Cardiotoxicity from Cancer Therapy: A Translational Approach to Biomarker Development

A thesis submitted to the University of Manchester for the degree of PhD in the Faculty of Faculty of Medical and Human Sciences

2015

Laura Suzanne Cove-Smith

School of Medicine

List of Contents

Word Count: 57,604

List of Figures

List of Tables

Abstract

Cardiotoxicity from Cancer Therapy: A Translational Approach to Biomarker Development. A thesis submitted to the University of Manchester for the degree of doctor of philosophy (PhD) by Laura Suzanne Cove-Smith (March 2015)

Background

Heart damage from cancer therapy is a significant problem for survivors. Some of the most effective treatments, such as anthracyclines, cause heart toxicity that can lead to significant morbidity and mortality. Cardiotoxicity also contributes to the loss of promising cancer drugs in early development and is notoriously difficult to predict. This translational project employs parallel pre-clinical and clinical studies to explore circulating biomarkers and cardiac magnetic resonance imaging (CMR) during development of anthracycline associated cardiotoxicity with the aim of finding biomarkers to aid clinical decision making and enable forward/back translation.

Methods

Pre-clinical work: A rat model of chronic anthracycline-induced cardiomyopathy was developed involving 8 weekly intravenous boluses of doxorubicin followed by a 4 week 'washout' period. A time course assessment of cardiac function using multiple MRI parameters was performed alongside a panel of circulating biomarkers measured prior to dosing.

Clinical work: In parallel following ethical approval, 30 cancer patients receiving standard anthracycline chemotherapy were recruited. Serial CMR scans were performed using standard and new exploratory techniques before, during and after treatment and blood was taken to evaluate a similar panel of cardiotoxicity biomarkers using multiplex ELISA at corresponding time points.

Results

Pre-clinical results: Systolic and diastolic function declined progressively, culminating in left ventricular dysfunction (LVEF <50%) by 12 weeks. Myocardial electron microscopy revealed myofibrillar and mitochondrial damage after one dose and gross histopathological damage after 5 doses. Myocardial contrast enhancement and troponin I increased significantly after eight doses and preceded LV dysfunction. Extensive fibrosis was seen 1 month after drug cessation.

Clinical results: LVEF declined progressively in all patients and 7 patients (23%) had persistent LV dysfunction 12 months after therapy. Troponin I elevations were seen towards the end of therapy and peak troponin I corresponded with LVEF decline. None of the other circulating biomarkers correlated strongly with outcome. Lower baseline extracellular volume (ECV) was associated with greater LVEF decline but little change in ECV was seen over time. Baseline dyssynchrony was associated with worse outcome and deteriorated with time alongside LVEF decline.

Conclusions

Results suggest that troponin I and cardiac MRI are sensitive translational tools in drug-induced cardiotoxicity. However, troponin I is a relatively late marker, peaking after substantial myocardial damage, too late to halt or change treatment. The imaging suggests that fibrosis and inflammation cannot be detected within a year of chemotherapy but baseline ECV and strain analysis may have a role in risk stratification.

Declarations

No portion of this work has been submitted for another degree or qualification at this or any other university or institute of learning.

Pre-Clinical Work

The pre-clinical work was run in collaboration with Astra-Zeneca Global Safety Alliance at Astra-Zeneca Alderley Park, UK. The overall project design and data interpretation was carried out by Dr Laura Cove-Smith[2,3,6], Dr Howard Mellor[1] and Dr Neil Woodhouse[1] in collaboration with all members of the supervisory team (clinical and pre-clinical). The animal handling, welfare and scanning was carried out by Jason Kirk[1] and Dr Neil Woodhouse assisted by Dr Laura Cove-Smith. The imaging analysis was performed by Dr Neil Woodhouse at the Astra-Zeneca imaging facility, overseen by Dr Paul Hockings[1]. The histological wet work was carried out by Dr Laura Cove-Smith, Susan Smith[1] and Melanie Galvin[1]. Interpretation and quantification of histology was carried out by Adam Hargreaves[1] and Dr Laura Cove-Smith. The work was overseen by Dr Sally Price[1]. The electron microscopy was performed by Simon Brocklehurst[1] and interpreted by Adam Hargreaves. The circulating biomarker work was performed by Dr Laura Cove-Smith[2,3] at the Cancer Research UK Manchester Institute, supervised by Dr Alison Backen[2] and overseen by Professor Caroline Dive[2] excluding Troponin I which was measured using a clinical platform at Astra-Zeneca overseen by Dr Catherine Betts[1]. The results were collated by Dr Laura Cove-Smith and the overall pre-clinical project was supervised by Howard Mellor from Global Safety Alliance.

Clinical Work

The clinical study protocol design was carried out by Dr Laura Cove-Smith, Dr. Kim Linton[3,6], Professor John Radford[3,6], Dr Matthias Schmitt[4,6], Professor Alan Jackson[5,6] and Professor Caroline Dive[2,6]. The cardiac MRI protocol was developed and optimised by Dr Laura Cove-Smith, Neal Sherratt[5,6] and Dr. Matthias Schmitt. The statistical analysis plan was written with the help of statistician Susan Lovick[1] and Linda Ashcroft[2]. The statistical analysis was performed by Dr Laura Cove-Smith with input from Clare Hodgson[2] and Dr Cong Zhou[2]. The code for T1 and T2 mapping analysis in the clinical study was developed by Dr Joanne Naish[5,6] and Dr David Morris[5,6] at the Manchester Biomedical Imaging Institute and supervised by Professor Alan Jackson. Scan acquisition was performed by staff at the Wolfson Molecular Imaging Centre and medical supervision was provided by Dr Laura

Cove-Smith (or Dr Nerissa Mescallado[3] in her absence). Scan analysis was performed by Dr Laura Cove-Smith (with guidance and help from Dr Christopher Miller[4], Dr Mark Ainslie[4] and Neal Sherratt). The circulating biomarker work was performed by Dr Laura Cove-Smith at the Cancer Research UK Manchester Institute. Data interpretation was performed by Dr Laura Cove-Smith with the supervision of her supervisors. The overall clinical project was supervised by Dr Kim Linton, Professor John Radford and Professor Caroline Dive.

[1]Astra-Zeneca Alderley Park UK, [2]Cancer Research UK, Manchester Institute, [3]The Christie NHS Foundation Trust, [4]University Hospital of South Manchester NHS Foundation Trust, [5]Manchester University Biomedical Imaging Institute, [6]University of Manchester

Copyright Statement

Acknowledgements

I would like to acknowledge the help of my enthusiastic and supportive supervisors Dr Kim Linton and Professor John Radford at the Christie, Professor Caroline Dive at the Cancer Research UK, Manchester Institute, Professor Alan Jackson at the Manchester Biomedical Imaging Institute, Dr Matthias Schmitt at the University Hospital of South Manchester and Dr Howard Mellor and Dr Ruth Roberts at Astra-Zeneca. The multifaceted nature of this project meant their time, expertise and guidance were much needed and much appreciated.

I would like to thank the lymphoma and breast cancer teams at the Christie with their help recruiting patients and getting the clinical study off the ground, particularly Dr Kim Linton, Professor John Radford, Dr Adam Gibb, Joanna Dash, Professor Richard Cowan, Dr Maggie Harris, Suzanne Allibone, Caroline Hamer, Andrea Whitmore, Dr Sasha Howell, Dr Anne Armstrong, Dr Andrew Wardley and Sally Bennett. I would like to thank Dr Nerissa Mescallado for providing medical supervision of MRI scans in my absence and the staff in the Christie clinical trials unit and outpatients for their phlebotomy and sample preparation skills.

I would like to thank Dr Alison Backen at the Cancer Research UK, Manchester Institute for teaching me the ins and outs of multiplex ELISA and to Dr Danielle Shaw and Dr Alistair Greystoke for their help and support with the logistics of setting up a clinical trial within clinical and experimental pharmacology. I would like to acknowledge the help of Grace Hampson ensuring the quality of biomarker data through the initiation of the computerised results system and the statisticians, Cong Zhou, Linda Ashcroft, Susan Lovick and Claire Hodgson for their guidance and patience with me.

I would like to thank the cardiologists from Wythenshawe particularly Dr Matthias Schmitt, Dr Christopher Miller and Dr Mark Ainslie for their cardiology expertise without which I would have struggled (even more) and the team at the biomedical imaging institute including Neal Sherratt, Sarah Fitzpatrick, Barry Whitnall, Amy Watkins, Dr David Morris and Dr Joanne Naish who always went out of their way to help me with the MRI scanning and analysis.

I would like to thank all the people at Astra-Zeneca who helped me to carry out the fruitful pre-clinical work, particularly Dr Howard Mellor, Adam Hargreaves, Jason Kirk, Dr Sally

Price, Melanie Galvin, Susan Smith and Dr Neil Woodhouse for their time, effort and guidance. My experience at Astra-Zeneca was fascinating and I feel privilege to have had the opportunity to learn about drug safety and development from these experts.

Thanks also go to the Teenage Cancer Trust who provided funding for the multiplex camera and Cancer Research UK and Astra-Zeneca for funding the highly successful clinical fellowship scheme.

Lastly, but most importantly I would like to thank the patients who took part in the clinical trial which was truly altruistic. Unlike some trials, this study did not directly benefit patients and involved many extra visits and blood tests during an extremely difficult time. I will be forever grateful to the patients who took part and was touched by their willingness and dedication to help others.

The Author

Dr Laura Cove-Smith is a Medical Oncology Speciality Trainee in the North Western Deanery (appointed 2008). She graduated from Sheffield University Medical School in 1998 and carried out her core medical training in Sheffield where she worked at the Weston Park Cancer Hospital and developed a love of oncology, particularly lymphoma. She gained membership of the Royal College of Physicians in 2007 before moving to Manchester to pursue a career in medical oncology. She started her registrar training with the lymphoma team at the Christie and became interested in late effects from cancer therapy. She was appointed to a competitive 3 year clinical research fellowship funded jointly by Astra-Zeneca and Cancer Research UK in 2011 as part of a highly successful training scheme in conjunction with Manchester University. The fellowship was based within Clinical and Experimental Pharmacology in the Cancer Research UK, Manchester Institute (University of Manchester) with input from the Biomedical Imaging Institute (University of Manchester), Astra-Zeneca Global safety Alliance and the Christie. The research presented in this thesis was conducted during this clinical fellowship post.

Publications arising from this Thesis

Cove-Smith L, Woodhouse N, Hargreaves A, Kirk J, Smith S, Price SA, Galvin M, Betts CJ, Brocklehurst S, Backen A, Radford J, Linton K, Roberts RA, Schmitt M, Dive C, Tugwood JD, Hockings PD, Mellor HR. An Integrated Characterisation of Serological, Pathological, and Functional Events in Doxorubicin-Induced Cardiotoxicity. Toxicol Sci. 2014 Jul;140(1):3-15

Cross MJ, Berridge BR, Clements PJ, **Cove-Smith L**, Force TL, Hoffmann P, Holbrook M, Lyon AR, Mellor HR, Norris AA, Pirmohamed M, Tugwood JD, Sidaway JE, Park KB. Physiological, pharmacological and toxicological considerations of drug-induced structural cardiac injury. Br J Pharmacol. 2014 Oct 10.

International Presentations arising from this Thesis

Cove-Smith L - oral abstract presentation at the International CardiOncology Society (ICOS) Annual Meeting, 'Circulating and imaging biomarkers of treatment induced cardiotoxicity in cancer patients; a translational approach.' September 2012

Cove-Smith L - invited speaker at Biomedical Imaging Institute Cardiovascular symposium, University of Manchester. 'Cardiotoxicity in cancer patients' April 2014.

Cove-Smith L – invited speaker at the annual meeting of the British Society of Toxicological Pathology and Safety Pharmacology Society 'Cardiovascular safety risk assessment for new candidate drugs from functional and pathological data' Alderley Park, Cheshire, UK 14-15th November 2013

Cove-Smith L - Invited speaker at the Oxford Global International Oncology Clinical Development Congress, 'A translational approach to safety biomarker development ' Manchester, UK, October 2012

International Poster Presentations arising from this Thesis

Cove-Smith L, Radford J, Schmitt M, Roberts R, Mellor H, Sherratt N, Morris D, Naish J, Gibb A, Dash J, Mescallado N, Harris M, Cowan R, Howell S, Armstrong A, Wardley A, Backen A, Jackson A, Dive C, Linton K. 'Cardiotoxicity from cancer therapy: a translational approach to biomarker development' Poster presentation at the National Cancer Research Institute Conference, Liverpool, UK, 2-5th November 2014

Laura Cove-Smith, Neil Woodhouse, Adam Hargreaves, Jason Kirk, Susan Smith, Sally A. Price, Melanie Marsden, Catherine Betts, Simon Brocklehurst, Alison Backen, John Radford, Kim Linton, Ruth Roberts, Matthias Schmitt, Caroline Dive, Jonathan Tugwood, Paul D. Hockings & Howard R. Mellor. 'An integrated characterisation of serological, pathological and functional events in doxorubicin-induced cardiotoxicity' Congress of the European Societies of Toxicology, Edinburgh, UK, 7-10th September 2014

Claire Barnes, Janet Kelsall, Susan Smith, **Laura Cove-Smith,** Howard Mellor, Adam Hargreaves and Sally Price. 'Localisation of novel miRNA biomarkers of doxorubicin-induced cardiotoxicity in rats' Congress of the European Societies of Toxicology, Edinburgh, UK, 7-10th September 2014

Mellor H, **Cove-Smith L**, Kirk J, Hargreaves A, Price S, Betts C, Dive C, Hockings P and Woodhouse N. 'An integrative approach to Identify Functional, Structural and Pathological

Biomarkers of Doxorubicin-induced cardiotoxicity' Poster presentation at Society of Toxicology, San Antonio, Texas, March 10-14, 2013

Other Related Publications

Chow S, **Cove-Smith L**, Schmitt M, Hawkins R. High-dose interleukin 2-induced myocarditis: can myocardial damage reversibility be assessed by cardiac MRI? J Immunother. 2014 Jun;37(5):304-8

Abbreviations

2D	2 Dimensional
ABVD	Doxorubicin, Vinblastine, Bleomycin, Darcarbazine
ACE	Angiotensin Converting Enzyme
AF	Atrial Fibrillation
AKT	Protein kinase B
ANP	Atrial Natriuretic Peptide
ATP	Adenosine triphosphate
BMI	Body Mass Index
BNP	Brain Natriuretic Peptide
BP	Blood Pressure
BSA	Body Surface Area
CCD	Charged Coupled Device
CK	Creatine Kinase
CMR	Cardiac MRI
CO	Cardiac Output
CR	Complete Response
CRP	C-Reactive Protein
CTC	Common Toxicity Criteria
CV	Coefficient of Variation
DNA	Deoxyribonucleic Acid
DVT	Deep Vein Thrombosis
E/A ratio	Ratio of velocity of flow through the mitral value in early (E) and late (A) diastole
ECG	Electrocardiogram
ECHO	Echocardiogram
ECV	Extracellular Volume
EDTA	Ethylenediaminetetraacetic Acid
EDV	End Diastolic Volume
EF	Ejection Fraction
EGFR	Epidermal Growth Factor Receptor
ELISA	Enzyme Linked Immunosorbant Assay
EM	Electron Microscopy
ESV	End Systolic Volume

FABP	Fatty Acid Binding Protein
FEC-T	5-Fluorouracil, epirubicin, cyclophosphamide, docetaxel
FH	Family History
FOV	Field of View
GCP	Good Clinical Practice
GFR	Glomerular Filtration Rate
H&E	Hematoxylin and eosin
HER2	Human Epidermal Growth Factor Receptor 2
hFABP	heart type Fatty Acid Binding Protein
HL	Hodgkin Lymphoma
HTN	Hypertension
ICC	Intra-Class Correlation
IHD	Ischaemic Heart Disease
IL	Interleukin
IMP	Investigational Medicinal Product
LA	Left Atrium
LGE	Late Gadolinium Enhancement
LLOQ	Lower Limit of Quantification
LV	Left Ventricle
LVEF	Left Ventricular Ejection Fraction
LVM	Left Ventricular Mass
MAP-K	Mitogen-activated protein kinase
MI	Myocardial Infarction
Mirna	Micro Ribonucleic Acid
MMP	Matrix Metallo Proteinase
MPO	Myeloperioxidase
MRI	Magnetic Resonance Imaging
mTOR	Mammalian target of
MUGA	Multi-gated acquisition scan
NADH	Nicotinamide adenine dinucleotide (reduced)
NHL	Non Hodgkin Lymphoma
NHS	National Health Service
NTproBNP	N-terminal Brain Natriuretic Peptide
PAPPA	Pregnancy Associated Plasma Protein

PI3-K	phosphatidylinositide 3-kinase
PR	Partial Response
QC	Quality Control
RCF	Relative Centrifugal Force
RCHOP	Rituximab, cyclophosphamide, vincristine, doxorubicin and prednisolone
RECIST	Response Evaluation Criteria In Solid Tumours
RNA	Ribonucleic Acid
ROC	Receiver Operator Curve
ROS	Reactive Oxygen Species
SD	Stable Disease
SV	Stroke Volume
SVT	Supra-ventricular Tachycardia
TE	Echo Time
TIMP	Tissue inhibitor of Matrix Metallo Proteinase
TNF	Tissue Necrosis Factor
TR	Repetition time
Trop	Troponin
ULOQ	Upper Limit of Quantification

1 Introduction

1.1 Cardiotoxicity from Cancer Therapy

The development of treatment-induced cardiotoxicity is becoming increasingly relevant as cancer survival rates improve [1]. Childhood survivors of cancer are eight times more likely to die from cardiac causes and 15 times more likely to develop cardiac failure than their contemporaries [2,3]. Anthracycline chemotherapies are thought to be some of the main contributors to cardiac morbidity in cancer survivors [3-5] but remain some of the most effective anti-cancer agents, particularly against haematological malignancies and breast cancer. Currently, there is no consensus about how to monitor patients for chemotherapy-induced cardiotoxicity. The need for formal guidance on cardiotoxicity was highlighted by the American Association of Clinical Oncology survivorship panel in 2007 [6] and international consensus guidelines are currently being devised by the international cardio-oncology society [7]. Assessment of left ventricular (LV) function before, during and after therapy is now recommended [8, 9] but this approach has not been universally adopted in adult cancer patients largely because it remains unclear whether close monitoring of this type improves outcome. Assessment of LV function using older imaging techniques, such as radionucleotide scanning are relatively insensitive and have only been able to detect damage when significant potentially irreversible cardiac dysfunction is present. However, newer imaging techniques may have the potential to detect damage at an earlier potentially reversible stage. The national cancer survivorship initiative, formulated by the department of health in partnership with Macmillan cancer support, has raised awareness about cardiotoxicity amongst clinicians and the public thus highlighting the need for more research in this area [10]. However, one of the biggest challenges is detecting which patients are at highest risk as clinical examination and simple bedside tests such as electrocardiograms (ECG) often remain normal throughout treatment. Circulating biomarkers of cardiac damage could have great potential to predict cardiotoxicity during treatment allowing early intervention with the aim of improving outcome.

Anthracyclines are not the only systemic treatments that have detrimental off-target effects on the heart. Many of the newer ‘targeted’ agents share cancer and cardiac receptor targets and awareness about this issue in drug development is rising. Many potentially promising anti-tumour drugs are discarded during pre-clinical development and early phase clinical trials due to unforeseen cardiotoxicity which is notoriously difficult to predict. Being able to evaluate

accurately the cardiotoxicity profile of an agent during early stages of development could be more cost effective, prevent unforeseen toxicity and lead to the development of safer compounds. However, there does not appear to be a common molecular structure - pharmacophore - associated with drug induced cardiotoxicity and current methods of assessing cardiotoxicity during drug development are relatively unsuccessful. Therefore finding useful biomarkers of cardiac toxicity could be beneficial in early drug development as well as clinical practice.

1.2 Pathophysiology of the Heart

Determining which biomarkers to investigate requires an understanding of the molecular mechanisms of drug induced cardiotoxicity and the pathophysiology of the heart. The heart consists of 4 main chambers, the right and left ventricle which expel their blood volume during systole (ventricular contraction), and the right and left atria which contract during diastole (the relaxation phase of the cardiac cycle) to aid filling of the ventricles. The atria and ventricles are separated by the atrio-ventricular valves (mitral and tricuspid valves) which are forced shut during systole to prevent retrograde flow. The right ventricle receives deoxygenated blood from the venous system and pumps it into the lungs through the pulmonary valve into the pulmonary circulation where it is oxygenated. Oxygenated blood is returned via the pulmonary veins to the left side of the heart to enter the systemic circulation through the aortic valve (**Figure 2**). The volume of blood ejected from each ventricle during systole is termed the stroke volume (SV). This can be calculated by working out the volume of blood remaining in the ventricle following contraction i.e. SV = the end diastolic volume (EDV) minus the end systolic volume (ESV). This can be expressed as a percentage fraction called the 'ejection fraction' (EF) which is the most commonly used parameter of cardiac dysfunction in clinical practice. It is measured by various imaging techniques including echocardiogram. However, increasingly it is being realised that diastolic dysfunction is equally important in terms of clinical impact and potential reversibility, as it almost always precedes systolic dysfunction. The diastolic function can be assessed in several different ways but the most widely used is the E/A ratio. This is the ratio of flow through the mitral valve during early and late diastole which measures the efficiency of ventricular filling.

The heart itself is comprised of the myocardium, consisting of specialised muscles cells called cardiac myocytes, an outer fibrous sack called the pericardium and the endocardium, a layer of endothelial cells lining the chambers of the heart. A specialised conducting system,

originating in the right, atrium co-ordinates rhythmical contraction of the heart. Depolarisation starts in specialised conducting cells at the sino-atrial node and spreads through the atrium to the atrio-ventricular node via specialised inter-nodal tracts where it is slowed to allow adequate filling time before spreading through the bundle of His to the Purkinje fibres (large rapid conducting cells) and bundle branches in the right and left ventricle. Cardiac cells themselves are connected by gap junctions to form a functional syncytium allowing action potentials to spread rapidly from one cell to another to facilitate unified contraction. The myocardium is the functional component of the heart which acts as the 'pump' supporting the cardiovascular system. Cardiac failure occurs when the 'pumping action' is insufficient to meet the haemodynamic and metabolic needs of the body. There are many different causes of cardiac failure including ischaemia, hypertension, valvular damage, metabolic disorders and drugs. The events that lead to cardiac failure at a cellular level may initially differ, but the common end point is a dysfunctional myocardium with ineffective contraction and inadequate cardiac output.

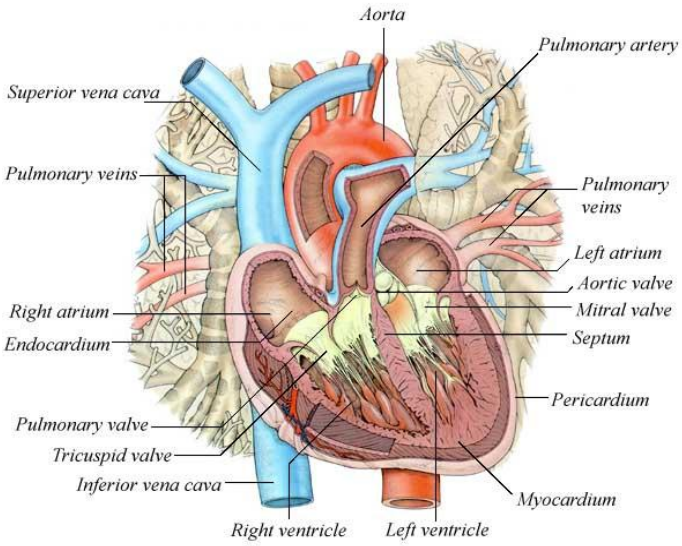

Figure 2. 'The Heart Structure.' (http:// www.chelation-uk.com/heart-structure.html)

Myocytes differ from other cells due to their ability to deform and enable myocardial contraction. Similar to skeletal muscle cells, they have a cytoskeleton made up of thick myosin and thin actin filaments which can be phosphorylated resulting in conformational changes that lead to contraction. These filaments form contractual units called sarcomeres, in which myosin filaments slide over actin through the binding and release of cross bridges formed at the actin binding site on myosin heads. Each sarcomere is bounded by a z line

linking myosin with giant myofilament titin which acts as a coil linking the sarcomeres and enabling unified contraction. The myocytes are bounded by a basement membrane involving a specialised structure called the sarcolemma which allows interaction between the intra and extracellular environments. The cells are linked by intercalated discs allowing further inter-cell interaction and coordination of contraction throughout the myocardium (**Figure 3**). The ability to contract means myocytes have a high energy utility and greater number of mitochondria than other cells to enable the binding and unbinding of myosin heads through ATP hydrolysis. Contraction is regulated by intracellular calcium which is stored and released from the sarcoplasmic reticulum, a smooth specialised endoplasmic reticulum specific to cardiac cells. Once released, high intracellular calcium concentration triggers cell depolarisation which activates the binding of filaments leading to subsequent contraction (often termed excitation contraction coupling) [11].

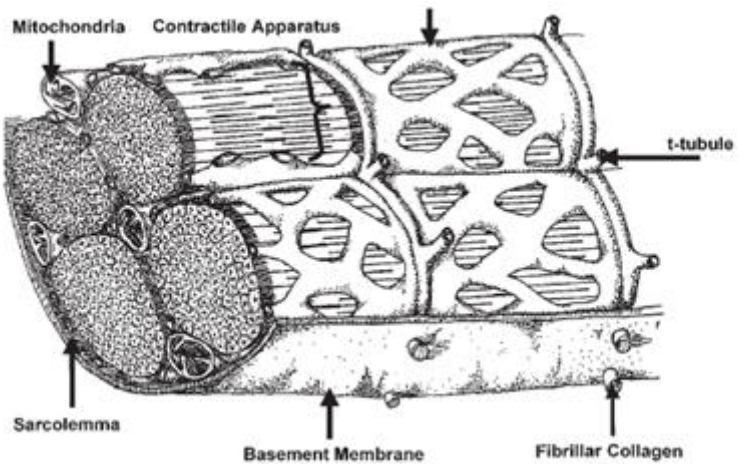

Figure 3. The Structure and Function of a Cardiac Myocyte: a review of the fundamental concepts [12].

1.3 Anthracyclines

Studying anthracyclines could help to investigate the effects of chemotherapy on the myocardium and the potential role of circulating and imaging biomarkers. Anthracyclines are antibiotic agents derived from streptomyces peucetius, a gram positive bacterium originally isolated from soil in the Adriatic region in the 1950s [13]. They have often been described as ‘the physician’s classical anti-cancer drug’ due to their multi-faceted action against tumour cells. They are thought to cause cell death through several processes including intercalation into DNA, inhibition of topoisomerase 2 and formation of reactive oxygen species.

Doxorubicin is the most widely used anthracycline and remains the cornerstone of successful first line treatment for haematological malignancies such as lymphoma, leukaemia and breast cancer.

1.3.1 Anthracycline-induced Cardiotoxicity

Unfortunately the use of anthracyclines is limited by their potential to cause cardiotoxicity. There are very few systemic agents that offer a safer yet equally efficacious alternative despite rapid advances in oncological management [14]. Heart failure has been a reported in survivors of childhood malignancy for many decades and the incidence has been shown to increase with time (**Figure 4**). Anthracyclines are believed to be one of the main contributing factors to the development of heart failure in cancer survivors. This presents a significant clinical problem as, in the USA alone, the number of cancer survivors is estimated to be above 10 million and approximately half will have received an anthracycline. Survivorship studies show that severe, sometimes fatal cardiomyopathy is seen in 5-10% of cancer survivors. Yet some studies suggest that up to half of patients treated with anthracyclines may have evidence of subclinical damage at 5 years [5, 15-19]. The incidence of cardiac failure in breast cancer patients who have had anthracyclines is lower (~3.2%) [20]. The anthracycline epirubicin, a stereoisomer of doxorubicin, is often used in preference to doxorubicin as it was initially thought to be less cardiotoxic following comparative pre-clinical and early clinical studies carried out in the 1980s [21, 22]. Despite this, the incidence of cardiac failure is still rising in breast cancer patients. This may be due to the recent addition of trastuzumab to adjuvant therapy. Trastuzumab is a humanised monoclonal antibody targeting tumours with over-expression of human epidermal growth factor 2 (HER2). It was found to be highly cardiotoxic with rates of left ventricular dysfunction up to 34% when given concurrently with anthracyclines [23].

Anthracycline induced cardiac damage can be acute, early or late onset. Acute cardiotoxicity is thought to be independent of dose and manifests as an acute pericarditis-myocarditis, arrhythmia or acute coronary syndrome [8]. Early cardiotoxicity can present as progressive congestive cardiac failure shortly after therapy but most commonly, late onset chronic congestive cardiac failure develops many years after treatment [8, 24]. Late cardiac damage appears to be dose dependent. This was demonstrated in a large retrospective study by Von Hoff [25] and reinforced by work from Swain *et al* who demonstrated a steep dose correlation curve in patients receiving doxorubicin [26]. In this analysis, cardiac failure was

reported in 48% of patients when the dose exceeded 700mg/m^2. This led to modification of anthracycline dosing in clinical practice but, even at standard treatment doses of 200-400 mg/m^2, significant cardiotoxicity is seen [17, 25-29]. Therefore, oncologists have to carefully balance the risk of cardiac morbidity and mortality with the benefits of cancer therapy.

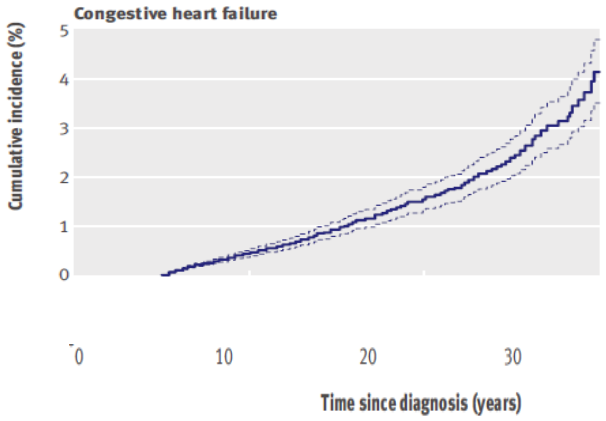

Figure 4. Cardiac outcomes in a cohort of adult survivors of childhood and adolescent cancer: retrospective analysis of the Childhood Cancer Survivor Study cohort [5].

1.3.2 The Molecular Mechanism of Anthracycline Cardiotoxicity

The mechanisms leading to anthracycline cardiotoxicity are difficult to delineate. They are not fully understood but may result from their broad anti-neoplastic properties [27, 30]. The main anti-tumour actions of anthracyclines involve the disruption of replication and transcription through intercalation into DNA and RNA causing interference with DNA strand separation and inhibition of topoisomerase II [31]. They also cause free radical formation which leads to cellular and mitochondrial membrane damage through lipid peroxidation. Some of these mechanisms are likely to contribute to cardiotoxicity and unlike some tissues i.e. bone marrow and liver, the heart has less capacity to regenerate leading to irreversible damage [32]. Several proposed mechanisms of myocyte damage have been identified from *in vitro and in vivo* studies but it is not clear which are most relevant in clinical practice.

1.3.2.1 Free Radical Damage

The most commonly explored theory involves the formation of reactive oxygen species (ROS) [33]. Oxidative stress occurs in all tissues but, under normal conditions the oxidant-antioxidant systems are in equilibrium and tissue damage only occurs if this balance is disrupted. Cardiac muscle is highly active therefore mitochondria rich, producing high

quantities of ROS during cardiomyocyte metabolism [34]. Anti-oxidants such as glutathione prevent free radical damage in cardiomyocytes however the level of antioxidants is insufficient to cope with the enhanced production of ROS induced by anthracyclines leaving the heart susceptible to oxidative stress [34-36]. Free radicals are formed due to the quinone moiety of anthracyclines. Anthracyclines are readily reduced to form highly reactive semiquinones which causes uncoupling of the electron transport chain and catalyses the formation of more ROS. Highly reactive anions such as superoxide are generated and cause DNA and membrane damage in the mitochondria and cell itself (**Figure 5**) [1, 37, 38]. The formation of free radicals can also damage heart enzymes, such as creatine kinase (CK), which are vital for myocardial contraction, as they control interaction of the thick and thin myofilaments [39]. Free radicals can also directly damage the myofilaments themselves leading to reduced contractility and subsequent cardiac dysfunction (**Figure 6**) [40]. Anthracyclines also bind readily to intracellular iron generating anthracycline-iron complexes. Although the interaction of anthracyclines and iron are not fully understood, iron binding is thought to catalyse further redox reactions leading to more free radical generation and cellular damage [41]. Reduction occurs via membrane bound NADH dehydrogenase [38] and can lead to dissipation of the mitochondrial membrane potential. Mitochondrial membranes are rich in cardiolipin which has a high affinity for anthracyclines, readily binding them and leading to high intra-mitochondrial concentrations [42]. This results in the activation of pro-apoptotic proteins Bid and Bax and it has been proposed that myocyte death occurs via the mitochondrial pathway involving Bid, Bax, cytochrome-c, and caspase-3 [43] [30]. This mitochondrial damage leaves myocytes energy depleted leading to myocardial dysfunction [44].

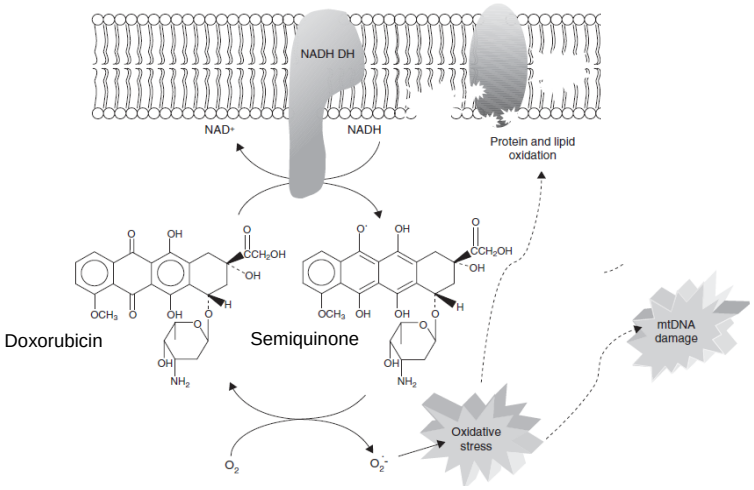

Figure 5. Adapted from 'Drug-induced mitochondrial dysfunction in cardiac and skeletal muscle injury' [45].

1.3.2.2 Doxorubicin Induced Cell Death in Myocytes

The formation of ROS is thought to be one of the initial steps leading to cardiomyocyte death. Several *in vitro* and *in vivo* studies have shown that free radical damage leads to apoptosis and that inhibition of free radical formation reduces cell death [30, 37, 46]. Dose dependent myocyte death has been demonstrated *in vitro* [37] and it is feasible that cumulative damage occurs due to fractionated myocyte death with each dose of anthracycline. Apoptosis has been shown on human myocardial biopsy directly after doxorubicin with visible chromatin contraction and nuclear condensation. However, evidence of necrosis and cytoplasmic swelling were also seen [47] and growing evidence that circulating sarcomeric proteins can be released in anthracycline toxicity suggests that both apoptosis and necrosis occur [48, 49].

1.3.2.3 The Role of Endothelial Cell Damage

Endothelial cell damage may also contribute to chemotherapy-related cardiotoxicity through the disruption of vessel integrity by the initiation of inflammatory, atherosclerotic and pro-thrombotic pathways. Several *in-vivo* studies have demonstrated direct endothelial as well as myocyte damage and death following doxorubicin [50] [51].

1.3.2.4 Disruption of Protein Synthesis

Anthracyclines can directly intercalate into nucleic acids disrupting protein synthesis. Coupled with the inhibition of DNA regulating enzymes such as topoisomerase 2 this process

can halt the production of key proteins involved in maintenance of cardiac muscle homeostasis [52]. This results in reduced myofilament synthesis and in the presence of increased myofilament degradation leads to an overall loss of cytoskeletal proteins [30].

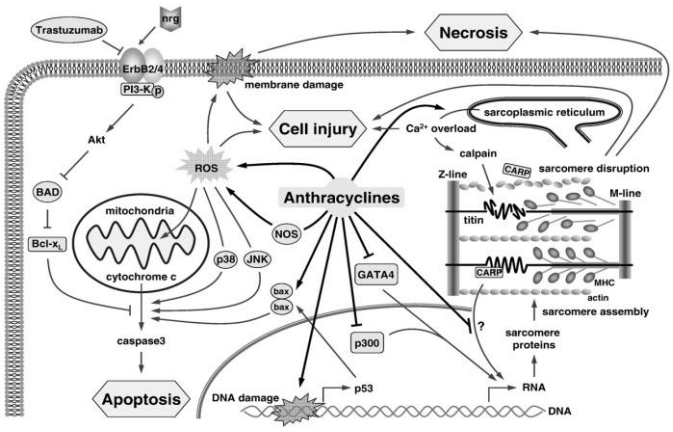

Figure 6. 'Mechanisms of anthracycline cardiac injury' [30].

1.3.2.5 Growing Knowledge through Trastuzumab

Treatment with trastuzumab in breast cancer has improved our understanding of the potential mechanisms of anthracycline induced cardiotoxicity. The HER2 receptor belongs to a family of membrane receptor tyrosine kinases which, when activated, dimerise to initiate downstream PI3-K/AKT and MAP-K pathways promoting cell growth and survival. Unlike anthracyclines, trastuzumab related cardiomyopathy appears to be reversible (now called type 2 cardiotoxicity). Studies examining the nature of this unforeseen side effect have shown that HER2 is expressed in adult myocytes and is essential for normal myocyte growth and function. In the presence of trastuzumab, HER2 signalling is suppressed and degradation of cardiac proteins by anthracyclines is accelerated [27, 30]. This suggests that the PI3K-Akt-mTOR pathway is involved in preserving cardiac integrity and potentially cardiac function [53]. These findings are becoming increasingly relevant because many new cancer drugs are being developed to target this pathway and therefore have the potential to cause cardiotoxicity.

1.3.2.6 Electrophysiological Toxicity

Finally anthracyclines have adrenergic properties affecting the control of calcium and dynamic function [30, 54]. This effect may not be dose dependent and may be responsible for the rarer acute arrhythmogenic or sudden acute contractility problems.

1.3.3 Prognosis from Anthracycline-induced Cardiomyopathy

Previous studies have suggested that anthracycline-induced cardiomyopathy (type 1 cardiotoxicity) is relatively resistant to conventional heart failure therapies. Doxorubicin related cardiomyopathy carries a worse prognosis than some other forms of left ventricular dysfunction with a 2 year mortality of 60% (**Figure 7**) [55]. However, recent studies suggest that there may be an element of reversibility and the evidence base for prompt recognition and intervention by cardiology specialists is growing [56, 57]. Cardinale *et al* demonstrated complete recovery of cardiac function (LVEF) in 60% of patients with cardiac dysfunction after chemotherapy following the initiation of Enalapril (ACE1 inhibitor) +/- betablockade within 2 months of completing chemotherapy. However no reversibility was seen if treatment was initiated more than 6 months post chemotherapy [56]. Therefore risk stratification, timely diagnosis and treatment of chemotherapy-related cardiac damage could significantly reduce the incidence of long term complications.

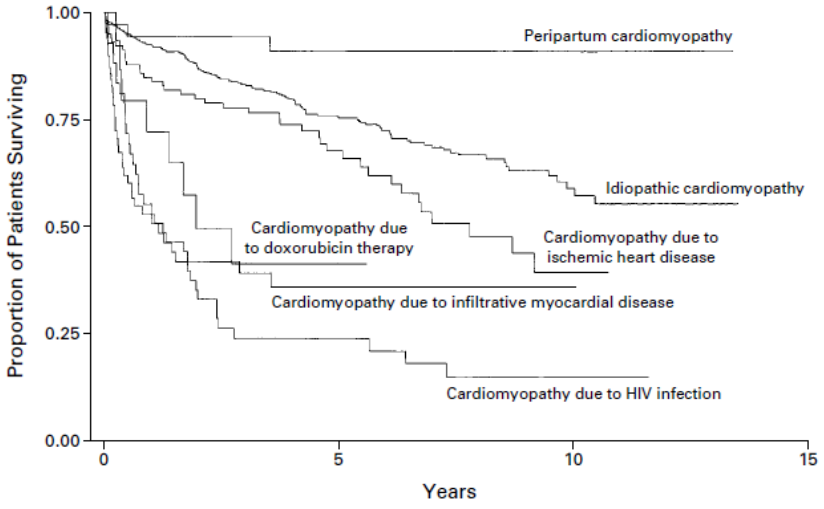

Figure 7. Adjusted Kaplan-Meier estimates of survival according to underlying cause of cardiomyopathy. Underlying lying causes and long term survival in patients with unexplained cardiomyopathy [55].

1.4 Predicting Drug-Induced Cardiomyopathy in Clinical Practice

The risk of developing significant cardiac disease from chemotherapy is unpredictable using current clinical tools. There are no reliable predictive biomarkers of cardiotoxicity and in most cases cardiac damage is not detected until clinical heart failure develops years after chemotherapy [24]. Patients often have confounding risk factors and long time lapses

between cancer treatment and the onset of symptoms, therefore cardiac failure in cancer survivors may be mislabelled, underestimating the true incidence [58]. A 'multi-hit hypothesis' has been proposed, suggesting that initial subclinical damage occurs during chemotherapy but does not lead to overt heart failure unless the heart undergoes a second 'hit', such as hypertension. However, events could occur the other way round with occult cardiac damage, due to pre-existing cardiovascular risk factors increasing the likelihood of cardiac failure following chemotherapy [59]. This makes the accurate assessment of the aetiology of cardiac failure in a population of pre-treated cancer patients difficult.

Currently, risk stratification of patients receiving potentially cardiotoxic anti-cancer agents is largely done on a clinical basis. Alternative treatments are usually sought for patients with a history of overt cardiac disease and patients with multiple risk factors will undergo cardiac imaging to formally assess the function of the heart prior to therapy. However, those without known cardiovascular disease often receive treatment without cardiac assessment at baseline, during treatment or during follow up. Several studies which were summarised in a paper by Singal *et al* identified key factors which carried a higher risk of cardiotoxicity with anthracyclines. These were found to be age over 70, combination chemotherapy, mediastinal radiotherapy, previous cardiac disease, hypertension, liver disease and hyperthermia [60]. These findings may to hold true for many cardiotoxic agents but no unified strategy to guide monitoring of these high risk individuals exists.

Following work by Unverferth, Billingham and Bristow in the early 1980s, myocardial biopsy was considered the most sensitive and specific way to assess anthracycline-induced cardiotoxicity [61]. Billingham and Bristow developed a histological grading scale of anthracycline-related cardiotoxicity based on the typical changes seen following doxorubicin (**Table 1**). Their grading system measured the loss of myofibrils, mitochondrial and nuclear degeneration, distension of sarcoplasmic reticulum and vacuolisation of cytoplasm [62]. However, the high risk and invasive nature make the use of cardiac biopsy clinically and ethically impractical. Circulating biomarkers could offer a non-invasive, clinically practical modality for predicting cardiotoxicity in cancer patients [8]. They could be used to elicit cardiac damage prior to the detection of changes on cardiac imaging, providing a better way to risk stratify and monitor patients. They could also be used in drug development to assess the cardiotoxicity profile of new agents preventing loss of novel drugs at a late stage.

Grade	Billingham scoring system of morphological characteristics of anthracycline cardiotoxicity (Billingham *et al* 1978)
0	Normal myocardial ultrastructural morphology
0.5	Not completely normal but no evidence of anthracycline specific damage
1	Isolated myocytes affected and/or early myofibrillar loss; damage to <5% of all cells
1.5	Changes similar to grade 1 except damage involves 6-15% of all cells
2	Clusters of myocytes affected by myofibrillar loss and/or vacuolisation, with damage to 16-25% of all cells
2.5	Many myocytes (26-35% of all cell) affected by vacuolisation and/myofibrillar loss
3	Severe diffuse myocyte damage (>35% of all cell)

Table 1. Pathological scoring of anthracycline damage, adapted from 'Billingham and Bristow histological staging of doxorubicin cardiotoxicity' [63].

1.4.1 The Role of Biomarkers in Cardiotoxicity

A biomarker is defined as 'a characteristic which can be objectively measured and evaluated as an indicator of normal or pathological biological processes, or pharmacological responses to a therapeutic intervention' [64, 65]. The clinical utility of circulating biomarkers depends on their ability to inform the risk/benefit ratio and aid clinical decision making in a way that is superior, quicker, easier and cheaper than other existing approaches [66]. Biomarkers can be used to identify target populations and streamline novel drug development. Pharmacodynamic biomarkers can be used to measure desired drug effect during early clinical trials by monitoring upstream or downstream effects. Biomarkers can also be used to guide prognosis or to predict response to therapy. They are becoming increasingly used as surrogate endpoints for clinical outcomes but their validity in this setting is still debatable. Diagnostic, screening and predisposition biomarkers have been used for decades and all offer valuable additional information to aid clinical decision making. Safety biomarkers are used to report toxicity from treatment in clinical trials and clinical practice. **Table 2** lists the different types of biomarkers with an example of where they are currently used in the clinical setting.

Biomarker Category	Role	Example
Screening	To identify individuals with a disease at an early stage to enable intervention and improve outcome	Detection of dysplasia in cervical smear testing used to screen for potential cervical carcinoma
Prognostic	To indicate the likely disease course and outcome	Number of lymph nodes involved predicts for relapse in breast carcinoma
Predictive	To predict who is likely to respond to a given treatment	EGFR mutation status predicts for response to EGFR small molecule inhibitors such as Gefitinib in lung cancer
Pharmacological	To measure the effect of a treatment on a specific target	Receptor blockade or enzyme inhibition report for proof of mechanism or proof of concept in drug development trials
Diagnostic	To confirm or define a type of medical condition	Immunohistochemistry used to determine the type of cancer
Pre-disposition	To identify individuals at risk of developing a certain condition	Presence of BRCA1 mutation infers a greater risk of developing breast or ovarian carcinoma
Surrogate	To use as substitutes for a clinically meaningful endpoint such as response to a treatment	Tumour markers such as PSA falling in response to therapy
Toxicity/Safety	To measure the toxicity of a treatment on normal tissues	Alaninine aminotransferase (ALT) for reporting liver toxicity

Table 2. The role of biomarkers, adapted from the Cancer Research UK website March 2011. http://www.cancerresearchuk.org

Historically we have relied on clinical assessments to detect side effects and document the toxicity profile of our treatments. The most commonly used method is the 'Common Terminology Criteria for Adverse Events' (the CTC grading system). This is a standardised grading system for the most commonly seen drug toxicities. The grading system runs from grade one, which is mild, to grade five which is death related to a treatment (**Table 3**). This system is notoriously subjective and relatively crude. It relies on the development of overt clinical manifestations of toxicity which do not always occur until significant damage has been done and may be permanent. Despite this, it is currently used to guide dose escalation in phase 1 trials and dose reduction in clinical practice. The effect of chemotherapy on the bone marrow is commonly used as a surrogate for toxicity. However, as the bone marrow can readily regenerate it is not an ideal surrogate as it does not reflect the incipient irreversible damage that may be occurring in other tissues such as lung parenchyma, myocardium or nerves. Tissue specific biomarkers of toxicity could offer a more objective way to measure the effects of treatment on normal tissues. They could potentially report on damage at a much

earlier stage, before clinical symptoms arise. They could guide decision making in clinical practice and in drug development to avoid severe toxicity and development of lasting damage.

Grade	Description of adverse event
Grade 1	Mild
Grade 2	Moderate
Grade 3	Severe
Grade 4	Life-threatening or disabling
Grade 5	Death related to adverse event

Table 3. CTC grading system. 'Common Terminology Criteria for Adverse Events, Version 4.0, DCTD, NCI, NIH, DHHS', 28th May 2013, http://ctep.cancer.gov.

Circulating biomarkers are relatively non-invasive, cost effective and practically amenable in a busy clinical setting. In an era of personalised medicine, developing biomarkers that can assess toxicity could enable treatment to be tailored for an individual to avoid severe or permanent effects. Several specific circulating protein biomarkers of toxicity are making their way into early phase trials but are yet to be used in routine care [67]. Incorporating toxicity biomarkers into early phase trials could also avoid development of highly toxic agents and help in the development of protective strategies. Biomarkers of cardiac toxicity would be invaluable as cardiac damage is one of the most limiting toxicities in drug development.

1.4.2 Review of Existing and Potential Cardiotoxicity Biomarkers

Multiple circulating biomarkers have been validated and established for diagnostic use in the setting of ischaemic damage and congestive cardiac failure. Several of these have been explored in chemotherapy-related cardiotoxicity but none, as yet, has shown strong predictive value. The field of chemotherapy-induced cardiotoxicity suffers from a lack of standardisation, and few studies have explored multiple biomarkers simultaneously using robustly validated protocols. The natriuretic peptides (NPs) and troponins (Trop) have been most widely explored and several others including heart type fatty acid binding protein (hFABP), creatine kinase (CK), myoglobin, interleukins (IL), C-reactive protein (CRP) and tumour necrosis factor-a (TNFa), have been looked at with variable results. Several newer biomarkers of fibrosis have been explored in cardiomyopathy, including the matrix metalloproteinases (MMPs) and the tissue inhibitor matrix metalloproteinases (TIMPs). They have rarely been studied in chemotherapy-related cardiotoxicity but could be potential candidates for exploration in this setting.

1.4.2.1 Troponins

Troponins are some of the most important biomarkers of cardiac damage and are used for the diagnosis and risk stratification of ischaemic cardiac damage [68]. Troponins are a group of 3 regulatory proteins, troponin T, I and C, involved in muscle contraction through interaction with tropomysin binding protein. At rest, tropomysin overlays the actin binding sites on myosin heads preventing interaction of myosin filaments (thick) with actin filaments (thin). In action, influx of calcium through the sarcoplasmic reticulum results in translocation of the tropomysin-troponin complex away from the actin outer domains through interaction with the three regulatory proteins (**Figure 8**). This releases the actin binding site and allows binding of actin to myosin. Movement of the myosin heads through ATPase activity causes the filaments to slide along each other resulting in sarcomeric shortening and muscle contraction [69].

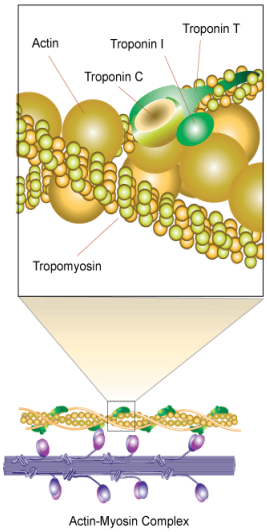

Figure 8. 'Structure and interaction of cardiac troponins within the actin-myosin complex' (http://www.sigmaaldrich.com).

Troponins are some of the most widely studied cardiac biomarkers in anthracycline and chemotherapy-related cardiotoxicity. Raised circulating troponin levels have been demonstrated in many clinical studies, some of which show a correlation with cardiac dysfunction and some which show no clinical utility. An Italian group led by cardiologist Danielle Cardinale have carried out the greatest body of work about troponins in this setting and their work led to proposals about monitoring troponin in clinical practice [7]. One of their first studies in breast cancer patients receiving high dose chemotherapy showed that elevation of trop I following chemotherapy predicted the development of LV failure within 1 year and

their seminal study demonstrated that persistent elevation of trop I one month after therapy indicated a high risk of subsequent cardiac events [70]. Patients with no observed rise in Trop I showed no significant LVEF decline and only 1% had a significant cardiac event suggesting that trop I has a high negative predictive value and could be used to exclude low risk patient from subsequent monitoring [71]. A study of patients with haematological malignancies receiving anthracycline chemotherapy showed a greater decline in ejection fraction in those with raised Trop T during therapy, however only 28 patients were assessable at the time of follow up making the numbers very small [72]. A study in children with acute lymphoblastic leukaemia assigned to receive standard anthracycline chemotherapy with or without dexrazoxane (a potential cardio-protective agent) used trop T as a surrogate marker of cardiotoxicity. Results suggested that elevated trop T in the first 90 days post chemotherapy was associated with reduced left ventricular mass and left ventricular end-diastolic posterior wall thickness 4 years post therapy [70].

Table 4 summarises eight clinical studies exploring troponins in chemotherapy-related cardiotoxicity. Studies were heterogeneous in their sampling protocols, patient populations and treatment regimens therefore the best approach for biomarker sampling remains unclear. The majority of patients with elevated troponin levels across studies remained asymptomatic with no overt cardiac failure but correlations were seen with subclinical imaging parameters. There are however, many studies that showed no correlation between circulating troponins and cardiac dysfunction. The majority of these were small studies with fewer than 40 patients but a larger study in 95 breast cancer patients receiving anthracyclines followed by trastuzumab showed that Trop T did not predict for subsequent LV dysfunction despite 50% of the cohort having elevated levels during treatment. [73].

More recently, advances in assay development have raised questions about whether the new high sensitivity troponin assays may be more informative than the traditional assays used in these studies. Several recent studies have used high sensitivity assays to evaluate troponin changes in breast cancer patients receiving trastuzumab (+/- prior anthracyclines). Results appear to be very similar with elevations in troponin correlating with LVEF decline but no improvement in the predictive power of troponin [74]. One group retrospectively re-tested their samples using a high sensitivity troponin I assay and showed high concordance and no improvement in the prediction of cardiotoxicity [75].

Author	No. of pts	Cancer Diagnosis Chemotherapy type	Methods	Biomarkers (ELISA)	Outcome
Auner *et al* [72]	n=78	Haematological malignancies Various regimens (all anthracycline based)	Prospective longitudinal study **Cardiac assessment:** Echo	Trop T	Patients with raised Troponin T had a greater decline in LV function.
Cardinale *et al* [71]	n=703	Breast cancer Various regimens (not all anthracycline based)	Prospective longitudinal study **Cardiac assessment:** Echo	Trop I	Trop I was found to have a high negative predictive value. Persistent elevation 1 month post treatment carried a worse prognosis in terms of LV dysfunction and cardiac events.
Cardinale *et al* [76]	n=211	Breast cancer Various regimens (not all anthracycline based)	Prospective longitudinal study **Cardiac assessment:** Echo	Trop I	A higher number of cardiac events were seen in patients with elevated Troponin I during and one month after chemotherapy. Persistent elevation of troponin I can be used to risk stratify patients at risk of cardiac events.
Cardinale *et al* [48]	n=204	All malignancies Various regimens (not all anthracycline based)	Prospective longitudinal study **Cardiac assessment:** Echo	Trop I, CK, CKMB	Troponin I was the only marker with prognostic sensitivity.
Kilickap *et al* [77]	n=41	Haematological malignancies Various regimens (all anthracycline based)	Prospective longitudinal study **Cardiac assessment:** Echo	Trop T	Increased serum Trop T level can be detected in the early stages of anthracycline therapy and is associated with diastolic dysfunction of the left ventricle.
Lipshultz *et al* [78]	n=154	Acute lymphoblastic leukaemia Doxorubicin	Randomised controlled trial of doxorubicin +/- dexrazoxane Prospective longitudinal biomarker study **Cardiac assessment:** Echo	Trop T, NTpro BNP, CRP	Elevated troponin T in the first 90 days post chemotherapy was associated with reduced left ventricular mass and left ventricular end-diastolic posterior wall thickness 4 years post therapy. Raised NT pro BNP was associated with evidence of left

					ventricular remodelling at 4 years. CRP was not informative.
Sandri *et al* [79]	n=179	All malignancies Various regimens (not all anthracycline based)	Prospective longitudinal study **Cardiac assessment:** Echo	Trop I	Elevated Troponin I was observed in 32% with a mean fall in LVEF of 18%. Trop –ve pts had change in LVEF of 2.5%.
Sawaya *et al* [80]	n=43	Breast cancer Various regimens(all anthracycline based)	Prospective longitudinal study **Cardiac assessment:** Echo	Trop I, NTproBNP	Trop I and longitudinal strain on echo were independent predictors of development of cardiotoxicity. NT pro BNP was not informative.

Table 4. Troponins as circulating biomarkers of chemotherapy-induced cardiotoxicity. Studies involving n > 40 patients.

Troponins have already been adopted in pre-clinical and clinical drug safety testing as surrogate markers for cardiovascular drug toxicity. They have similar characteristics between species making them good translational biomarkers [81]. Pre-clinical in vivo studies have shown that circulating troponins can be detected in drug induced cardiotoxicity animal models [82, 83]. High troponin T levels have been shown to correlate with dose dependent cardiotoxicity demonstrated by histological analysis following necropsy [84]. Taken together the pre-clinical and clinical evidence suggest that troponins are useful biomarkers of cardiotoxicity. They have the potential to be predictors of subsequent cardiac dysfunction but how to implement their use remains unclear. They have not as yet been adopted in routine clinical practice and, although they are measured in some areas of drug development, more research into their precise role is needed.

1.4.2.2 Natriuretic Peptides

N-terminal pro brain natriuretic peptide (NTproBNP) and brain natriuretic peptide (BNP) are established diagnostic and prognostic markers of heart failure. Their specific use as biomarkers of anthracycline-induced cardiotoxicity remains unclear [85]. They are neurohormones produced in response to stretch in the myocardium and act as a signal to

cause diuresis, natriuresis, vasodilation and suppression of the rennin-angiotensin-aldosterone system. Circulating levels of natriuretic peptides have been shown to be proportional to the degree of cardiac failure [86] and prognostic in terms of response to heart failure therapy [87]. They are now used in the diagnosis of heart failure alongside assessment of ejection fraction and clinical symptoms [88]. NTproBNP is the amino terminal fragment of brain natriuretic protein which is raised in the presence of on-going LV dysfunction [89]. Natriuretic peptides are the most widely studied blood borne biomarkers in chemotherapy-induced cardiomyopathy. Studies are heterogeneous in terms of patient population, study design, chemotherapy regimen and sampling protocol. The data suggest that natriuretic peptides are raised in established LV dysfunction but are not necessarily predictive of its development. Much of the work on natriuretic peptides has been carried out in paediatric centres. A small cross-sectional clinical study of 63 children who received anthracycline-based regimens for paediatric cancers revealed that 41% had cardiac dysfunction as demonstrated by echocardiography at 5 years. Simultaneous BNP sampling revealed significantly elevated levels in those with cardiac dysfunction and higher levels in those with multiple abnormal echo parameters but BNP was not measured during chemotherapy receipt so did not assess the predictive ability of BNP [90]. A study of 107 adults receiving epirubicin or doxorubicin for various malignancies involved longitudinal natriuretic peptide sampling with cardiac imaging assessment. The aim was to evaluate whether these circulating biomarkers could replace cardiac assessment for the monitoring of post-anthracycline cardiotoxicity. A strong correlation was seen between ANP, BNP and reduced LVEF but neither biomarker predicted for change in cardiac function and results suggest that neither biomarker can be used for patient monitoring in clinical practice [91]. Similarly, in a small study of 28 patients with non-Hodgkin lymphoma, ANP, BNP and NTProANP were measured but only became elevated when cardiac dysfunction was already demonstrable on echocardiogram [92]. One of the largest studies exploring the neuropeptides as biomarkers of chemotherapy-induced cardiotoxicity was a cross-sectional study of 122 childhood cancer survivors. All participants received anthracycline therapy over 5 years prior to the study and were asymptomatic. Interestingly none had elevated troponin T levels but 13% of patients had elevated NTpro-BNP. The level of elevation was related to the cumulative anthracycline dose but there was no correlation with LV dysfunction on echo. In fact, only 2 of the 9 patients with a reduced LVEF had elevated neuropeptides leaving interpretation of the clinical utility of these biomarkers unclear [93]. More recently however, NTproBNP was explored by prospective measurement of NTproBNP 24 hours after each cycle of

chemotherapy in 71 breast cancer patients. Results suggested NTproBNP was predictive of subsequent LV dysfunction on echo if it is persistently raised [94]. Similarly a larger study of 70 breast cancer patients receiving anthracyclines or trastuzumab demonstrated that elevated BNP correlated positively with anthracycline dose and negatively with ejection fraction [95]. Together, the outcomes of these studies are conflicting. Some suggest that the natriuretic peptides are capable of reporting the presence of cardiac dysfunction once it has developed but cannot be used as predictors whereas others support their use as predictive biomarkers of chemotherapy-induced damage.

1.4.2.3 Biomarkers of Acute Myocyte Damage

Fatty acid binding proteins (FABPs) are a family of cytoplasmic lipid binding proteins. Heart Type fatty acid binding protein (hFABP) is one of the most sensitive markers of ischaemic cardiac damage and is thought to be more sensitive but less specific than the troponins [96]. It can be detected in the circulation rapidly after a cardiac event with reported diagnostic sensitivity of 84% within 6 hours making it the earliest marker of ischaemia [97]. hFABP has been studied in chemotherapy-related cardiotoxicity but not extensively. hFABP and BNP levels were measured in 40 patients receiving doxorubicin chemotherapy for non-Hodgkin lymphoma and LV dysfunction was assessed on echo. High levels of hFABP following the first cycle showed a significant correlation with reduction in LVEF at the end of treatment suggesting that hFABP has the potential to be a good predictive biomarker of subsequent doxorubicin induced cardiac dysfunction. Due to its rapid release, hFABP could be a clinically useful biomarker to guide alternative oncological treatments or instigation of cardio-protective intervention at an early stage [29]. However, Horacek *et al* carried out several small circulating biomarker studies on patients with haematological malignancies, 3 of which looked at hFABP and their findings were less promising showing no change in hFABP during or after anthracycline therapy [98].

1.4.2.4 Biomarkers of Inflammation

Events preceding overt cardiotoxicity are likely to involve an inflammatory process. Cytokine mediated inflammatory markers have been shown to predict development of heart failure in large population studies [99-101]. High levels of pro-inflammatory cytokines such as TNFa have been detected in patients with established heart failure and are associated with a worse outcome [102, 103]. High sensitivity CRP and MPO are both predictors of mortality following myocardial infarction (MI) [104-106] and can be used to risk stratify patients

presenting with acute MI [107]. CRP has been explored as a potential cardiotoxicity biomarker during chemotherapy in several studies. One showed an increased level following therapy but no correlation with subsequent LV dysfunction [73] and another showed no change in levels pre or post treatment [78]. IL8 is involved in the recruitment of neutrophils in damaged tissue and has been shown to increase during myocardial infarction although it's precise role and use as a predictive biomarker is unclear [108]. Recent pre-clinical studies have highlighted the role of inflammatory cytokine IL1b in anthracycline toxicity and identified the IL1b receptor as a potential target for cardio-protective drug therapy. It was already known to play a role in the pathogenesis of other forms of heart disease [109] and Zhu *et al* demonstrated that serum levels of IL1b and IL1Ra were significantly higher in their doxorubicin-treated mouse model compared to controls [110]. The potential issue of using inflammatory markers to report cardiotoxicity in a cancer population is the lack of specificity. This could present a problem in patients with cancer due to the inflammation involved in tumorigenesis and infection which is common during cytotoxic treatment. Several studies in breast cancer patients receiving taxane-based chemotherapy demonstrated elevation in IL-6 and TNFα following therapy but this was thought to be due to systemic rather than cardio-specific inflammation [111].

1.4.2.5 Biomarkers of Fibrosis and Cardiac Remodelling

Matrix metalloproteinases (MMPs) are a family of enzymes responsible for matrix remodelling. They are regulated by a group of proteins called tissue inhibitor matrix metalloproteinases (TIMPs) and are collectively responsible for the turnover of the extracellular matrix [112]. Changes in ventricular geometry and myocardial architecture result from increased activity of MMPs with decreased activity of TIMPs when myocardial injury occurs. This results in abnormal collagen turnover and disruption of myocyte interaction [113]. More recently they have been found to be involved in regulation of sarcomeric and cytoskeletal proteins within cardiac myocytes themselves [114]. Several studies in congestive cardiac failure patients and in experimental animal models have shown changes in myocardial expression of MMPs and TIMPs [115]. One animal study inducing cardiomyopathy in a pig model by injection of intra-cardiac doxorubicin demonstrated strong transcription activation of MMP1, MMP2 and MMP9 and weaker activation of TIMP1. Histological assessment supported the development of fibrosis, however circulating levels were not assessed [116]. If circulating levels are proportionally detectable in the circulation, these enzymes could be novel biomarkers in doxorubicin induced cardiotoxicity which may

also involve diffuse remodelling and fibrosis. Circulating levels of MMP2 and MMP9 have been shown to rise in several other cardiac conditions including ST elevation MI, hypertensive heart disease, dilated cardiomyopathy and congestive cardiac failure [117, 118]. Yamazaki showed that levels of serum MMP2 were significantly higher in patients with chronic cardiac failure than in healthy controls [119]. They also demonstrated that levels positively correlated with severity of heart failure. A study of patients admitted with acute heart failure demonstrated that prognosis was significantly better in patients who showed a rapid reduction in circulating levels of MMP2 following initiation of treatment than those with persistently elevated levels [120]. Pregnancy associated plasma protein A (PAPPA) is also a matrix metalloproteinase involved in cell proliferation and metabolism through interaction with insulin-like-growth factor 1. High levels are associated with worse outcome in patients with acute coronary syndromes and sepsis related cardiac dysfunction [121, 122] but it has not been investigated as a marker of chemotherapy-induced cardiotoxicity.

1.5 Cardiac Imaging in Anthracycline Toxicity

Due to their widespread availability, the most frequent imaging modalities in clinical practice and research into chemotherapy-induced cardiotoxicity are echocardiography and radionucleotide scanning. A relatively large number of cross sectional studies monitoring cardiac function in cancer survivors have been performed but few have carried out imaging before, during and after treatment. Most studies measure basic functional parameters such as ejection fraction, fractional shortening, E/A ratio and left ventricular mass to report cardiac damage. As imaging techniques evolve, cardiac magnetic resonance imaging (CMR) is becoming the clinical gold standard for assessing a wide range of cardiac parameters. It has high spatial resolution, good temporal resolution and is highly reproducible. It is non-invasive, does not use radiation and is able to produce high quality images which provide detailed information above and beyond basic functional measurements. CMR is one of the only clinically available imaging modalities able to perform myocardial tissue characterisation and being able to image the myocardial tissue detail may enable early damage to be picked up prior to functional decline. CMR is able to assess regional myocardial motility which can be informative in early development of cardiomyopathy. Phase-contrast velocity mapping can be used to assess blood flow in valvular or vascular abnormalities. CMR is also increasingly used for assessment of ischaemic heart disease as 3D whole heart imaging can non-invasively assess coronary artery patency [123]. For these reasons it has become the imaging mode of choice in cardiovascular research [124].

Myocarditis-like syndromes have been seen with anthracyclines and CMR has become the clinical gold standard for assessing oedema and inflammation of the myocardium [8, 16, 125]. The use of late gadolinium enhancement techniques has also facilitated the assessment of myocardial viability. Damaged tissue undergoes replacement fibrosis and becomes hyper-enhanced as gadolinium accumulates secondary to increased extracellular distribution volume. This delays washout leading to increased signal intensity on T1 weighed sequences. Using this technique combined with assessment of regional wall motion it is possible determine whether tissue remains viable [124]. Late-gadolinium-enhancement techniques can assess localised and diffuse replacement fibrosis which can occur in cardiomyopathy. It is possible that this process could also be seen in chemotherapy-induced cardiotoxicity. Myocardial fibrosis is a common histological feature of end stage cardiac failure [126] and the mechanisms leading to fibrosis are likely to involve a common end pathway regardless of the initial insult.

1.5.1 Principles of MRI

Magnetic resonance scanning uses magnetisation of protons and radiofrequency waves to create images. When a person is placed within a strong magnetic field the protons within water molecules in their body align with the magnetic field. When energy is given to the protons, in the form a radiofrequency wave, the protons alter their spin and 'flip' 180 degrees to a higher energy state perpendicular to the magnetic field. When the energy is removed, the protons return to their natural lower energy state in parallel with the magnetic field and this is called 'relaxation'. The electromagnetic energy released when the protons 'relax' can be measured by a transceiver and used to create an image. Different tissues generate different signal intensities depending on their water composition. Some tissue will have longer relaxation times than others and this difference can be used to create an image. Varying the strength of the magnetic field alters the amount of energy needed for the protons to resonate and absorb energy to 'flip'. Varying the timing of the radiofrequency (RF) pulses allows differences in relaxation time to be exploited and these two principles can be used together to create contrast between different tissues. Applying 'gradients' to the field by passing electrical current through a coil within the scanner alters the magnetic field in different areas in the body and allows localisation of the energy that is released so an accurate image can be obtained. Protons are subject to two different types of force within a magnetic field. They have a longitudinal force (T1), when their overall charge is in parallel with the magnetic field, and a transverse force (T2), a rotational force resulting from the constant precession of

protons in the centre of the field. The expected decay of T1 (longitudinal relaxation) and T2 (transverse relaxation) have characteristically different appearances as shown by the graphs below (**Figure 9**). The decay constant (T1 or T2 value) is representative of the time in milliseconds for a tissue to recover it magnetisation (reach equilibrium) following inversion by a RF pulse. Differences in these values can be used to show contrast between tissues and build up an image. The T1 relaxation time depends on the interaction between the natural frequency of the molecules and the larmor frequency. The Larmor frequency (ω) is a measurement of the precessional frequency in megahertz of a nucleus around a magnetic field and is made up of the rate of precession in a field strength of 1 Telsa (γ) multiplied by the actual strength of the external magnetic field applied (β) i.e. $\omega = \gamma\beta$. Molecules that have frequencies markedly different from the Larmor frequency take longer to relax. Tissues that have a similar frequency to the Larmor frequency release energy quickly and have a shorter T1. Small molecules like water and large proteins have significantly different frequencies from the Larmor frequency and hence have a long T1 appearing dark on scan. Medium size molecules such as those in fat have frequencies similar to the larmor frequency and appear bright on scan. Conversely fat appears dark on T2 images and water appears bright as they have different transverse magnetisation and different relaxation times. T2 sequences are able to pick up inflammation and oedema within tissues due to their high water content whereas T1 images are better for imaging structures such as muscle or lipid rich areas

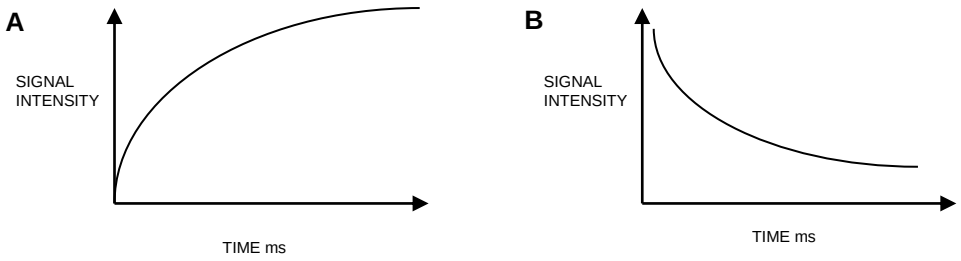

Figure 9. T1 (longitudinal) decay (A). T2 (transverse) decay (B).

1.5.2 MRI in Chemotherapy-related Cardiotoxicity

As yet there have been very few clinical studies exploring cardiac MRI in patients receiving anthracyclines. Several case studies have been reported showing intra-myocardial late gadolinium enhancement on MRI after anthracyclines which correlated with histological changes in one case [127, 128]. A small longitudinal study was carried out by Wassmuth *et al*

in 2001. Cardiac MRI was performed before, on day 3 and day 28 after commencement of anthracycline chemotherapy in 22 patients with differing cancers, predominantly breast cancer and lymphoma. Interestingly they found that an increase in contrast enhancement on day 3 predicted for a subsequent fall in ejection fraction within 1 month and could be an early predictor of cardiotoxicity [129]. A further small study of 28 patients who were receiving anthracycline chemotherapy demonstrated oedema on cardiac MRI directly following chemotherapy and reduced right and left ventricular ejection fraction during treatment but gadolinium enhancement was not performed [130]. A small study of 10 patients with non-Hodgkin lymphoma receiving standard doxorubicin based chemotherapy demonstrated a concerning level of potential cardiotoxicity 3 months after completion of chemotherapy. 50% of patients had a fall in EF of >10% and 70% had some structural or functional abnormality measurable by CMR [131]. This could due to small numbers or it may suggest that CMR is more sensitive and may detect changes in LVEF earlier than other methods.

1.5.3 Measuring Diastolic Function with Imaging

Diastolic dysfunction is extremely hard to assess accurately and cannot be easily estimated by one method alone. Measuring flow through the mitral value during early and late filling to obtain the E/A ratio is the most well-known way of assessing diastolic function. The E wave represents 70-75% of the filling resulting from ventricular relaxation and the A wave results from atrial contraction and accounts for the remaining 20-25%. In the presence of normal function the ratio of E:A is between 1 and 2 (E>A). Three different patterns of diastolic dysfunction can occur: 1) E<A, where there is reversal of ratio due to impaired ventricular relaxation, 2) pseudonormalisation, when both values are reduced proportionally and 3) E:A>2, indicative of restrictive filling. The mitral annular tissue velocity, pulmonary pressures and left atrial volumes can also be used to look at diastolic function and a combination of several parameters is often used to diagnose diastolic dysfunction [132]. New methods of detecting more subtle changes in diastolic function are evolving such as dyssynchrony. This is a measure of ventricular relaxation and how quickly and efficiently the myocardium untwists. The most widely explored measures of dyssynchrony are strain and strain rate. Strain is a measure of deformation (the change from original shape i.e. change in length) and strain rate is the speed of deformation. Due to the arrangement of myocardial fibres within the heart, ventricular relaxation should occur rapidly and synchronously to enable efficient suctioning of blood into the chamber. If damage occurs, this process of unwinding can become inefficient leading to inadequate ventricular filling and diastolic

dysfunction. It is possible to track myocardial movement throughout a cardiac cycle using cardiac MRI (tagging or contouring) and speckled tracking echo to measure strain and strain rate. Estimations of longitudinal, circumferential and radial strain can be obtained and may give earlier information about myocardial damage during the development of cardiomyopathy. Deformation and dyssynchrony have not been widely explored in the development of chemotherapy-induced cardiotoxicity. Three recent papers suggest that strain and strain rate worsen following anthracycline and/or trastuzumab treatment but they have limited follow up and are unable to correlate changes in deformation with LVEF decline or the development of cardiac events [133, 134]. However, one study suggested that changes in longitudinal strain during chemotherapy are predictive of subsequent cardiotoxicity within a year of therapy [135]. Further research into the clinical utility of dyssynchrony in this setting are needed.

1.5.4 Tissue Characterisation using MRI

T1 mapping is a technique which can detect the presence of diffuse fibrosis in the myocardium by direct myocardial signal quantification on a standardised scale enabling inter-study comparison [136]. Normal T1 values for myocardial tissue are still being determined but it is thought that longer T1 values correlate with the presence of fibrosis. Quantification of signal from tissues could enable the detection of subtle changes in the composition before they are discernible with the naked eye. It is still being developed in the research setting but the aim is to be able to quantify the longitudinal relaxation of a specific tissue regionally, globally and on a voxel by voxel scale. This technique has been explored in patients with end stage heart failure awaiting transplant. Segmental estimation of extracellular volume (ECV) was calculated from the T1 maps and correlated with histopathological findings. Areas of expanded ECV identified with imaging showed a strong correlation with areas of fibrosis at histological assessment suggesting that CMR can be used to characterise changes in myocardial tissue [137]. T1 mapping could be a useful tool to look for subclinical diffuse fibrosis that may occur with drug induced cardiotoxicity by detecting change in the T1 value of the myocardium during or after treatment. Similarly T2 mapping could enable quantification of myocardial inflammation or oedema even if it is not visible and one hypothesis is that a subclinical drug induced myocarditis may occur acutely during or shortly after therapy followed by myocyte death and eventually diffuse fibrosis. This project hopes to explore whether quantifiable tissue changes are seen during the development of cardiotoxicity using serial T2 and T1 mapping sequences before, during and after

anthracycline therapy, and determine if these changes are reflected in blood borne biomarkers. These techniques had not been explored in anthracycline cardiotoxicity prior to this project but 3 recent studies have been published. Two of the studies explored T1 mapping in cancer survivors several years after receipt of anthracycline therapy and their results suggest that fibrosis is occurring and is detectable [138, 139]. Only one study has looked at this technique prospectively before and after chemotherapy and found that T1 signal intensity increased but T1 mapping values did not change within 3 months of anthracycline therapy. Clearly these studies were small and statistical significance was not reached highlighting the need for larger clinical trials of this nature.

1.6 Predicting Cardiotoxicity in Drug Development

Cardiotoxicity from cancer treatment is difficult to predict during early drug development, particularly the chronic subclinical toxicity seen with some agents. The cardiotoxic potential of drugs like trastuzumab and sunitinib was underestimated during drug development and even in the early phase clinical trials. The impact of their toxicity was only realised once the drugs reached real life patient populations when some centres reported that 50% of their patients had cardiovascular events with sunitinib [7]. It is possible to predict certain acute cardiac effects using *in-silico*, *in-vitro* and *in-vivo* models and promising agents undergo rigorous safety testing before entering clinical trials. However, current models struggle to detect more insidious chronic damage that may translate into clinical events in humans. Many toxicity models use large single bolus doses to induce severe acute cardiac failure [140-142]. These studies are helpful but cannot inform about the chronology of events leading to cardiotoxicity or aid exploration of potential early cardiotoxicity biomarkers. Therefore clinically relevant models of drug-induced cardiotoxicity are needed to learn about the sequence of events leading to cardiac failure and aid discovery of new biomarkers.

1.7 Hypotheses

To successfully develop biomarkers of chemotherapy-induced cardiotoxicity it is important to explore a panel of biomarkers that reflect the pathological processes occurring when the heart undergoes drug induced damage i.e. inflammation, myocyte damage, myocyte death, cytoskeletal damage, strain and fibrosis. As outlined above there are already multiple biomarkers, both diagnostic and exploratory that have been investigated in other cardiac diseases, therefore exploring their role in chemotherapy-related cardiotoxicity is a logical first step. Using cardiac MRI to report cardiac damage will enable subtle subclinical damage to be

detected at an early stage for correlation with the circulating biomarkers. Furthermore, exploring multiple imaging and circulating biomarkers simultaneously may provide greater information to advance biomarker development.

Hypothesis 1: Circulating biomarkers may have the potential to report sub-clinical cardiac damage prior to the development of overt cardiac dysfunction in anthracycline-induced cardiotoxicity

Hypothesis 2: Pathological processes including inflammation, fibrosis and dyssynchrony may contribute to the development of anthracycline-induced cardiotoxicity therefore quantitative assessment of myocardial oedema, extracellular volume and strain using novel imaging techniques may detect damage prior to the development of overt cardiac dysfunction

1.8 Aims and Objectives

Overall project aim: To evaluate a panel of potential circulating proteins alongside novel cardiac imaging techniques in anthracycline-induced chemotherapy in the pre-clinical and clinical setting with the aim of identifying potential biomarkers to aid detection of cardiac damage at an early potentially reversible stage

Overall project objectives:

- To develop a pre-clinical rat model of anthracycline-induced induced cardiotoxicity that is clinically relevant and can be used to characterise the chronology of events leading to cardiotoxicity and aid discovery of potential circulating biomarkers
- To design and carry out a clinical study to evaluate a panel of potential circulating cardiotoxicity biomarkers and novel cardiac imaging techniques in cancer patients receiving anthracycline-base therapy
- To evaluate the translational potential of promising biomarkers identified

2 Pre-clinical Cardiotoxicity Model

(adapted from Cove-Smith L & Woodhouse N et al. 'An Integrated Characterisation of Serological, Pathological, and Functional Events in Doxorubicin-Induced Cardiotoxicity.' Toxicol Sci. 2014 Jul;140(1):3-15)

2.1 Introduction

Anthracyclines have been in widespread use and greatly studied since the 1960s however certain gaps still exist in the understanding of anthracycline-induced cardiotoxicity, particularly a detailed definition of the steps leading to severe impairment of cardiac function [143]. As previously discussed, advances in cardiac imaging have started to reveal early subclinical damage, such as diastolic dysfunction, in patients receiving chemotherapy [133, 144]. Furthermore, cardiac magnetic resonance imaging (CMR) enables objective characterisation of myocardial tissue that allows subtle cardiac damage and pathologies to be detected and this could be applied to detect anthracycline-induced cardiotoxicity [145]. Myocardial degeneration is known to occur during anthracycline-induced cardiotoxicity and this cell death is associated with release of cardiac proteins into the circulation. However, it is unclear 1) exactly which proteins are detectable 2) when they are released with respect to development of pathological damage and 3) when myocardial degeneration occurs in relation to cardiac contractile impairment and 4) if these events are linked. Ultimately, such information could enable the earlier detection of chemotherapy-induced subclinical cardiomyopathy in the clinic and support pre-clinical strategies in the safety assessment of novel drug candidates. In light of this, a pre-clinical rat model was developed with which to undertake an integrated characterisation of the serological, pathological and functional events associated with the development of chronic anthracycline-induced cardiotoxicity and help identify potential biomarkers for translation into humans. In order to achieve this, the initial aim was to identify a dosing regimen that resulted in a chronic, rather than acute, cardiomyopathy, consistent with clinical presentation [146]. The mechanisms leading to anthracycline-induced cardiotoxicity appear to be similar in rats and humans, and therefore the rat is an appropriate model species for obtaining translationally-relevant data regarding the development and progression of anthracycline-induced cardiotoxicity [47, 147]. Doxorubicin was used as the classic and most widely used anthracycline. Previously, large single bolus doses of doxorubicin, or multiple doses over 1-2 weeks, have been administered

to rodents to evoke *acute* cardiotoxicity [140, 148, 149]. The aim of this work was to establish a more progressive cardiomyopathy, through weekly dosing over a 2 month period followed by a 1 month follow-up, in order to provide the optimal opportunity to gain insight into the chronology and inter-relationships between the changes (functional, serological and pathological) associated with cardiotoxicity development in a clinically relevant animal model. A panel of circulating biomarkers were chosen from a comprehensive literature search and/or their established use in other cardiac conditions such as ischaemia. Troponin I, Troponin T, MMP9, MMP2 IL8, IL1b, TNFa and hFABP were measured at baseline and over time in treated and control rats. Cardiac MRI was chosen to detect cardiac damage using a comprehensive array of standard parameters including volumetric analysis, systolic function, diastolic function and contrast (gadolinium) enhancement.

Aims:

- To develop a clinically relevant model of chronic anthracycline-induced cardiotoxicity
- To characterise the behaviour of functional parameters and tissue signal intensity during the development of chronic anthracycline-induced cardiotoxicity
- To characterise the behaviour of circulating biomarkers during the development of chronic anthracycline-induced cardiotoxicity
- To explore the histopathological events occurring during the development of chronic anthracycline toxicity in relation to the imaging and circulating biomarker changes

Objectives:

- To develop a rat model of cardiotoxicity using fractionated dosing of doxorubicin and perform longitudinal circulating biomarker analysis and cardiac MRI to correlate with histological findings

2.2 Methods

2.2.1 Study Outline

All studies utilised 10 week old male Hannover Wistar rats housed two animals per cage. The animals were randomly allocated to control and treatment groups. Animal identification, conditions of housing, acclimatisation, environment, diet and water were in accordance with the standard AstraZeneca operating procedures. Clinical observations and food consumption were monitored daily and body weights were monitored bi-weekly. Treated rats (n=6 for pilot study and n=8 for longitudinal imaging study) were administered with a single intravenous bolus dose of doxorubicin 1.25 mg/kg (equivalent to approximately 50mg/m^2 in humans) or vehicle alone (0.9% sterile sodium chloride) via tail vein once per week for 8 weeks followed by an off-dose 'recovery' period of 4 weeks. For the pilot study, imaging was performed at week 12 under terminal anaesthesia (inhaled isofluorane) prior to necropsy. For the longitudinal imaging study, CMR was performed under anaesthesia (prior to doxorubicin dosing) on days 1 (baseline), 15, 29, 43, 57 and under terminal anaesthesia on day 78. Blood samples for biomarker analysis were taken at baseline and prior to each dose. Where imaging and dosing days corresponded, contrast was given through the same cannula. A satellite pathology study was performed using treated rats (n=6 per group) and control rats (n=3 per group) culled at each scanning time point for histological analysis of the heart. The animals were treated, sampled and terminated by taking one animal from each treatment group sequentially, and then repeating this until all the animals were processed.

2.2.2 CMR Imaging

All imaging experiments were carried out at AstraZeneca, Alderley Park led by Neil Woodhouse using a 4.7T Bruker system with Avance III electronics (Bruker BioSpin GmbH, Germany) and contrast enhanced sequences were performed using Gadolinium diethyltriaminepentaacetic acid contrast agent. Intragate short axis and long axis views were initially obtained to ensure correct positioning in the heart. Ventricular volumes were obtained using a retrospectively gated short axis stack of the left ventricle from the apex to the atrio-ventricular ring with 1mm contiguous slices. Image analysis was performed using Segment® (Medviso, Sweden) software [150]. Parameters assessed were left ventricular ejection fraction (LVEF), stroke volume (SV), cardiac output (CO) and LV mass. A single slice ECG triggered velocity encoded phase contrast image in the short axis plane at the level of the mitral valve was performed to measure the early (E) to late (A) ventricular filling

velocities for diastolic assessment. ECG and respiratory gated T1 weighted short axis images through the whole left ventricle were taken pre-contrast and retrospectively gated dynamic contrast enhanced images were taken during injection of gadolinium contrast to measure peak enhancement. Delayed myocardial enhancement was measured 15 minutes after the contrast agent bolus. Contrast was administered via an indwelling tail vein cannula as a bolus dosed at 0.3 mM/kg.

2.2.3 Serological Biomarker Analysis

Blood was collected into lithium heparin tubes at the time of tail vein cannuation if possible and plasma prepared by centrifugation at 3000rpm for 10 minutes at 4^{o}C. Plasma was stored at -80^{o}C until analysis.

2.2.3.1 Troponin I

Cardiac troponin I was assessed using a human ultrasensitive troponin I assay kit (Siemens, Camberley, UK) validated for use in the rat on the Advia Centaur CP automated analyser (Siemens). Analysis was conducted as per manufacturer's guidelines at AstraZeneca Alderley park.

2.2.3.2 Troponin T, MMP9, MMP2, IL8, IL1b, TNFa and hFABP

Troponin T, MMP9, MMP2, IL8, IL1b, TNFa and hFABP were measured by Multiplex Immunosorbant Assay (ELISA). Analysis took place within the Clinical Experimental Pharmacology department at the Cancer Research UK, Manchester Institute. 96 well Multiplex ELISA plates were custom made by Aushon BioSystems and experiments were performed in line with manufactures guidelines. In brief, 50µl of plasma sample (diluted as per manufacture instructions) was spotted in duplicate onto 96 well plates. Samples were incubated for 1-3 hours (assay dependent) at room temperature on a horizontal orbital micro-plate shaker at 750rpm. Following incubation the plates were washed three times with wash buffer using an automated plate washer. 50µl of biotinylated detection antibody was added to each well and incubated for a further 30 minutes on the plate shaker as above. Following this, the plates were washed as before and 50µl of streptavidin-HRP reagent was added to each well. The plates were incubated for a further 30 minutes under the same conditions. The plates were washed again and 50µl of supersignal substrate was added. Plates were imaged using the SearchLight plus CCD imaging system and data were analysed using the

SearchLight array analyst software. Acceptance criteria was taken as an R^2 of >0.985 for the standard curve and a CV% <30% for plasma samples.

2.2.4 Tissue Processing and Histopathological Assessment

Pathological assessment was performed on rats taken from a satellite pathology group that were treated in exactly the same way as the longitudinal imaging group animals. Rats were sacrificed on days 8, 15, 29, 43, 57 and 78, allowing direct comparison of the cardiac pathology with imaging and plasma biomarkers. The hearts were carefully removed and processed as follows: The tip of the right atrium was taken from all animals, fixed in 2.5% glutaraldehyde and stored for processing and examination by electron microscopy (EM). For histopathological examination, 4μm tissue sections were cut and air dried onto strongly adhesive slides and then deparaffinised in xylene (2 x 3 min) and rehydrated. Tissue sections were stained with haematoxylin and eosin and examined by light microscopy.

2.2.5 Pathological Scoring of Doxorubicin-Induced Cardiac Damage

Pathological scoring of the H&E stained cardiac sections from individual animals was performed according to a grading system developed for the study based on Billingham and Bristow's criteria with refinement to incorporate extracellular damage [62]. Note that, unless stated, the pathological descriptors of each ascending severity grade are additional features to those of the lower grades: Grade 1, multi-focal intracellular vacuolation of cardiomyocytes (minimal disruption of tissue architecture); Grade 2, multi-focal neutrophilic and lymphoplasmacytic inflammation (chronic active myocarditis) and endothelial hypertrophy; Grade 3, multi-focal cardiomyocyte degeneration/apoptosis/necrosis; Grade 4, multi-focal displacement of cardiomyocyte alignment/architecture with replacement macrophage/fibroblast infiltration; Grade 5, diffuse grade 4 with multi-focal cardiomyocyte hypertrophy/cytomegaly; Grade 6, diffuse grade 4 with diffuse cardiomyocyte hypertrophy/cytomegaly; Grade 7, multi-focal inter-cellular vacuolation (oedema) and fibroblast proliferation with collagen deposition (fibrosis); Grade 8, diffuse grade 7; Grade 9, atrial dilatation; Grade 10, intra-atrial thrombosis.

2.2.6 Sirius Red Staining

Fibrosis assessment was performed by staining for collagen using picro sirius red [151, 152]. 4 μm-thick sections were prepared as above and stained with picro-sirius red (0.1%), in saturated aqueous picric acid (Sigma, UK) for 1 hour to allow equilibrium to be reached.

Sections were washed briefly in 2 changes of acidified followed by vigorous shaking to remove the excess water. Finally, sections were dehydrated rapidly in 3 changes of 100% alcohol, cleared in xylene and mounted. Images of the slides were captured using a ScanScope Scanner and analysed using ImageScope software (Aperio Technologies Incorporated, Vista, USA) using the 'Color Deconvolution v9' algorithm to quantify the percentage of strongly staining collagen present in the myocardium. The left ventricle and left atrium were considered as separate regions of interest which were drawn manually.

2.2.7 Electron Microscopy

Approximately 1mm thick slices of heart (left atrium) were fixed in 2.5% glutaraldehyde in 0.1M sodium cacodylate (Agar Scientific, UK). Fixed samples were trimmed and post fixed in 1% osmium tetroxide (Agar Scientific, UK), dehydrated through a series of increasing acetone concentrations and then polymerized with araldite resin (Agar Scientific, UK) for 48 hours at 60ºC. Resin sections (semi-thins) were taken for light microscopy to assess tissue quality and help choose areas for further examination. Ultrathin sections were cut at approximately 100µm thickness and suspended on nickel grids (Agar Scientific, UK). Grids were then stained with saturated uranyl acetate (Sigma, UK) and 1% lead citrate (Leica, Germany) and viewed on a JEOL 1400 Transmission Electron Microscope (JEOL Ltd, Japan) and digital images captured. This work was performed by Simon Brocklehurst and interpreted by Adam Hargreaves.

2.2.8 Statistical Methods

All statistical analyses were performed using Microsoft Excel 2010 and Graphpad Prism version 5.03 (GraphPad Software, San Diego California USA, www.graphpad.com). Inter-group comparisons were made using two tailed paired Student's t-test and 95% confidence intervals calculated. Non-paired t-tests were used for inter-group comparisons. Correlations between biomarkers used in the same animals were made using Pearson correlation coefficient. Statistical significance was taken as $p<0.05$.

2.3 Results

2.3.1 Development of a Rat Model of Chronic Doxorubicin-Induced Cardiomyopathy

To develop a rat model of chronic doxorubicin-induced cardiomyopathy, an initial 12 week pilot study was performed, applying CMR approaches to assess cardiovascular function in Hannover Wistar rats after doxorubicin administration at 1.25 or 2.5 mg/kg/week for 8 weeks followed by a 4 week off-dosing period. Due to intolerance, animals in the 2.5 mg/kg dose group had to be dose-reduced to 1.75 mg/kg during week 4 and the majority of these animals were terminated for welfare reasons between weeks 5 and 8. Adverse signs included respiratory effects (increased depth and decreased rate), cold extremities, decreased activity, pale skin, hunched posture, pilo-erection, tip toe gait, reduced food consumption and unacceptable loss of body weight (up to 19% in total). A dose of 1.25 mg/kg/week was generally well tolerated, with some reduced body weight gains and slightly reduced food consumption (compared to controls), throughout the 12 week study. Of note, 8 weeks of the 1.25 mg/kg dosing regimen equates (mg/kg basis) to approximately the maximum recommended life time doxorubicin exposure in humans [9, 26].

CMR assessment of the 1.25 mg/kg doxorubicin group at 12 weeks demonstrated a statistically significant reduction in LVEF (treated versus control $p = 0.0008$) to a mean value of <50% in the treated group. Having established a doxorubicin-induced cardiomyopathy rat model, the next step was to investigate the functional, structural and pathological events encompassing the development of doxorubicin-induced cardiotoxicity in more detail and to understand the exact chronology of these changes. Serial CMR assessments were therefore performed alongside pathological characterisation and serological biomarker measurements to define the behaviour of these overlapping indices of heart structure and function.

2.3.2 Longitudinal Assessment of Doxorubicin-Induced Cardiac Dysfunction Using CMR

The functional indices derived from the volumetric analysis revealed significant differences between doxorubicin treated rats and control animals over time. Multi-slice cine CMR revealed statistically significant decreases in multiple indices of cardiac function (**Figure 10**). LVEF was significantly lower in doxorubicin-treated animals relative to controls at the first post-doxorubicin assessment (day 15), after only two doses (**Figure 10**). Left ventricular ejection fraction (LVEF) decreased incrementally with each subsequent doxorubicin dose and continued to decline further during the post-dosing ‘rest’ period (day 50 onwards), indicating that the doxorubicin schedule had triggered a continuous and irreversible functional

deterioration. Despite the steady decline in cardiac contractility, the mean rat LVEF remained in what is considered to be the 'clinically normal human range' [153] until day 78 when it dropped to <50% (mean 49.2 %, **Figure 10a**), a level universally considered as left ventricular dysfunction.

The incremental decline observed in both cardiac output (CO) (**Figure 10b**) and stroke volume (SV) (**Figure 10c**) in the doxorubicin-treated rats was consistent with the LVEF profile of these animals. Of note, in the control group, CO increased 13% between baseline and day 57 (P=0.018) in line with growth of the rats, whereas the doxorubicin group did not significantly change weight post the second dose (day 15). There were no significant changes in left ventricular mass (LVM) and end diastolic volume (EDV), suggesting that these parameters did not deteriorate with doxorubicin treatment. Diastolic function was estimated by measuring the E/A ratio. This fell incrementally with time and also showed a statistically significant difference between doxorubicin-treated and control rats from day 15 (p=0.02) onwards. The E/A ratios were 0.85 and 1.14 (doxorubicin-treated versus controls) by the end of study (**Figure 10d**) representing significant diastolic dysfunction in the doxorubicin group [132].

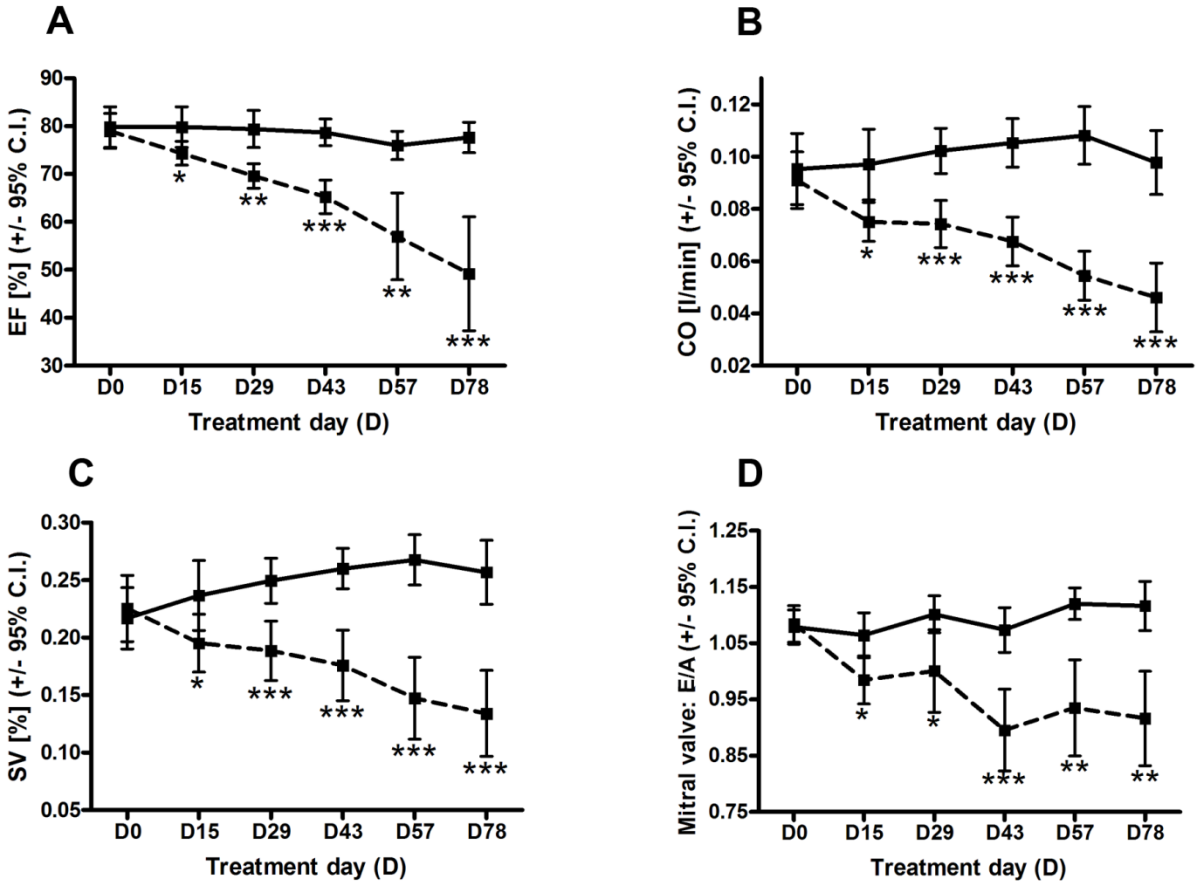

Figure 10. Detection of cardiovascular functional impairment by CMR during the development of chronic doxorubicin-induced cardiomyopathy. *Rats (n=8) were dosed once weekly with doxorubicin (1.25 mg/kg, dashed line) or vehicle (solid line) for 8 weeks followed by a 4 week off-dosing period. Ejection fraction (EF) (A), Cardiac output (B), Stroke volume (C) and E/A ratio (D) were assessed by cardiac MR at baseline and throughout the 12 week study as described in the methods. Error bars represent 95% confidence intervals. Star symbols represent statistical significance (* p=<0.05; **p=<0.01; ***p=<0.001).*

2.3.3 Elevations in Gadolinium Myocardial Enhancement and Serum Troponin I are Biomarkers Of Doxorubicin-induced Cardiac Injury

Gadolinium enhancement is used to assess late-enhancing cardiac damage, such as infarcts, in clinical practice [154]. Dynamic CMR imaging acquired during the infusion of gadolinium demonstrated statistically significant increases in both peak myocardial enhancement (from day 57, **Figure 11a**) and delayed myocardial enhancement (from day 43, **Figure 11b**) in the doxorubicin-treated group. Interestingly, when troponin I levels were assessed in serum

samples taken from the same rats, circulating troponin I levels significantly increased during the non-dosing period (day 50-78, **Figure 11c**). Furthermore, it was clear that the troponin I profile mirrored the myocardial enhancement profiles (**Figure 11a-c**), suggesting that these biomarkers may be reporting a common event, for example the onset of myocardial degeneration. In support of this, statistically significant correlations were found between serum troponin I levels and the degree of peak myocardial enhancement on Day 57 ($r=0.8$ $p=0.0008$) (**Figure 12a**) and troponin I levels on day 57 also correlated with final LVEF ($r=0.8$ $p=<0.0001$) suggesting it may have role in predicting LVEF decline (**Figure 12b**). Little change was seen in peak enhancement in control animals throughout the time course study and troponin I levels remained unchanged (**Figure 11a-c**). No significant change was seen in the other circulating biomarkers (**appendix 1**).

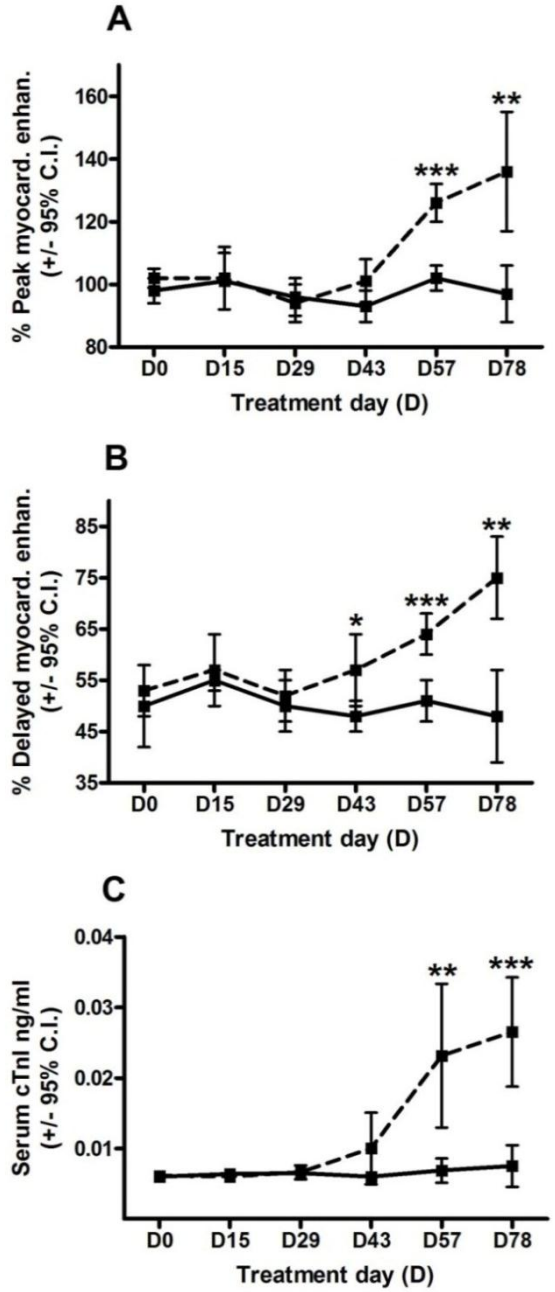

Figure 11. Elevations in serum troponin I and Gadolinium myocardial enhancement are biomarkers of doxorubicin-induced cardiac injury. *Rats (n=8) were dosed once weekly with doxorubicin (1.25 mg/kg, dashed line) or vehicle (solid line) for 8 weeks followed by a 4 week off-dosing period. Peak (A) and delayed (B) Gadolinium myocardial enhancement was assessed by CMR at baseline and throughout the 12 week study as described in the methods. Serum troponin I (C) was assessed using a Siemens human ultrasensitive troponin I assay kit. Error bars represent 95% confidence intervals. Star symbols represent statistical significance (*p=<0.05; **p=<0.01; ***p=<0.001).*

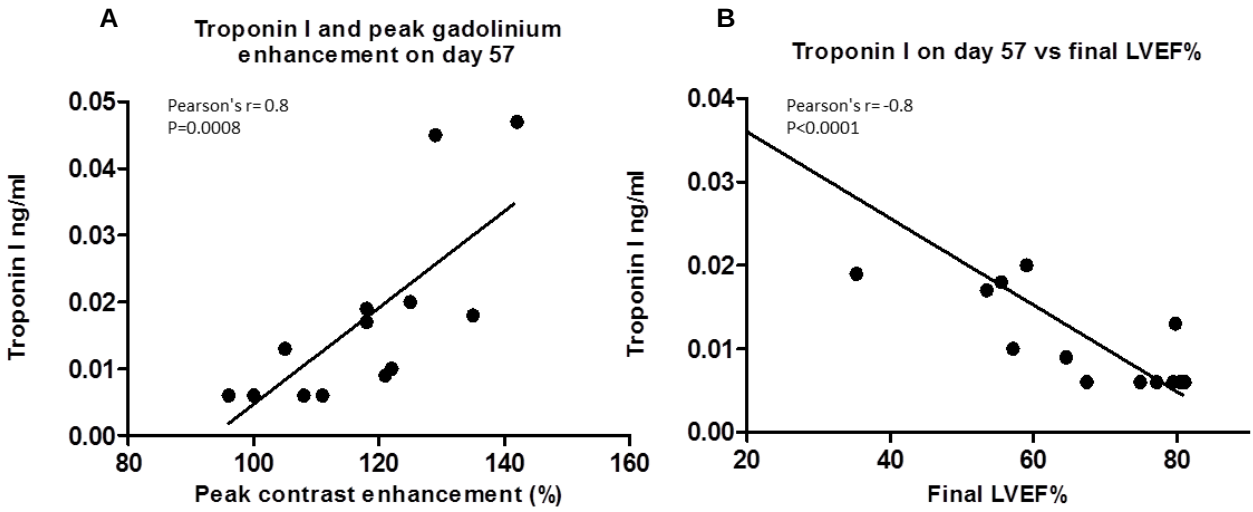

Figure 12. Correlation of circulating Troponin I with peak gadolinium enhancement on day 57 (A) and troponin I on day 57 with final LVEF (B).

2.3.4 Doxorubicin-induced Pathological Effects in the Heart

H&E stained sections of the hearts taken from the rats at necropsy were examined and assessed. Vehicle-treated control animals exhibited heart morphology equivalent to normal rats, with no discernible microscopic damage throughout the 78 day experiment (**Figure 13a, Figure 14a & b**). Doxorubicin treated rats exhibited normal cardiac morphology one week after a single dose (day 8, **Figure 13b**). However, after two doses (day 15), some animals had developed subtle multi-focal intracellular vacuolation of cardiomyocytes (**Figure 13c**) in the atria (3/6 rats) and ventricles (2/6 rats). Of note, these early (grade 1) intra-cellular changes were associated with minimal disruption of the overall tissue architecture (**Figure 13c**). After 4 doxorubicin doses (day 29), (grade 2) multi-focal neutrophilic and lymphoplasmacytic inflammation (chronic active myocarditis) and endothelial hypertrophy was prevalent in the atria and to a lesser extent, the ventricles. By day 43 (after 6 doses), multi-focal cardiomyocyte degeneration (apoptosis and or necrosis) was evident in the atria of rats (grade 3, **Figure 13d**), in some cases extending to displacement of cardiomyocyte alignment with replacement inflammatory cell infiltration (grade 4) and cardiomyocyte cytomegaly (grade 5). While the ventricular pathology was consistently less severe than the atrial observations, the nature of the findings was consistent and progressively worsened over time (**Figure 14a & b**). By day 57 (8 doses), inter-cellular vacuolation (oedema) and fibroblast proliferation with collagen deposition (fibrosis) was observed in the atria (**Figure 13e**). During the off-dosing period (day 50-78) the cardiac damage progressively worsened to ultimately include

atrial dilatation in all animals. Diffuse cardiomyocyte hypertrophy/cytomegaly was observed (**Figure 13e**) along with extensive intra and inter-cellular vacuolation (**Figure 13e & f**). Diffuse disruption of the overall tissue architecture was clearly evident (**Figure 13f**). Regions of haemorrhage were frequently observed (**Figure 13f**) and in some hearts, large intra-atrial thrombi were also present at day 78.

Interestingly, a correlation between the degree of diastolic dysfunction (E/A ratio) in rats at the end of the study (day 78) and both the atrial and ventricular pathology severity scores was seen (r=0.70 p=0.03, r=0.73 p=0.03 respectively), suggesting that these indices may be coupled with respect to the progression of the cardiotoxicity. Correlations between troponin I levels and both atrial and ventricular pathology grade on day 43 (r=0.94 p=0.002, r=0.76 p=0.04 respectively) and between troponin I and ventricular pathology only on day 57 (r=0.80 p=0.03) were also found.

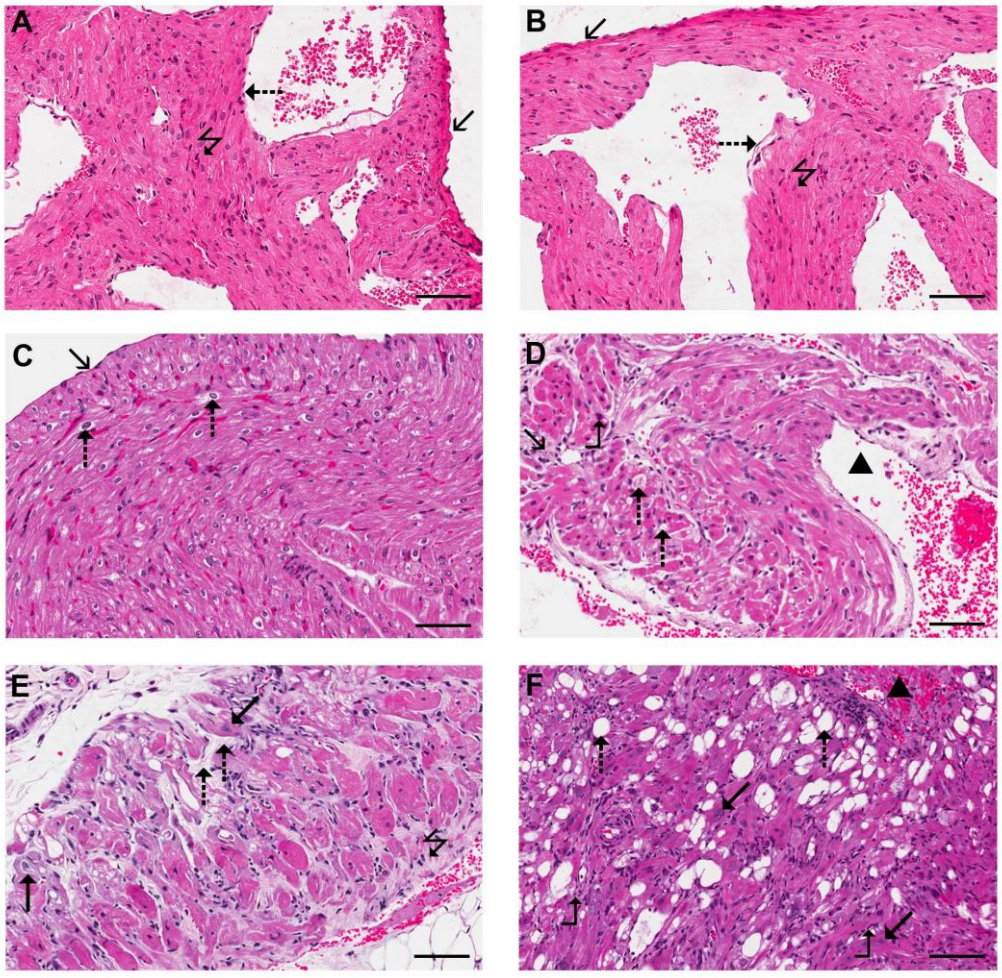

Figure 13. Pathological characterisation and severity scoring of the doxorubicin-induced cardiac injury. *The scale bar on each panel represents 100 µm. A, Control animal*

*(day 78). B, Doxorubicin-treated rat heart section (day 8). C, Doxorubicin-treated rat atrial section (day 15). D, Doxorubicin-treated rat atrial section (day 43). E, Doxorubicin-treated rat atrial section (day 57). F, Doxorubicin-treated rat atrial section (day 78). A, shows typical myocardial architecture. The pericardial surface (solid arrow), the endocardium of the atrial lumen (filled with red blood cells) and the normal arrangement of cardiomyocytes (zig-zag arrow) are highlighted. B, shows normal myocardial architecture. The pericardial surface (solid arrow), the endocardium of the atrial lumen and the normal arrangement of cardiomyocytes (zig-zag arrow) are all highlighted. C, shows grade 1 pathology. The pericardial surface is shown (solid arrow) and multi-focal intracellular vacuolation of cardiomyocytes highlighted (dashed arrows). D, shows grade 3 pathology. Minimal disruption of overall architecture observed. Atrial lumen illustrated (triangle). Multi-focal and well-demarcated intracellular vacuolation of cardiomyocytes (dashed arrows); lymphoplasmacytic inflammation (solid arrow) and a degenerate cardiomyocyte (bent arrow) are highlighted. E, shows grade 7 pathology. Diffuse cardiomyocyte hypertrophy/cytomegaly (solid arrows), inter-cellular vacuolation (oedema; dashed arrows) and fibroblast proliferation with collagen deposition (fibrosis; zig-zag arrow) are highlighted. F, shows grade 7 pathology. Diffuse cardiomyocyte hypertrophy/cytomegaly (solid arrows), intra and inter-cellular vacuolation (dashed arrows) and diffuse disruption of architecture. Haemorrhage (triangle) and fibrosis (diagonal arrow) are also highlighted.***

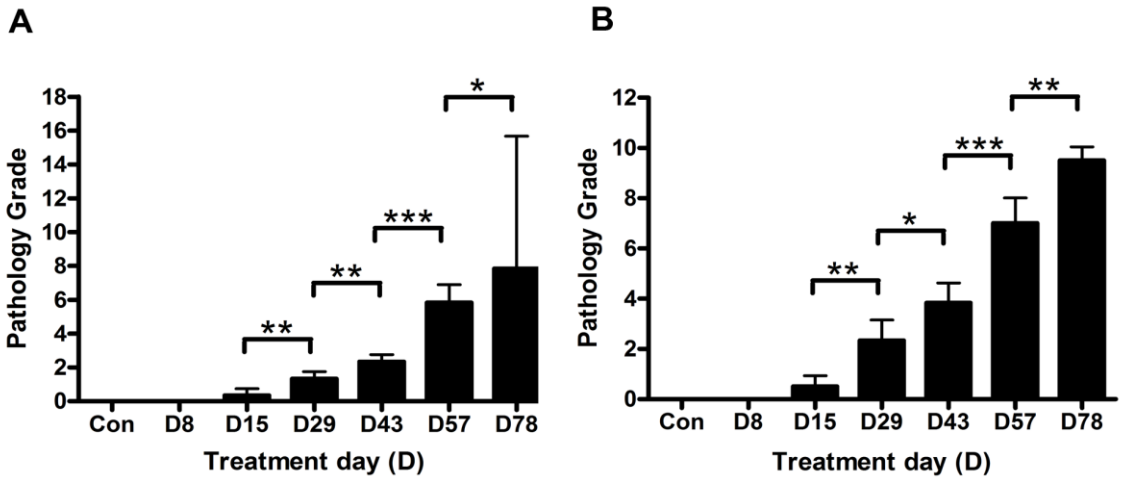

Figure 14. Grading of ventricular (A) and atrial (B) cardiac pathology in rats over the time course of Doxorubicin dosing. *The control data shown represents combined D57 and D78 vehicle-only control groups (n=6). Error bars represent 95% confidence intervals. Star symbols represent statistical significance (*p=<0.05; **p=<0.01; ***p=<0.001).*

2.3.5 Subcellular Effects of Chronic Doxorubicin Treatment on Rat Cardiomyocytes

Subcellular changes induced by doxorubicin treatment were assessed by electron microscopy (EM) performed on rat heart sections and interpreted by a board qualified veterinary pathologist from AstraZeneca. Cardiomyocytes from control rat atrium displayed a typically uniform myofibrillar, mitochondrial and Z-line presentation with a highly regular Z-line orientation and a normal microvascular profile (**Figure 15a**). Overall, there was a time-dependent progression in cardiomyocyte structural degeneration associated with doxorubicin treatment (**Figure 15b-f**; time-points Day 8 to Day 78 respectively). A key feature of the subcellular damage was longitudinal myofibrillar splitting and Z-line distortion, which was marked in individual cardiomyocytes even one week after a single doxorubicin dose (day 8, **Figure 15b**) and when no changes were evident at the cellular/tissue level in the H&E stained sections (**Figure 13b**).

Of particular prominence were early mitochondrial changes, characterised by swelling, membrane distortion, dense-body deposition and general loss of structural integrity (**Figure 15b,c & d**). These were accompanied by areas of membrane blebbing, lysosomal prominence and marked intra-cellular vacuolation (**Figure 15d & e**). Interestingly, earlier changes were often more prominent in individual cells, with adjoining cells frequently displaying changes of lesser severity. At later time-points, individual cellular changes assumed confluence and groups of cells were similarly affected. This corresponded with areas of focally extensive degeneration as seen by light microscopy (**Figure 13**). Although there was a general preservation of intercalated disc configuration, scattered cells appeared to have lost all muscle fibre content and contained myriad clear vacuoles surrounded by partially-intact basal laminae (**Figure 15f**). After chronic treatment (day 57 and day 78), cardiomyocytes displayed marked microvascular congestion or intravascular ‘sludging’ (**Figure 15e & f**).

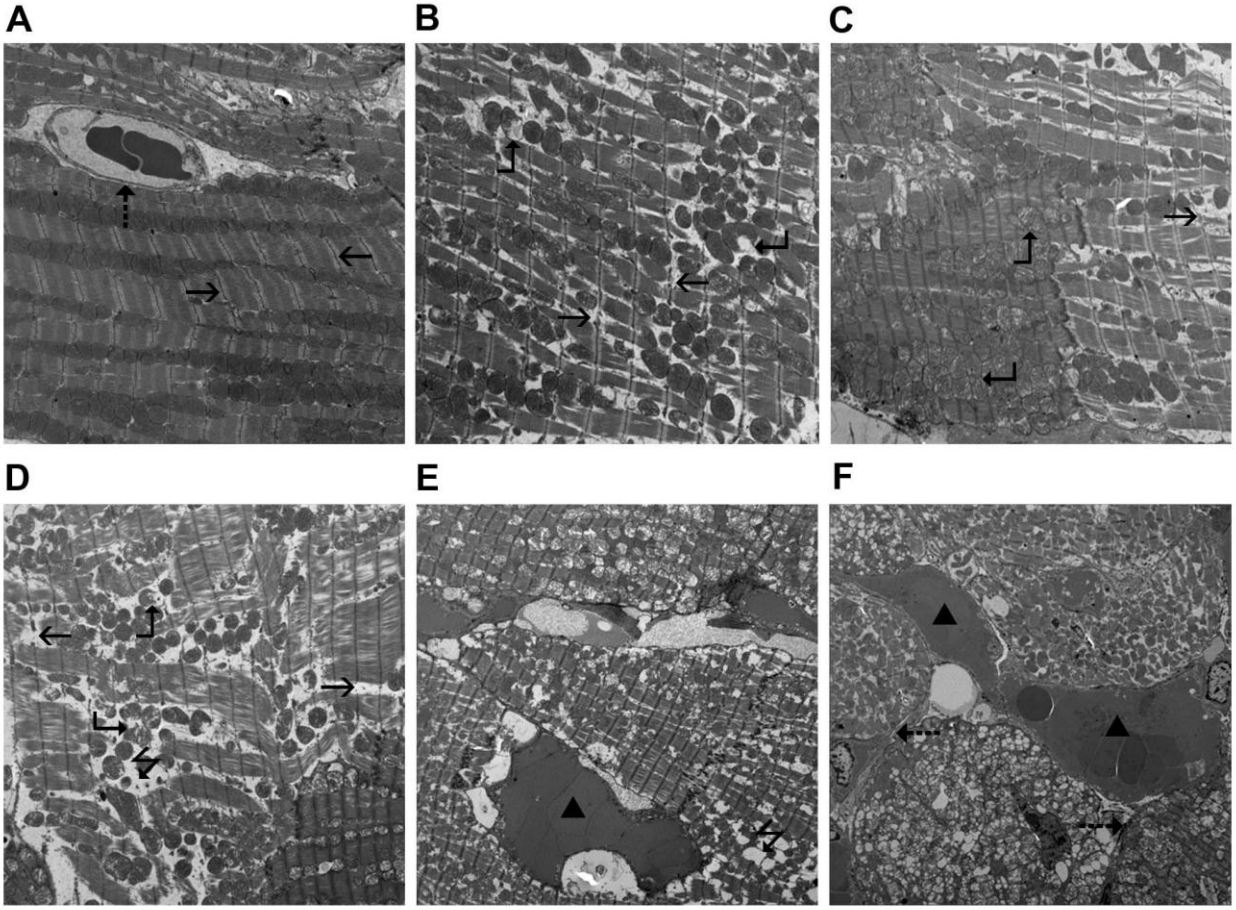

Figure 15. Subcellular morphological characterisation of doxorubicin-induced changes in rat cardiomyocytes. *Micrographs were prepared of representative cardiomyocytes. A, Control rat (day 8); B, Doxorubicin -treated (day 8); C, Doxorubicin -treated (day 29); D, Doxorubicin -treated (day 48); E & F, Doxorubicin -treated (day 72). Highlighted features - regularity of myofibrillar Z-line orientation (solid arrows) and the unadulterated microvascular profile (dashed arrow) within control rat cardiomyocyte (A). Longitudinal myofibrillar splitting and Z-line distortion (solid arrows) in cardiomyocytes from doxorubicin-treated rats (B). Mitochondrial changes, characterised by swelling, membrane distortion, dense-body deposition and general loss of structural integrity (bent arrows B, C and D). Scattered cells appeared to have lost all muscle fibre content (F) and contained myriad clear vacuoles surrounded by partially-intact basal laminae (dashed arrows, F). Terminal samples displayed microvascular congestion (intravascular "sludging", triangles, E and F)*

2.3.6 Replacement Fibrosis Development upon Chronic Doxorubicin Dosing

Based on the observed fibroblast infiltration and apparent collagen deposition, particularly in the atria, observed in the H&E stained sections (**Figure 13e**), collagen deposition was examined within the myocardium in more detail. Pico sirius red staining for collagen highlighted a fine trabecular fibrous stroma between cardiomyocytes within both the atria and ventricles of control animals (**Figure 17a**). Digital quantification of the sirius red staining in control animals revealed no significant changes in collagen content during dosing. However the normal collagen content of the atria was greater than that of the ventricle (**Figure 17c**). Doxorubicin-treated rat hearts exhibited thickened and expanded intercellular fibrous stroma (scarring) in the ventricles, and more extensively in the atria, at the end of the study on day 78 (**Figure 17**) and quantification revealed statistically significant increases in the collagen content at this time point (**Figure 16**). At earlier time points, doxorubicin-treated rat hearts did not show quantifiably significant collagen deposition, indicating that this is primarily a late event in the development of chronic doxorubicin-induced cardiotoxicity.

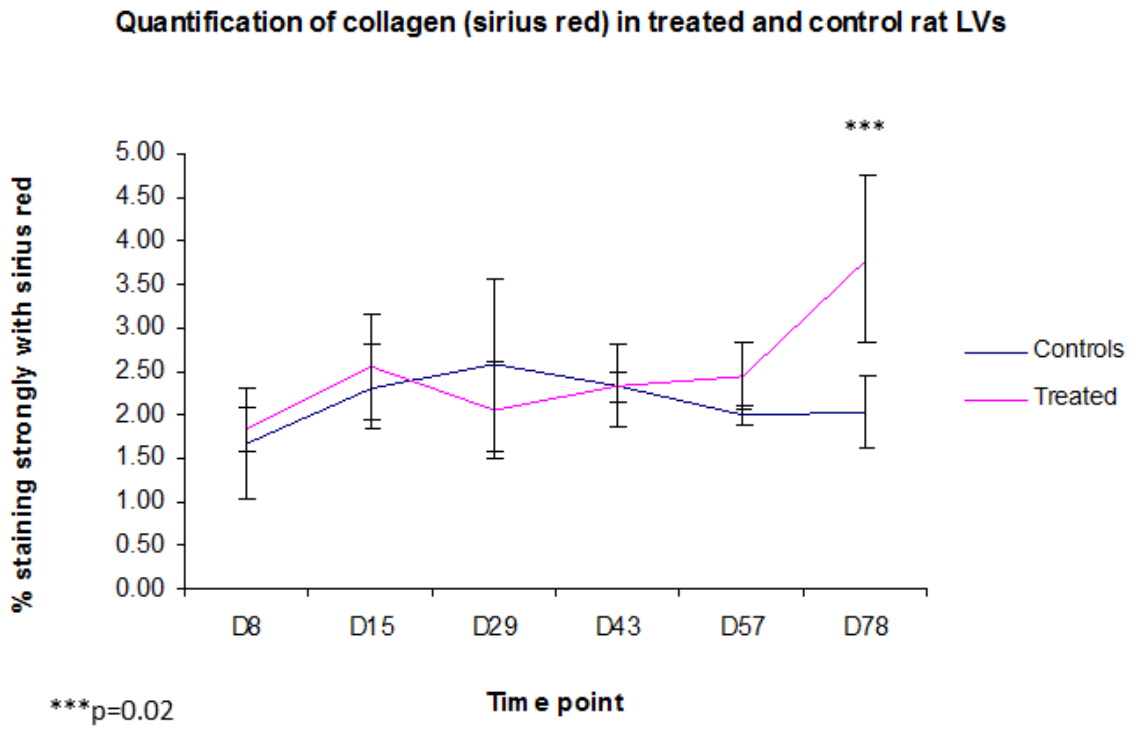

Figure 16. Longitudinal quantification of collagen using picro sirius red staining. *No difference in treated and control rats is seen until day 78 when a significant increase in collagen was seen in treated rats (p=0.02)*

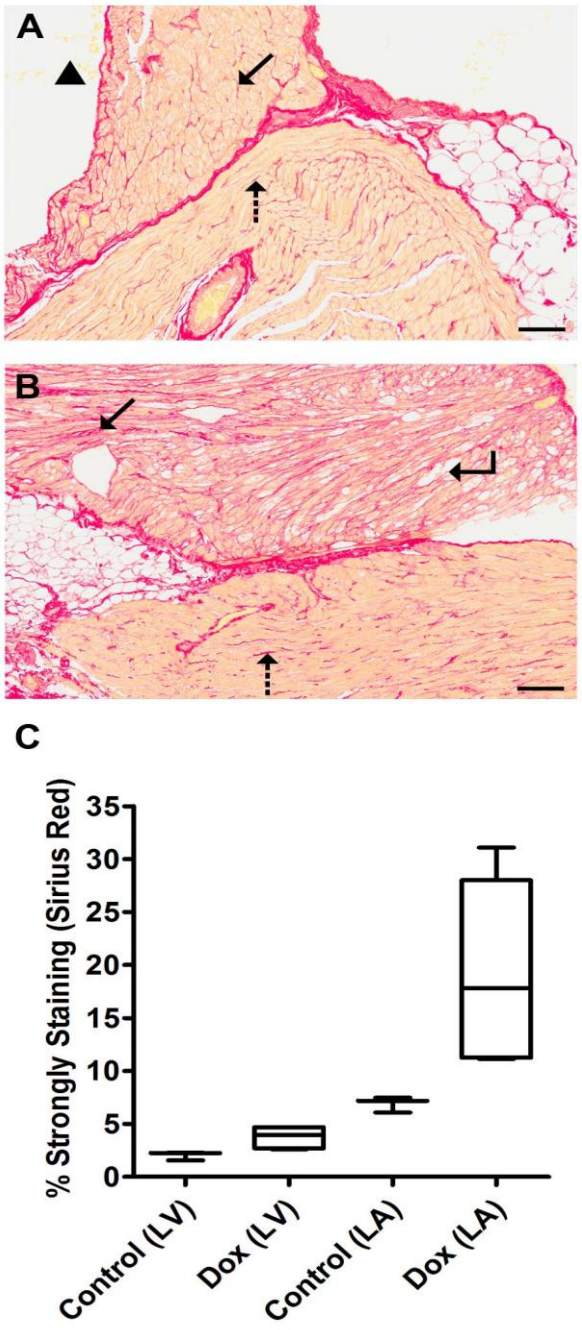

Figure 17. Chronic doxorubicin treatment is associated with replacement fibrosis in rat hearts. *Fibrosis assessment was performed using Picro sirius red staining for the presence of collagen and quantifying the percentage of myocardium with strong staining as described in the methods. The left ventricle and left atrium were considered as separate regions of interest and were quantified independently. A, Control rat (day 78) atrioventricular junction. Sirius red highlights the fine trebecular fibrous stroma found between cardiomyocytes within the atria (solid arrow) and ventricles (dashed arrow). Chambers contain residual red blood cells (triangle). B, Doxorubicin-treated rat (day 78) atrioventricular junction. Sirius red*

highlights the thickened and expanded intercellular fibrous stroma (scaring) within the atria (solid arrow) and ventricles (dashed arrow). Vacuolation (cell loss) is clearly evident (bent arrow). C, Box-plot showing a significant increase in sirius red staining between control and doxorubicin-treated rat left ventricles (LV, p=0.01) and left atria (LA, p=0.026). Whiskers represent the upper and lower quartiles.

2.4 Discussion

In this study, chronic dosing of rats with doxorubicin led to the development of progressive cardiotoxicity and a number of key findings. Firstly, when measured by the sensitive modality of CMR, significant functional decline was one of the earliest, rather than latest features of doxorubicin-induced cardiotoxicity. Secondly, steady state circulating troponin I and myocardial Gadolinium-enhancement elevations formed part of the progression of doxorubicin-induced cardiotoxicity and preceded the LV dysfunction, but these are not predictive biomarkers of the onset LVEF decline *per se*. Thirdly, subcellular myofibrillar and mitochondrial degeneration coincided with (and is likely to be mechanistically linked to) early doxorubicin-induced functional impairment and this preceded any overt cardiomyocyte degeneration.

CMR revealed statistically significant doxorubicin-induced decreases in both systolic (LVEF, CO, SV) and diastolic (E/A ratio) parameters simultaneously from day 15. Pseudo-improvement was seen in diastolic function from day 15 to 29 reflective of atrial damage preceding ventricular changes. This perceived improvement may result from poor atrial compliance raising intra-atrial pressures and driving passive filling. However, from day 29 a steep decline in diastolic function was seen as the damage progressed and atrial contraction was lost. In the clinical setting diastolic dysfunction has been reported to precede systolic dysfunction [155-157] but this study showed a decline in systolic and diastolic indices from day 15. The functional indices continued to decrease incrementally with each subsequent doxorubicin dose and declined further during the post-dosing 'recovery' period (day 50 onwards), indicating that, by the end of dosing, the doxorubicin schedule had triggered a continuous and irreversible functional deterioration.

Despite the steady decline in cardiac contractility, the mean rat LVEF remained in what is considered to be the 'clinically normal (human) range' [153] until day 78 when it dropped to <50% (mean 49.2 %, **Figure 10**), a level clinically indicative of left ventricular dysfunction. Although there were no premature deaths in the current study, in a previously published rat study dosing for 10 weeks with a higher dose of doxorubicin (2.5 mg/kg), mortality significantly increased in the follow-up period (weeks 12-14) [158], providing further evidence of the progressive/irreversible nature of the damage. Also consistent with the rodent findings, a significant decline in mean patient LVEF (versus baseline) has been observed

upon cessation of doxorubicin therapy, which progressively worsens over the subsequent 12 months [76, 159].

The significant functional contractile decline observed at day 15, after two doxorubicin doses, coincided with low level (grade 1) multi-focal vacuolation in the hearts of some of the treated rats, and more notably, profound sub-cellular structural changes in cardiomyocytes as assessed by electron microscopy (from day 8) including longitudinal myofibrillar splitting, Z-line distortion and marked mitochondrial changes. Consistent with this, disruption of normal cardiomyocyte cytoskeleton, cross-striations and a profound alteration in desmin localisation (an intermediated filament protein required for contractile element anchorage) has previously been observed after acute doxorubicin treatment in rats [149]. It is highly likely that the early functional decline observed is a consequence of the observed doxorubicin-induced damage to the sub-cellular contractile machinery, either directly or via defective protein synthesis in response to DNA damage. These subcellular doxorubicin-induced features are highly consistent with previous findings in humans, particularly the extensive myofibrillar degeneration and swelling to mitochondria and the sarcoplasmic reticulum [160]. Interestingly, human cardiac biopsies examined post first dose of doxorubicin have revealed mitochondrial swelling within the first 24 hours [47].

At much later time points (after day 43), dynamic CMR imaging acquired during the infusion of Gadolinium demonstrated statistically significant increases in both peak and delayed myocardial enhancement, which mirrored steady state troponin I elevations. Further to this, significant correlations were found between myocardial enhancement and troponin I levels, suggesting that these biomarkers may be reporting a common event in chronically doxorubicin-exposed hearts, most likely the onset of myocardial degeneration. Consistent with this, from day 43 (after 6 doses) onwards, multi-focal cardiomyocyte degeneration (apoptosis and/or necrosis) became evident, particularly in the atria of rats. As described, correlations between troponin I levels and cardiac pathology grade on days 43 and 57 were also observed. In a previous study of anthracycline-induced cardiomyopathy in rat, elevated serum troponin T correlated with a pathological ‘cardiomyopathy score’, which encompassed the extent of cytoplasmic vacuolation and myofibrillar loss [161]. There is strong clinical evidence linking troponin elevation with cardiac ischaemia (acute coronary syndromes) in man, which is thought to be due to myocardial necrosis from infarcted tissue [68]. It is becoming evident that troponin can rise in other types of cardiac injury and this study supports this as troponin I was raised in the presence of the diffuse cardiac injury induced by

doxorubicin [162]. Myocyte necrosis is characterised by cellular swelling, leading to uncontrolled leakage of cellular contents and an associated inflammatory response and appears to dominate (over apoptosis) in response to chronic doxorubicin dosing [149]. Troponin T and I are both highly sensitive and specific for cardiac injury [163, 164]. Although the mechanism(s) of myocardial degeneration induced by doxorubicin is still not fully understood, it seems to be widely accepted that serum troponin elevations are a direct consequence of the cardiomyocyte degenerative process [84]. However, whether troponin is solely released from necrotic cardiomyocytes or if it can be liberated as part of an apoptotic process, or even in response to reversible damage, all remain points of debate [165, 166]. As the majority of the troponin pool is complexed to the myocyte contractile machinery, it is possible that even mild-to-moderate troponin release may represent irreversible cardiac injury. Assuming loss of cardiomyocyte membrane integrity always precedes troponin release, early or acute troponin elevation is thought to derive from the smaller (~5%) soluble cytosolic troponin pool, which can be rapidly released after myocyte damage. In contrast, the sustained troponin elevation observed likely results from breakdown of the contractile organelles, for example through oxidative damage to the sarcolemma together with loss of cardiomyocyte membrane integrity via necrosis [68]. None of the other proteins rose significantly during the study although troponin T rose non-significantly in line with Troponin I which would be expected. The multiplex ELISA assays were not as robust as the troponin I clinical assay. Human capture antibodies were used for these assays, and although they were validated for cross reactivity with rat prior to use, affinity for the rat protein was suboptimal and baseline variability was high which may have contributed to the lack of overt signal change during treatment.

This study focussed on the development of progressive cardiotoxicity and looked for significantly sustained troponin I elevations, or high steady-state levels, i.e. raised troponin I one week after the previous dose. These sustained elevations were only observed from week 6 (day 43) onwards and reached significance at day 57 onwards, one week after the last of the 8 doses. The magnitude of the troponin elevations (0.02-0.03ng/ml) is consistent with the low level release previously observed in both rats and humans after anthracyclines [76, 161]. In the absence of continuous cardiac damage, raised serum troponin levels will quickly return to baseline after a few days. In drug induced cardiotoxicity, the diagnostic window is likely to be drug-dependent and the mechanism of cardiac injury may be a crucial factor in the mode of myofibril loss and troponin release [165]. These data demonstrate that a combination of

continuous myofibrillar system damage combined with sustained troponin release are key underlying features of the developing stages of progressive doxorubicin toxicity.

In this rodent study, the troponin I elevation persisted for the four weeks between cessation of dosing and necropsy. The mean troponin I value increased to a maximum on day 78 and importantly, the LVEF decline mirrored this finding. By the end, the rodents had undergone a profound cardiac functional decline consistent with the onset of heart failure. One clinical study has shown that the timing and extent of troponin I elevation is prognostic with respect chemotherapy-associated cardiac risk. Patients without troponin I elevations had no change in LVEF on follow-up (1 month to 3 years) [71]. Marked 'early' elevations in troponin I measured within 72 hrs of a high-dose chemotherapy cycle were associated with an enhanced risk of subsequent systolic dysfunction and clinical heart failure on follow up. However, the cardiovascular risk is greatest for those patients exhibiting a persistent or 'late' troponin I elevation 1 month after ending chemotherapy [48, 71, 76].

Like the functional indices, the pathological severity score increased with the total cumulative dose of doxorubicin and the damage continued to progress after cessation of dosing. The microscopic pathological features observed at later time points in this study and others [158, 167] are highly consistent with those observed in post-mortem human cardiac tissue after doxorubicin-induced heart failure, namely disruption of the normal cellular architecture, cytoplasmic vacuolation, cellular loss, replacement fibrosis and even ventricular and atrial thrombi [160].

In a study by Lightfoot *et al*, the effects of 10 weekly doses of doxorubicin (1.5 or 2.5 mg/kg) on CMR parameters in Hannover Wistar rats was assessed [168]. In contrast to the present study, authors did not observe a significant early drop in LVEF that incrementally declined with repeat dosing. A significant LVEF decline was observed at the week 4 time point for the high dose group but not at the lower dose or at other time points. The authors showed that individual animals (from either doxorubicin dose group) that experienced a 'primary event' (deterioration in LVEF >10% of baseline, absolute LVEF <65% or unanticipated death) also exhibited myocellular degeneration. An increase in delayed myocardial Gadolinium-enhancement was found to precede a 'primary event' and was therefore a predictive biomarker of LV dysfunction [168]. Considering these data in the context of the Lightfoot *et al* primary event criteria, a significant LVEF decline to below 10% of baseline in the doxorubicin-treated rats from day 29 (-12%) was seen, absolute LVEF was <65% from day

57 (58%) and no unexpected deaths occurred. Significant elevations in delayed and peak Gadolinium-enhancement were seen from days 43 and 57 respectively. Therefore, it is likely that the predictivity of Gadolinium-enhancement for LV dysfunction ultimately depends upon the dysfunction criteria set. Nonetheless, it is clear from this study that significant LV impairment commences several weeks prior to elevations in myocardial Gadolinium-enhancement, overt myocyte degeneration and the release of troponin I. Highly significant elevations in both peak and delayed Gadolinium-enhancement were evident in the doxorubicin group at day 57 when mean LVEF was 57% (<27% of baseline). The continued decline in cardiac function in the 'recovery period' from day 50 indicates that the cardiotoxicity was already irreversible when robust elevations in the myocardial Gadolinium signal was observed. In the future, it would be informative to explore if the progressive cardiotoxicity can be halted or even reversed by ceasing after fewer doses, e.g. prior to the overt pathological changes and Gadolinium-enhancement and troponin I elevations.

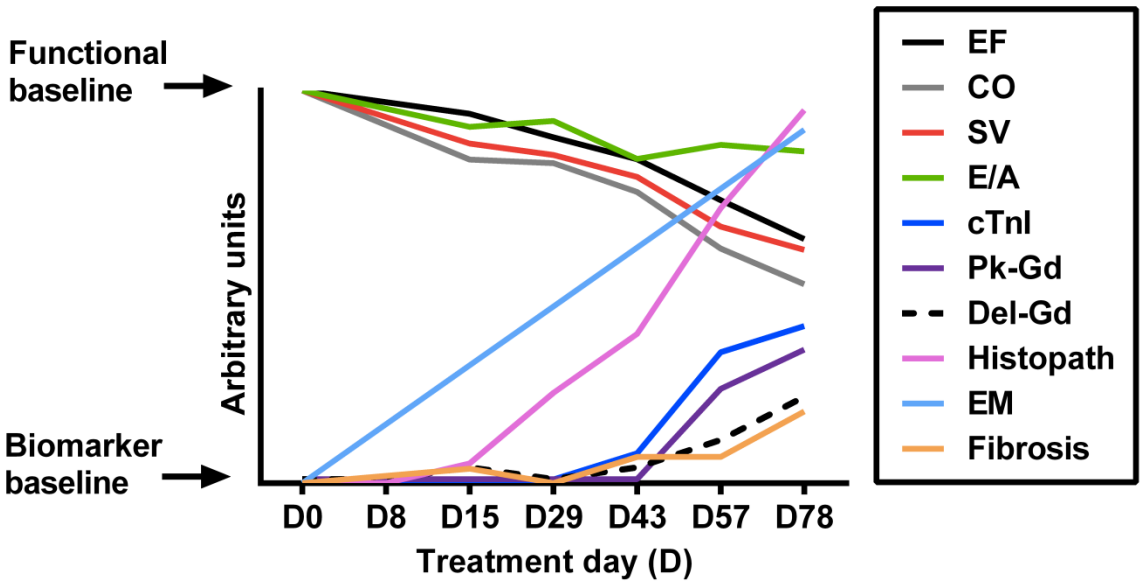

Figure 18. Summary illustration of cardiac changes associated with the development of doxorubicin-induced cardiomyopathy. *Cartoon illustration showing the chronology of doxorubicin induced cardiac changes. Key functional parameters (EF, CO, SV and E/A) declined significantly from baseline when assessed at day 15 (after 2 doxorubicin doses) and continued to decline throughout the study. Subcellular (EM) changes were marked at day 8 (after a single doxorubicin dose) and progressed thereafter. Doxorubicin-associated pathological changes at the tissue level were not evident at day 8 but developed from day 15.*

Significant elevations were observed in delayed Gadolinium-enhancement (from day 43), in peak Gadolinium-enhancement and troponin I (from day 57), consistent with the pathological onset of cardiomyocyte degeneration. Fibrosis development was a late event (significant at day 58), consistent with collagen deposition in regions of cardiomyocyte loss.

2.5 Conclusions

In summary, this study comprehensively characterised the chronology and nature of not only the functional events, but also the pathological and serological changes underlying doxorubicin-induced cardiotoxicity in a rodent model (**Figure 18**). It is hoped that the findings from this study in conjunction with the clinical study have helped gain a better understanding of the translational and patient-related aspects of anthracycline-induced cardiac injury, inform predictive biomarker research and can help to support the development of safer future medicines.

3 Clinical Cardiotoxicity Biomarker Study

3.1 Introduction

Despite the development of many new targeted systemic cancer therapies, anthracyclines remain extremely effective and are unlikely to be readily superseded in the curative treatment of lymphoma or breast cancer [169]. Unfortunately, as discussed at length in the main introduction, they can also cause substantial damage to normal tissues including the heart. Therefore breast cancer and lymphoma survivors are at risk of cardiovascular morbidity and mortality following treatment. Current methods of detecting which patients are at highest risk of cardiotoxicity are lacking. If high risk patients could be identified, either prior to or during therapy, their treatment could be tailored to be less cardiotoxic or cardio-protective strategies could be implemented. There is growing evidence that early intervention with standard heart failure therapies such as beta blockers and ace inhibitors may reduce the risk of cardiac events following therapy [170]. Therefore ways of identifying patients who are at greatest risk or who are developing early cardiac damage during treatment are greatly needed. This clinical study was carried out with the aims of identifying early clinically applicable biomarkers of cardiotoxicity and of relating findings to the pre-clinical work to assess translatability of the potential biomarkers.

Aims:

- To characterise changes in cardiac function using cardiac MRI in cancer patients receiving 1st line anthracycline chemotherapy
- To characterise the behaviour of circulating biomarkers in cancer patients receiving 1st line anthracycline chemotherapy
- To evaluate myocardial tissue changes (fibrosis and oedema) in cancer patients receiving 1st line anthracycline chemotherapy
- To evaluate myocardial strain in cancer patients receiving 1st line anthracycline chemotherapy
- To explore the relationship between circulating biomarker changes and cardiac MRI findings

Objectives:

- To design and conduct a clinical trial exploring cardiac MRI and circulating protein biomarkers in cancer patients receiving anthracycline chemotherapy

3.2 Clinical Study Materials and Methods

3.2.1 Study Overview

This study was carried out in patients with lymphoma or breast cancer as they receive anthracyclines as part of standard treatment and have a high chance of survival putting them at risk of long term cardiac toxicity. The study was conducted at The Christie NHS Foundation Trust, a tertiary referral centre for lymphoma and breast cancer. The site already runs a large number of translational trials in partnership with the Cancer Research UK Manchester Institute (for analysis of circulating protein biomarkers) and the Wolfson Molecular Imaging Institute (for CMR imaging) with well-established processes in place to ensure success.

3.2.2 Study Population

38 patients receiving standard 1st line anthracycline based chemotherapy for lymphoma or breast cancer (adjuvant, curative or palliative) at the Christie NHS Foundation Trust, Manchester, UK were recruited to this study from November 2011 to May 2013. The protocol gained ethical approval from the UK Research and Ethics Committee (North West Cheshire) in June 2011 (ref. 11/NW/0274) and adhered to the Declaration of Helsinki and Good Clinical Practice (GCP) principles. Informed consent was taken from all patients prior to entering the study but patients who were unable to undergo cardiac MRI scanning (for reasons such as claustrophobia) were excluded. Inclusion criteria are listed below but were briefly as follows, age over 16 years and a histologically confirmed diagnosis of cancer requiring standard first line anthracycline based chemotherapy. Exclusion criteria were prior anthracycline therapy, prior or planned radiotherapy treatment to cardiac structures, patients with HER2 positive breast cancer requiring trastuzumab therapy, creatinine clearance <30ml/min/1.73m^2, patients already participating in another clinical study involving an investigational medicinal product (IMP), patients with uncontrolled arrhythmias such as AF that would be incompatible with cardiac MRI scan acquisition. Breast cancer patients requiring adjuvant radiotherapy were only eligible if the radiotherapy was given solely to the right side, avoiding cardiac structures. Patients who were unable to attend for both of the post treatment cardiac assessments due to progressive disease or cancer related death were also excluded from the study.

Inclusion Criteria:

1. Age >16 years
2. Histologically confirmed diagnosis of cancer requiring standard first line anthracycline based chemotherapy, including but not limited to patients with lymphoma such as hodgkin lymphoma, diffuse large B cell lymphoma and breast cancer
3. No previous anthracycline (or other potentially cardiac damaging) drug treatments
4. No previous or planned radiation treatment involving the myocardium
5. No contraindications to magnetic resonance scanning
6. Patients must be able to receive and understand verbal and written information regarding the study and give written, informed consent

Exclusion Criteria:

1. Previous anthracycline base chemotherapy treatment
2. Previous or planned radiation therapy involving the myocardium
3. Patients for whom anthracycline treatment is deemed inappropriate due to significant medical co-morbidity
4. Left ventricular function as measured by MUGA scan or echocardiography below 50% (if known)
5. Patients in atrial fibrillation or other uncontrolled cardiac arrhythmias including frequent recurrent ectopy
6. Patients who will receive trastuzumab following anthracycline treatment
7. A previous diagnosis of cancer except for non melanomatous skin cancer or cervical carcinoma in situ
8. Patients unable to safely undergo MRI i.e. due to MRI incompatible devices/implants
9. Creatine clearance <30ml/min/1.73m^2

3.2.3 Study Protocol

Physical examination, ECG and blood pressure measurements were taken at baseline. Cardiac co-morbidities and medications were documented to record baseline cardiac risk. Three baseline blood samples were taken for biomarker analysis, two at baseline (on different days) and one directly prior to the first chemotherapy cycle. Further biomarker bloods were taken at 2, 24 and 72 hours following cycles 1, 3 and 6 of a 6 cycle regimen (**Figure 19**) (biomarker analysis methods are described in detail in section 3.5). Cardiac assessment was performed

using CMR at baseline (pre-chemo) half way through treatment (mid-chemo), 4-6 weeks (post-chemo) and 1 year after treatment (**Figure 19**). Assessments of left ventricular systolic and diastolic function, left atrial volume, myocardial oedema, and strain/strain rate were performed each time. Assessment of extracellular volume took place at baseline, 4-6 weeks post treatment and at one year (full CMR methods are described in section 3.2.5). ECG and blood pressure measurements were taken prior to the final cycle of chemotherapy and patients underwent clinical review for development of cardiac complications 3, 6 and 12 months after treatment. The biomarker and imaging data were anonymised at collection and neither the patients nor treating physicians were made aware of the findings therefore all treatment decisions made during the study were made according to standard clinical practices without the knowledge of the study results.

Figure 19. Clinical study schema

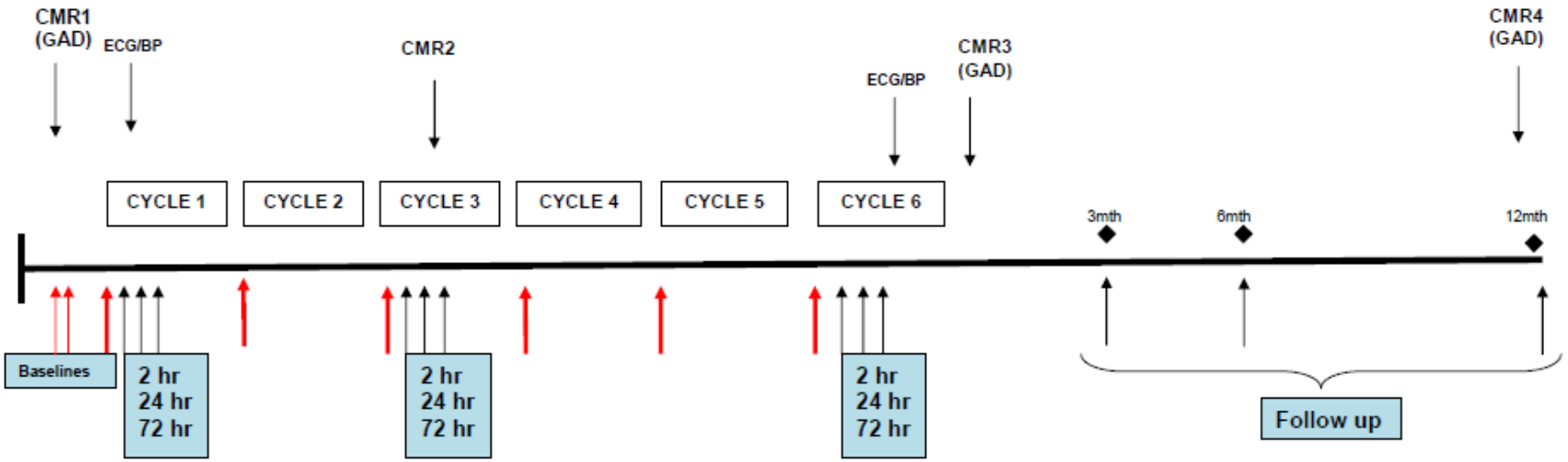

KEY

CMR - Cardiac magnetic resonance scan

♦ - Clinical review & cardiac examination

GAD - Gadolinium contrast enhanced scan

↑ - baseline & pre-chemotherapy biomarker bloods

↑ - post chemotherapy & follow up biomarker bloods

3.2.4 Study End Points

Primary end point:

- An asymptomatic or symptomatic decline in LVEF of ≥ 10% to an absolute LVEF of ≤ 55%

Secondary end points:

- A significant deterioration in cardiac function deemed as an absolute fall in LVEF of ≥10% during the study
- The development of left ventricular failure LVEF ≤ 50%
- The development of a clinical cardiac event

The primary end point was based on current guidelines and practice in the subspecialty of cardio-oncology however there is still uncertainty and lack of consensus about the threshold that constitutes cardiotoxicity [171, 172]. This study was designed to explore biomarkers that report cardiotoxicity at an early, potentially reversible stage therefore the secondary end point of fall in LVEF by ≥ 10% was included to capture patients who had an element of cardiac damage even when the LVEF remained in the normal range.

3.2.5 Cardiac MRI Methods

Cardiac imaging techniques have improved greatly over the past few decades and it is now possible to get a detailed assessment of the cardiac anatomy, function, strain, tissue and potentially tissue metabolism using cardiac MRI (CMR). CMR has therefore become the gold standard imaging tool in cardiovascular research but has not been widely explored in chemotherapy-induced cardiotoxicity. It was appealing and novel to use a comprehensive CMR protocol to characterise the time course and nature of heart damage occurring during anthracycline therapy in cancer patients. CMR has the potential to detect early subclinical damage prior to the onset of symptoms therefore correlation of imaging findings with changes in circulating protein biomarkers could give more insight into the damage process and help identify patients at risk.

A unique CMR imaging protocol was designed in conjunction with the cardiologists at University Hospital of South Manchester to reflect the possible pathological processes that may occur during the development of anthracycline-induced cardiomyopathy and to complement a circulating biomarker panel under simultaneous exploration. Four CMR scans

were performed over 18 months; one at baseline, one half way through treatment, one directly after treatment and the final scan 12 months after therapy. This schedule was designed with the hope of detecting early changes in imaging parameters during or shortly after treatment and subsequent cardiac dysfunction a year after therapy. Systolic LV function was measured with standard volumetric analysis to determine whether cardiac dysfunction occurred and LV function was used as the end point for this study as it was thought unlikely that a significant number of clinical events would occur in this small cohort during the study period. Elements of diastolic function were estimated by measuring the E/A ratio and carrying out strain analysis to determine whether diastolic dysfunction may precede systolic dysfunction and whether it could be used to identify cardiotoxicity at an earlier stage. The histology findings from the pre-clinical rat model (see chapter 2) suggested that inflammation (infiltration of neutrophils and lymphocytes) occurred during anthracycline therapy and fibrosis (collagen deposition and fibroblast proliferation) occurred 4 weeks after drug cessation. Therefore tissue characterisation using T2 mapping to quantify oedema/inflammation and T1 mapping to quantify fibrosis were explored to determine whether these processes important in the development of anthracycline-induced cardiomyopathy in humans.

3.2.5.1 Overall scanning procedure

Cardiac imaging was acquired using a 1.5 tesla MRI scanner (Philips Healthcare, The Netherlands) at baseline (pre-chemo) half way through treatment (mid-chemo), 4-6 weeks (post-chemo) and 1 year after treatment. Scans were carried out at the Wolfson Molecular Imaging Centre and were supervised by a medically qualified clinical research fellow. Patients were scanned in the supine position using a five phased array cardiac coil with prospective electrocardiographic (ECG) gating and respiratory monitoring. Patients were cannulated with a 20 gage cannula for administration of a gadolinium bolus for contrast sequences using Dotarem 0.15mmol/kg (excluding the mid treatment scan to minimise venous access problems). Prospective ECG gated, end expiratory balanced steady state free procession cines were acquired of the horizontal long axis (4 chamber view), vertical long axis (2 chamber view), 3 chamber view, left ventricular outflow tract and AV valve. A short axis stack of the left ventricle was acquired from the atrio-ventricular ring to the apex using 8mm slices with a 2mm gap. The typical parameters included flip angle 60°, field of view (FOV) 350mm x 300mm, repetition time (TR) 3.3ms, echo time (TE) 1.6ms, in plane pixel size of 1.7mm x 2.0mm and matrix 208 x 136.

3.2.5.2 Volumetric Analysis

Assessment of Left Ventricular Volumes and Function:

LV volume analysis was performed using semi-automated contouring with Philips clinical workstation (View Forum Cardiac package 2009, Philips Healthcare, The Netherlands). Endocardial contours (excluding papillary muscles) were drawn on each short axis slice in ventricular end diastole and end systole. Basal slices were included if more than 50% of the blood pool was surrounded by ventricular myocardium throughout the cardiac cycle. Apical slices were included if blood pool remained visible throughout the cardiac cycle. Epicardial contours were drawn on end diastolic slices only. End systole and end diastole selection was automated based on the greatest and smallest cavity volume calculated. The end diastolic volume (EDV), end systolic volume (ESV) and LV mass were automatically calculated by adding the area of each slice and multiplying by the thickness using Simpson's rule. The LV ejection fraction was subsequently calculated using the following standard equation LVEF = LVEDV – LVESV/ LVEDV x 100 and the stroke volume (SV) and cardiac output (CO) were determined using the heart rate at time of acquisition. All measurements were then corrected for body surface area where appropriate. Volumetric analysis was performed by 2 individual blinded analysts. Where measurements differed significantly (CV>5%), invariably due to basal slice selection, the scans were reviewed and re-analysed once basal slice selection was agreed.

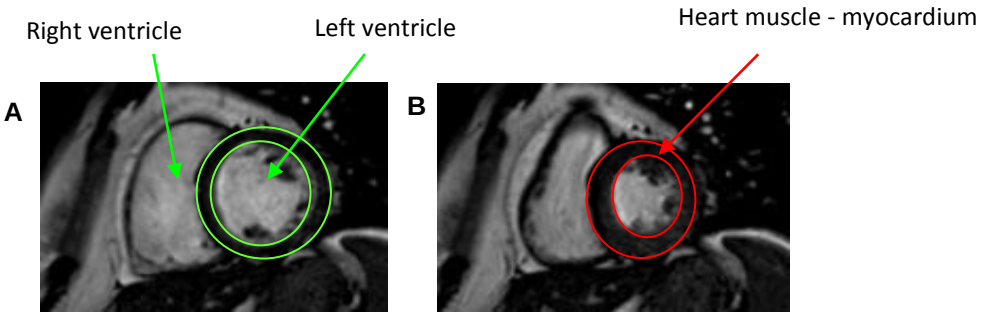

Figure 20. Estimating left ventricular volumes with Philips work station. Short axis view of the heart in diastole (A) and short axis view of the heart in systole (B)

Left Atrial Volume Assessment:

Left atrial (LA) volumes were estimated using the biplane area length method (8/(π x 3)x((LA area 4Ch x LA area 2Ch)/LA length 4 ch) from 2D 4 chamber and 2 chamber views correcting for body surface area [173].

Diastolic Function (E/A ratio):

Phase contrast sequences were acquired in a single plane across the mitral valve to measure velocity of blood flow in diastole. Peak velocity (cm/s) in early (E) and late (A) diastole were measured in order to calculate the E/A ratio as an estimate of diastolic function.

3.2.5.3 Tissue Characterisation

Oedema Assessment (T2 Mapping):

Single slice, mid ventricular black blood T2 prepared STIR pulse images were acquired for visual assessment of oedema. Four T2 prepared single-shot SSFP sequences with differing preparation times (TE 14ms, 35ms, 56ms and 77ms) were acquired of the mid ventricular slice in separate breath holds to generate pixel based T2 maps of the myocardium for quantitative assessment of oedema [174]. Typical parameters included flip angle 90°, repetition time 2000ms, matrix 216 x 116, in plane pixel size 2.2mm x 2.6mmm, FOV 320 x 320mm. The myocardial ring was isolated using osiriX (region of interest pluggin) and the median T2 value was calculated using MATLAB (mathworks 2009a TM) for the whole mid myocardial slice.

Estimation of the Extracellular Volume Fraction (T1 mapping):

T1 maps of the mid ventricular slice were generated using a modified look locker inversion recovery sequence in a single breath hold before and 10 minutes after a bolus infusion of 0.15mmol/kg gadolinium (inversion time sampling in a 3,3,5 scheme at identical times in the cardiac cycle as described by Messroghli *et al*, 2004) [175]. Typical parameters include flip angle 35°, TR 2.6ms, TE 1.05ms, in plane pixel size 2mm x 2mm, matrix 160 x 160, FOV 320 x 320. The myocardial ring was isolated using osiriX (region of interest pluggin) and the median T1 (pre and post contrast) values were calculated using MATLAB (mathworks 2009a TM) for the whole mid myocardial slice. The extra-cellular volume fraction (ECV) was estimated as previously described by Wong *et al* using the patients' most recent haematocrit and the following equation: extracellular volume fraction (ECV) = λ x (1- haematocrit).

Where λ = ΔR1(myocardium) / ΔR1(blood). ΔR1 = R1(post-contrast) – R1(pre-contrast). R1 = 1/T1. This method enables quantification of T1 solely from the gadolinium sequested in the extracellular space after reaching equilibrium by accounting for the signal generated from myocardial blood vessels (ΔR1blood) and the myocytes themselves (R1 pre-contrast) [176].

Late Gadolinium Enhancement:

Late gadolinium enhancement of the LV was assessed by acquiring a short axis stack of the left ventricle as described above (in section 3.2.5.2) 15 minutes after the bolus of 0.15mmol/kg gadolinium. Inversion recovery gradient echo sequences were taken using manually established inversion times to null the normal myocardium. Visual assessment of localised contrast enhancement was then made and documented.

3.2.5.4 Myocardial Deformation Analysis

Strain analysis was performed using image-arena™ (TomTec imaging systems, Munich, Germany) to calculate longitudinal and circumferential strain and strain rate. Manual endocardial contouring was performed on the 4 chamber view, 2 chamber view and short axis stack to enable automated endocardial tracking and calculation of segmental strain and strain rate. Global dyssynchrony was estimated using three methods. Firstly, by calculating the maximum delay in time to peak systolic velocity for the left ventricle (12 LV myocardial segments for longitudinal and 16 for circumferential analysis), secondly by calculating the standard deviation for the time peak velocity for the myocardial segments based on methods described by Yu *e* and thirdly by calculating the basal septal – lateral wall delay [177, 178]. The 4 chamber and 2 chamber views were used for longitudinal strain and the basal, mid and apical ventricular rings were used for circumferential strain calculation.

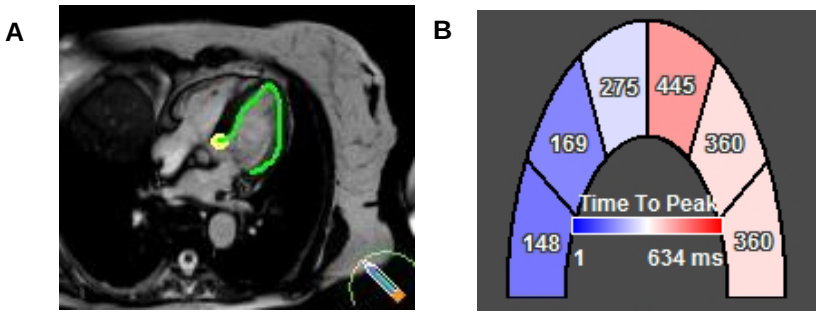

Figure 21. Deformation analysis a) left ventricular endocardial tracking on a 4 chamber view b) calculation of segmental longitudinal time to peak strain of the left ventricle from the 4 chamber view

3.2.6 Optimisation of the Cardiac MRI Protocol

Prior to use in the clinical study the bespoke imaging protocol was optimised using healthy volunteers to ensure it was tolerable, time efficient and able to generate high quality robust data. 5 healthy volunteers were scanned as described in the clinical study material and methods (section 3.2.5). Volumetric assessment was performed on all five and tissue characterisation was tested on 2 of the five volunteers. The protocol was tolerable and able to generate robust standard volumetric data. The novel imaging sequences were successful and generated high quality data for analysis of exploratory imaging biomarkers such as tissue characterisation. The imaging protocol optimisation work is shown in **appendix 4**.

3.3 Statistical Analysis

This was an exploratory study producing investigative circulating biomarker and imaging data therefore the study was not powered to detect a specific outcome. The sample size was largely pragmatic but statistical considerations were made based on other similar clinical studies suggesting that around 30% (12 patients) would be expected to have elevation of at least one biomarker [71]. The study was designed to recruit 40 patients and from a cohort this size one would expect to be able to gain useful data to determine biomarker distribution, behaviour with treatment and correlation with cardiac dysfunction. With this number of patients, any change in biomarker would have to be large to be significant but large changes would be expected if they are clinically relevant. Statistical analysis was performed using three statistical packages, Graphpad Prism version 5.03 (GraphPad Software, San Diego California USA, www.graphpad.com), STATA (version 10), Statistical Package for the Social Sciences (SPSS) version 20 (release 13.0.2004, SPSS Inc., Chicago, IL) and Microsoft Excel.

3.3.1 Imaging End Points

Descriptive statistics i.e. mean, median, standard deviation and inter-quartile range of the imaging end points were calculated and plotted to determine the behaviour of systolic function (LVEF) and other volumetric parameters during anthracycline receipt. These descriptive statistics were also applied to the novel imaging biomarker data (i.e. extracellular volume fraction and strain rate). Student's T-test and analysis of variance (ANOVA) tests were used to determine whether there was a significant difference between the results at each scanning time point and Chi squared was used to explore associations between categorical

clinical variables and the development of cardiotoxicity. Statistical analysis of the circulating biomarker and combined data is discussed later in section 3.5.3.

3.4 Clinical and Imaging Results

3.4.1 Study Population

100 patients were found to be eligible and were given written information about the cardiotoxicity biomarker study. 38 patients were recruited in total and 30 patients completed the study with evaluable data (taken as at least one post treatment cardiac MRI scan). Of the excluded patients, 5 were unable to tolerate the MRI scans, 2 patients died from progressive disease during chemotherapy and 1 was initially misdiagnosed and did not require anthracycline chemotherapy. From herein the reported data are from the 30 fully evaluable patients only.

3.4.2 Baseline Demographics

19 patients (63%) had a diagnosis of non-Hodgkin lymphoma, 6 (20%) had Hodgkin lymphoma and 5 (17%) had breast cancer. Patients were aged between 22 and 88 years old with a mean age of 57 years. 14 (47%) were male, 16 (53%) were female and all patients had a performance status of 0-1. Three patients (10%) had previously received non-anthracycline containing chemotherapy (R-CVP) and two went on to have unplanned radiotherapy to the mediastinum. The cancer staging was equally spread from stage 0 (adjuvant) to stage 4 (widespread) but the majority were receiving chemotherapy with curative intent (93%). Of the patients with active cancer at the time of starting therapy 20 (80%) had a complete response at the end of treatment and 5 (20%) had a partial response. 4 patients (16%) went on to develop progressive disease within 12 months of completing therapy. **Table 5** shows the baseline demographics for the study population.

Baseline demographic		Number (%)	Baseline demographic		Number (%)
Gender	Male	14 (47)	Chemotherapy regimen	R-CHOP	19 (63)
	Female	16 (53)		ABVD	6 (20)
Age	Range (years)	22-88		FEC-T	5 (17)
	Mean (years)	57	Cancer stage	No cancer (adjuvant)	5 (17)
Ethnicity	White	28 (93)		1	7 (23)
	Afro-Caribbean	1 (3)		2	6 (20)
	Asian	1 (3)		3	5 (17)
Diagnosis	NHL	19 (63)		4	7 (23)
	HL	6 (20)	Treatment Intent	Curative	23 (77)
	Breast Cancer	5 (17)		Adjuvant	5 (17)
Performance Status	0	20 (67)		Palliative	2 (7)
	1	10 (33)	Response (end of treatment)	Complete response	20 (67)
Previous chemotherapy	No	27 (90)		Partial response	5 (17)
	Yes	3 (10)		Progression	0 (0)
Mediastinal XRT (consolidation)	Yes	2 (7)	Disease status end of study	Remission/SD	26 (87)
	No	28 (93)		Relapse/progressed	4 (13)

Table 5. Baseline demographics for the study population, n=30.

3.4.3 Cardiovascular Risk Factors

21 patients (70%) had at least one pre-existing cardiovascular risk factor, namely hypertension (HTN), hyperlipidaemia, family history (FH) of ischaemic heart disease (IHD), obesity (deemed as a BMI ≥30), previous myocardial infarction (MI) or smoking. 4 patients (13%) had hypertension, 4 (13%) had hyperlipidaemia and 3 (10%) had both. No patients had diabetes and only one had a previous cardiac event (MI). 15 patients (50%) were current or ex-smokers, 11 (37%) were overweight and 10 (33%) were obese according to body mass index (BMI). Although only 23% (7 patients) had a diagnosis prior to starting treatment 40% (12 patients) had a raised BP at baseline (≥140/90). All patients were deemed fit for anthracycline chemotherapy by the treating physician but patients with a significant cardiovascular history were confirmed to have normal systolic function on standard ECHO or MUGA prior to starting anthracycline therapy. 9 patients (30%) were already on cardiac medication for hypertension, hypercholesterolaemia or pre-existing heart disease (details of cardiac risk factors and concurrent medications are given in **Table 6a and b**).

A

Cardiac risk factor	Number (%)
Pre-existing cardiac risk factor	21 (70)
Smoker or ex-smoker	15 (50)
Previous cardiac event	1 (3)
Hypertension	7 (23)
Hyperlipidaemia	7 (23)
Strong FH of IHD	4 (13)
Diabetes	0 (0)
Obesity	10 (33)
Baseline blood pressure raised	13 (46)
Abnormal baseline ECG	11 (37)

B

Cardiac Medication	Number (%)
Statin	6 (20)
Calcium channel blocker	3 (10)
Anti-platelet	2 (6)
ACE inhibitor	1 (3)
Beta-blocker	1 (3)
Angiotensin 2 inhibitor	1 (3)
Alpha-blocker	1 (3)
Diuretic	1 (3)

Table 6. Pre-existing cardiac risk factors (A) and concomitant cardiac medications (B)

3.4.4 Anthracycline Dosing

25 patients (83%) received the anthracycline drug doxorubicin and 5 (17%) received epirubicin. The mean anthracycline dose received was 255mg/m^2, well below the life time recommended dose of 450mg/m^2. An epirubicin dose of 450mg/m^2 is considered equivalent to 300mg/m^2 of doxorubicin therefore epirubicin doses were converted to the equivalent doxorubicin dose to enable comparison and aid statistical analysis (epirubicin dose x 0.6) [9]. Patients with NHL received 6 cycles (doxorubicin 50mg/m^2) every 3 weeks with the exception of one patient who was treated with 2 cycles for early stage disease. Patients with Hodgkin lymphoma received split dosing (doxorubicin 25mg/m^2) every 2 weeks for 12 doses and patients with breast cancer received epirubicin (100mg/m^2) every 3 weeks for 3 cycles.

3.4.5 Cardiotoxicity from Anthracycline Therapy

3.4.5.1 Incidence of Asymptomatic Cardiotoxicity

The primary end point of cardiotoxicity (LVEF decline of ≥10% to ≤55%) was met by 12 patients (40%) during the study. However, 5 patients (17%) recovered to the normal range by 12 months leaving just 7 (23%) with a persistent decline. 17 patients (57%) had a fall of ≥ 10% points from baseline but 6 patients (20%) showed an improvement by 12 months. 5 patients (17%) had clinical LV dysfunction with a LVEF <50% by the end of study but all were asymptomatic with no symptoms of heart failure. 5 patients (17%) were unable to attend for the final 12 months scan and 3 of them had a fall of ≥10% to ≤55% following chemotherapy. The greatest drop seen was an absolute decline of 28% to an LVEF of 31%

post treatment in one patient who remained asymptomatic. Only 13 patients (43%) had no significant decline in LVEF during the study (**Table 7**).

End point	Number (%)
Primary	
LVEF decline to ≤ 55% by ≥10% (at any point)	12 (40)
Secondary	
LVEF decline by ≥10% from baseline (at any point)	17 (57)
LV dysfunction LVEF ≤50% (end of study)	5 (17)
Cardiac event	4 (13)

Table 7. Study end points – decline in LVEF

3.4.6 Determining Cardiotoxicity for Analysis of Exploratory Biomarkers

The clinical parameters and exploratory imaging/circulating biomarkers and were evaluated against all end points to investigate possible relationships and associations that could give insight into the nature of anthracycline toxicity and highlight potential biomarkers as prognostic or predictive markers. Due to the small number of patients meeting the primary end point of LVEF decline of ≥10% to ≤55% and the low rate of clinical events during the 18 month study the secondary end point of LVEF decline of ≥ 10% was used for evaluation of circulating biomarkers and exploratory imaging parameters.

3.4.6.1 Left Ventricular Function Declined with Anthracycline Therapy

The mean (and median) left ventricular ejection fraction (LVEF) fell during and after anthracycline therapy from a baseline of 64 (63)% to 59 (60)% mid treatment, 55 (56)% directly after treatment and 57 (58)% at one year (**Figure 22**). The mean decline in LVEF was statistically significant at the first scan (mid-treatment $p=0.01$) and dropped by a peak of 9% directly after therapy ($p<0.0001$) however the population LVEF remained in the normal range (55-70%) throughout the study.

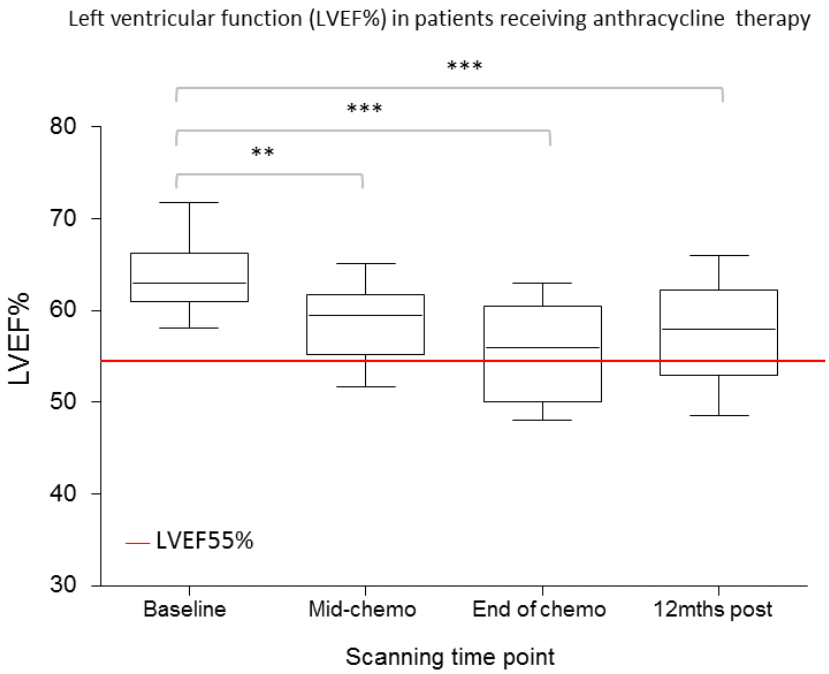

Figure 22. Box and whisker plot showing longitudinal LVEF measurements in patients receiving anthracycline chemotherapy. *Whiskers represent the 5-95% confidence intervals and significance was testing using one way ANOVA with post analysis multi-comparison testing, p<0.0001*** and **p<0.01.*

3.4.6.2 Identification of Three Different Populations

Within the whole population there were three groups of patients with differing behaviour of LVEF; patients with a persistent decline in LVEF (of ≥ 10%), patients with a transient fall in LVEF recovering by 1 year and patients with very little change in LVEF. 5 patients were unable to attend for the final cardiac MRI scan at 1 year due to cancer progression or patient choice (**Figure 23**).

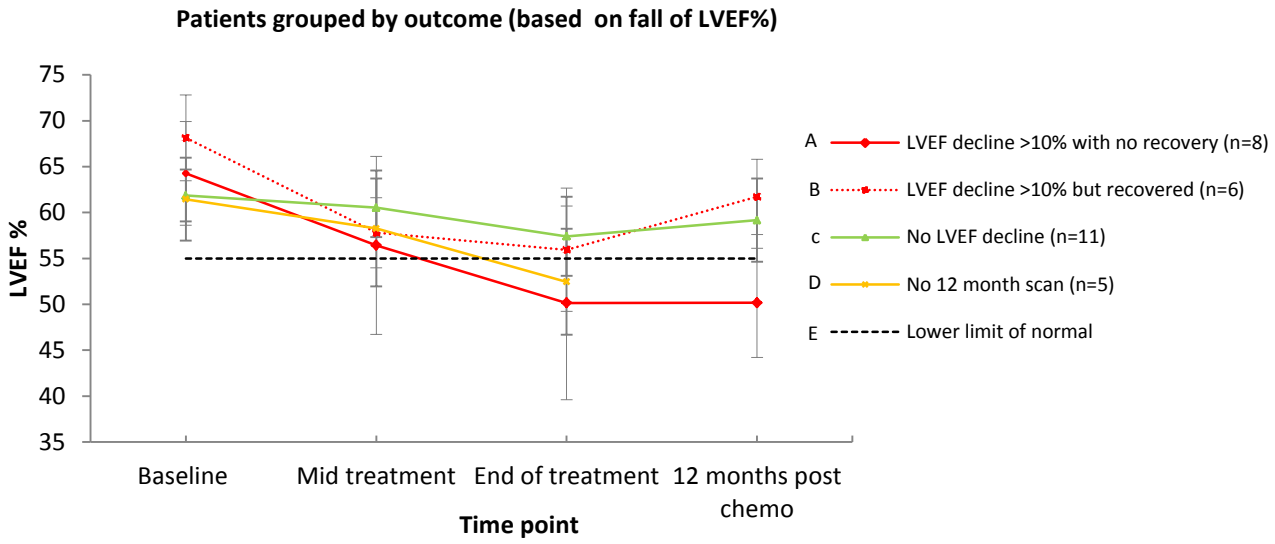

Figure 23. Differing behaviour of LVEF decline with anthracycline therapy. *A, patients with sub-clinical cardiotoxicity (LVEF decline of ≥10%) at 12 months (p=0.003). B, patients with transient sub-clinical cardiotoxicity (LVEF decline of ≥10%) but recovered at 12 months (p=0.01). C, patients with no sub-clinical cardiotoxicity (decline in LVEF p=ns). D, patients unable to attend for final cardiac assessment. The error bars represent the standard deviation of the mean and significant decline was measured by one way ANOVA.*

3.4.6.3 Development of Clinical Cardiac Events

Four patients had a clinical cardiac event within 18 months of starting therapy. Three were diagnosed with supraventricular arrhythmias (two tachy-arrhythmia and one brady-arrhythmia) during treatment. Two patients were switched to non cardiotoxic chemotherapy regimens but one was able to continue doxorubicin following specialist cardiology input. The fourth patient had a myocardial infarction (MI) 10 months after completing chemotherapy. Only the patient who suffered the MI had a significant and sustained fall in LVEF (from 58% to 52% to 47%) and the initial decline occurred prior to the MI. The other patients showed no significant change in systolic function. All four received doxorubicin but the patients with arrhythmias only received 2-3 cycles before they occurred. One patient had previously been treated with non-cardiotoxic chemotherapy but none had radiotherapy. **Table 8** shows the clinical characteristics of the patients who had cardiac events.

Event nature	Time to event (wks from start)	Gender	Anthracycline	Anthracycline stopped	Dose (mg/m2)	LVEF decline prior to event?	Previous chemo
Bradycardia/AF	12	M	Doxorubicin	Yes	210	No	No
SVT	9	F	Doxorubicin	Yes	150	No	Yes
SVT	6	F	Doxorubicin	No	295	No	No
MI	60	M	Doxorubicin	N/A	300	Yes	No

Table 8. Clinical cardiac event characteristics. *(AF = atrial fibrilation, SVT = supraventricular tachycardia, MI = myocardial infarction)*

3.4.7 Clinical Prognostic Factors

3.4.7.1 Who is Getting Cardiotoxicity?

The mean age of patients with a significant decline in LVEF was marginally higher than patients who maintained their LVEF (60 years versus 57 years) but the difference was not statistically significant (p=0.4) and age was not prognostic. The mean baseline systolic blood pressure was higher in patients with a significant fall in LVEF (140mmHg versus 131mmHg) but again this was not statistically significant. None of the baseline clinical factors were strongly associated with decline in LVEF including gender, abnormal baseline ECG, body mass index, smoking, previous chemotherapy and hypertension. A pre-existing diagnosis of hyperlipidaemia was weakly associated with decline in LVEF (p=0.08). The presence of one or more pre-existing risk cardiovascular risk factors (including hyperlipidaemia) showed only a weak association with decline in LVEF (p=0.09). The only clinical factor found to have potential prognostic value was the anthracycline dose. The mean dose of anthracycline received in patients who developed cardiotoxicity was 271mg/m^2 compared to 250mg/m^2 in patients without cardiotoxicity and a higher total cumulative dose of anthracycline was associated with a significant fall in LVEF (p=0.02 for an LVEF decline ≥10%). The characteristics of patients with a significant LVEF decline are shown in **Table 9** and explored further in the following section 3.4.7.2.

Clinical factors	LVEF fall by ≥ 10% at all		Significance
	No (n=13)	Yes (n= 17)	Chi sq p =
Age (mean in yrs)	57	60	0.4
Gender Male (no. of pts)	4	10	0.13
Female (no. of pts)	9	7	
Pre-existing cardiac risk factor (no. of pts)*	6	14	0.09
Baseline systolic pressure (mean mmHg)	131	140	0.7
- Smoking (current or ex-smoker)	5	10	0.5
- HTN	3	4	0.7
- Hyperlipidaemia	1	6	0.08
Body mass index	28	27	0.9
Abnormal ECG (no. of pts)	4	7	0.6
Previous chemo (no. of pts)	1	2	1
Anthracycline dose (mean mg/m^2)	230	274	0.02 (dose> 280mg/m^2)

Table 9. Clinical characteristics of patients with LVEF decline. **Previous cardiac event, strong family history (FH) of myocardial infarction (MI), diabetes, hypertension (HTN), hyperlipidaemia, obesity, smoking.*

3.4.7.2 Dose Related Cardiotoxicity

Receiver operator curve (ROC) analysis was used to determine the optimum cut off dose separating good and poor prognosis patients (Figure 24). A dose of 280mg/m^2 resulted in a sensitivity of 82% and specificity of 62%. The incidence of cardiotoxicity (LVEF fall of ≥10% to ≤55%) in patients who received over 280mg/m^2 was 63% (12/19) compared to 36% (4/11) in patients receiving ≤ 280mg/m^2 but this was not statistically significant (p= 0.2). However, when looking at LVEF decline by ≥ 10% as a secondary end point there was a significant difference between patients who received over and under 280mg/m^2 (p=0.02). Univariate Kaplan Meier analysis showed a significant difference between patients receiving under and over 280mg/m^2 (**Figure 25**, p=0.027). The groups were equally matched for age and the presence of pre-existing risk factors.

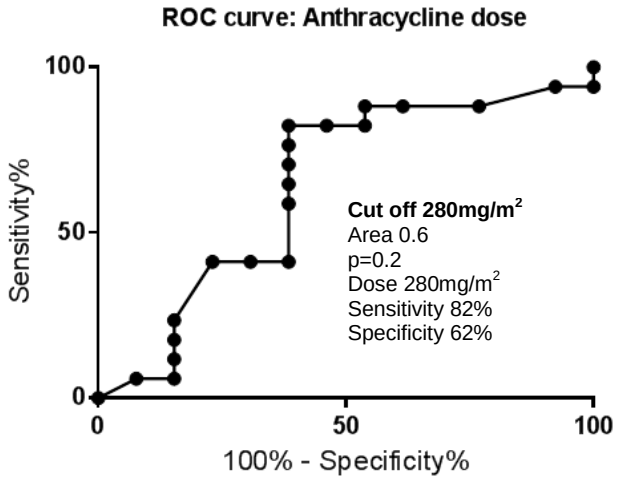

Figure 24. Receiver operator curve to determine the optimum sensitivity and specificity of anthracycline dose as a prognostic marker

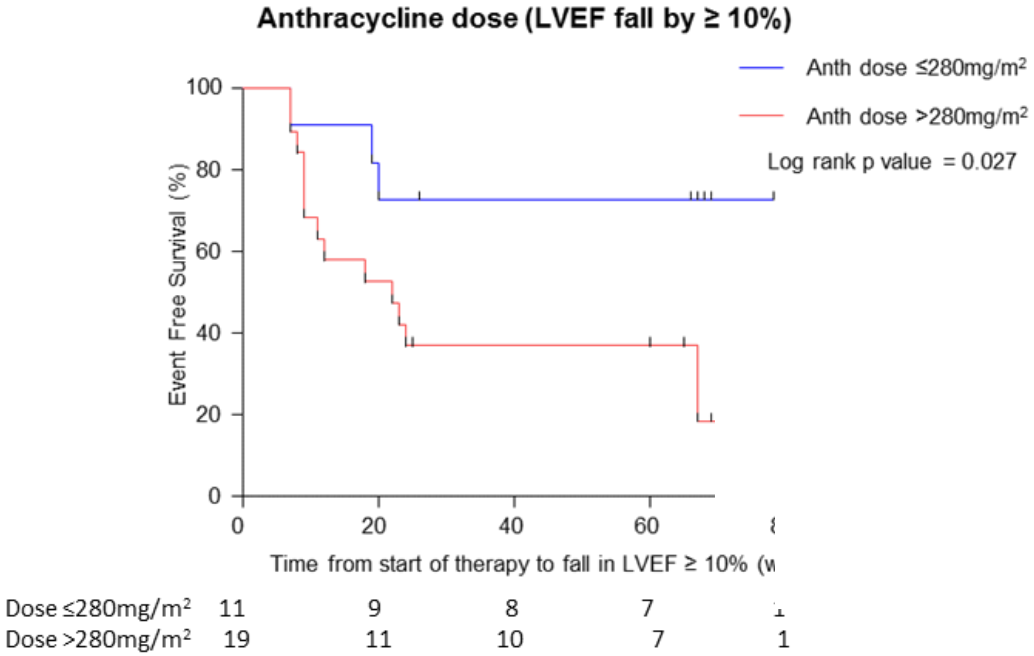

Figure 25. Cumulative cardiac event rate (LVEF fall by ≥10%) in two groups stratified by cumulative total dose of anthracycline

3.4.8 Volumetric Analysis

3.4.8.1 Baseline LVEF

Baseline LVEF correlated with peak LVEF decline (**Figure 26**) showing that patients with higher baseline LVEF had a greater decline in LVEF (Pearson coefficient =0.5, p=0.01). Univariate Kaplan Meier analysis of patients grouped according to baseline LVEF (split at the median, 63%) also showed a significant difference in LVEF decline. Only 5/16 (31%) patients with an LVEF below 63% had a drop of ≥ 10% compared to 12/14 (86%) patients with baseline LVEF above 63% (**Figure 27**).

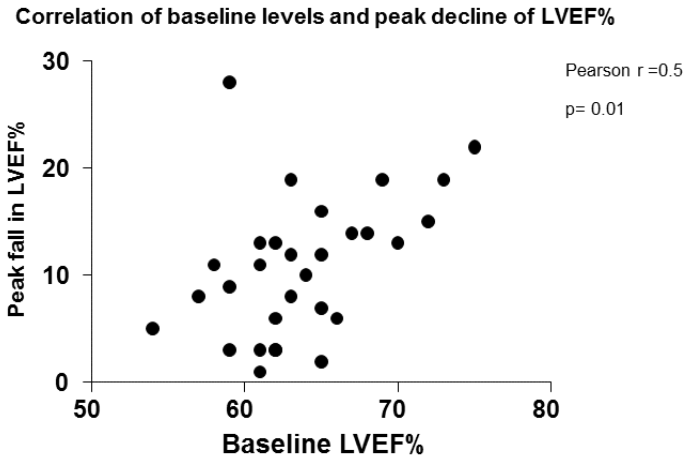

Figure 26. Correlation of baseline LVEF and absolute decline in LVEF

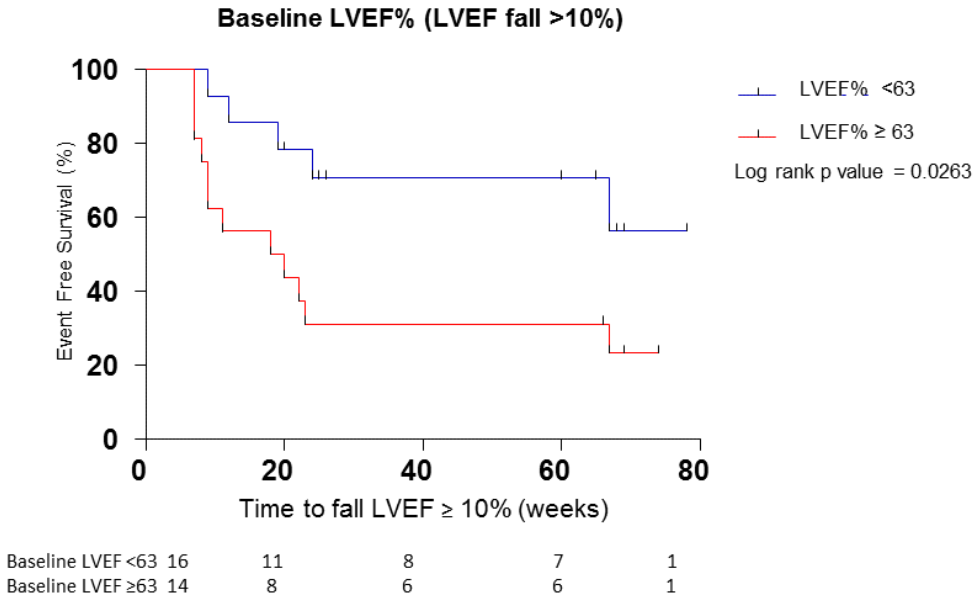

Figure 27. Cumulative cardiac event rate (LVEF decline by ≥10%) in patients stratified by baseline LVEF (cut off 63%)

3.4.8.2 Left Ventricular Volumes

The overall decline in LVEF resulted from a significant increase in left ventricular end systolic volume over time (**Figure 28**). End diastolic volume remained the same until 12 months when there was slight increase that was not statistically significant. Stroke index fell during treatment and reached a low of 41ml/min/m^2 directly post therapy and cardiac output also fell to 2.9l/min/m^2 at the end of treatment however neither fall was statistically significant. There was no change in LV mass during the 18 month study (**Table 10**).

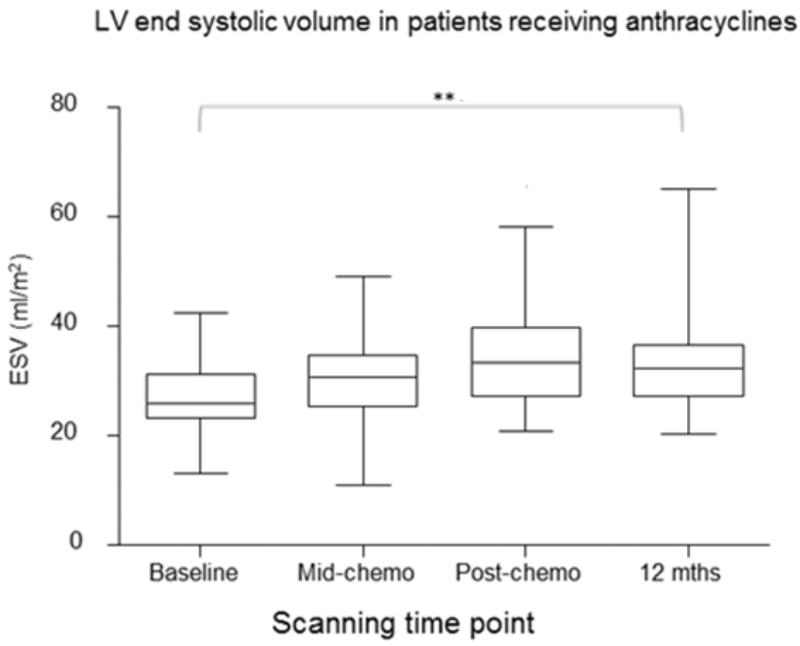

Figure 28. Box and whisker plot showing longitudinal LV end systolic volume measurements in patients receiving anthracycline chemotherapy *(whiskers represent the 5-95% confidence intervals and significant change was measured using one way ANOVA, **p=0.02)*

Cardiac imaging parameter (volumetric)	Baseline Mean (SD)	Mid-chemo Mean (SD)	End of chemo Mean (SD)	12 months post Mean (SD)	ANOVA
Pt number	30	28	29	24	N/A
LV mass (g/m^2)	48.81 (13)	46.92 (11)	46.25 (11)	46.90 (7)	ns
End diastolic volume(cc/m^2)	141.6 (37)	136.4 (41)	137.8 (39)	153.2 (45)	ns
End systolic volume (cc/m^2)	27.75 (8)	30.60 (9)	34.23 (9)	34.59 (10)	p=0.02
Stroke Index (SI ml/m^2)	48.22 (9)	42.83 (11)	40.65 (13)	44.63 (9)	p=0.05
Cardiac Index (CO l/min/m^2)	3.32 (0.7)	3.2 (0.6)	2.9 (0.6)	3.0 (0.8)	ns

Table 10. Longitudinal volumetric and functional analysis in patients receiving anthracycline chemotherapy *(significance value were calculated using a one way ANOVA with post analysis multi-comparison testing)*

3.4.9 Diastolic Function

3.4.9.1 E/A Ratio

Diastolic function declined in a similar manner to systolic function with the E/A ratio falling during and directly post chemotherapy but improving slightly after 12 months (**Figure 29**). However, the mean E/A ratio remained in the normal range (1-2) throughout and the change was not statistically significant. The E/A ratio is a crude measure of filling efficiency, in that if both early and late diastole filling velocities decrease proportionally, the ratio will not alter. Therefore, the velocities were also plotted separately at each time point to explore diastolic behaviour in more detail. This showed that both early and late filling velocities initially declined during chemotherapy resulting in very little change in the E/A. Directly after chemotherapy both velocities increased again but the A wave (late filling velocity) became higher than baseline suggesting an element of impaired LV relaxation. These changes normalised by 12 months but there was still a small but proportional decline from baseline in early and late filling suggesting less efficient ventricular filling.

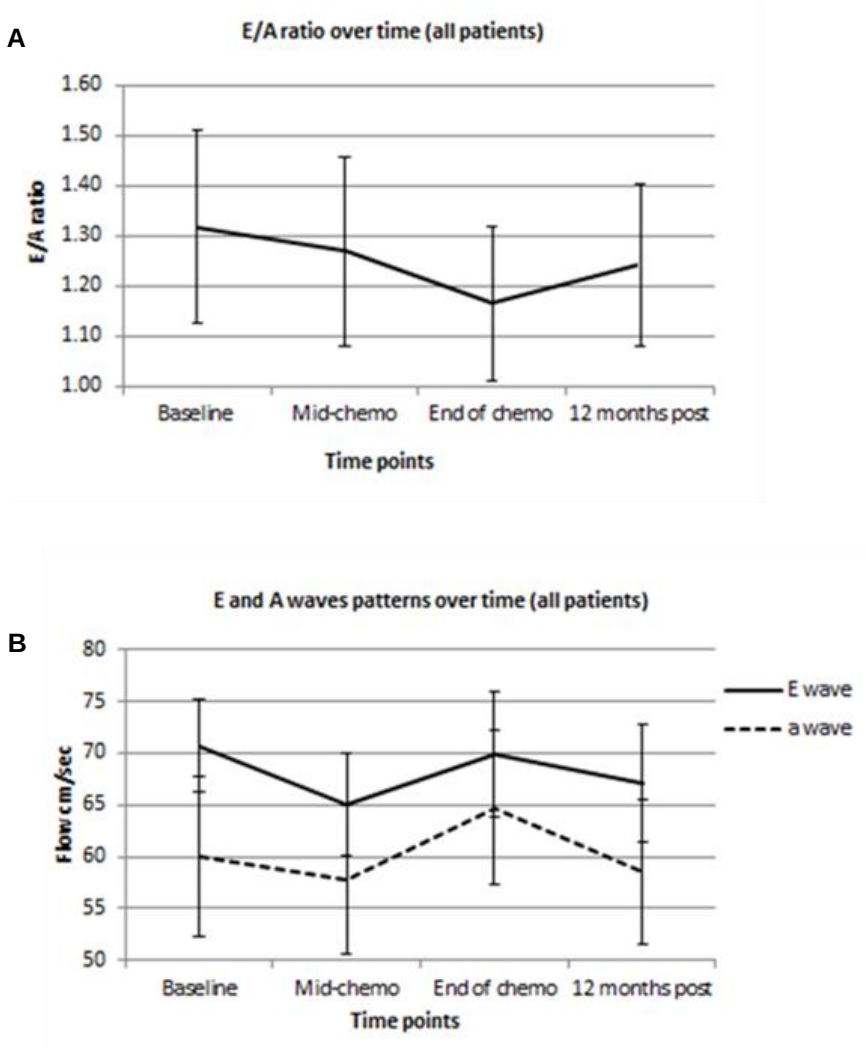

Figure 29. Longitudinal E/A ratio (A) and E and A wave (B) measurements in patients receiving anthracycline chemotherapy (error bars represent the standard deviation of the mean). *The mean E/A ratio fell during and shortly after therapy but remained in the normal range. Plotting the E and A waves separately suggests that LV relaxation may be impaired directly post anthracycline.*

The behaviour of E/A was explored further by looking at fold change from baseline in three subpopulations grouped by final decline in LVEF i.e. persistent fall in LVEF of ≥10%, transient fall in LVEF ≥10% and no fall in LVEF. Patients with no 12 month scan were grouped based on their end of treatment scan. This showed that there was little change from baseline in patients with little or transient LVEF decline but there was a greater fall in E/A ratio in patients with a persistent fall in LVEF (**Figure 30** & **Table 11**). However groups overlapped and the difference was only significant at the mid-chemotherapy.

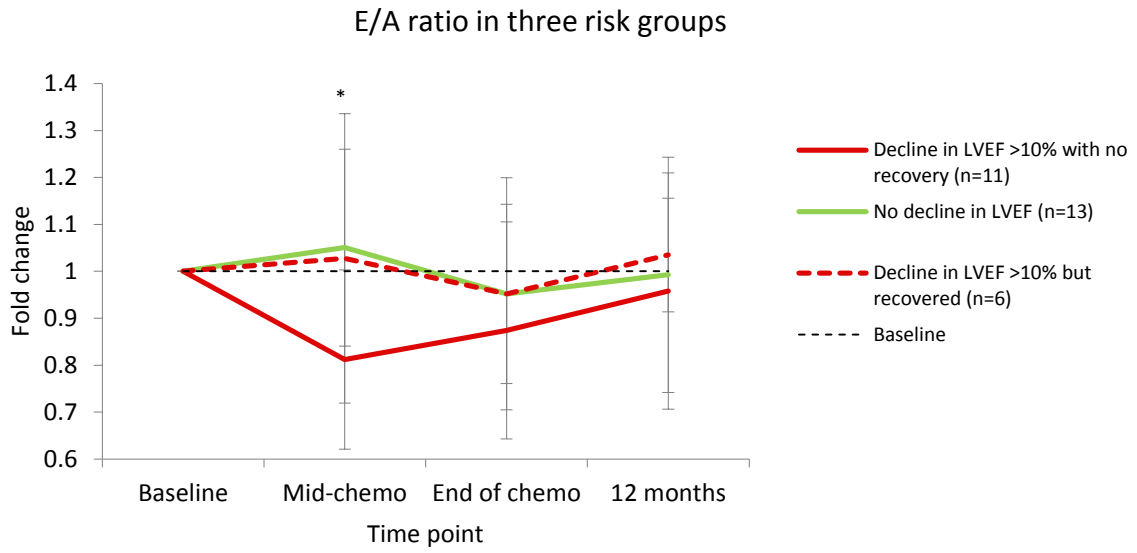

Figure 30. E/A ratio in patients grouped by decline in LVEF. *Fold change in E/A ratio was significant at the mid-point for patients with persistent LVEF decline (*p=0.02 using paired t test from baseline)*

3.4.9.2 Change in Left Atrial Volume

Impaired relaxation can result in atrial dilation and the histological findings from the pre-clinical rat model suggested that damage was more marked in the atria. Atrial volumes were therefore estimated at each time point to assess for dilation suggestive of damage but there was no significant longitudinal change in left atrial (LA) volume in the whole population or in subgroups based behaviour of LVEF (**Table 11**).

Cardiac imaging parameter (diastolic)	**Baseline Mean (SD)**	**Mid-chemo Mean (SD)**	**End of chemo Mean (SD)**	**12 months post Mean (SD)**	**ANOVA (p=)**
Pt number	30	28	29	24	NA
E/A ratio	1.32 (0.53)	1.27 (0.53)	1.17 (0.43)	1.24 (0.45)	ns
E wave	70.7 (12.5)	65.0 (13.7)	69.8 (16.9)	67.2 (15.9)	ns
A wave	60.0 (21.5)	57.8 (19.9)	64.7 (20.7)	58.5 (19.3)	ns
Left atrial volume (cc/m^2)	34.97 (12)	32.40 (11)	29.40 (11)	34.46 (13)	ns

Table 11. Mean diastolic parameters in patients receiving anthracycline chemotherapy *(significance was tested using ANOVA with post analysis multi-comparison testing)*

3.4.10 Tissue characterisation

3.4.10.1 Global Myocardial T1 and ECV Fraction Estimation

Pre contrast T1 values represent longitudinal relaxation of the myocardial tissue and are longer in damaged or scarred tissue. Paramagnetic contrast agents shorten the T1 time and in the presence of scarring shorten it even further as contrast is held in the extracellular space. T1 values were measured pre and post gadolinium to quantify the extracellular volume and determine whether expansion occurred during the development of cardiotoxicity. The ECV was calculated using haematocrit to correct for signal generate from the blood in the myocardial vasculature. There was very little dynamic change in native T1 values pre or post contrast over time (**Figure 31** & **Table 12**). Behaviour of T1 pre and post contrast did not differ significantly between subgroups based on LVEF decline but post contrast T1 values fell slightly in patients who had a persistent or transient decline in LVEF whereas they increased in patients who maintained LV function. No association was seen between baseline pre or post contrast T1 values and LVEF decline. Similarly, there was no significant change in ECV with treatment in the whole population however, a slight increase in ECV was seen post treatment (**Figure 31c**).

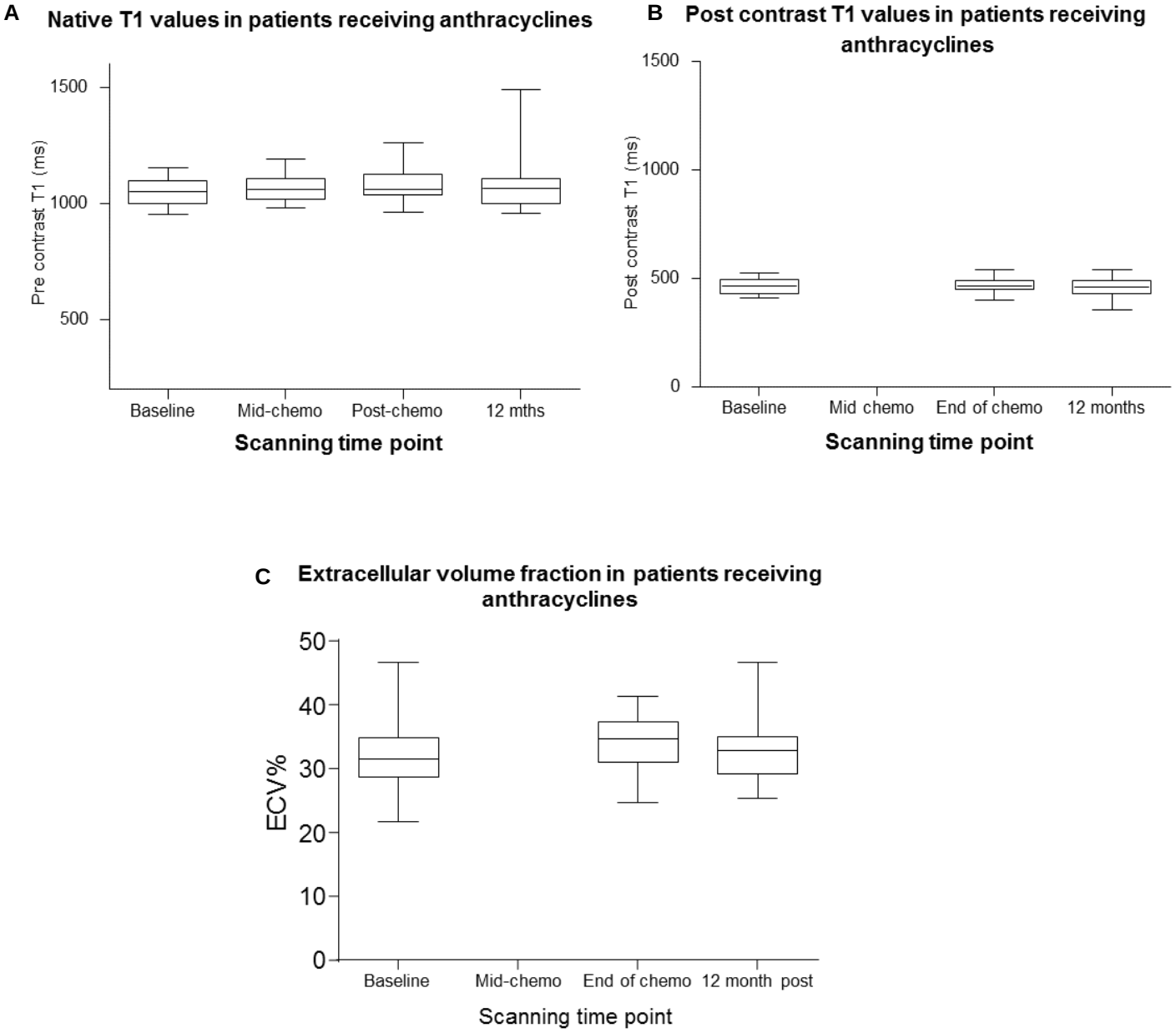

Figure 31. Mid slice myocardial native T1 (A), post contrast T1 measurements (B) and ECV values (C) in patients receiving anthracycline chemotherapy *(whiskers represent the 5-95% confidence intervals).*

Cardiac imaging parameter (mapping)	Baseline Mean (SD)	Mid-chemo Mean (SD)	End of chemo Mean (SD)	12 months post Mean (SD)	ANOVA
Pt number	30	28	29	24	N/A
Myocardial native T1 value (ms)	1052 (58.04)	1064 (52.85)	1079 (66.95)	1074 (107.2)	ns
Myocardial post contrast T1 value (ms)[$]	462.9 (36.4)	NA	466.2 (29.9)	454.4 (42.3)	ns
Myocardial ECV[$]	31.74 (5.5)	N/A	34.10 (4.5)	32.56 (4.6)	ns

Table 12. Pre and post-contrast T1 values and ECV estimation at each time point. *The population mean values are shown and significant change from baseline was tested by one way ANOVA with post analysis multi-comparison testing. [$]one patient was unable to have contrast due to falling renal function therefore the patient numbers were n-1 for post contrast and ECV scans.*

3.4.10.2 Subgroup Analysis of ECV

When subgroup analysis of the ECV data was performed, a significant fold increase in ECV over time was seen in patients who had a persistent decline in LVEF of ≥10% (p=0.02 using ANOVA with multi-comparison post testing) whereas patients who maintained LV function or had a transient fall of >10% had no significant change in ECV (**Figure 32**).

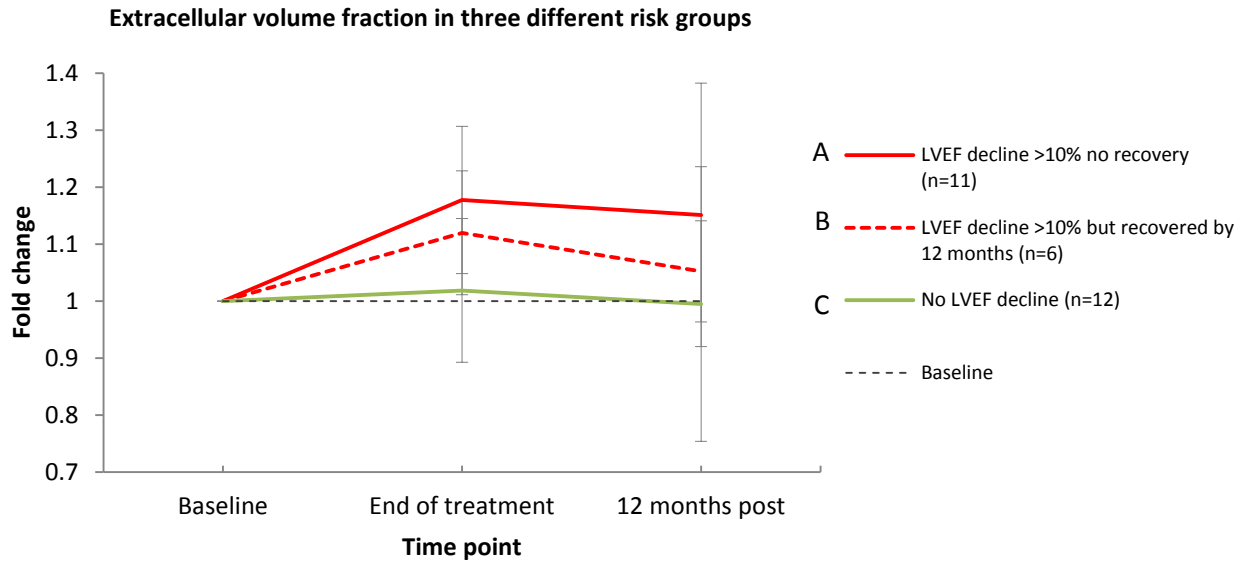

Figure 32. Fold change in ECV in patient subgroups based on LVEF decline. Error bars represent the standard deviation of the mean. Patients with persistent LVEF decline (A) had a *baseline mean ECV of 29% which increased significantly to 34% at the end of chemotherapy and 35% at 12 months (p=0.02). Patients with transient LVEF decline (B) had a baseline mean ECV of 31% which increased to 35% directly after chemotherapy and*

recovered to 32% at 12 months (p=ns). Patients with no significant LVEF decline (C) had a baseline ECV of 35%, which was 34% after therapy and dropped to 30% at 12 months (p=ns).

Univariate Kaplan Meier analysis showed that patients with a peak ECV change from baseline of > 2% (derived using ROC analysis, **Figure 33**a) did worse than patients with very little change in ECV (log rank 0.005) (**Figure 33**b). However, sensitivity and specificity of peak change at a cut off of 2% in ECV was relatively low (59% and 75% respectively). The mean age of patients in the group with a greater peak change in ECV was slightly higher (63 years versus 52 years) but age was not significantly associated with decline in LVEF and was therefore unlikely to be a confounding factor. The mean dose of anthracycline was similar (258mg/m^2 versus 256mg/m^2) however the proportion of patient with pre-existing cardiovascular risk factors was higher in the group with a greater change in ECV which may have been a confounding factor (46% compared to 82% of patients in the poor outcome group). When the analysis was re-run stratifying patients for pre-existing cardiovascular risk factors the difference between groups was no longer significant however there was still a trend to suggest that patients with a greater increase in ECV with treatment did worse (p =0.19, **Figure 34**). Patient numbers were too small to carry out formal multivariate analysis.

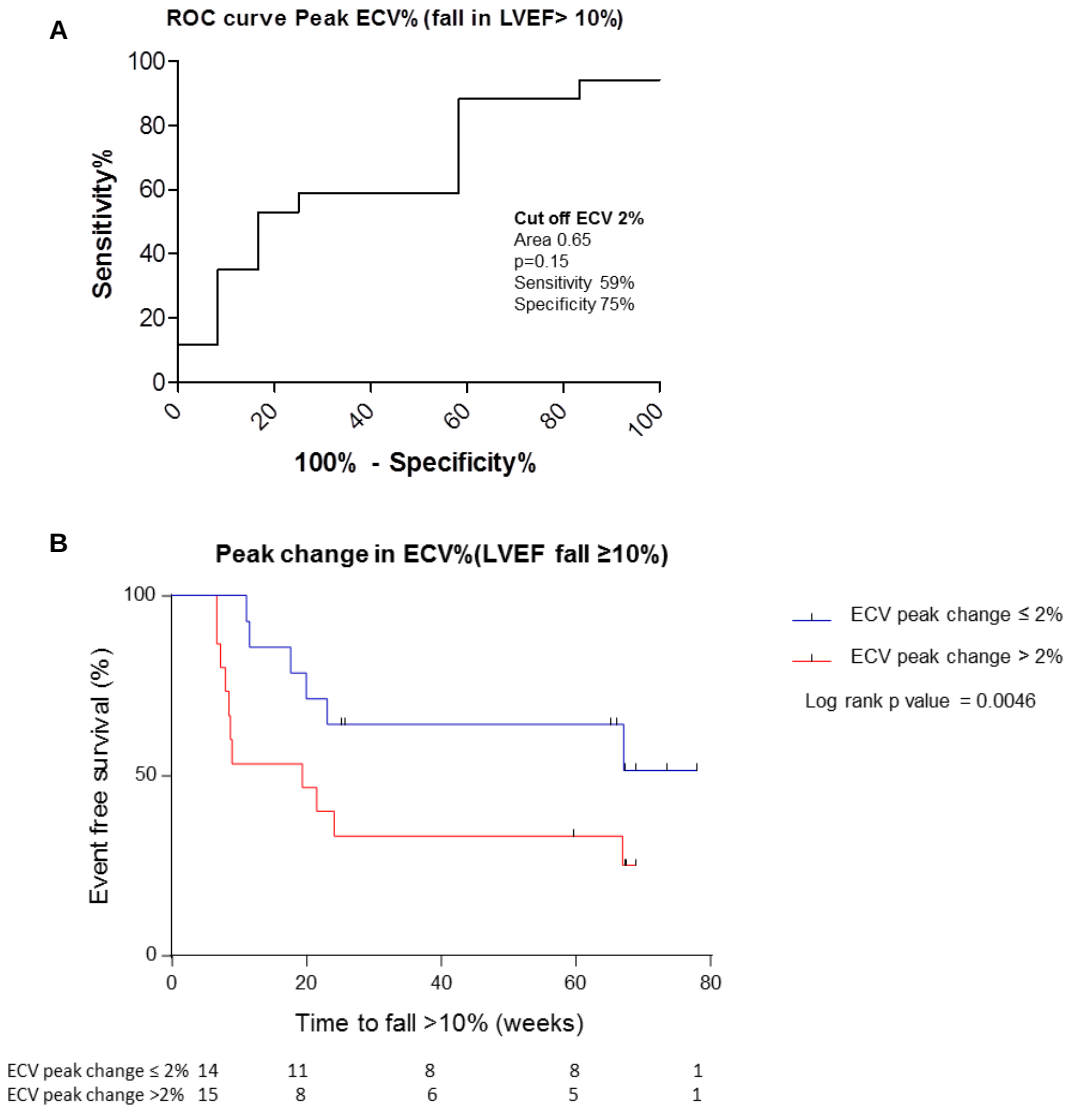

Figure 33. Receiver operator curve analysis to determine the optimum sensitivity and specificity of peak change in ECV as a prognostic marker (A) and cumulative cardiac event rate fall in (LVEF ≥ 10%) in patients stratified by peak change in ECV (B)

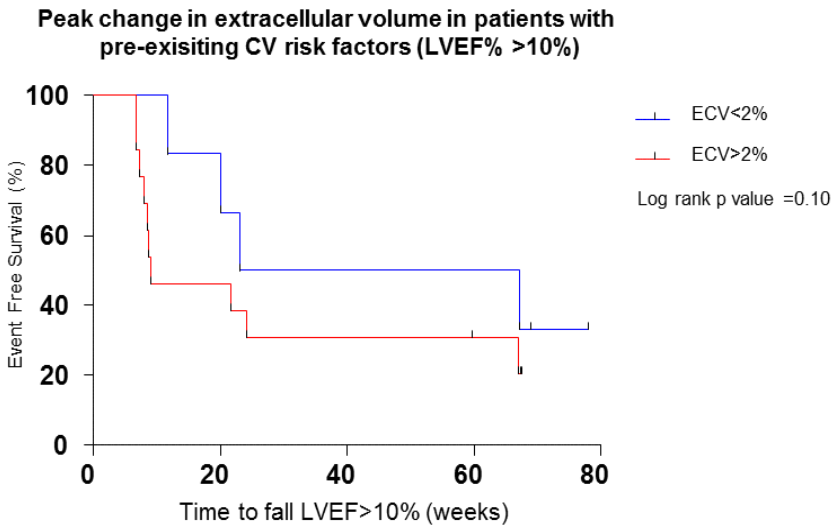

Figure 34. Cumulative cardiac event rate fall in (LVEF ≥ 10%) in patients with pre-existing cardiovascular risk factors stratified by peak change in ECV

3.4.10.3 Myocardial Extracellular Volume Fraction (ECV) as a Baseline Marker

It was hypothesised that patients with a higher baseline ECV, suggestive of pre-existing fibrosis, may be at greater risk of cardiotoxicity. In fact, the opposite was seen in this study. Baseline ECV fraction correlated negatively with peak LVEF decline (Spearman r= -0.6, p=0.0005) and patients with a lower baseline ECV appeared to do worse than patients with a higher ECV (**Figure 35**b). Patients with an LVEF decline of ≥ 10% during treatment had a mean ECV of 29% whereas patients with maintained LV function had a mean ECV of 37%. However, as expected lower baseline LVEF correlated with higher ECV values (**Figure 35a**).

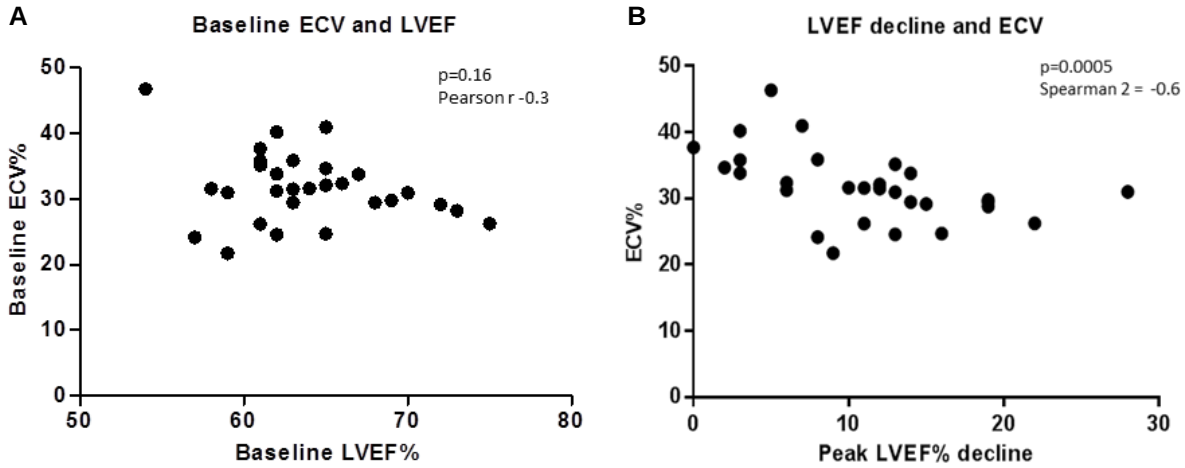

Figure 35. Correlation of baseline ECV and baseline LVEF (A) and baseline ECV and peak fall in LVEF (B)

Receiver operator curve (ROC) analysis was used to derive a cut off for ECV and a value of ≤33% gave a sensitivity of 88%, specificity of 75% (p=0.01) (**Figure 36**a). Patients were split into lower ECV and higher ECV groups using this cut off and a higher incidence of sub-clinical cardiotoxicity (LVEF decline ≥10%) was seen in patients in the lower ECV group, 79% (15/19) and 20% (2/10) respectively. Univariate Kaplan Meier analysis showed that there was a significant difference between the two groups (log rank 0.0078, **Figure 36**b) suggesting ECV has the potential to be a baseline prognostic marker. The groups were equally matched for age and pre-existing risk factors but the dose of anthracycline received in patients in the low ECV group was higher (means 276mg/m^2 and 219mg/m^2). The analysis was therefore re-run stratifying for anthracycline dose and although the difference between groups was no longer significant due to small patient numbers (p=0.17) there was still a trend towards patients with lower ECV having a worse outcome (**Figure 37**). Patient numbers were too small to carry out formal multivariate analysis.

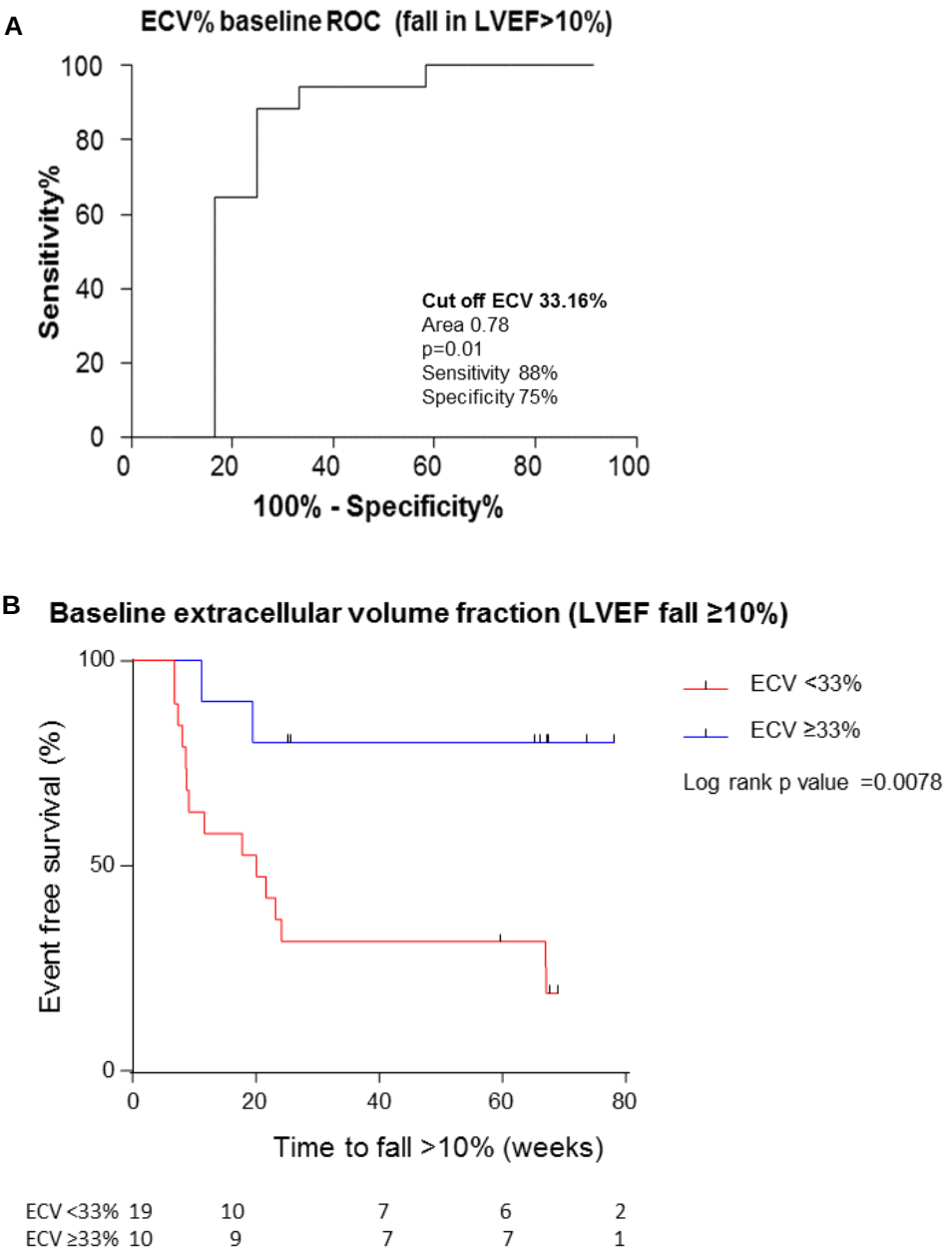

Figure 36. Receiver operator curve to determining the sensitivity and specificity of baseline ECV as a prognostic marker (A) and cumulative cardiac event rate (fall in LVEF ≥ 10%) in patients stratified by baseline ECV (all patients) (B)

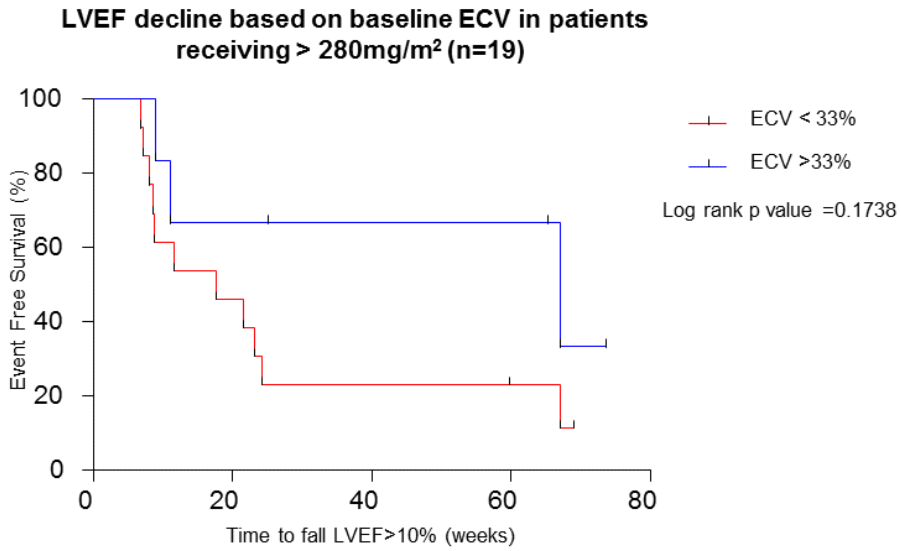

Figure 37. Cumulative cardiac event rate in patients receiving >280mg/m^2 stratified by baseline ECV

3.4.10.4 Late Gadolinium Enhancement

Late gadolinium enhancement was performed to look for areas of discreet localised myocardial fibrosis. One patient was found to have a small area of localised enhancement at baseline suggestive of a previous infarction despite having no history of prior cardiac events. This area remained unchanged during treatment and localised fibrosis was not seen in any of the other patients prior to or after treatment.

3.4.10.5 T2 Mapping for Assessment of Myocardial Oedema

T2 measurements are generated by the fluid content of a tissue therefore T2 mapping was performed to quantity myocardial oedema as it was hypothesised that cardiotoxicity may occur, in part due to a myocarditic process. A trend showing slightly higher T2 values directly post anthracycline therapy was seen but T2 values did not change significantly with time in the whole population or in the 3 subpopulations based on decline in LVEF (Figure 38). The baseline prognostic potential of T2 mapping was also assessed but no relationship between baseline T2 values and LVEF decline or cardiac events was seen. Figure 39 shows examples of the T1 and T2 maps generated from patients.

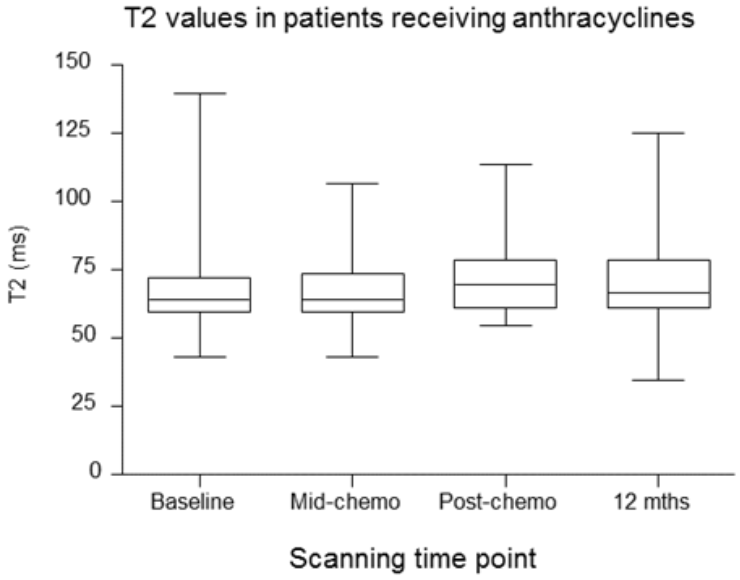

Figure 38. Mid slice T2 estimation in patients receiving anthracycline chemotherapy showed no significant change during or after anthracycline therapy. *Mean myocardial T2 values at baseline were 68.9ms, mid-chemo 68.4ms, end of chemo 72.8ms and 12 months post chemo 70.7ms. Whiskers represent the 5-95% confidence intervals.*

Examples of study cardiac MRI mapping images (**Figure 39**)

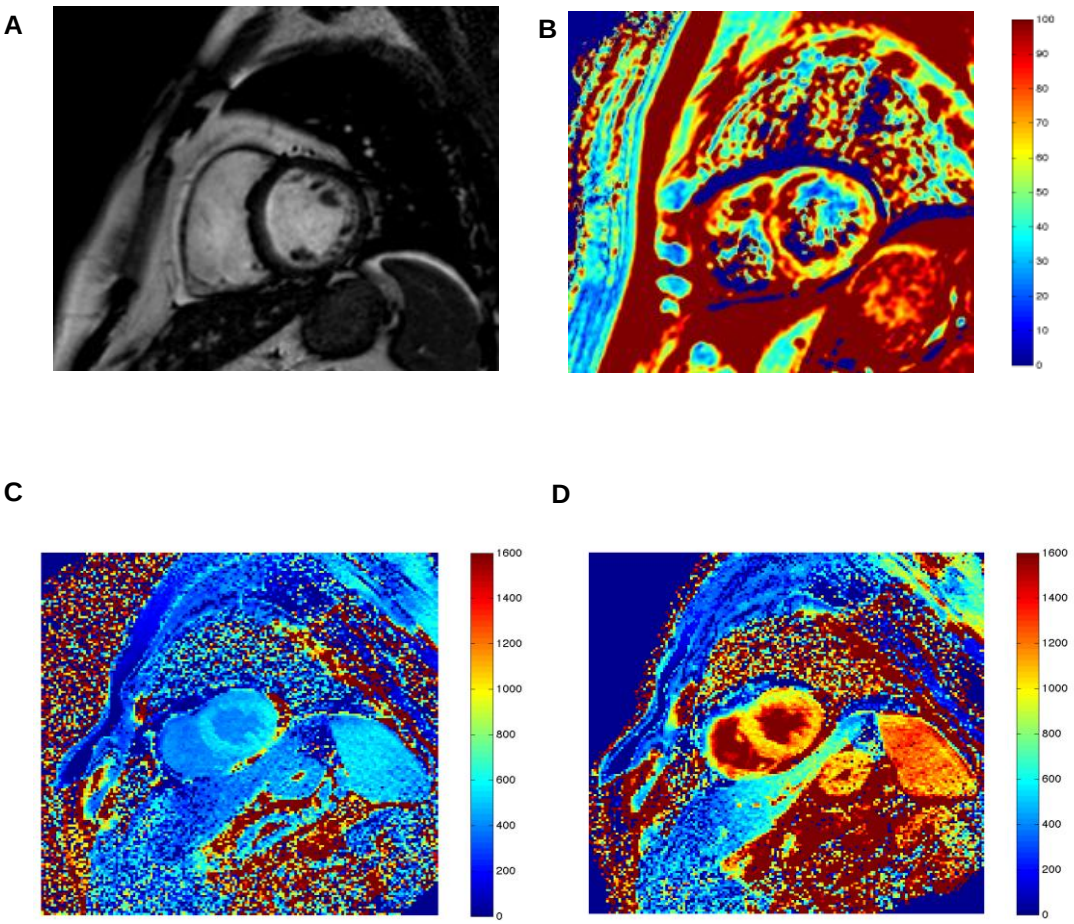

Figure 39. Example of a short axis mid ventricular slice (A), T1 map pre-contrast (B), T1 map post contrast (C) and T2 map (D) of the myocardium

3.4.11 Myocardial Deformation

3.4.11.1 Myocardial Strain

Strain analysis showed significant worsening in both longitudinal and circumferential strain during and after anthracycline chemotherapy. Longitudinal strain estimated by basal latero-septal wall delay, maximal wall to wall delay and the standard deviation of segmental strain all showed a significant increase in dyssynchrony directly after chemotherapy. Maximal longitudinal wall to wall delay continued to worsen at 12 months while the other parameters appeared to improve slightly. Changes in circumferential strain were less marked and only latero-septal wall delay showed a significant change (lengthening) directly after chemotherapy (**Figure 40**). Sub-group analysis showed that patients with a persistent or transient decline in LVEF (≥10%) had a greater fold change in longitudinal wall to wall delay with anthracycline therapy than patients with no decline in LVEF but the difference was not statistically significant (**Figure 41**).

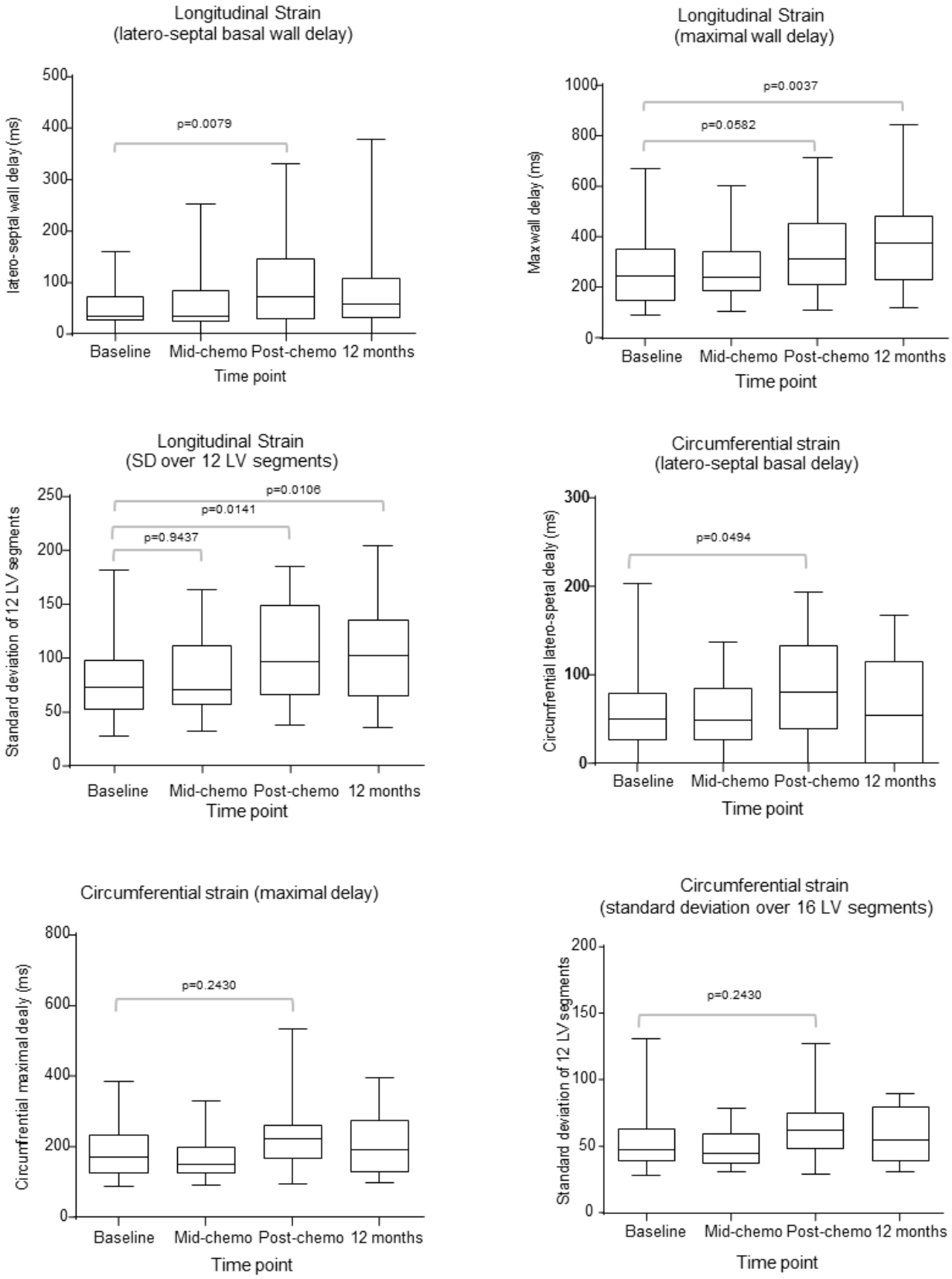

Figure 40. Box and whisker plots showing myocardial strain in patients receiving anthracycline chemotherapy (whiskers represent the 5-95% confidence interval). The p values shown were generated using paired t test compared to baseline.

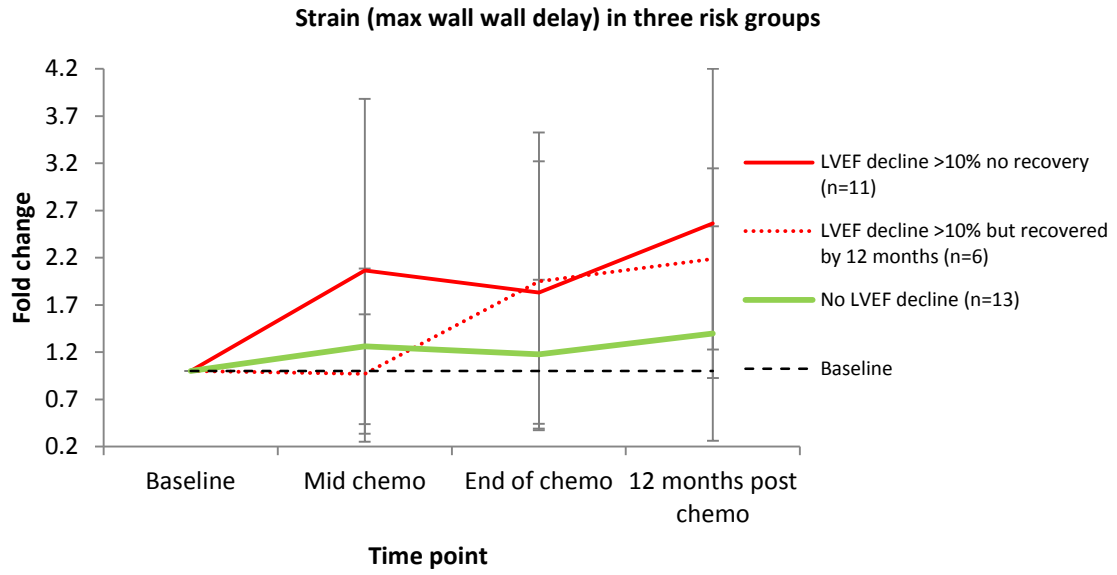

Figure 41. Fold change in longitudinal strain in patients grouped according to decline in LVEF. *A trend towards greater fold change in strain over time was seen in patients with transient or persistent LVEF decline but the changes were not significant (mean values are plotted and the error bars represent the standard deviation of the mean*).

3.4.11.2 Myocardial Strain Rate

Myocardial strain rate did not alter significantly during or after anthracycline therapy. Only one of the six parameters measured showed a marginally significant change post therapy and that was circumferential strain rate measured by latero-septal delay (**Figure 42**). However univariate Kaplan Meier analysis showed that patients with greater longitudinal dyssynchrony at baseline (estimated by maximal wall to wall delay in time to peak strain rate) did worse than patients with less dyssynchrony at baseline. The incidence of LVEF decline (by ≥10%) in patients with a maximum longitudinal wall to wall delay in time to peak strain rate over 207ms (determined with ROC analysis) at baseline was 80% (12/15) compared with 33% (5/15) in patients with a shorter time to peak strain rate (**Figure 43**). The groups were equally match for age, anthracycline dose and pre-existing cardiovascular risk factors.

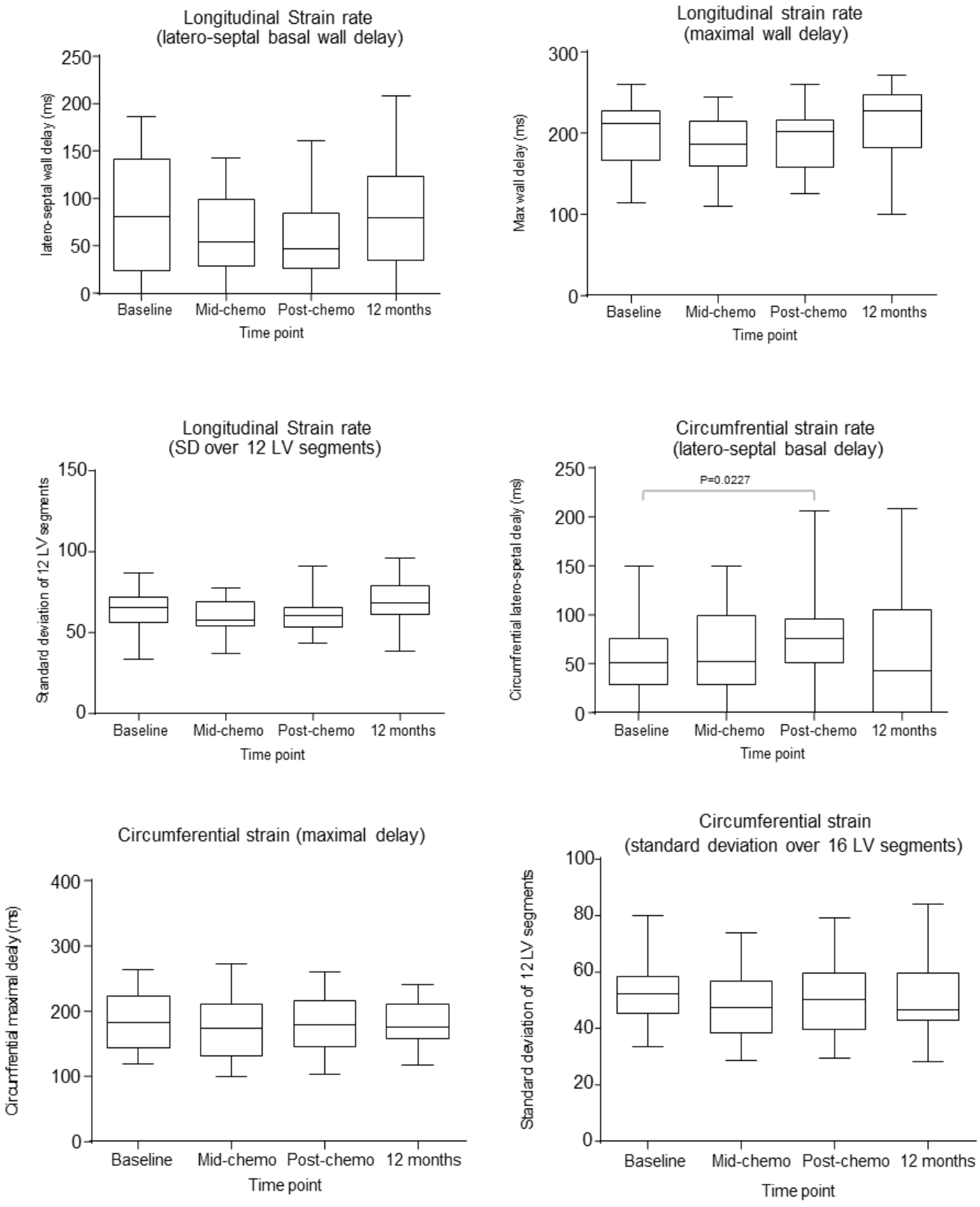

Figure 42. Box and whisker plots showing myocardial strain rate in patients receiving anthracycline chemotherapy (whiskers represent the 5-95% confidence interval and p values were generated using paired t tests)

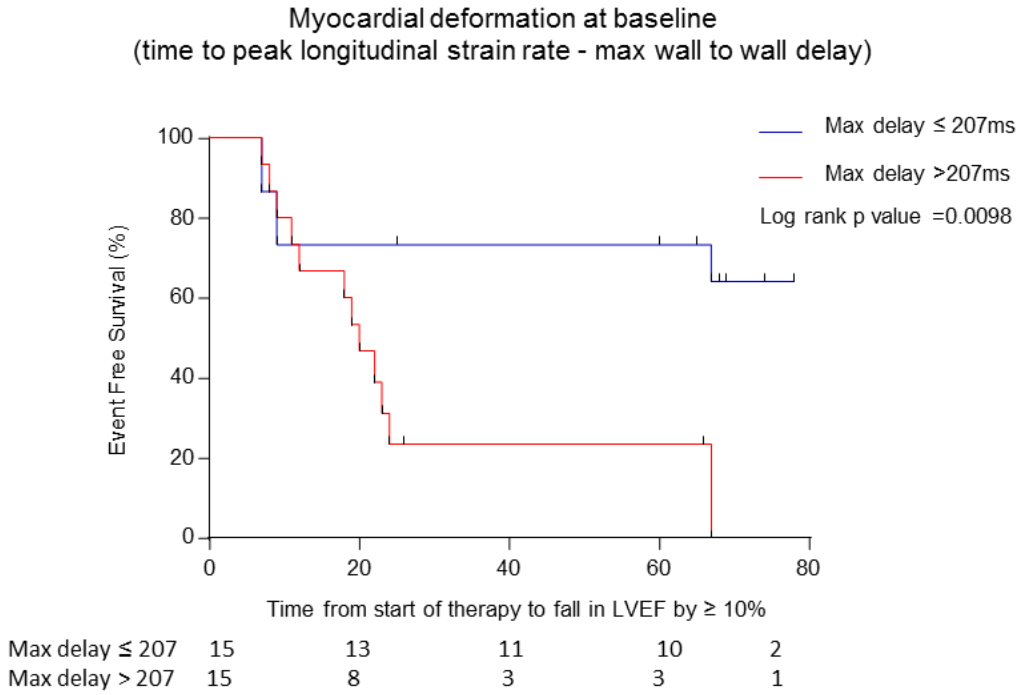

Figure 43. Cumulative cardiac event rate (LVEF fall by ≥10%) in patients stratified by baseline longitudinal strain rate (maximum wall to wall delay in time to peak strain rate)

3.4.12 Summary of Imaging Findings

3.4.12.1 LVEF Decline

The mean and median LVEF declined significantly in patients with anthracycline therapy but within the population there were three identifiable subgroups with differing behaviour in LVEF; patients with persistent decline in LVEF, patients with transient decline and patients with no significant decline. Baseline LVEF correlated positively with peak LVEF decline and counter intuitively suggested that higher pre-treatment LVEFs were associated with a greater decline in LVEF with anthracycline therapy.

3.4.12.2 Clinical Factors

The only clinical factor showing a strong association with decline in LVEF was anthracycline dose. Patients receiving a dose of >280mg/m^2 had a higher rate of LVEF decline and shorter time to LVEF decline than patients receiving lower doses. The presence of pre-existing cardiovascular risk factors (including smoking) was weakly associated with LVEF decline.

3.4.12.3 Imaging Biomarkers

End systolic volume increased with time whereas end diastolic volume remained relatively stable leading to the fall in LVEF. Cardiac output and stroke volume decreased slightly with treatment but recovered by 12 months. LV mass remained the same throughout. Diastolic function, estimated by E/A ratio did not alter significantly with anthracycline therapy despite a slight drop at the end of therapy and no change was seen in left atrial volume. Native T1, ECV fraction estimation and T2 values did not alter with treatment but a lower baseline ECV (under 33%) was associated with worse outcome in terms of LVEF decline. On subgroup analysis, the ECV fraction did increase over time in patients with a significant decline in LVEF and a greater increase in ECV with treatment (>2%) was associated with a higher rate of and time to LVEF decline. The presence of dyssynchrony at baseline measured by maximal longitudinal wall to wall delay was associated with worse outcome in terms of LVEF decline but strain rate did not alter with treatment. Longitudinal strain increased with anthracycline therapy but followed the same time course as decline in LVEF.

3.5 Circulating Biomarkers

Eleven proteins were explored; troponin I, NTproBNP, hFABP, MMP2, MMP9, TIMP1, IL1b, TNFa, IL8, PAPPA and MPO. These biomarkers were chosen following a comprehensive review of the literature and/or their utility in other cardiac conditions. The biomarker panel was chosen to reflect possible pathological processes occurring in anthracycline-related cardiotoxicity and complement the imaging protocol. The clinical biomarker panel was more comprehensive than the pre-clinical panel as rat-specific/compatible assays were not available for all the above proteins. However, in light of the pre-clinical findings troponin I was chosen for the clinical study as it proved to be more informative than troponin T. No significant changes were seen in the other proteins however biomarker time points in the rat model were limited by blood volume and the assays were less robust than human assays therefore none of the other biomarkers were excluded on the basis of the negative pre-clinical findings. The clinical study was designed with multiple circulating biomarker time points (20 in total) in order to capture cumulative changes prior to each dose and transient changes occurring shortly after each bolus. There is very little evidence surrounding optimal timing of biomarker analysis during the development of anthracycline-induced cardiotoxicity as it is not known whether and when all the proteins being investigated are released. Cardinale *et al* have published the most comprehensive body of work on cardiotoxicity biomarkers in humans, particularly the troponins, therefore the sampling schema was designed to incorporate elements of the sampling schedules that they employed [71]. The biomarker proteins were measured using plasma as some of the exploratory proteins such as the MMPs are thought to be released in high amounts following clot formation [179] therefore plasma is more likely to represent a true level of circulating protein.

3.5.1 Circulating Biomarker Methods

3.5.1.1 Measurement of Circulating Biomarkers

As multiple biomarkers were being explored at each time point, multiplex enzyme linked immunosorbant assay (ELISA) was chosen to measure the protein biomarker panel. This technique enables multiple proteins to be measured simultaneously from very small volumes of plasma (as little as 100ul) therefore minimising the volume of blood required from a patient at each time point. The sandwich ELISA technique enables highly specific quantification of each protein [180] to allow accurate detection of changes in a protein during

the development of cardiotoxicity. Multiplex ELISA is an ideal tool for biomarker detection and development in clinical studies as it is time efficient and patient friendly making a realistic technique for translation into clinical practice. It was not possible to plex similar proteins together due to the risk of cross reactivity therefore some of the proteins in the exploratory panel, namely MMP9, MMP2 and NTproBNP were measured as single plexes.
The above biomarkers with the exception of Troponin I were all measured using multiplex ELISAs, validated to GCP for laboratory standards. Troponin I was measured using a clinically validated diagnostic single ELISA platform.

3.5.1.2 Clinical Blood Sampling

Full sampling schedules are described in detail in the section 3.2.3 and **Figure 19**. Blood sampling was carried out by standard venepuncture or at cannulation by staff at the Christie NHS Foundation Trust. Where possible, biomarker blood was taken at the same time as routine blood tests. Blood was collected in 10ml collection tubes (containing EDTA anticoagulant) and processed within half an hour at The Christie NHS Foundation Trust Clinical Trials Unit Laboratory under GCP conditions. Plasma was obtained by centrifuge at 1000 RCF (Relative Centrifugal Force) for 10 minutes. Plasma was aliquoted and stored at -80°C before analysis.

3.5.1.3 Multiplex ELISA kits

Analyte specific 96 well multiplex plates, recombinant protein standards and quality control samples were custom made by Aushon BioSystems for IL1b, PAPP-A, TNFa, MPO, TIMP1, MMP2, MMP9, hFABP, IL8 and NT-pro BNP (**Table 13**). Where possible, the analytes were plexed in combination to enable multiple proteins to be detected simultaneously using minimal blood volume. Imaging of multiplex plates was performed using the SearchLight Plus CCD imaging system, from Aushon Biosystems.

Multiplex ELISA kit	Product No.	Kit contents
MPO/TIMP1 2 plex	85822	96 well plate (spotted with protein specific anti-human capture antibody) Diluent (10% foetal calf serum and 0.1% sodium azide) Lyophilized protein standard High and low protein QCs Biotinylated (murine/human) detection antibody reagent Streptavidin-horseradish peroxidase (SA-HRP) reagent SuperSignal stable peroxide solution SuperSigmol luminol enhancer solution Wash Buffer
MMP2 2 plex	85185	
MMP9 2 plex	84920	
hFABP/IL8 2 plex	85836	
PAPPA, TNFa, IL1 3 plex	85824	
NTproBNP 1 plex	85510	

Table 13. Multiplex ELISA kit details

3.5.1.4 Multiplex Immunosorbant Assay (ELISA) Method

Analysis took place within the Clinical Experimental Pharmacology department at the Cancer Research UK, Manchester Institute under GCP conditions. Multiplex ELISAs were performed in line with manufacturer's guidelines following in house validation of assay performance (see **appendix 3**). The multiplex ELISA technique was performed as described in section 2.2.3.2 of the pre-clinical study (and shown in **Figure 44. Schema for multiplex ELISA analysis method**). Acceptance criteria for plasma samples was taken as a CV% <30% between replicate wells.

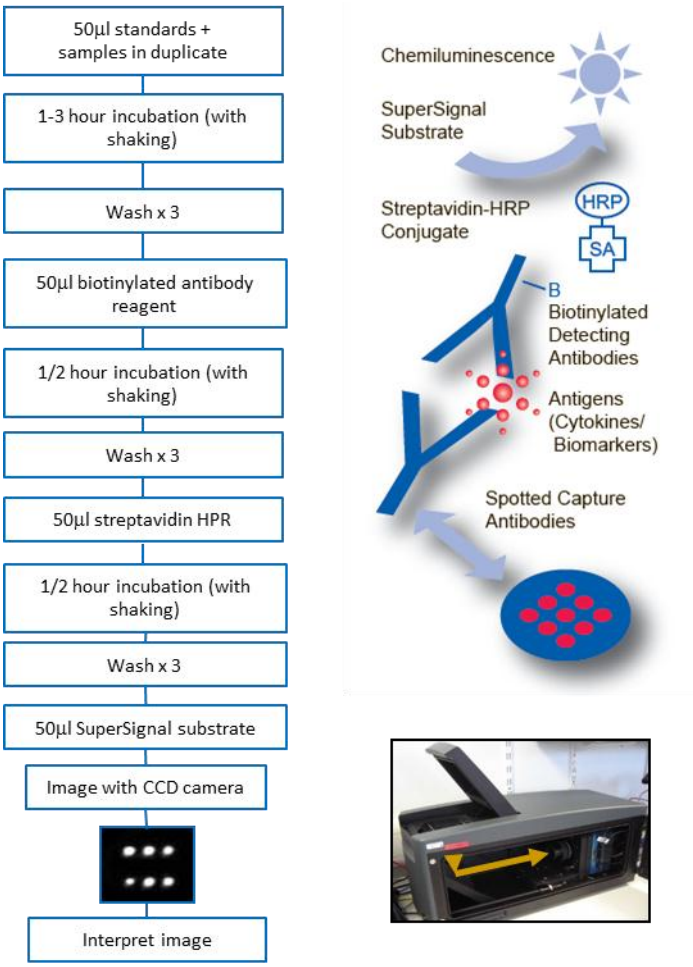

Figure 44. Schema for multiplex ELISA analysis method

3.5.1.5 Standard Curves

Standard curves were generated by reconstituting the supplied lyophilized protein in kit diluent and diluting to produce an eight point concentration curve from which to calculate protein levels (dilution regimen 1:16, 1: 2, 1: 4, 1: 4, 1: 4 , 1: 4 and 1: 2). Acceptance criteria for the standard curves was taken as an R^2 of over 0.985 and a CV% of <15% for technical replicates). The standard curves and R^2 values for each biomarker are shown in **appendix 3**.

3.5.1.6 Assay Ranges

The assay ranges were initially determined during validation and refined on completion of the clinical study ELISA work. The CV% of each technical replicate pair was plotted against concentration for each analyte to determine the level at which the assay became inaccurate demonstrated by poor agreement between technical replicates (CV%>30). The samples were plotted in concentration order and binned into groups of 20. The mean concentration and

CV% were calculated for each group and plotted. The lower limit of quantification (LLOQ) was taken as the point at which the mean for the group fell below a CV% of 30%. Results that fell below this level were reported as under the LLOQ. Workings for determining the LLOQ for each assay are shown in **appendix 2** and a worked example is shown below in **Figure 45**. The upper limit of quantification (ULOQ) for each assay was taken as the top of the standard curve and no clinical sample exceeded these limits. The individual assay ranges and assay specific methods are shown in **Table 14**.

Example of Determining the Lower Limit of Quantification for Multiplex ELISAs:

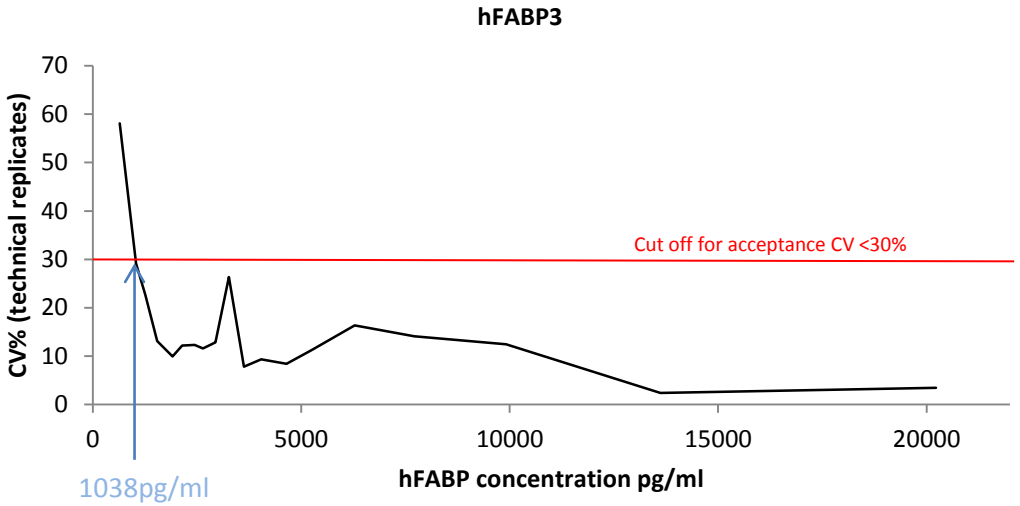

Figure 45. Determining the lower limit of detection for the hFABP assay. *A low level of agreement between technical replicates was seen below a concentration of 1038pg/ml with this assay (blue arrow - where the 30% CV level intersects the graph) therefore the lowest reportable value for HFABP was set at 2076pg/ml (1038pg/ml x 2 for the dilution factor).*

Plex	Assay	Incubation time	Dilution (with kit diluent)	Lowest reportable value pg/ml	Highest reportable value pg/ml
MPO/TIMP1 2 plex	MPO	1 hour	1 in 1000 (2ul in 2mls)	2000	1800000
	TIMP1			5000	5000000
MMP2 1 plex	MMP2	1 hour	1 in 100 (3ul in 297ul)	3100	3200000
MMP9 1 plex	MMP9	1 hour	1 in 100 (3ul in 297ul)	4900	5000000
IL1b, TNFa, PAPPA 3 plex	IL1b	3 hours	1 in 2 (150ul in 150ul)	3.4	400
	PAPPA			196	200000
	TNFa			4.6	4800
hFABP IL8 2 plex	hFABP	2 hours	1 in 2 (150ul in 150ul)	2076	960000
	IL8			0.8	800
NTpro BNP 1 plex	NTpro BNP	3 hours	1 in 2 (150ul in 150ul)	2.8	2800

Table 14. Multiplex ELISA method details

3.5.1.7 Quality Control (QC)

Quality control samples were added to each plate to ensure robust and reliable data was generated. The QC samples used in this study were supplied by Aushon Biosystems in single use vials and stored at -80°C. Six wells of QC (three high and three low) were added to each plate (top, middle and bottom) as shown below (**Figure 46**). The mean of the two technical replicates values was reported and the acceptance criteria was taken as a CV <15%. The QC ranges were set using the QC data from the first 10 plates of each multiplex assay and applied prospectively thereafter (**Table 15** & **Table 16**). The QC ranges were calculated by taking 2 standard deviations either side of the mean to represent the top and bottom limits of each high and low QC (**Figure 47**). Results that were clearly erroneous due to operational error or experimental failure were not used to calculate the mean values.

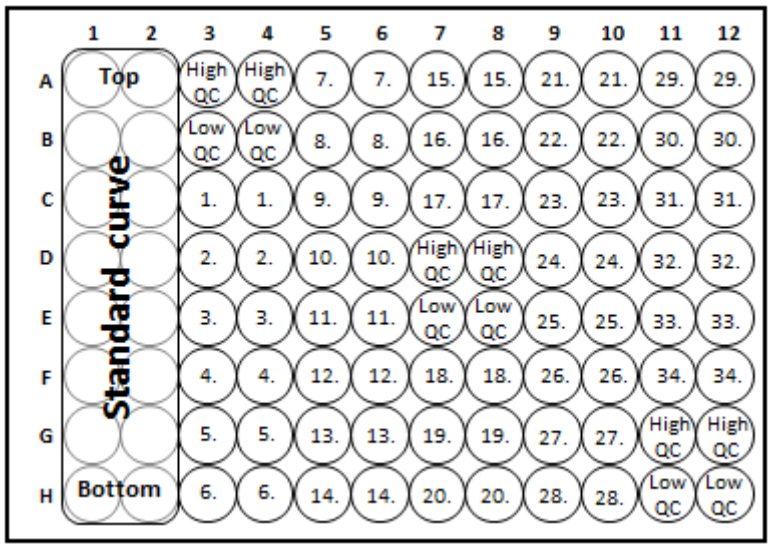

Figure 46. Plate plan for quality control samples and standard curve

Quality control samples were made for each assay by spiking known quantities of recombinant protein into diluent at low and high levels. Six replicate QC pairs (three high and three low) were added to each plate in different positions to ensure accuracy and uniformity across the plate in each experiment.

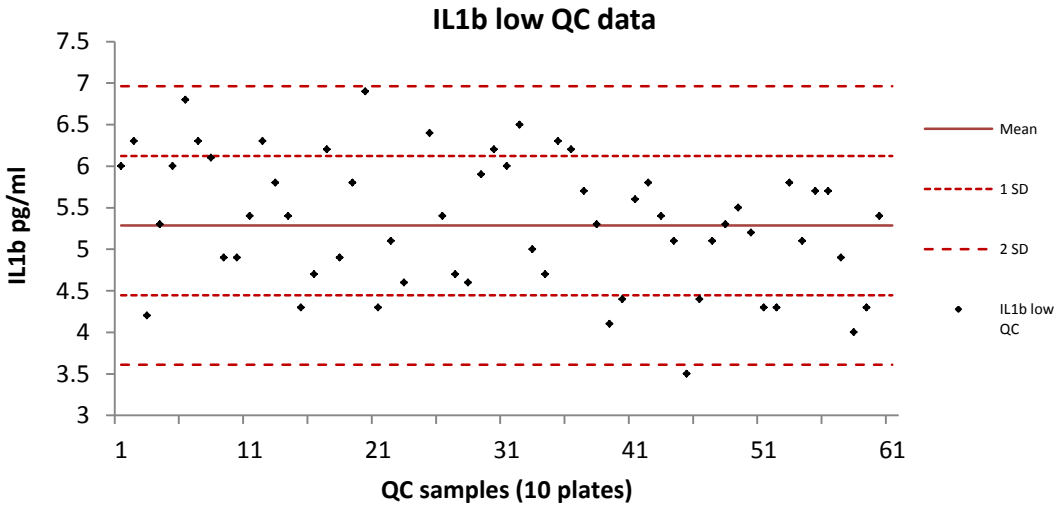

Figure 47. Example of plotting low QC data to set QC ranges for the IL1b assay

The low QC results for the first 10 plates of the IL1b assay were plotted. The QC range was set by calculating 2 standard deviations from the mean. This process was applied for the high and low QC for each assay.

HIGH QC	NTproBNP	IL1b	PAPPA	TNFa	MMP9	MMP2	MPO	TIMP1	hFABP	IL8
Mean (pg/ml)	321.8	25.96	11726.6	286.1	6727.9	4618.8	221.99	673.7	64796.5	48.96
SD (pg/ml)	82.6	4.5	2516.8	59.2	1091.7	740.8	44.05	104.4	8222.2	8.1
High limit (pg/ml)	487.1	34.95	16760	404.4	8911	6100	310	883	81241	65.1
Low limit (pg/ml)	156.5	16.96	6693	167.7	4544	3137	134	465	48352	32.8

Table 15. High QC values. n= 10 plates.

LOW QC	NTproBNP	IL1b	PAPPA	TNFa	MMP9	MMP2	MPO	TIMP1	hFABP	IL8
Mean (pg/ml)	69.6	5.33	2506.3	60.96	1442.8	955.3	49.95	137.5	13916.8	10.57
SD (pg/ml)	16.5	0.78	439.3	8.39	295.5	208.7	9.27	22.4	1835.5	1.57
High limit (pg/ml)	102.5	6.88	3385	77.7	2034	1373	68	182	17588	13.7
Low limit (pg/ml)	36.6	3.77	1628	44.2	852	538	31	93	10246	7.4

Table 16. Low QC values. n=10 plates.

3.5.1.8 Plate and Sample Failures

If more than one QC in the same range failed due to having a high CV% or being out of range the plate was failed, no data was reported and the plate was re-run. If an individual clinical sample failed due a high CV% the sample was re-analysed. If the sample failed for a second time or inadequate sample was available to repeat the experiment, the data was not reported and the time point was marked as missing.

3.5.1.9 Troponin I Analysis

Troponin I analysis was carried out at Stepping Hill NHS Foundation Trust (Clinical Biochemistry and Blood Sciences Laboratory) in accordance with GCP guidance. Troponin I was measured using an ultrasensitive troponin I diagnostic assay on the ADVIA Centaur analyser (Seimens). The standard diagnostic assay range was applied (LLOD 20ng/l – ULOD 50,000ng/L) and standard clinically significant values were used to aid data interpretation. In house assay validation was not required as the assay has already been fully validated for clinical diagnostic use.

Assay	Result	Clinical significance
Troponin	<20ng/l	Normal (no cardiac damage
	20-50pg/ml	Raised but clinical significance
	>50pg/ml	Diagnostic of myocardial infarction

Table 17. Troponin I clinical assay ranges

3.5.2 Multiplex ELISA Validation

Extensive validation of each assay was carried out prior to analysis of clinical samples in order to ensure that the assays were 'fit for purpose' i.e. robust and reproducible. Eight experiments were carried out to test the validity of the assays and all of the assays were shown to be fit for purpose. Some assays were shown to be more robust than others which was taken into account when interpreting the clinical data. The circulating biomarker assay validation work is shown in **appendix 3**.

3.5.3 Circulating Biomarkers Data Analysis

All circulating biomarker data were logged (to the base 10) prior to statistical analysis except Troponin I as it is a clinical diagnostic test with a standardised range. The baseline variability (intra-class correlation) of each circulating biomarker was determined using 2 (or when available 3) baseline samples and biomarker distribution was assessed to determine their utility as baseline prognostic biomarkers. Longitudinal biomarker analysis was performed by calculating fold change over time and plotting against baseline variability to determine if significant dynamic change was occurring. Biomarkers with significant change over time were taken forward for further investigation as dynamic biomarkers.

3.5.4 Combining Imaging and Circulating Data

Scatterplot matrices were plotted and potential correlations between the imaging and circulating biomarker data were tested using Spearman rank correlation coefficient. All of the exploratory circulating and imaging biomarkers were initially plotted against peak LVEF decline and final absolute LVEF. Positive correlations were explored further using receiver operator curve (ROC) analysis. Kaplan-Meier curves and log rank analysis were used to compare time-to-event rate (event being the development of cardiotoxicity or LVEF decline) between cohorts determined by exploratory imaging or circulating biomarker behaviour. Scatterplot matrices were also used to look at biomarker-biomarker relationships. A probability of $p<0.05$ was considered significant but due to the small numbers a $p<0.01$ was preferred.

3.5.5 Patient Plots

Individual patients profile plots of the circulating and imaging biomarkers were created to assess changes in trend for patients of particular interest i.e. those who had cardiac events.

3.6 Circulating Biomarkers Results

3.6.1 Baseline Levels in Cancer Patients

The baseline level of each cardiotoxicity biomarker was initially assessed to determine a) whether the protein was detectable in patient plasma (as the proteins may or may not be detectable in the absence of cardiac damage) and b) to measure baseline variability as many of the biomarkers are not cardio-specific and could be highly variable in the presence of cancer. For a biomarker to have baseline prognostic potential there should be minimal intra-patient variability but an element of inter-patient variability to distinguish between different prognostic groups. The intra-class correlation co-efficient (ICC) was calculated for each biomarker to measure agreement between baseline samples (where values closer to 1 show better agreement). The baseline values were then displayed graphically (**Figure 48**) to determine firstly, whether variability increased or decreased at lower concentrations and secondly, to assess whether there was reasonable inter-patient variability to dichotomise the population. Two baseline samples were available from 17 patients, three baseline samples from 9 patients and one baseline sample from 4 patients. Biomarker values were logged (to the base 10) prior to analysis as per standard practice for analysis of biological markers with the exception of Troponin I as this was measured using a diagnostic assay with a standardised clinical range. Levels of IL1b, TNFa and Trop I were undetectable at baseline therefore they cannot be used as baseline prognostic biomarkers. The other eight proteins were detectable at baseline and had good intra-class correlation ($\geq$0.7) suggesting they had potential for exploration as baseline prognostic biomarkers. Baseline variability did not worsen at the extremes of concentration and a reasonable range of baseline values were seen in all eight biomarkers. The mean baseline protein biomarker concentrations, intra-class correlation co-efficients and the significance values are shown in **Table 18** and **Figure 48** shows the baseline distribution of each biomarker in this cancer population

Circulating protein biomarker	Mean baseline level (pg/ml)	Baseline intra-class correlation	P value	Potential baseline biomarker
A				
hFABP	4548	0.914	<0.0001	Yes
IL1b	Undetectable	N/A	N/A	No
IL8	23.56	0.827	p<0.0001	Yes
MMP2	221158	0.714	p=0.001	Yes
MMP9	168953	0.827	p<0.0001	Yes
MPO	35406	0.7	p=0.002	Yes
NTproBNP	340	0.962	<0.0001	Yes
PAPPA	940	0.840	p<0.0001	Yes
TIMP1	107263	0.818	p<0.0001	Yes
TNFa	Undetectable	N/A	N/A	No
Trop I	Undetectable	N/A	N/A	No

Table 18. Inter-class correlation of circulating biomarkers at baseline in patients receiving anthracyclines for breast cancer and lymphoma.

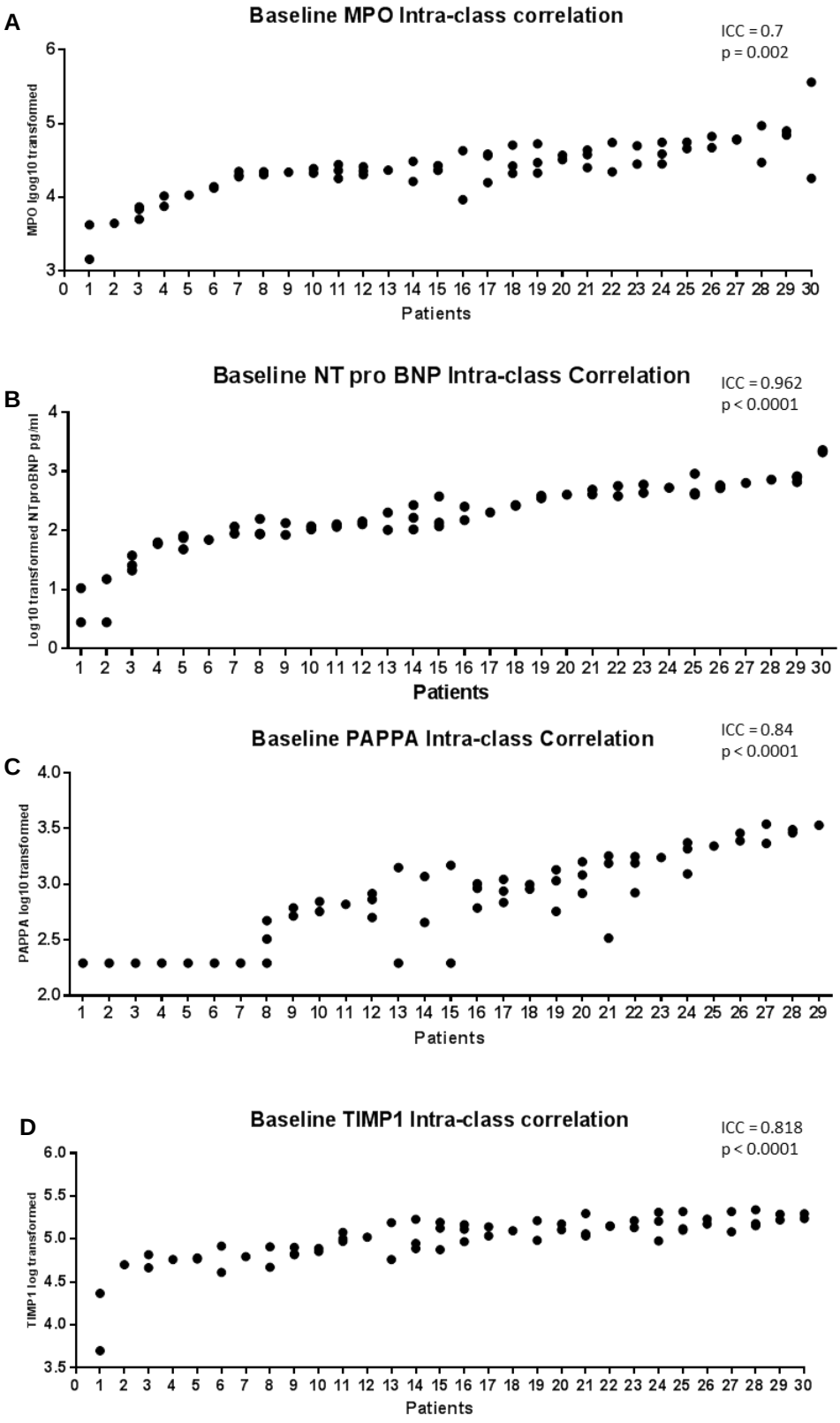

Figure 48. Baseline biomarker distribution for MPO (A), NTproBNP (B), PAPPA (C) and TIMP1 (D). Patients are listed on the x axis in order of the average baseline concentration and each baseline sample is plotted on the y axis to show inter and intra-patient

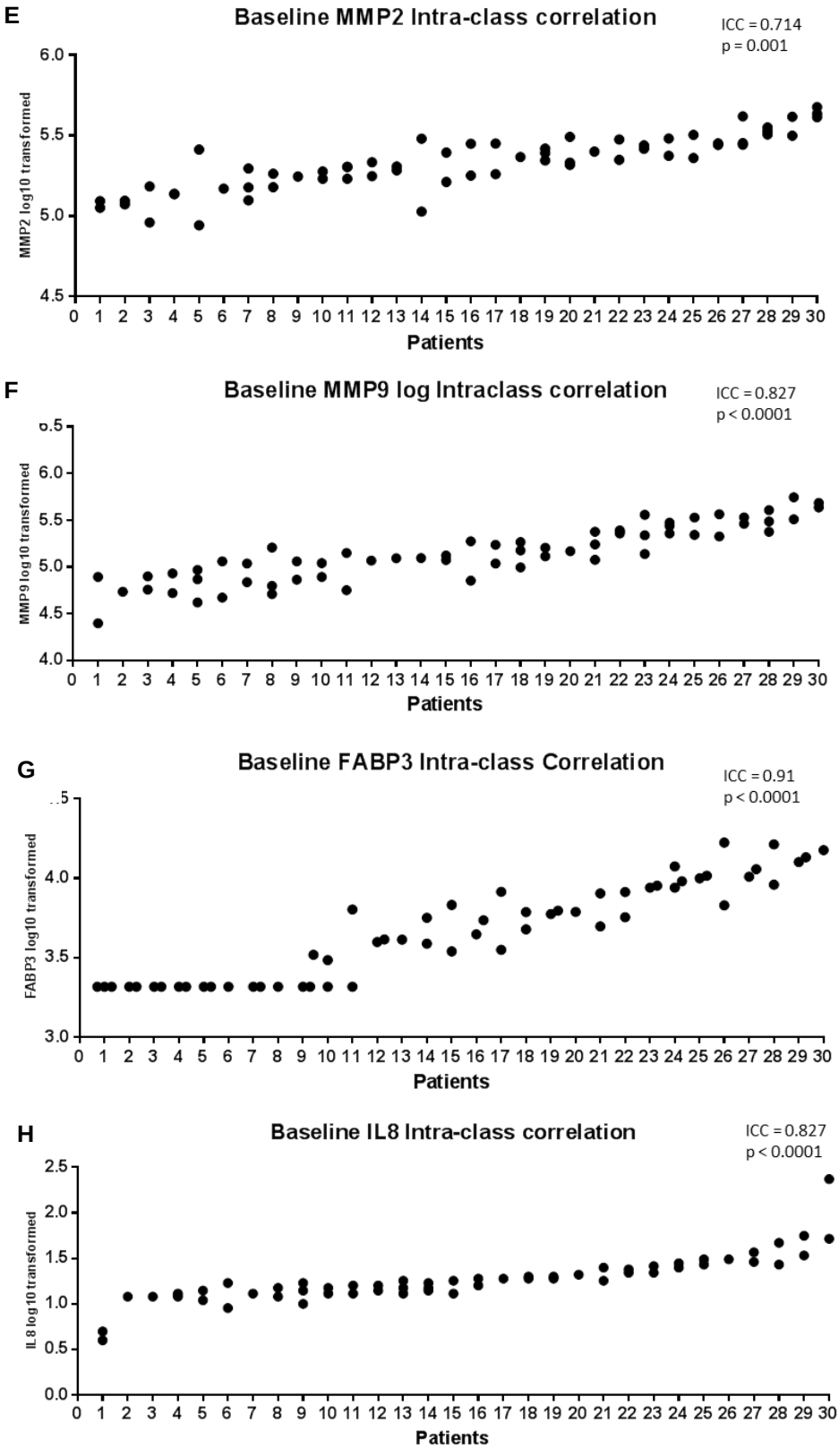

Figure 48 continued. Baseline biomarker distribution for MMP2 (E), MMP9 (F), hGABP (G) and IL8 (H). Patients are listed on the x axis in order of the average baseline concentration and each baseline sample is plotted on the y axis to show inter and intra-patient variability.

3.6.1.1 Baseline Correlations

Scatterplot matrices were constructed to explore correlations between the baseline levels of each biomarker and peak (and final) decline in LVEF (**Appendix 5: Figure 104**). Correlations were tested using Spearman rank correlation coefficient. Baseline MMP9 showed a weak positive correlation with LVEF decline (Spearman r 0.3, p=0.05), baseline MMP2 showed a weak but non-significant negative correlation with fall in LVEF (Spearman r -0.3, p=0.07) and there was a trend suggesting they negatively correlated with each other (Spearman r -0.2, p=0.4). There was no correlation between baseline levels of MMP9 or 2 with cancer stage but levels correlated with myocardial extracellular volume (ECV). None of the other circulating biomarkers showed prognostic value at baseline.

3.6.1.1.1 Baseline Circulating Matrix Metalloproteinase Levels and Extracellular Volume

The imaging data suggested that lower ECV values were associated with worse outcome in terms of LVEF decline and baseline levels of MMP2 and MMP9 showed a correlation, albeit relatively weak with ECV measurements. Both these parameters are thought to evaluate the extracellular matrix and would therefore be expected to correlate. Unexpectedly MMP2 and MMP9 behaviour differed, baseline MMP9 levels correlated negatively (Spearman r-0.6, p=0.17) and MMP2 correlated positively (Spearman r0.3, p=0.18) with ECV therefore patients with higher baseline levels of MMP9 and lower levels of MMP2 had lower ECV measurements and a greater rate of LVEF decline (**Figure 49**).

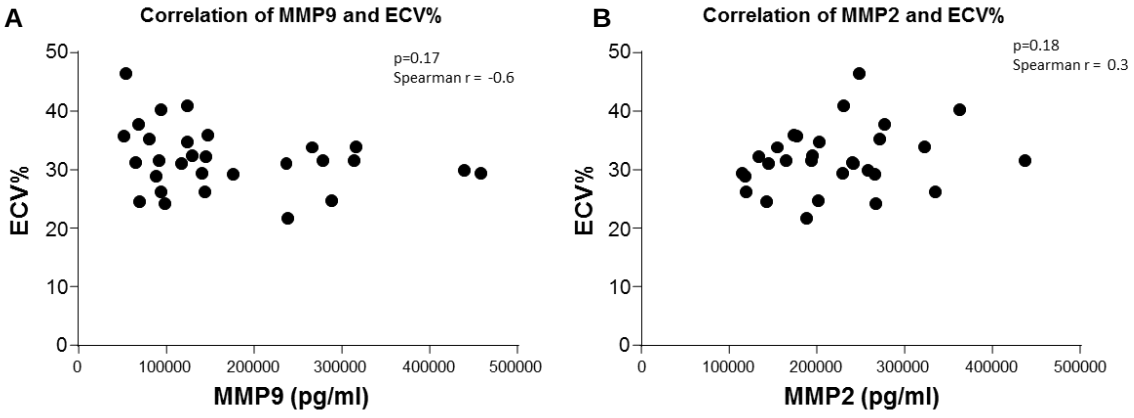

Figure 49. Correlation of baseline circulating MMP9 (A) and MMP2 (B) with baseline ECV

3.6.1.1.2 Baseline Correlation of hFABP and PAPPA

The strongest correlation was seen between hFABP and PAPPA (Spearman r = 0.95 p<0.0001). This was initially thought to be related tumour burden but levels did not correlate with cancer stage. However both proteins were shown to correlate closely with age.

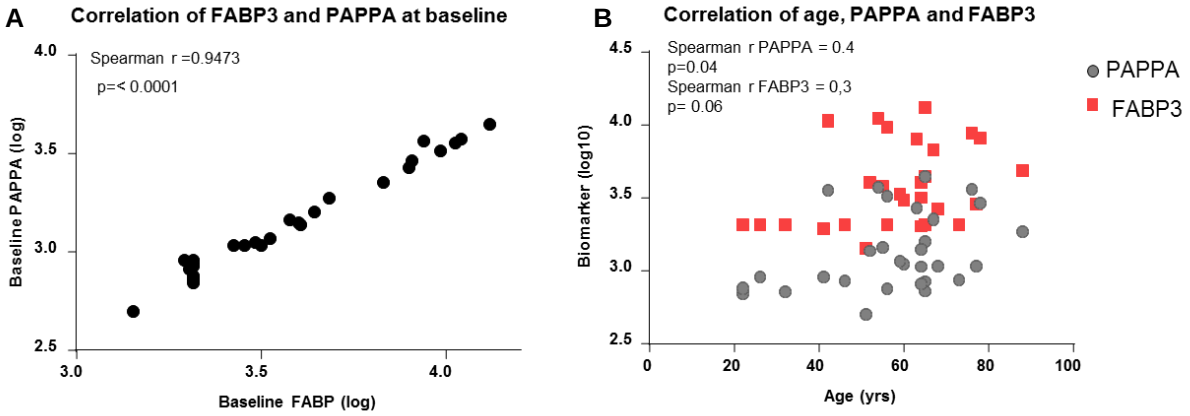

Figure 50. Correlation of baseline hFABP and PAPPA (A) and correlation of both proteins with age (B)

3.6.1.1.3 Matrix Metalloproteinases as Prognostic Markers

3.6.1.1.3.1 MMP2 as a Prognostic Marker

Baseline MMP2 levels were used to stratify the patients into two groups using an optimal cut off value determined with ROC analysis (**Appendix 5: Figure 105**). Patients with baseline levels of MMP2 below 201597pg/ml had a slightly higher event rate (LVEF fall of ≥10% to ≤55%) 62.5% (10/16) than patients with levels of MMP2 above 201597pg/ml 43% (6/14). Univariate Kaplan Meier analysis showed a significant difference between groups (p=0.03) (**Figure 51**). However, the sensitivity and specificity of MMP2 at this cut off were relatively low (59% and 69% respectively, AUC 0.7) and the difference between patients with high and low baseline MMP2 levels was not significant (p=0.16) when the secondary end of a LVEF decline of ≥ 10% was used. The groups were matched most clinical factors except anthracycline dose as patients in the low MMP2 grouped happened to receive higher doses of anthracycline which may be a confounding factor.

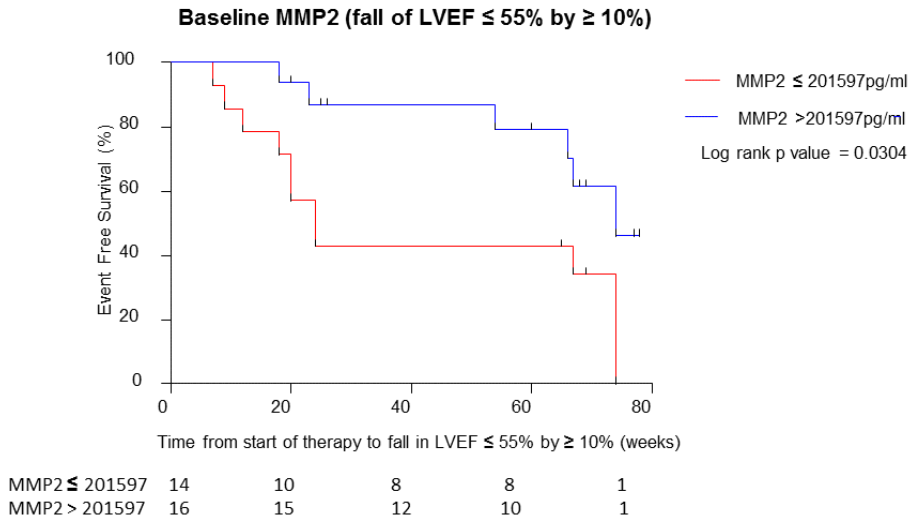

Figure 51. Cumulative event rate (LVEF fall of ≥10% to ≤55%) in patients stratified by baseline levels of circulating MMP2

3.6.1.1.3.2 MMP9 as a Prognostic Marker

Patients were stratified using baseline levels of MMP9 with an optimum cut off determined by ROC analysis (**Appendix 5: Figure 106**). Patients with baseline MMP9 levels above 129805pg/ml had a slightly higher incidence of LVEF decline (≥10%) than patients with lower MMP9 levels at baseline. Univariate Kaplan Meier analysis showed a significant difference between groups (p=0.003) (**Figure 52**) however the sensitivity and specificity of MMP9 were also relatively low (65% and 69% respectively, AUC 0.7). Groups were evenly matched for age but there were slightly more patients with pre-existing cardiovascular risk factors and higher anthracycline doses in the group with higher baseline MMP9 levels which could contribute to the different outcome. Kaplan Meier analysis showed no significant difference between patients with high and low baseline levels of MMP9 when the primary end point of LVEF fall of ≥10% to ≤55% was used.

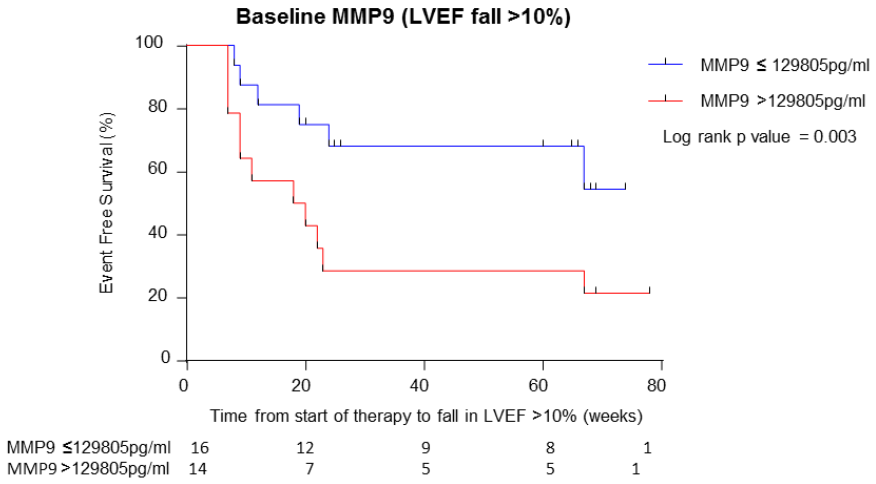

Figure 52. Cumulative event rate (LVEF fall by ≥ 10%) in patients stratified by baseline levels of MMP9

3.6.1.2 Longitudinal Biomarker Analysis

Longitudinal fold change from baseline was plotted for each biomarker to determine whether the biomarker had the potential to be a pharmacodynamic safety biomarker. Biomarker values were logged (to the base 10) prior to analysis and where necessary affine transformations were performed to aid interpretation and analysis. Baseline variability was calculated and plotted simultaneously to determine whether the dynamic change was significant i.e. outwith baseline variability. This was determined by measuring the greatest fold change between baseline samples for each patient and calculating the population mean and standard deviation of the logged data. The standard deviation was multiplied by 1.96 to encompass 95% of the data (therefore excluding erroneous baseline measurements) and the values were plotted either side of the population mean (+/- 1.96 x SD) on each biomarker graph to clearly show when significant dynamic change was being seen.

Example of longitudinal biomarker analysis using the hFABP3 results:

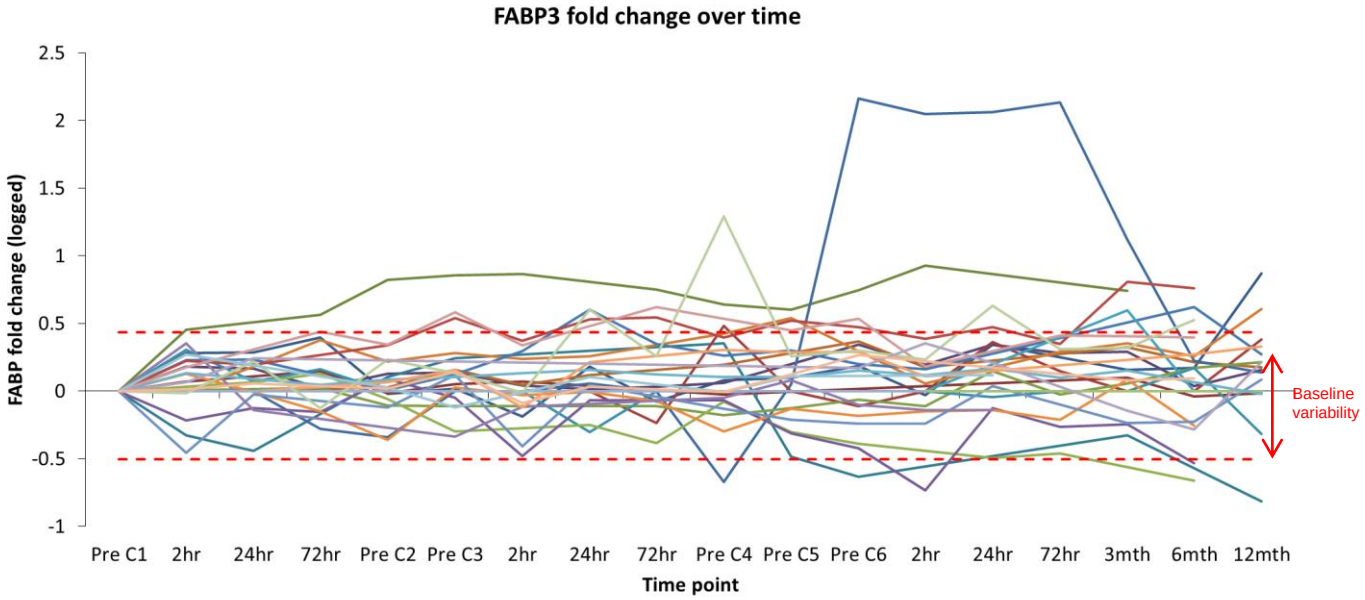

Figure 53. Fold change of circulating logged levels of hFABP (FABP3) during and after anthracycline therapy. Each line represents one patient and the dotted red lines show the limits of baseline variability. C= cycle. Fold change in hFABP over time plotted with baseline variability. From this plot it is possible to see that only a small number of patients showed dynamic change beyond baseline variability. The patient showing the most dramatic rise in hFABP during cycle 6 (represented by the blue line) also had marked elevations of NTproBNP, PAPPA and Troponin I at the same time point. This patient had a staphylococcus aureus skin infection requiring antibiotics during cycle 6 and was diagnosed with an extensive DVT shortly afterwards both of which may have contributed to the biomarker elevations.

3.6.1.2.1 Assessment of Longitudinal Biomarker Potential

Longitudinal analysis was performed for each biomarker and results were as follows: transient elevations in NTproBNP were seen 24-72 hours after each chemotherapy dose but levels returned to baseline prior to each cycle and during follow up (**Appendix 5: Figure 95**). The transient rises did not correlate with decline in LVEF or clinical cardiac events. A small number of patients showed marked elevations of PAPPA and hFABP but they did not correlate with LVEF decline or cardiac events (**Appendix 5: Figure 97, Figure 96**). Some of the rises corresponded with other clinical inflammatory events such as infection. IL8 rose

transiently 24 hours after the first dose of chemotherapy but subsequently remained unchanged (**Appendix 5: Figure 102**). This transient rise did not correlate with cardiotoxicity but may have resulted from tumour flare. MMP2, TIMP1 and MPO did not increase or decrease beyond baseline variability throughout the study (**Appendix 5: Figure 101, Figure 99, Figure 100**). Troponin I was not detectable at baseline but showed marked dynamic elevation towards the end of chemotherapy and this is discussed further in section 3.6.1.2.2.1. MMP9 levels fell incrementally and significantly during treatment and results are explored further in section 3.6.1.2.3. The results for each biomarker are summarised in **Table 19** and the data are displayed graphically in **Appendix 5**.

Circulating protein biomarker	Baseline variability Fold change (log)	Significant change from baseline	Biomarker potential
hFABP	1.7 (0.23)	Yes	Baseline and dynamic
IL1b	-	No	None
IL8	1.5 (0.17)	No	Baseline only
MMP2	1.447 (0.16)	No	Baseline only
MMP9	1.6 (0.22)	Yes	Baseline and dynamic
MPO	2.2 (0.35)	No	Baseline only
NTproBNP	1.6 (0.2)	Yes	Baseline and dynamic
PAPPA	2.2 (0.34)	Yes	Baseline and dynamic
TIMP1	1.6 (0.21)	No	Baseline only
TNFa	-	No	None
Trop I	-	Yes	Dynamic only

Table 19. Baseline variability and significant change from baseline for each potential circulating biomarker

3.6.1.2.2 Dynamic Changes in Circulating Biomarkers

3.6.1.2.2.1 Troponin I

Troponin I was undetectable at baseline but became markedly elevated during anthracycline therapy and appeared to be the most informative biomarker. Troponin I levels remained undetectable until cycle 4 when they began to rise following receipt of half of the cumulative anthracycline dose. Troponin I became significantly raised prior to cycle 5 ($p= 0.0014$ with paired t test), peaked 2 hours after the final cycle ($p<0.0001$ on paired t test) and returned to baseline by 6 months (Figure 54). 11 (37%) patients had a clinically significant rise in troponin I (>50ng/ml), 11 (37%) had a low level rise in troponin (20-50ng/ml) and the remaining 8 patients (26%) had no rise in troponin.

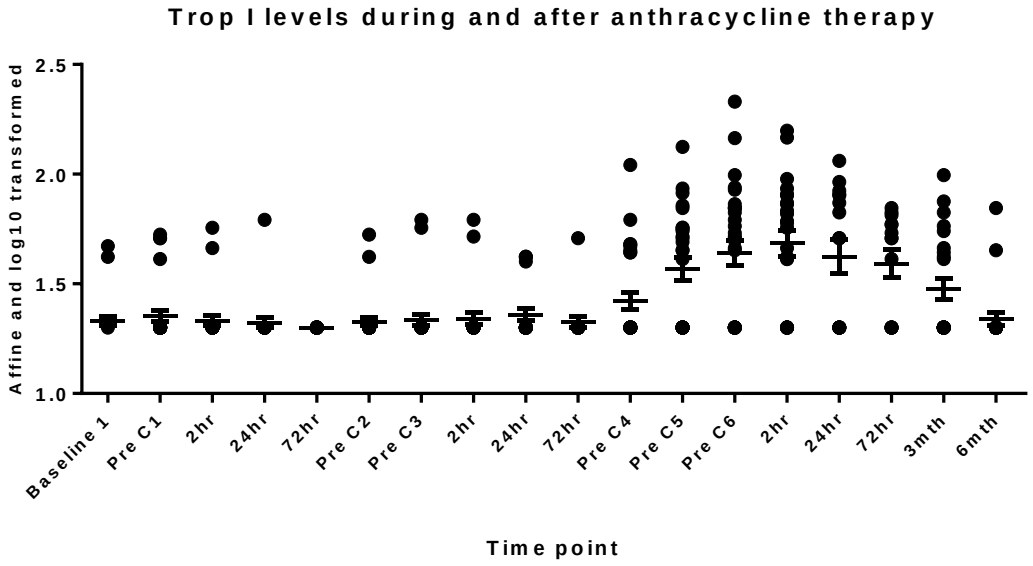

Figure 54. Circulating Troponin I levels during and after anthracycline treatment. *The graph shows the individual values (affine transformed and logged) and the population mean and standard deviation at each time point. C= cycle.*

3.6.1.2.2.1.1 Troponin I and LVEF Decline

Troponin elevations were seen in patients with and without a decline in LVEF but higher peak troponin levels were seen in patients with a LVEF decline of ≥ 10% (both persistent or transient) than patients with very little change in LVEF (**Figure 55**). Patients with a persistent decline of ≥ 10% had a significant increase in troponin I pre cycle 6 (p=0.0006 using one way ANOVA with post analysis multi-comparison testing) whereas patients with a transient or no LVEF decline had elevations which were not significant. Of note, troponin I rises were seen after a similar cumulative doses of anthracycline in both humans and rats (6.3mg/kg in rats and 5.4mg/kg in humans*) when the pre-clinical and clinical findings were compared.

**The standard human Doxorubicin dose given in RCHOP and ABVD regimens is 300mg/m^2 in total. An average male weighs 70kg giving a BSA of approximately 1.9m^2. This means the total dose received would be ~570mg or 570mg/70kg = 8.14mg/kg in 6 doses every 3 weeks therefore 1.36mg/kg each dose. Troponin I rose prior to cycle 5 after 1.36mg/kg x4= 5.44mg/kg in humans and after 1.25mg/kg x 5 = 6.3mg/kg in rats, although it must be noted that different assays were used.*

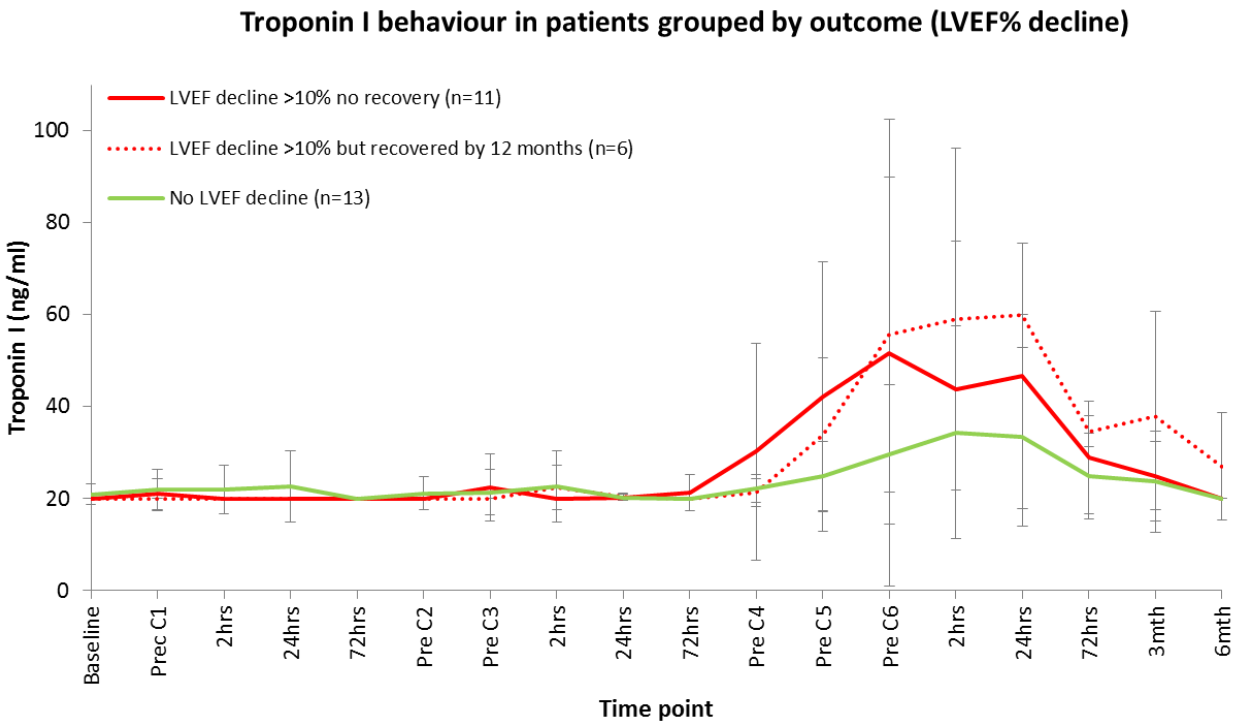

Figure 55. Characteristics of circulating Troponin I during and after anthracycline treatment in three groups based on LVEF behaviour *(green line: no LVEF decline, red line: persistant LVEF decline and red dotted line: transient LVEF decline). The mean values are shown and the error bars represent the standard deviation for the populations.*

3.6.1.2.2.1.2 Troponin I as a Safety Biomarker

A weak but significant correlation between peak fold change in Trop I and peak fall in LVEF was seen (Spearman r = 0.4, p= 0.04) (Figure 56) therefore ROC analysis was performed to determine the optimal cut off level (in terms of sensitivity and specificity) associated with a significant LVEF decline. A troponin I level of ≤ 39ng/ml resulted in an AUC of 0.76 with sensitivity of 85% and specificity of 71% (p=0.0171) (Figure 57). The patients were grouped into two prognostic groups based on this cut off of and univariate Kaplan Meier analysis was performed. This showed a significant difference between the two groups for decline in LVEF ≥ 10% (log rank p value = 0.02) (**Figure 57**) but the difference was not statistically significant when the event was classed as a fall of ≥10% to ≤55% and/or the development of a clinical cardiac event by 18 months.

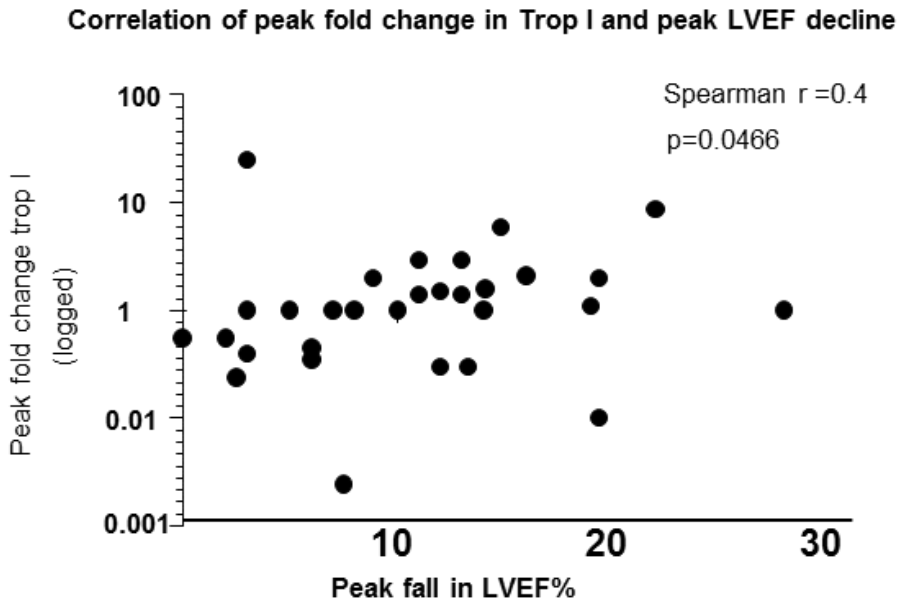

Figure 56. Correlation of peak fold change in Troponin I (logged) and peak LVEF decline

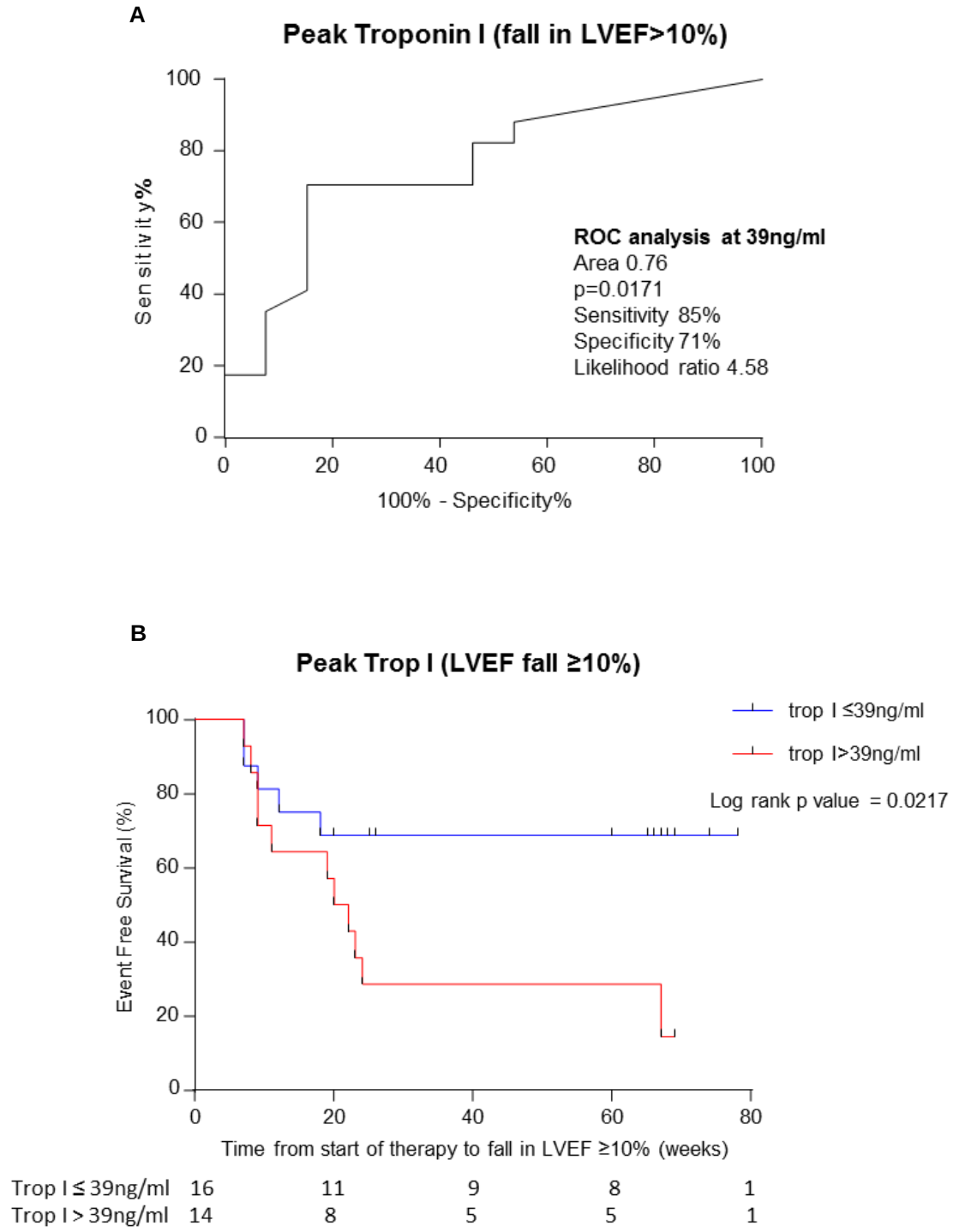

Figure 57. ROC analysis to determine the optimum cut off of Troponin I (A) and Cumulative event rate (LVEF fall by ≥ 10% at any point) in patients stratified by baseline levels of circulating Troponin I (B). *n=30.*

3.6.1.2.2.1.3 Positive and Negative Predictive Values for Troponin I

The positive and negative predictive value of troponin I for significant LVEF decline (by ≥10%) was calculated (**Table 20**). With this small data set Troponin I had a positive predictive value of 86% and a negative predictive of 69%. Five patients had a decline in LVEF ≥10% with only minor or no elevation of Troponin I (<39ng/ml) and only two patients had a rise in troponin I (>39ng/ml) with no significant fall in LVEF.

LVEF decline ≥ 10%	**True positive**	**False positive**	**Total**	**PPV TP/(TP+FP)**
Positive test (peak Trop >39ng/ml)	12	2	14	85.7%
	False negative	**True negative**		**NPV TN/(FN+TN)**
Negative test (peak Trop >39ng/m)	5	11	16	68.8%
Total	17	13	30	

Table 20. Positive and negative predictive values for Troponin I and LVEF decline (≥10%)

3.6.1.2.2.1.4 Troponin I in Patients with Clincial Cardiac Events

Longitudinal troponin I levels were plotted for the patients who had cardiac events during the study (**Figure 58**). Troponin I levels remained undetectable prior to the arrhythmias in two patients but rose afterwards and the other patient had low level elevation of troponin prior to starting therapy. The fouth patient had marked elevation of Troponin I co-inciding with a drop in LVEF prior to the cardiac event (MI).

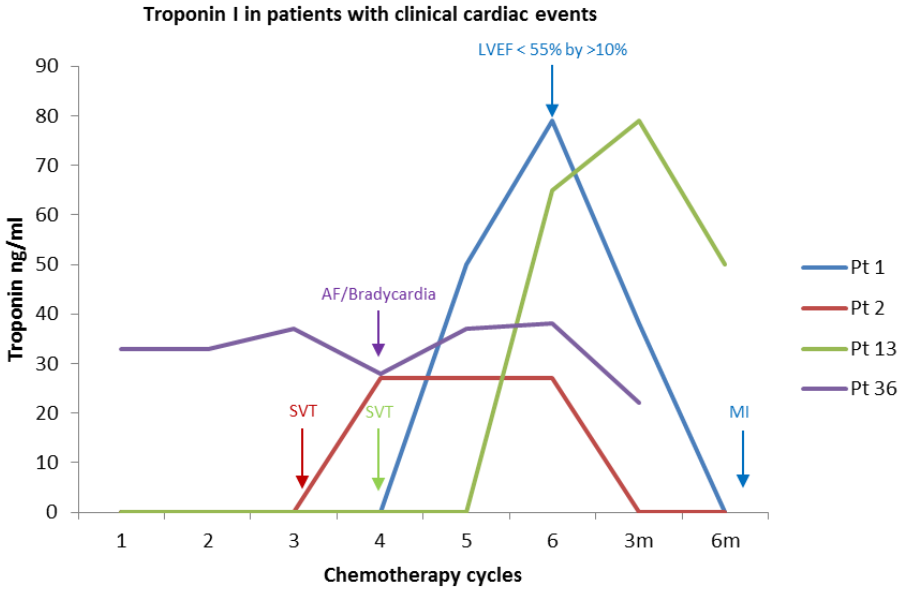

Figure 58. Troponin I characteristics in the patients with clinical cardiac events

3.6.1.2.3 MMP9

A significant decrease from baseline was seen in circulating MMP9 levels during anthracycline therapy. MMP9 levels fell significantly at cycle 2 and remained significantly lower than baseline (p=0.0001 using paired t testing) before each cycle until 12 months post therapy when level started to rise again (p=0.07 at 12 months) (**Figure 59).** Transient (non-significant) elevations 2-72 hours post anthracycline dose were seen suggesting possible bolus related acute release (Figure 98).

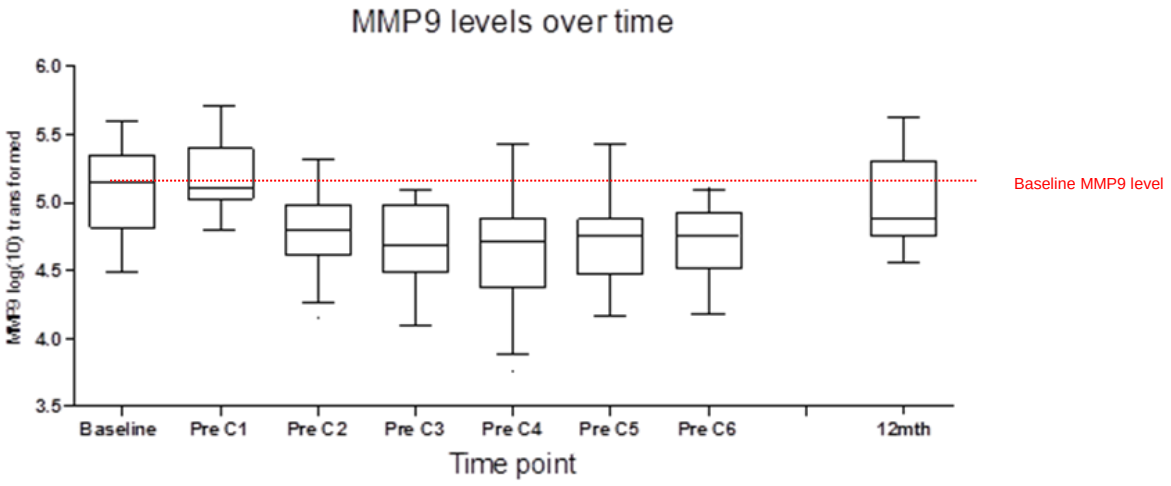

Figure 59. Box and whisker plot showing a decline in circulating MMP9 levels prior to each anthracycline dose and recovery at 12 months. The whiskers represent 95% confidence intervals.

3.6.1.2.3.1 MMP9 and Neutropenia

As MMP9 is not a cardio-specific protein the initial hypothesis was that MMP9 levels may be related to tumour shrinkage. However, MMP9 levels at baseline did not correlate with cancer stage but correlated closely with baseline neutrophil count (Spearman r 0.6, p<0.0001) (**Figure 60**). A close relationship between the decline in MMP9 and neutrophil count during therapy was seen and is shown in **Figure 61**. The surge in neutrophil level prior to cycle 5 was thought to result from the instigation of granulocyte-colony stimulating factor (GCSF) in several patients.

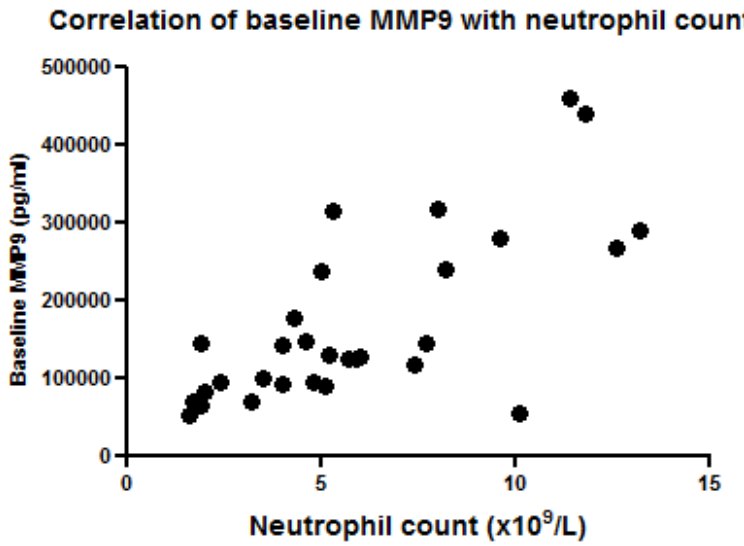

Figure 60. Correlation of circulating MMP9 levels and neutrophil count at baseline

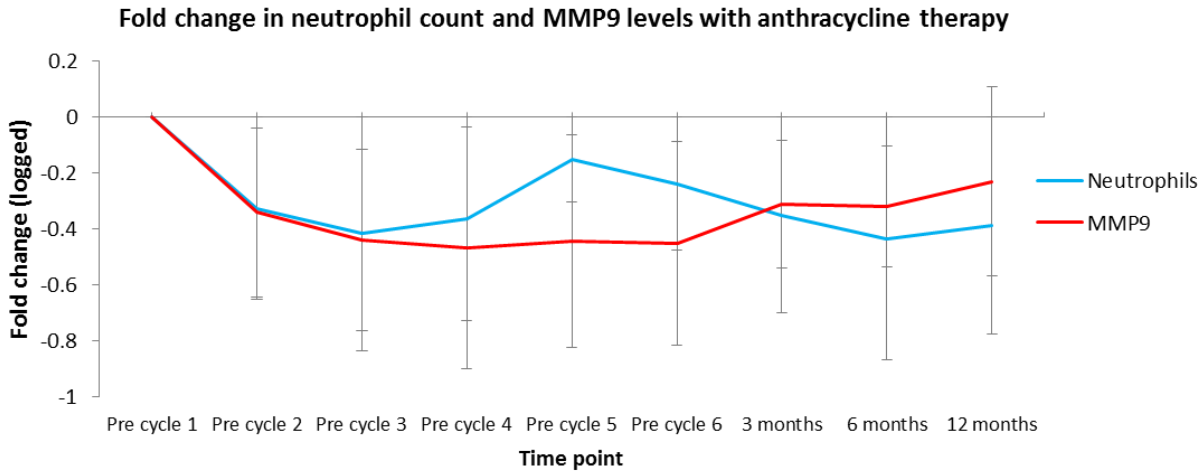

Figure 61. Behaviour of circulating MMP9 and neutrophil levels in patients during and after anthracyclines (logged fold change). The error bars shown represent the standard deviation of the populations.

3.6.1.2.3.2 MMP9 and LVEF Decline

The behaviour of MMP9 during and after anthracycline therapy was plotted in subgroups groups based on LVEF decline (persistent LVEF decline, transient LVEF decline and no LVEF decline) to determine whether the biomarker had potential to discriminate between high risk and low risk patients. All groups changed significantly from baseline and there was no significant difference between the groups, however **Figure 62** shows that patients with no decline in LVEF had a less significant fall in MMP9 during treatment. A weak negative

correlation was also seen between fold change in MMP9 and peak LVEF decline (Spearman r – 0.3, p=0.06).

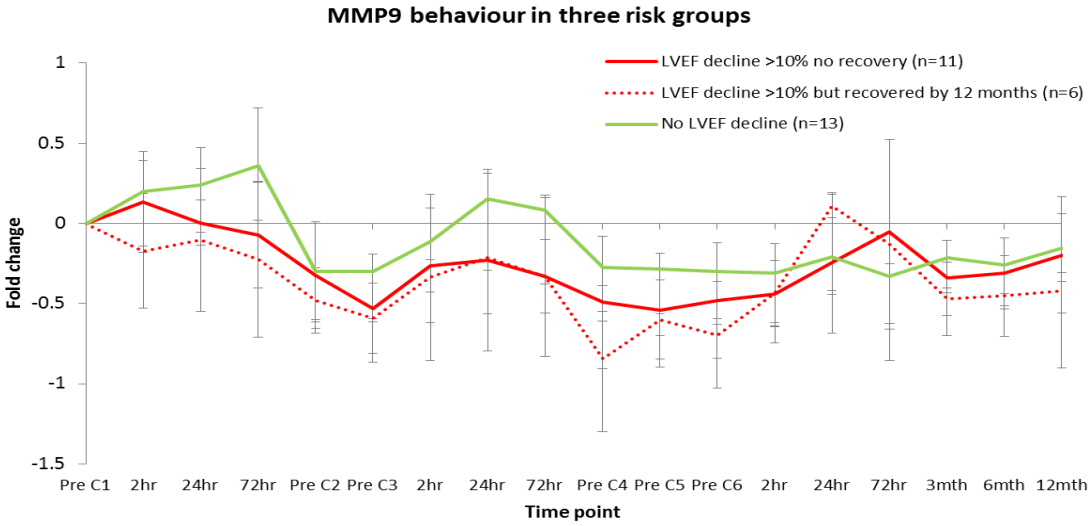

Figure 62. Characteristics of circulating MMP9 during and after anthracycline treatment in three groups based on LVEF behaviour (no LVEF decline, persistant LVEF deceline and transient LVEF decline). The mean values are shown and the error bars represent the standard deviation for the populations.

Fold decrease in MMP9 was explored further by ROC and Kaplan Meier analysis. A fold decrease of 0.6 (logged data) gave an area under the curve of 0.7, sensitivity of 62% and specificity of 65% with ROC analysis (Figure 63). This cut off was used to stratify patients for Kaplan Meier analysis and results suggested that patients with a greater decline in MMP9 did worse than patients who maintained levels of MMP9 throughout treatment (Figure 63), although the difference was not statistically significant (p=0.2). A cut off of log 0.6 equates to an absolute fold decrease of 4 (or fold change of -0.25 x baseline) and patients who had a more dramatic fall in MMP9 seem to have done slightly worse.

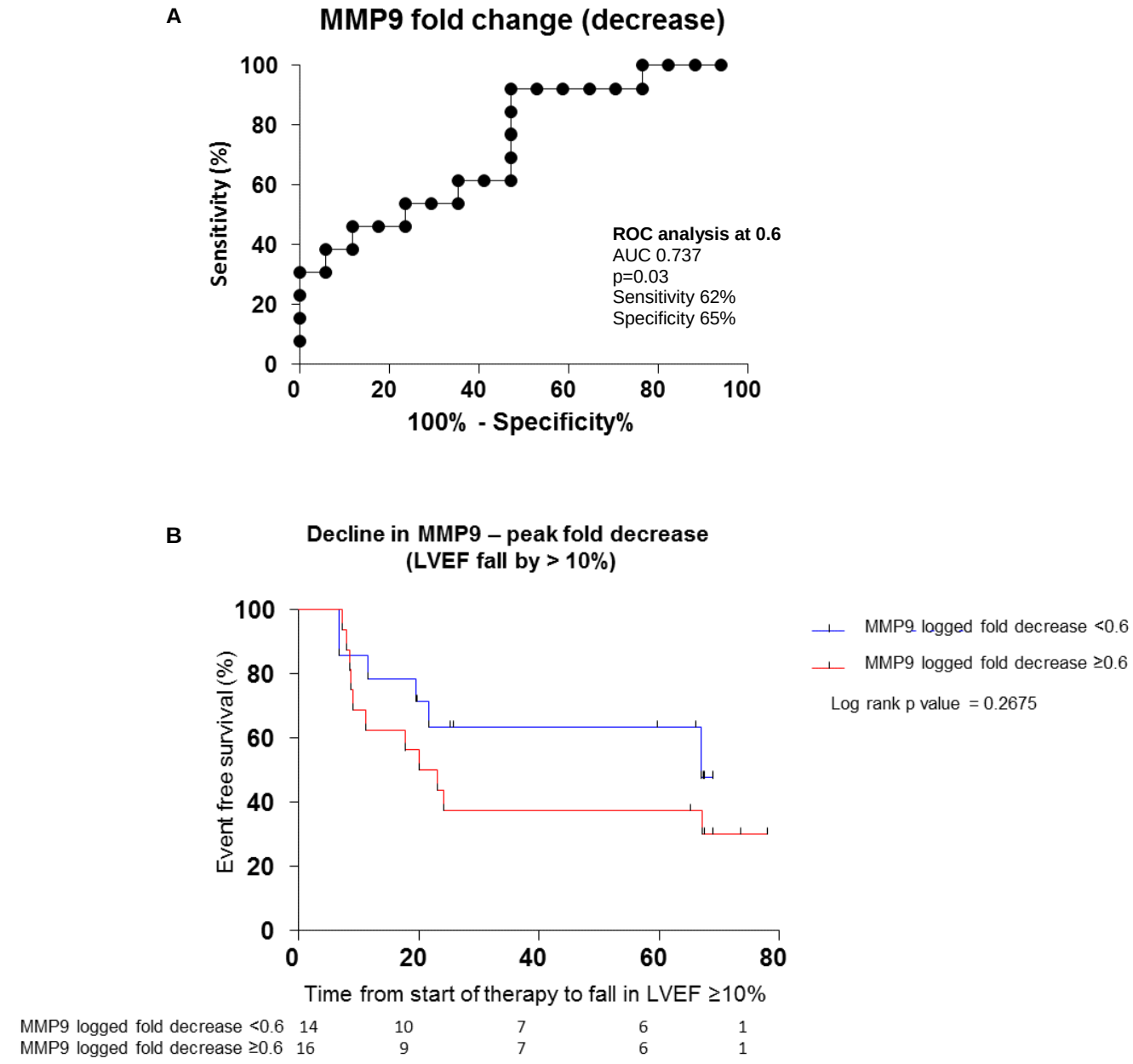

Figure 63. ROC analysis to determine the optimum cut off of MMP9 fold change (decline) (A) Cumulative event rate (LVEF fall by ≥ 10%) in patients stratified by peak fold decline in circulating MMP9 (B)

3.6.1.3 Individual Patient Plots

Individual patient plots were made for patients of particular interest (patient 001 and 028) in order to learn more about the behaviour and interaction of the circulating and imaging biomarkers in cardiotoxicity.

*Patient 001 – Myocardial Infarction (**Figure 64**):*

Patient 001 had a Myocardial infarction (MI) 10 months after chemotherapy. This patient had an LVEF of 58% at baseline which remained the same during treatment and dropped to 52% post therapy (prior to the MI) and finally to 49% at 12 months. Troponin I peaked (at 79ng/ml) prior to the MI and prior to the development of LV dysfunction. MMP9 levels fell to their lowest half way through chemotherapy. This patient had an element of diastolic dysfunction prior to starting therapy (baseline E/A ratio 0.9) which initially dropped further due to an increase in a wave before undergoing pseudo-normalisation due to a fall in both wave velocities after treatment. Again T1 was unchanged and T2 actually showed a decline mid treatment before returning to baseline at 12 months. Little change was seen in longitudinal dyssynchrony despite the development a MI and LV dysfunction.

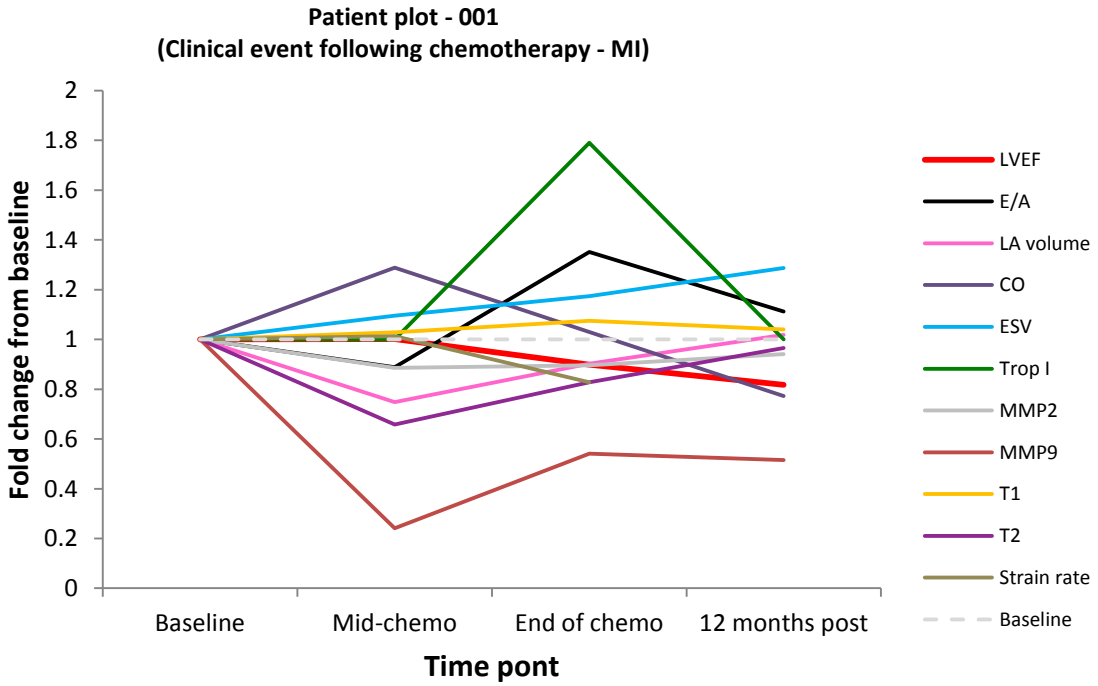

Figure 64. Patient 001 had a myocardial infarction 10 month after chemotherapy. *This graph shows the integrated behaviour of the imaging and circulating biomarkers prior to and following the event*

Patient 028 – Asymptomatic LV Dysfunction ***(Figure 65)****:*

Patient 28 had the greatest decline in LVEF and developed asymptomatic LV dysfunction half way through treatment. This patient had an LVEF of 59% at baseline which dropped to 42% half way through treatment, reached a low of 31% directly after therapy and recovered marginally to 37% at 12 months. ESV steadily increased throughout the study resulting in the LVEF decline but the apparent improvement in LVEF at 12 months was due to an increase in EDV at the final time point which could be due to dilation from myocardial damage. The E/A ratio dropped to 0.6 (normal 1-2) half way through chemotherapy and LA volume steadily increased but neither preceded LV dysfunction. Troponin I did not predict for the development of LV dysfunction as elevations were not seen until after chemotherapy, peaking at a relatively low level of 40ng/ml (although just above the cut off for high risk patients determined in the above analysis). MMP9 levels fell dramatically half way through chemotherapy prior to the rise in Troponin I and worsening in longitudinal dyssynchrony. Relatively modest changes were seen in T1 values but a slightly bigger although transient fold change was seen in T2 values directly post therapy.

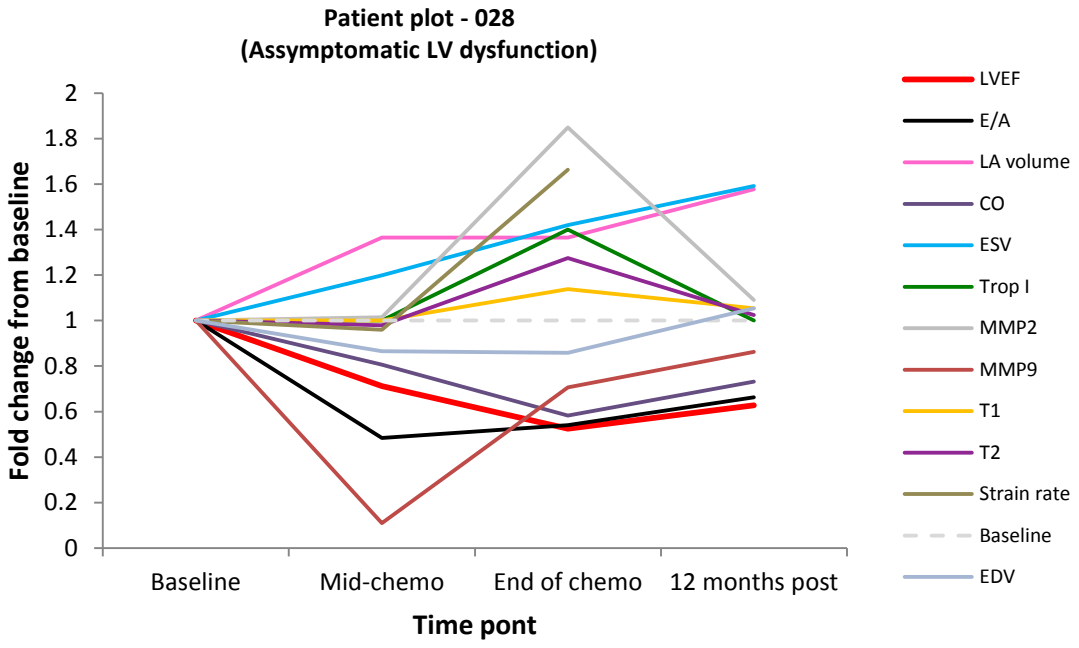

Figure 65. Patient 028 had the greatest decline in LVEF during the study and had asymptomatic LV dysfunction at 12 months. *This graph show the integrated behaviour of the imaging and circulating biomarkers during the development of LV dysfunction*

3.6.2 Summary of Circulating Biomarker Findings

3.6.2.1 Baseline Circulating Biomarkers

MMP2 and MMP9 were the only circulating biomarkers that showed potential as baseline prognostic markers. Intra-patient variability was low and a reasonable range of baseline values were seen within the population. MMP2 levels correlated negatively and MMP9 levels correlated positively with LVEF decline although the relationships were relatively weak. Three biomarkers (IL1b, TNFa and Trop I were not detectable at baseline and the remaining six biomarkers (hFABP, IL8, MPO, NTproBNP, PAPPA and TIMP1) did not show a strong correlation with LVEF decline or cardiac events.

3.6.2.2 Longitudinal Circulating Biomarkers

Troponin I was not detectable at baseline in the majority of patients but rose during cycles 4 and 5 reaching a peak 2 hours post cycle 6. Peak Troponin I levels were associated with peak LVEF decline and patients with higher peak levels (>39ng/ml) did worse in terms of the rate of significant LVEF decline. MMP9 levels fell during treatment in the whole population and closely followed the trajectory of neutrophils for the first 3 cycles. Patients who had a less dramatic fall in MMP9 appeared to do slightly better i.e. have a lower rate of significant LVEF decline, than patients who showed a large drop in MMP9 during therapy.

3.6.2.3 Patients of Particular Interest

The individual patient plots highlight the complex nature of anthracycline-related cardiotoxicity and the fact that it can occur through different mechanisms in different people. It is therefore unlikely that a single biomarker would be able to predict for all types of cardiotoxicity and suggests that different approaches may be required to detect different toxicity i.e. acute arrhythmias versus chronic cardiomyopathy.

3.6.2.4 Relationship of Imaging and Circulating Biomarkers

Figure 66 shows the behaviour of the key circulating and imaging biomarkers and their relationships with each other during and after anthracycline therapy. Troponin I levels rise during treatment, peak at the end of treatment and return to near baseline 12 months after therapy. MMP9 levels fall and follow a similar time course to Troponin I reaching the lowest level directly after therapy and increasing again at one year. Levels of MMP2 change very little throughout the study. ESV volume increases during and after therapy resulting in the

fall in LVEF which reaches the lowest point at the end of anthracycline therapy and shows some recovery by 1 year. Longitudinal dyssynchrony increases at the mid point of chemotherapy and continues to worsen until end of the study. The E/A ratio falls in line with LVEF decline and is not an earlier event. T1 and T2 values remain relatively unchanged throughout the study.

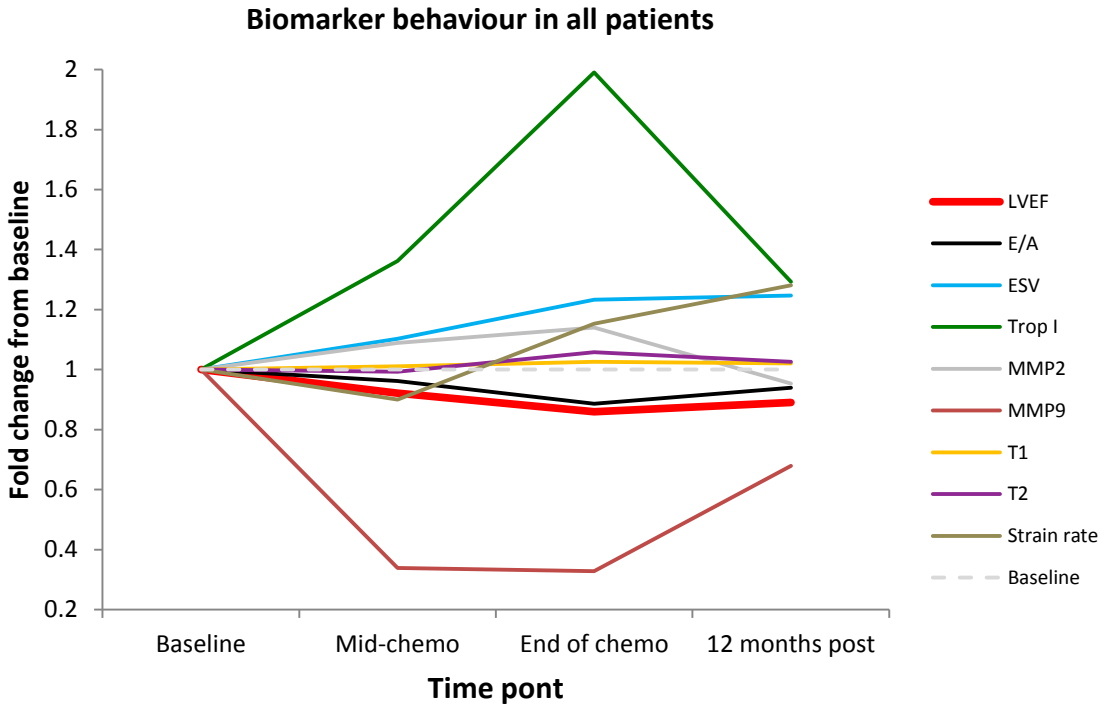

Figure 66. This graphs summarises the integrated behaviour of the key circulating and imaging biomarkers *(fold change from baseline) during and after anthracycline chemotherapy in all patient)*

3.7 Discussion

3.7.1 Population Characteristics

Patients were recruited from the Christie NHS Foundation Trust having been referred for treatment for lymphoma or breast cancer. All but 2 of the patients were being treated with curative intent and the 2 exceptions were having second line treatment for follicular lymphoma with an expected prognosis of over 5 years. Therefore the potential of late effects, particularly cardiotoxicity, in these patients is a significant issue. The cohort was representative of a normal breast cancer and lymphoma population. 70% of patients had at least one cardiovascular risk factor which is in keeping with this centre's usual treatment population [181]. The age range was also in line with the normal treatment population and the anthracycline doses were part of standard international regimens [181, 182]. The population was split equally in terms of gender and cancer stage. The performance status (0-1) reflected the fact that patients were generally fit. Two patients went on to have mediastinal radiotherapy due to an inadequate response to chemotherapy. This is unlikely to have had a significant impact on the reported results as LVEF is rarely acutely affected by radiotherapy. It may however increase the chance of cardiac morbidity in the future for these patients [183]. Self-selection bias may have impacted on the results as the nature of the trial may appeal to patients who are more health conscious. The majority of patients were Caucasian although the trial was offered to patients of all ethnic groups and some high cardiovascular risk groups were unable to enter the study due to the MRI scanning process (i.e. patients with severe truncal obesity or uncontrolled arrhythmias) and this may have had an effect on results by excluding key patient groups.

3.7.2 Cardiotoxicity was seen within 18 Months of Anthracycline Initiation

Due to the small number of patients and relatively short follow up it was uncertain whether many patients would develop cardiotoxicity during the course of the study. It was anticipated that very few patients would develop cardiac events therefore the final absolute LVEF and change in LVEF were the main study end points. Only a small number of patients (23%) met the pre-determined criteria of cardiotoxicity (fall in LVEF of $\geq$10% to $\leq$55% by the end of study. This was slightly higher than some studies but in line with others [18, 71, 79, 80, 135, 184]. However, many of the studies incorporated a mixed population of cancer patients receiving a range of different chemotherapies including trastuzumab and high dose stem cell transplant therapies making it difficult to directly compare the reported rates of

cardiotoxicity. Sawaya *et al* reported a similar rate of cardiotoxicity (21%) using identical criteria for cardiotoxicity (LVEF decline of ≥10% to ≤55%) but their study included patients receiving trastuzumab which would increase the likelihood of acute LVEF decline over a short time frame [80]. Another more recent study in patients receiving anthracycline-based therapy alone showed that only 13% of patients developed cardiotoxicity [135]. They used the same criteria for cardiotoxicity but follow up was shorter (8 months) and cardiac function was assessed using echo rather than MRI. It could be argued that cardiac MRI is more sensitive at picking up LVEF decline and several recent studies, although small, have demonstrated much higher rates of cardiotoxicity when cardiac function was assessed with MRI [138, 184]. Therefore, differences in study design, duration, cardiac assessment and definition of cardiotoxicity mean that direct comparison between studies is very difficult.

3.7.3 Significant LVEF Decline Occurred in a Large Proportion of Patients

A significant fall in LVEF (≥ 10%) during or within a year of anthracycline therapy was seen in a relatively large number of patients (40%). Cardinale *et al* reported a much lower rate of LVEF decline (23%) but deemed a significant fall to be > 15% and not all of their patients had anthracycline-based therapy. Many had non-cardiotoxic regimens such as ICE (ifosfamide, carboplatin and etoposide) [71]. A small study of lymphoma patients receiving doxorubicin base therapy suggested that 50% of their patients had significant LVEF decline (taken as >10%) when assessed with cardiac MRI which is more in keeping with these results. The majority of patients had persistent decline in LVEF but a proportion of patients (17%) had a transient fall that recovered by one year. The clinical relevance of this is unknown and it may still represent significant damage that could impact on the future cardiovascular health of these patients.

3.7.4 LV Dysfunction was seen in a Small Number of Patients

Only 5 patients (17%) had LV dysfunction (LVEF ≤50%) by the end of study, although 6 more had a transient fall under 50% which recovered by 12 months. All were asymptomatic throughout the study. The rate of LV dysfunction shown by Cardinale *et al* was only 5% but this may be explained by the differences outlined above [71]. Other studies have shown higher rates of LV dysfunction for instance, Drafts *et al* reported LV dysfunction in 26% of patients 6 months after doxorubicin therapy in a study of lymphoma, breast cancer and leukaemia patients [185].

3.7.5 LVEF Decline was Driven by Increasing End Systolic Volume (ESV)

LV systolic function declined in all patients during (mid-chemo) and after chemotherapy with some recovery evident at 12 months. The decline in LVEF was driven by an increase in left ventricular ESV from mid-chemotherapy onwards suggesting that LV contractility was affected from the outset. This is in keeping with findings from Jordan *et al* who also explored cardiotoxicity using CMR in 65 patients receiving chemotherapy for breast cancer or haematological malignancies and demonstrated an incremental increase in ESV with time [186].

3.7.6 Clinical Events were Rare

The number of clinical events was very small (4 in total) so very little can be deduced from this. However, the event rate was in line with other clinical studies of a similar follow up duration (16% reported by Cardinale *et al*) [71]. Three of the events were supraventricular arrhythmias that occurred during therapy and were not preceded by LVEF decline. They are more likely to have resulted from acute doxorubicin effects on either calcium regulation or the conductive system itself [54]. The pre-clinical model showed that atrial damage occurred earlier than ventricular damage in the receipt of doxorubicin and was ultimately more severe. This could have contributed to the development of SVTs due to disruption of the sino-atrial node and the atrial conduction fibres through myocardial degradation. Saying that, the arrhythmias occurred relatively early during treatment, before significant morphological damage would be expected from our pre-clinical translational work which makes the theory of intracellular calcium changes more likely.

3.7.7 Cardiotoxicity was Associated with Cumulative Anthracycline Dose

As previously discussed there is evidence to suggest that anthracycline induced cardiotoxicity is dose related [25, 26] and cumulative anthracycline dose was the only clinical factor that was strongly associated with LVEF decline in this patient population. Final total anthracycline dose was strongly associated with peak LVEF decline and patients who received over 280mg/m^2 did worse than patients who received lower doses. This fits with the cumulative dose related myocardial degradation demonstrated in the rat model and supports findings by other authors [25, 26, 62]. Some guidelines now advise clinicians to carry out cardiac imaging prior to and post receipt of 300mg/m^2 of doxorubicin and these findings add to evidence that patients receiving higher doses are at greater risk [9].

3.7.8 No Other Clinical Factors were Strongly Associated with LVEF Decline

Although older age (>70 years) has been shown to be a potential risk factor for anthracycline-related cardiotoxicity [25, 60] age was not strongly associated with peak LVEF in this small study. The mean age of patients with cardiotoxicity (LVEF decline of ≥10% to ≤55%) was higher than patients without cardiotoxicity (66 versus 54 years) but the difference was not statistically significant and there was no significant difference in the age of patients with and without a decline in LVEF ≥10% (60 versus 57 years). This may have been due to the size and the duration of the study, and age may still be a risk factor for the development of clinical cardiotoxicity in the future regardless of change in LVEF within 18 months of treatment. Pre-existing cardiovascular risk factors (such as hypertension and coronary artery disease) have also been shown to be associated with a higher risk of anthracycline-induced cardiotoxicity [187]. A weak association between pre-existing CV risk factors and LVEF decline (>10%) was seen in this study (p=0.09) but this factor alone was not strong enough to be used as an independent predictor. Anthracyclines are metabolised by the liver and there is some evidence suggesting that patients who have liver dysfunction are at greater risk of cardiotoxicity [60, 188]. None of the patients in this study had liver dysfunction but 16 patients had mildly elevated liver enzymes at baseline however no association was seen with cardiotoxicity. All the patients received combination chemotherapy which is thought to increase the risk of cardiotoxicity [25, 189] and two had radiotherapy to the mediastinum (unplanned) but these patients both experienced a decline in LVEF of ≥ 10% to ≤ 55% prior to the receipt of radiotherapy suggesting the cardiotoxicity at that point was solely drug induced. 11 patients had mildly abnormal ECGs at baseline (i.e. T wave inversion, prolonged PR or partial bundle branch block) but having an abnormal ECG was not associated with the development of cardiotoxicity even though this has been suggested in other studies [187]. There is some evidence from childhood cancer survivorship studies that women may be more susceptible to chemotherapy-related cardiotoxicity than men but this was not something that was seen in this study [190].

3.7.9 Baseline LVEF was Associated with LVEF Decline

One might expect patients with borderline poor LV function to be at greater risk of subsequent cardiotoxicity and this may be true in terms of risk of developing clinical symptoms of heart failure. For instance if a patient dropped their LVEF from a baseline of 54% to 44% it is more likely that they will develop clinical symptoms than a patient who has

a baseline of 64% and drops to 54% despite the same percentage drop in function. However, the results from this study suggest that patients with higher baseline LVEF measurements had greater falls in LVEF which was somewhat unexpected. A positive correlation was seen between baseline LVEF and peak LVEF decline and patients with higher baseline LVEF measurements (>63%) did significantly worse in terms of developing a significant drop (≥10%) during the study. It is difficult to know what the implications of this are and whether this will translate into a greater number of clinical events in these patients in the future. Despite the exponential growth of research in this area there was very little about using baseline LVEF as a predictor of subsequent cardiotoxicity. This is largely because patients with clinically significantly low baseline LVEF measurements are precluded from receiving anthracyclines/cardiotoxic therapy. Jordan *et al* showed no association with baseline LVEF and subsequent LVEF decline in the whole population but showed that lower baseline LVEF levels were predictive of LVEF decline (>20%) in a sub population of patients with ≥ 2 pre-existing CV risk factors [186].

3.7.10 Diastolic Function Declined with Systolic Function

Measuring LA volumes can help to determine whether significant atrial damage has occurred but unfortunately, the LA volume measurements were not as robust as hoped due to suboptimal image quality, particularly while patients were on chemotherapy. This made it difficult to draw strong conclusions about change in LA volume with treatment. Volumetric assessment of the LA was performed using standard 2D images of the 4 chamber and 2 chamber views which requires acquisition of high quality 2D images of the same atrial slice each time for accurate inter-scan comparison. Due to the nature of the study this was difficult to achieve as patients struggled to comply with the breath holds while they were on and directly after chemotherapy. A more accurate way of estimating the LA volumes would have been to do a short axis stack of the LA (as performed for LV volumes) which requires shorter breath holds and would be more reproducible from scan to scan. However it would have meant the patients were in the MRI scanner for a further 5-10 minutes therefore it was no incorporated into the original CMR protocol.

Another measure of diastolic function is the efficiency of ventricular filling during diastole. To recap, the E/A value is a ratio of early to late flow velocity through the mitral value during ventricular filling. E/A ratio alone is a relatively crude way of trying to estimate diastolic function and this is one of the current disadvantages of cardiac MRI. Echo can obtain more

detailed diastolic information such as tissue velocities and this is the measurement that is often used clinically in combination with the E/A ratio, LA volumes and pulmonary pressures to get a comprehensive assessment of all elements of diastolic function [132]. Therefore, although this study can give some insight into diastolic changes occurring during and after anthracycline therapy it is unable to comprehensively assess changes in all aspects of diastolic function during the development of anthracycline-induced cardiotoxicity. However, this study showed a decline in E/A ratio during and directly after treatment but the population mean remained in the normal range (1-2) throughout the study. The pattern of A wave change suggested that there was an element of impaired LV relaxation directly after therapy rather than a decline in atrial contractility that might be expected if marked atrial damage was occurring as in the rat model. However this raises the possibility that impaired LV relaxation may be one of the initial changes contributing to accelerated atrial damage. Fold change of E/A ratio from baseline dropped significantly during chemotherapy in patients who had persistent LVEF decline but it did not alter in patients who had transient or no LVEF decline. Diastolic and systolic functional decline occurred simultaneously going against the theory that diastolic dysfunction precedes systolic dysfunction negating the potential as an earlier marker. This simultaneous decline in function was also described by Cottin *et al* in a similar patient population [191]. Cochet *et al* have shown that pre-existing diastolic dysfunction can be used to predict for cardiotoxicity in patients receiving trastuzumab [144]. 11 patients had an abnormal baseline E/A ratio in this study but it did not predict for LVEF decline or the development of subsequent anthracycline-induced cardiotoxicity.

3.7.11 T1 Mapping and Extracellular Volume did not Change with Anthracycline Therapy

Baseline T1 values in this cancer population were slightly higher than those reported in healthy volunteers [192] but the mean age of the cancer patients in this study was significantly higher (57 years versus 24 years in the healthy volunteers) and this, together with the presence of cancer may explain the difference in baseline values. Pre and post contrast T1 imaging was performed to determine whether myocardial fibrosis could be detected with imaging and quantified during or after anthracycline therapy. This technique has been used to quantify fibrosis in patients with end stage heart failure requiring heart transplantation. ECV estimation calculated from pre and post contrast T1 values was shown to correlate closely with histologically confirmed myocardial fibrosis [137]. It was hypothesised that anthracycline-related cardiotoxicity may also involve diffuse fibrosis and remodelling and this was shown in the rat model with increased fibrosis at the end of study.

However, no significant change in T1 (pre or post) contrast occurred in patients during the 18 month study. There was a small transient rise in the T1 and ECV values directly after therapy but this is likely to represent myocardial oedema which can also affect T1 relaxation. This transient rise was also seen (although not significant) in T2 directly post therapy supporting the theory of increased myocardial fluid content at this time point. The lack of dramatic change in T1 and ECV was not entirely unexpected as fibrosis is a relatively late feature of cardiomyopathy and the follow up in this study may be too short to pick up quantifiable fibrotic changes in patients. Not only that, but patients had relatively mild LV dysfunction which may not be associated the with severe fibrotic changes that were seen in end stage heart failure patients [137]. Having said that, patients with persistent LVEF decline had a significant fold change in ECV from baseline whereas patients with no or a transient LVEF decline showed no significant change from baseline. This trend was also seen in post contrast T1 values but was not significant. This suggests that patients with persistent LVEF decline were getting an expansion of the ECV which could be due to myocyte degradation and collagen deposition in line with the findings in the rat study. Patients with an expansion of >2% did significantly worse in terms of LVEF decline than patients with little change in ECV. Native T1 may have been less informative in this setting as it reflects changes in signal from the ECV and the myocytes themselves. Therefore, although expansion of the ECV was occurring, there may have been simultaneous myocyte degradation (as seen in the rat model) resulting in little overall change in native T1.

ECV evaluation has rarely been explored in patients during the receipt of chemotherapy. The only similar study carried out CMR in 65 cancer patients at baseline and 3 months after anthracycline based chemotherapy. They showed an increase in late gadolinium enhanced signal intensity 3 months after treatment and this was associated with LVEF decline. However, they only performed T1 mapping in a small subset of 10 patients and found no change in T1 value from baseline [186]. A study by Tham *et al* performed T1 mapping in paediatric patients who had been in remission for at least 2 years following anthracycline based chemotherapy and found that ECV correlated with anthracycline dose and exercise capacity but all patients had normal LV function at the time of scan and no baselines were performed to look at change in ECV with treatment [139]. Neilan *et al* also investigated ECV/T1 measurement in 42 patients who had previously received anthracycline therapy (median 84 months) and found that they had increased ECV values compared to age matched

controls and ECV was higher in patients with LV dysfunction [138] so this suggests that significant ECV expansion may be a later development.

3.7.12 Baseline ECV may have Potential to Risk Stratify Patients

It was hypothesised that patients with pre-existing cardiac conditions leading to a higher ECV at baseline may be more susceptible to cardiotoxicity, however the opposite was observed in this study. A greater number of patients with apparent lack of scarring (ECV <33%) had a significant decline in LVEF than patients with higher ECV values. This was confounded by the higher doses of anthracycline received by patients with low baseline ECV values but when this was taken into account there was still a trend showing that these patients did worse. There are no published studies that can support or refute this finding currently and it has generated a new hypothesis. It is possible that anthracycline/drug induced cardiotoxicity is more likely to occur in patients without pre-existing scarring due to increased drug delivery directly to myocytes. Fibrosis of blood vessels and cardiac tissue may decrease the concentration of drug able to reach the myocytes themselves resulting in less toxicity. It has already been shown that drug delivery can affect cardiotoxicity as higher rates of cardiotoxicity are seen when doxorubicin is given as a rapid IV bolus (creating high peak circulating and intra-cardiac levels) rather than slower infusions [193] and recent cardiac MRI research suggests that fibrosis reduces myocardial perfusion making it a plausible hypothesis [194]. The results also support the finding that patients with better baseline cardiac function were more susceptible to LVEF decline, and even though other research has shown that patients with lower LVEF and higher ECV values are more susceptible to cardiac events from other conditions like ischaemia [176], the mechanism around drug-induced cardiotoxicity may differ. However, these findings need to be confirmed in a larger study to ensure they are not erroneous due to small numbers before further exploration.

3.7.13 Late Gadolinium Enhancement (LGE)

Only one patient was found to have an area of late gadolinium enhancement at baseline, suggestive of a previous infarction prior to treatment. There was no known history of ischaemic heart disease in this patient which shows the insensitivity of using clinical parameters like past medical history to risk stratify patients as occult conditions can be missed. No changes in LGE were seen during or after treatment in this or any other patient.

3.7.14 Inflammation did not appear to be a Key Feature of Cardiotoxicity

The lack of change in T2 with treatment goes against one of the original hypotheses that a subclinical myocarditic process occurs during therapy and leads to subsequent LVEF decline. Jordan *et al* also showed that there was no change in T2 shortly after therapy in their patients [186]. Inflammation was seen in the rat model but this followed cessation of doxorubicin and was not the most prominent feature of toxicity. The circulating inflammatory markers were largely supressed during treatment in most patients so these findings together suggest that inflammation is not a strong contributor to LVEF decline. The subtle changes seen in T1 and T2 post therapy were likely to be due to a mild increase in oedema from vascular permeability rather than overt myocarditis as doxorubicin is known to cause endothelial dysfunction and patients often develop generalised clinically appreciable oedema towards the end of treatment [195].

3.7.15 Changes in Dyssynchrony were seen and Coincided with LVEF Decline

Myocardial longitudinal and circumferential strain and strain rate were measured using multiple parameters to get an overview of changes in myocardial deformation during and after anthracycline therapy. Global longitudinal and circumferential dyssynchrony (measured by strain) worsened significantly from baseline directly after chemotherapy but showed some improvement by 12 months in all of the parameters except longitudinal maximal wall-to-wall delay that continued to worsen. Overall, the deterioration in dyssynchrony appeared to occur concurrently with LVEF decline however, patients with permanent LVEF decline showed worsening of longitudinal dyssynchrony (max wall to wall delay) half way through chemotherapy, patients with transient LVEF decline showed worsening of dyssynchrony later, directly post chemotherapy and patients with no LVEF decline showed very little change in dyssynchrony over time. The changes in patients with LVEF decline were not statistically significant and longitudinal dyssynchrony could not be deemed an early predictive marker of cardiotoxicity based on these findings however, this may be due to the small patient numbers and should be explored further. Very little change in global longitudinal or circumferential strain rate was seen during the study but patients with an element of dyssynchrony (assessed by maximal wall to wall delay in time to peak longitudinal strain rate) at baseline appeared to do worse in terms of LVEF decline than patients with less evidence of dyssynchrony prior to treatment. Strain and strain rate assessment have only been explored in treatment related cardiotoxicity over the last few years

so data is lacking but one study showed that global longitudinal strain after 4 cycles of anthracycline-based chemotherapy was predictive of subsequent cardiotoxicity (LVEF decline of ≥10% to ≤55%) [135]. Another study in lymphoma patients receiving epirubicin found a deterioration in longitudinal, circumferential and radial strain with treatment but scans were only preformed before and directly after treatment and LVEF remained normal throughout [134]. A longer study also reported a concurrent decline in peak strain rate and LVEF during the first year post treatment in patients receiving trastuzumab [196]. One study showed that baseline longitudinal strain measurements were predictive of reduced peak early longitudinal strain rate directly after anthracycline chemotherapy but due to short follow up they were unable to relate this to subsequent LVEF decline or clinical events [133]. These studies all estimated deformation using speckled tracking echo (some 2D and some 3D), not CMR and various different methods were employed to calculate changes in strain and strain rate making comparison between studies difficult. The findings all suggest that dyssynchrony occurs during and after anthracycline-base chemotherapy and that looking at cardiac deformation may have potential to inform about subclinical damage prior to LVEF decline but methods need to be optimised and more studies are needed before strong conclusions can be drawn.

3.7.16 Circulating Biomarkers

3.7.16.1 Baseline Biomarkers

The clinical study showed that levels of circulating MMP9, MMP2, TIMP1, IL8, PAPPA, NTproBNP and hFABP were detectable and quantifiable at baseline in this cancer population. Baseline intra-patient variability was relatively low and a reasonable range of baseline concentrations were seen within the population enabling comparison of LVEF behaviour in high and low biomarker groups. However, very few biomarkers showed strong prognostic potential when correlated with decline in LVEF and/or clinical events at 18 months. Only MMP2 and MMP9 showed promise as potential baseline prognostic biomarkers and they are discussed in section 3.7.16.3. Levels of TNFa, IL1b and Troponin I were undetectable at baseline. The validation process showed that the sensitivity of the TNFa and IL1b assays was relatively low (33% and 38% respectively) which may account for the apparent lack of detection of these proteins at baseline and during therapy. However, high levels of both proteins were detected in one particular patient during an episode of infection and thrombosis. The elevations corresponded with markedly elevated levels of several other

proteins (NTproBNP, hFABP, PAPPA and IL8) which would suggest that if there had been large and clinically meaningful changes in these biomarkers due to the development of cardiotoxicity, it would have been detected. The troponin I assay was a diagnostic assay therefore the lack of detectable levels at baseline are likely to be real, reflecting the absence of cardiac damage prior to the receipt of chemotherapy.

3.7.16.2 Troponin I

Troponin I was the most informative biomarker with the greatest potential for use in clinical practice. Troponin I levels rose markedly at cycle 4 following half the cumulative dose of anthracycline. Elevations were seen in 73% of patients but only half of these rose above the level used to diagnose myocardial infarction in clinical practice (>50ng/ml), the other half had low level rises (20-50ng/ml) suggestive of cardiac damage but of uncertain clinical relevance when applied to ischaemic damage. Low level troponin rises have been seen in other studies of chemotherapy-induced cardiotoxicity although the use of different assays makes direct comparison difficult [71]. Patients with and without a decline in LVEF had elevations in troponin I. Only 8 patients (26%) had no elevation in troponin I during the study and five of these patients still had a significant LVEF decline (>10%). These patients had relatively complete data sets with minimal missing data therefore the low troponin I levels cannot be explained by missing time points. Two patients had high peak troponin I levels with no significant fall in LVEF but the follow up for these patients is relatively short therefore it is possible they may go onto develop LV dysfunction or clinical events in the future. Peak fold change in troponin I correlated with LVEF decline and the positive and negative predictive value of peak troponin I were 86% and 69% respectively. Cardinale *et al* found that persistent raised troponin I one month after therapy had a very similar positive predictive value of 84% but a higher negative predictive value of 99% [71]. This difference may be due to the greater number of patients, longer follow up (2 years) and greater number of cardiac events. Troponin I levels did not peak until the final cycle of chemotherapy, cycle 6 in most patients which would be too late to switch treatment or intervene with cardio-protective agents during therapy which was the initial aim of the project. This is in keeping with several other studies that showed troponin I did not peak until the end of anthracycline therapy [71, 77, 197, 198]. The CMR imaging revealed that the population LVEF declined by 5% half way through treatment prior to significant troponin elevation. This would suggest that although troponin is a useful marker of cardiac damage that correlates with LVEF decline, it is not a marker of *early* cardiotoxicity and damage is occurring prior to release of

troponin into the circulation. However, it could still have useful clinical application as it could be used to identify patients for closer follow up or instigation of cardio-protective strategies such as lifestyle advice, ace inhibitors and betablockers as shown by Cardinale *et al* in 2006 [170]. The translational pre-clinical model showed that the release of Troponin I coincided with significant histopathological damage. If troponin I rises reflect similar subclinical damage in humans, they are likely to be the patients at risk of future cardiac events if/when future 'hits' occur to the heart. To that end, patients that had a rise of Troponin I >39ng/ml had a greater rate of significant LVEF decline (>10%) during the study and it could be argued that these patient warrant intervention to improve their cardiac function and prevent further decline. This shows the potential of troponin I to be used to prompt imaging in patients with significant rise in troponin I and avoid expensive imaging in all patients which is something that is being increasingly advised although not routinely done [7]. Although circulating Troponin I levels may have the ability to report myocyte and myocytoskeletal damage they were not elevated prior to the development of acute events in 2 of the 3 patients who had arrhythmias. The mechanisms behind acute arrhythmias with anthracyclines is unlikely to be due to overt histological damage but may result from calcium dysregulation therefore circulating biomarkers such as troponin I would struggle to predict such acute toxicity. This highlights the complexity of cardiotoxicity and suggests that a single biomarker alone is unlikely to have the ability to predict cardiotoxicity and perhaps a combination of clinical factors, imaging and circulating biomarkers is required to enable a more comprehensive assessment in these patients. Since the start of this project the use of circulating troponins in pre-clinical toxicology has grown and they are also being adopted in the clinical setting although not routinely in the UK. These results show the potential of troponin I to report myocardial damage in patients receiving chemotherapy but there is still uncertainty about how to manage these patients to improve outcome, Therefore, until a successful management strategy has been established, the benefit of monitoring remains questionable.

3.7.16.3 MMP2 and MMP9

Baseline levels of MMP2 and MMP9 showed prognostic potential. Higher baseline levels of MMP9 and lower baseline levels of MMP2 correlated with greater LVEF decline although correlations were relatively weak. MMP9 and MMP2 have been shown to be elevated in patients with established heart failure and ischaemia but their exact role in cardiac damage is not fully understood [118, 120, 199]. They are thought to be involved with cardiac

remodelling through collagen degradation [200] but very little is known about their role as prognostic markers. One paper suggested that higher baseline levels of MMP9 were prognostic for further cardiac events in patients undergoing cardiac revascularisation [199]. Another clinical paper showed that rapid decline in MMP2 during an episode of acute heart failure was predictive of better outcome [120] but very little is known about their behaviour in anthracycline-induced cardiotoxicity. One paper showed increased activation of MMP2 in the ventricular tissue of rats with chronic doxorubicin-induced cardiotoxicity however, circulating levels were no different in treated versus control rats [201]. Circulating levels of MMP2 did not alter during the receipt of anthracyclines in this clinical study but levels of MMP9 declined over time during therapy. MMPs are not cardio-specific and the initial theory was that the decline must be due to decreasing tumour volume with response to therapy. However, patients with no active malignancy (i.e. breast cancer patients) still showed a decline in MMP9 and baseline line levels did not correlate with cancer stage. There is some evidence to suggest that inflammatory cells such as neutrophils are one source of MMP9 release and the inflammatory response associated with myocardial damage during ischaemia leads to activation and elevation of MMP9 [202]. The correlation between MMP9 and neutrophils was therefore explored. Results showed that levels of circulating MMP9 correlated closely with neutrophil number at baseline and MMP9 declined in a similar manner to neutrophils during anthracycline therapy. Patients who had a greater decline in MMP9 from baseline appeared to do worse in terms of LVEF decline than patients who maintained their MMP9 levels throughout, although the changes were not statistically significant. Together these findings suggest that high circulating levels of MMP9 at baseline are associated with greater LVEF decline but the ability to maintain MMP9 and enable continued collagen breakdown during and shortly after anthracycline therapy could be cardio-protective. Conversely low MMP2 levels at baseline were associated with greater LVEF decline and MMP2 and MMP9 levels appeared to correlate negatively with each other suggesting they have opposing roles. The literature suggests they are both gelatinases and would be expected behave in a similar way but, as research into extracellular matrix protein evolves, their exact roles appear more and more complex [200, 203]. It must also be noted that circulating levels may not reflect the activity or concentration of these proteins in cardiac tissue as it is only a measure of release into the circulation. However, baseline levels of MMP9 and 2 correlated with baseline extracellular volume (ECV) measurements. Higher levels of MMP9 correlated with lower ECVs supporting that hypothesis that MMP9 can break down collagen and prevent scarring, however higher MMP2 levels were associated

with greater ECV, again suggesting that they have opposing roles. The MMP data supports the findings about ECV as patients with higher MMP9 but a lower ECV at baseline did worse. These data show that circulating levels of these extracellular matrix proteins correlate with the measurements of ECV and support the imaging findings that suggested patients with lower baseline ECV had a greater LVEF decline. Although the relationships were relatively weak these findings highlight a potential area for further research around the role of circulating MMPs, their relationship with ECV and LVEF during chemotherapy-induced cardiotoxicity. The findings are hypothesis generating and would need to be explored further in a much larger study before conclusions could be drawn.

3.7.16.4 PAPPA and hFABP

Baseline levels of PAPPA and hFABP correlated closely with each other which was initially thought be linked to tumour burden, however neither biomarker correlated with cancer stage and both correlated strongly with age. There is very little in the literature about the relationship between PAPPA and hFABP but they would be expected to correlate closely due to their roles in cellular metabolism and proliferation. The majority of papers about PAPPA are related to pregnancy or acute coronary syndromes and none discuss the relationship with age however, hFABP has previously been shown to increase with age in the general population [204]. Neither biomarker correlated with LVEF decline which is not unexpected as age was not related to cardiotoxicity in this study.

3.7.16.5 NTproBNP

The baseline and longitudinal behaviour of NTproBNP showed potential for use as a prognostic and safety biomarker as good intra-class correlation and dynamic changes were seen during treatment however, no strong correlation with LVEF decline or clinical events was seen. This is not unexpected as the literature around the role of natriuretic peptides in anthracycline toxicity is very mixed with some studies showing no correlation with cardiotoxicity and others suggesting that is may have potential [78, 80, 91, 92]. The strongest evidence remains in the post treatment setting where it can be used to aid diagnosis of subclinical cardiac dysfunction in cancer survivors many years later [90, 93]. The validation findings also raised some concern over the stability of NTproBNP when stored for long periods suggesting that levels could rise when stored for 6 months or more. This phenomenon did not appear to affect the longitudinal behaviour of NTproBNP in the study but the subtle post processing changes could affect the validity of the results.

3.7.16.6 IL8 and Rituximab

The validation process also suggested that rituximab could affect the IL8 assay due to competitive binding leading to slightly lower results in patients receiving rituximab. Levels of IL8 rose transiently 24 hours after the first cycle of chemotherapy and are more likely to reflect changes in the tumour than in the heart. This transient rise was seen equally in patients who were and who were not receiving rituximab but the only patient with clear elevations during the rest of treatment was not on rituximab. These changes were linked to an infective episode complicated by thromboembolism and were not thought to be related to cardiac damage. No overall link with LVEF was seen with the population as a whole.

3.7.16.7 MMP2, TIMP1, IL8,

The remaining circulating biomarkers (MMP2, TIMP1, IL8, PAPPA and hFABP) showed no significant change with time in the overall population or subgroups based on LVEF decline. hFABP is the only one of these biomarkers that has been explored in patients with chemotherapy-induced cardiotoxicity before. Several studies also showed no change in hFABP during or after chemotherapy but one study showed an acute rise within 24 hours of the first dose of chemotherapy that correlated with LVEF decline [29, 205, 206]. A non-significant rise from baseline was also seen 24 hours after cycle 1 in this study but the rise remained within the limits of baseline variability and was thought to result from initial tumour breakdown rather than cardiotoxicity. Overall the findings are not entirely surprising and it is possible that very little is published about these biomarkers as they have not been found to be useful in other studies of chemotherapy-induced cardiotoxicity.

3.8 Conclusions

The exploratory imaging biomarkers were unable to identify patients prior to the decline in LVEF and in most cases changes occurred simultaneously with deterioration in LV function. LVEF itself was one of the earliest changes to occur but how this will relate to subsequent cardiac morbidity remains to be seen. Contrary to the initial hypotheses, **better baseline cardiac function and lower baseline ECV were associated with greater LVEF decline suggesting that patients without pre-existing damage are still at high risk of cardiotoxicity.** Diastolic function assessed by E/A ratio and dyssynchrony both worsened during treatment but changes happened concurrently with LVEF decline. No significant changes in myocardial tissue characterisation were seen during the study suggesting that fibrosis is a much later event and inflammation is not a key feature of anthracycline-related

cardiotoxicity. Significant Troponin I elevations were seen in patients receiving anthracyclines and peak troponin I levels correlated with peak LVEF decline. However, elevations did not occur until the end of chemotherapy following LVEF decline therefore Troponin I cannot be used as an early biomarker to aid cessation of anthracyclines or initiate of cardio-protective strategies. However, peak Troponin I levels had relatively high positive and negative value for predicting LVEF decline and could still be useful to risk stratify patients post therapy. This data adds to the growing body of evidence around the use of Troponin I in patients receiving cardiotoxic chemotherapy but highlights the need for an even earlier marker of cardiac damage. The pre-clinical and clinical data certainly suggest that troponin I release signifies the presence of myocardial damage but this study is unable to fully determine the clinical relevance and therefore how it would be implemented into clinical practice. The matrix metalloproteinases showed potential as cardiotoxicity biomarkers. MMP9 levels fell during treatment and patients with a greater decline did worse in terms of deterioration of LV function. Baseline levels of MMP2 and 9 may help to identify patients at higher risk and they appear to be related to myocardial extracellular volume however the associations were relatively weak and more exploration into their role in cardiotoxicity and relationship with LV function and myocardial fibrosis is needed. The remaining eight circulating biomarkers did not show potential in this setting.

4 Closing remarks

4.1 Project Limitations

The main limitations of the clinical study were the short time frame and relatively small patient population. The length of follow up was dictated by the time frame of the PhD and it would have been surprising to have seen a large number of clinical events in this short period hence the need for surrogate markers of cardiotoxicity such as LVEF decline. However, LV function is internationally recognised as a surrogate for cardiotoxicity and standard criteria were used. The number of patients was limited a) due to the time frame and b) due to the nature of the study. Although 100 patients were approached, only 36 were recruited. Some of the main reasons for the low recruitment rate were competing trials (usually involving new cancer agents), multiple blood tests and the MRI scans. Many patients were put off by having to have extra scans when they had already had multiple CT and PET scans prior to diagnosis. There was also an element of stigma around the MRI scans as people associated them with claustrophobia and were reluctant to participate. Several patients were unable to have cardiac MRI because of claustrophobia and a small number were excluded due to the presence of pre-existing atrial fibrillation or obesity. The latter two are important as they could influence the study results by excluding some potentially high risk patient groups. Most of the studies investigating cardiac MRI in cancer patients are relatively small and this may be because other investigators have had similar issues with recruitment. There were several other issues with cardiac MRI. Some of the imaging sequences required relatively long breath holds which some patients struggled with when they were in the middle of chemotherapy. This resulted in suboptimal image quality and therefore data. We were also unable to give contrast in some cases due to problems with venous access or worsening renal function. So despite the breadth of information obtainable with cardiac MRI the practicalities make it a difficult tool to use in cancer patients. Calculation of ECV requires measurement of haematocrit to determine the contrast volume of distribution but it was not always possible to measure haematocrit on the same day as the scan therefore the nearest haematocrit had to be used. This may have led to some inaccuracy in the ECV results if haematocrit varied significantly between the blood test and scan therefore for future projects it would be important to ensure a full blood count was taken on the same day as the scan. The sensitivity of two of the multiplex assays (IL1b and TNFa) was suboptimal and although dynamic change was seen in some patients, subtle changes may have been missed due to the low sensitivities. Assay sensitivity was also an issue in the pre-clinical work. The rat multiplex assays used human

capture antibodies that were validated by the manufacturer and shown to be compatible with rat plasma but the sensitivities were relatively low and the variability was high. No significant change was seen in any of the circulating biomarkers using multiplex ELISA which could have been a true finding (in line with the clinical study findings) but the suboptimal assay quality means these biomarkers cannot be confidently excluded as they may have been measureable using different methods. In the clinical study we were able to measure blood at multiple time points to pick up transient and well as cumulative changes in biomarker however the number of blood draws was limited in the rat due to animal welfare and tail vein damage. However, the transient rises seen in humans did not translate into useful predictors of cardiotoxicity making the smaller time point number in the rat model less important. Not all the novel exploratory imaging methods were possible in the rat due to the rapid heart rates. Endocardial tracking was not possible using the strain analysis software therefore strain analysis could not be performed. Tissue mapping has previously been performed in rats but is difficult to achieve and was therefore not performed in this project [207]. Peak contrast enhancement (T1 signal intensity) was performed in the rats. However, this method does not account for the contrast within vessels and is more likely to be a measure of vascular permeability and overall cardiac integrity than fibrosis. Therefore peak contrast enhancement could still be a useful marker of cardiotoxicity especially as elevations correlated well with troponin release. Finally, the use of Kaplan Meir analysis in the clinical study enabled basic assessment of the potential prognostic and predictive value of the exploratory biomarkers but took into account time to event, which may or may not be clinically relevant in this setting. Also, like most statistical tests, Kaplan Meir analysis did not account for the recovery of cardiac function over time which occurred in a small number of patients. As the group of patients showing transient LVEF decline was very small, separate statistical analysis of this group was not meaningful therefore a bigger study would be needed enable patients to be divided into three groups (based on LVEF behaviour over time) large enough to enable meaningful statistical analysis.

4.2 Preclinical Study Closing Remarks

A rat model of chronic anthracycline-induced cardiotoxicity using clinically relevant intravenous dosing was developed and successfully used to explore the changes in circulating and imaging biomarkers during the onset of cardiotoxicity. Cardiac MRI was a practical and sensitive way of detecting cardiotoxicity and LVEF declined incrementally with each dose of anthracycline. Electron microscopy revealed mitochondrial and cytoskeletal changes after the

first dose which may have led to the early decline in cardiac function before being visible with other methods. Circulating Troponin I levels increased towards the end of therapy and corresponded with the development of overt microscopic histological damage and peak contrast enhancement on CMR.

4.3 Clinical Study Closing Remarks

LVEF decline was seen during and within a year of anthracycline-based chemotherapy. LVEF decline appeared to be dose related but no other clinical factors were strongly associated with cardiotoxicity. No single circulating biomarker or imaging parameter was able to independently predict the development of cardiotoxicity in this small cohort and LVEF decline was one of the earliest changes to be seen, prior to changes in the exploratory markers. Troponin I rose during treatment and peak levels correlated with decline in LVEF however levels did not peak until the final cycle of chemotherapy therefore troponin I was found to be a relatively late marker of damage. However, it may have potential to risk stratify patients for cardio-protective strategies following treatment but is too late to be used to change cancer therapy or instigate cardio-protection during treatment. Extracellular volume estimation using cardiac MRI showed potential as a baseline prognostic marker and correlated with baseline levels of circulating MMP2 and 9 generating new hypotheses about susceptibility to anthracycline induced cardiotoxicity. Worsening of myocardial dyssynchrony was seen during treatment but changes occurred concurrently with decline in LVEF. Baseline longitudinal dyssynchrony (measured by maximal wall to wall delay in time to peak strain rate) shows potential as a baseline prognostic marker but this would need to be explored further in a large study before strong conclusions could be made.

4.4 Translation of the Chronic Anthracycline-Cardiotoxicity Rat Model

LVEF decline followed the same pattern of incremental decline in rats and humans and significant troponin I elevations occurred at a similar cumulative doses of anthracycline. This suggests that the rat model is a good translational model of progressive drug-induced cardiotoxicity and has the potential to aid cardiac safety profiling of other anti-cancer agents. It supports the use of cardiac MRI as a translation imaging tool for detecting cardiotoxicity and suggests that troponin I is a good safety biomarker for use in translational studies. It was not possible to perform all the imaging parameters in the rat model (i.e. strain and tissue characterisation) due to the rapid heart rate, but as imaging techniques improve this may be possible and enable direct histological comparison with imaging findings. Not all of the

circulating biomarkers were as informative in the rat model as they were in the human which was largely due to assay quality but troponin I proved to be a robust, clean and potentially useful circulating biomarker. However, it was a relatively late marker of damage, and earlier markers of cardiotoxicity to detect damage and guide management during treatment are needed. This translational rat model could be used to look for earlier biomarkers of anthracycline-induced cardiac damage such as circulating microRNAs that may be released into the circulation prior to proteins. **The changes seen on electron microscopy suggest that circulating markers of mitochondrial damage could provide the earliest indication of cardiac damage but finding cardiac specific markers of this nature may be challenging**.

4.5 Hypothesis Testing

Hypothesis 1 stated that circulating biomarkers may have the potential to report cardiotoxicity prior to the development of cardiac dysfunction whereas this project has shown that functional decline (both systolic and diastolic) is one of the earliest changes during anthracycline therapy and precedes detectable changes in circulating proteins. Hypothesis 2 stated that cardiac MRI may have the potential to detect changes in tissue character or deformation prior to functional decline. In fact only transient and non-significant changes in tissue character were detectable and dyssynchrony worsened concurrently with LV decline. However the project identified several circulating and imaging markers that warrant further investigation and could be useful in both drug safety testing and clinical practice namely Troponin I, MMP9, MMP2, ECV and strain analysis.

4.6 Future Directions

Further pre-clinical work is in process at Astra-Zeneca in collaboration with the University of Manchester, Institute of Cancer Sciences using the established rat model to look for earlier biomarkers of cardiac damage having estabilished that troponin I is a relatively late marker. A discovery proteomic and miRNA biomarker approach will be employed to look for up-regulated markers in myocardial tissue showing earlier signs of anthracycline damage and provide a targeted approach to determine whether these markers are detectable in the circulation. A group at Imperial College London have are also using this rat model to investigate mitochondrial function and miRNAs with the hope of identifying earlier biomarkers for translation into humans. From a clinical perspective, the speciality of cardio-oncology is growing rapidly and clinical research is becoming a priority. There is potential to extend the discovery proteomic and miRNA program into humans using the data already

gathered and the plasma stored during this project if promising biomarkers arise from the pre-clinical work. There is also potential to extend follow up in the current cohort to further explore the imaging parameters, particularly T1 mapping and ECV estimation at the 5 and 10 year point to determine whether patients with highest peak troponin I go on to develop fibrosis and LVEF decline at a later stage. It would also be interesting to expand the cohort and explore the hypothesis that a lower baseline ECV is associated with greater drug delivery to myocytes and a greater risk of cardiotoxicity as this is a new area of research which has not been explored before.

An interventional project in lymphoma survivors (>2 years) is being planned with the aim of determining whether intervention with lifestyle changes and primary prevention with a combined statin, aspirin and angiotensin 2 inhibitor polypill could reduce the rate of cardiac events. Troponin I is unlikely to be useful to stratify patients 2 years after therapy but it could be used to risk-stratify patients for similar intervention with primary pharmacological prevention and life style changes during or shortly after therapy and this hypothesis needs testing in a large prospective randomised controlled trial in order to break into routine clinical use.

Finally, it is unlikely that a single biomarker would have the power to independently predict or detect all aspects of cardiotoxicity in patients or during drug development. Therefore, a member of the statistical team at Manchester University is currently looking at combining the factors that show the most potential from this project i.e. change in Trop I, baseline LVEF, baseline ECV, anthracycline dose and dyssynchrony using principle component analysis to try and determine whether the combined approach can more accurately predict which patients will develop cardiotoxicity.

Appendix 1: Pre-Clinical Rat Cardiotoxicity Model Multiplex ELISA Results

Troponin T levels rose on day 43 in doxorubicin-treated rats in line with troponin I but the change was not significant as levels only rose in the worst affected rats. The behaviour of TNFa, MMP9, IL1b and IL8 in treated and control rats is shown below. FABP3 was not detectable in the majority of rat plasma samples at baseline or during treatment. The MMP2 assay did not meet acceptance criteria therefore data was not reported or interpreted.

Trop T

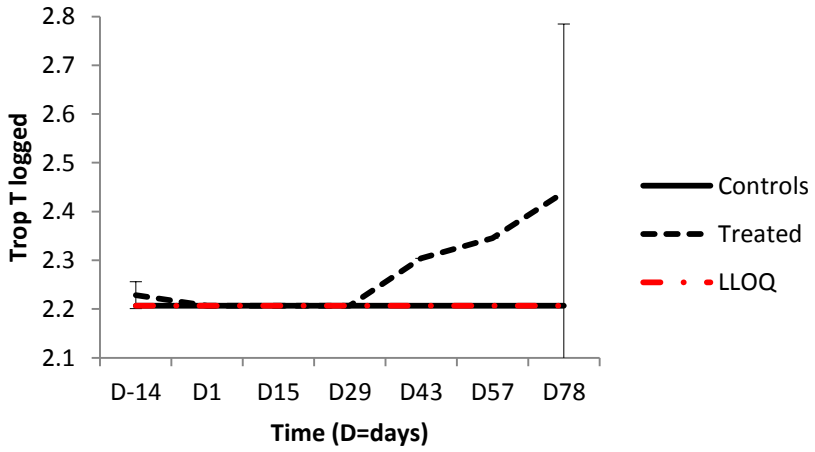

Figure 67. Troponin T levels in treated and control rats (n=8 per group). *Rats were dosed once weekly with doxorubicin (1.25 mg/kg, dashed line) or vehicle (solid line) for 8 weeks followed by a 4 week off-dosing period. Error bars represent the standard deviation for the group.*

TNFa

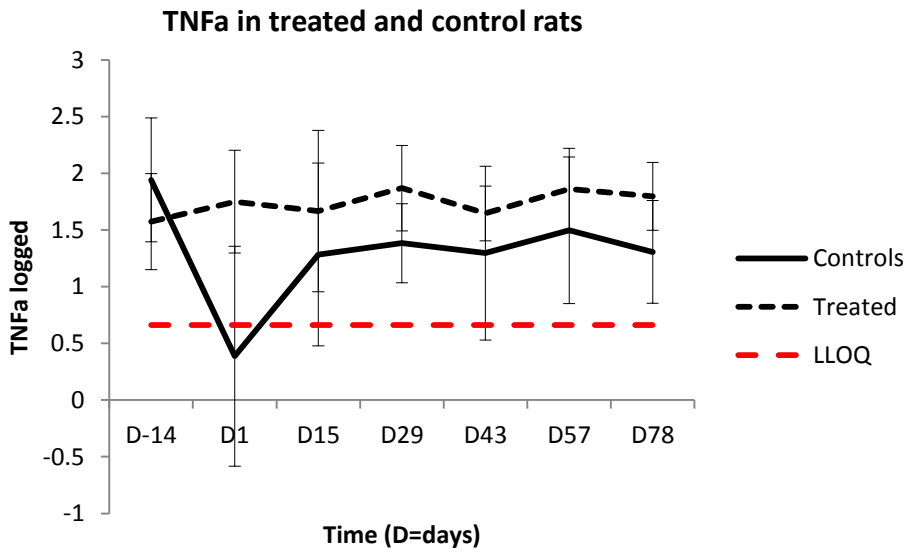

Figure 68. TNFa levels in treated and control rats (n=8 per group). *Rats were dosed once weekly with doxorubicin (1.25 mg/kg, dashed line) or vehicle (solid line) for 8 weeks followed by a 4 week off-dosing period. Error bars represent the standard deviation for the group.*

MMP9

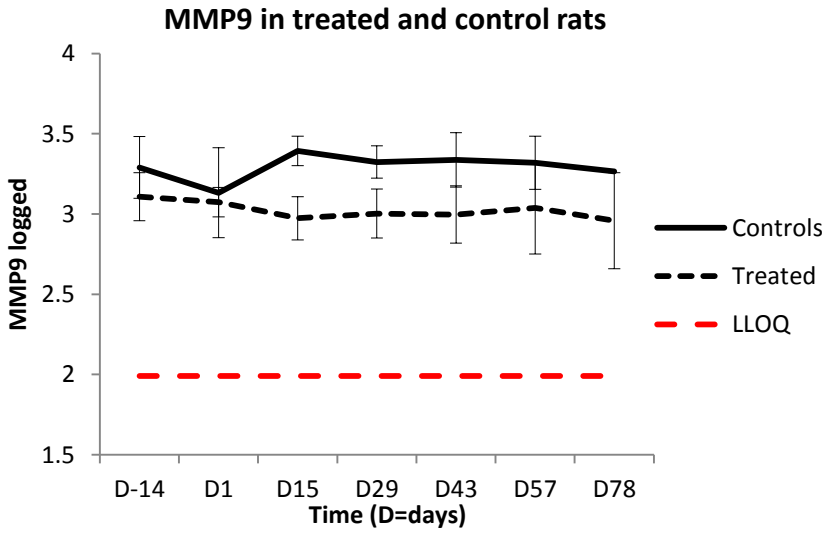

Figure 69. MMP9 levels in treated and control rats (n=8 per group). *Rats were dosed once weekly with doxorubicin (1.25 mg/kg, dashed line) or vehicle (solid line) for 8 weeks followed by a 4 week off-dosing period. Error bars represent the standard deviation for the group.*

IL1b

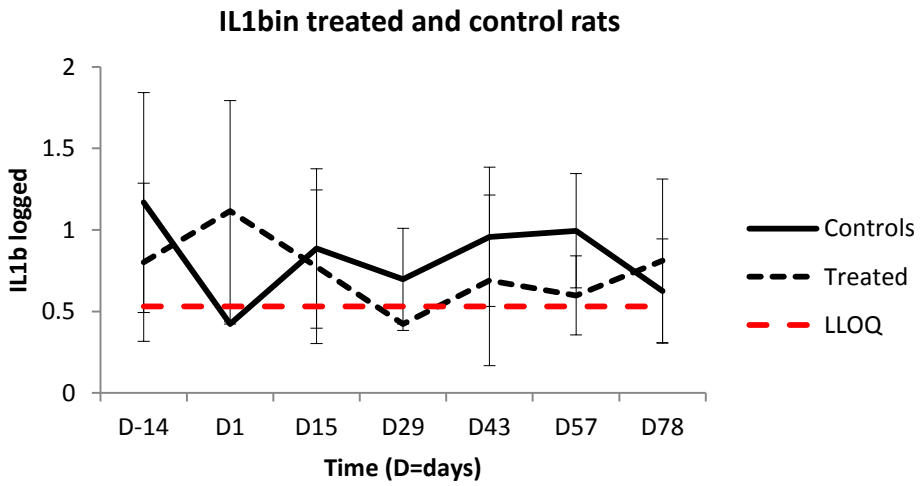

Figure 70. IL1b levels in treated and control rats (n=8 per group). *Rats were dosed once weekly with doxorubicin (1.25 mg/kg, dashed line) or vehicle (solid line) for 8 weeks followed by a 4 week off-dosing period. Error bars represent the standard deviation for the group.*

IL8

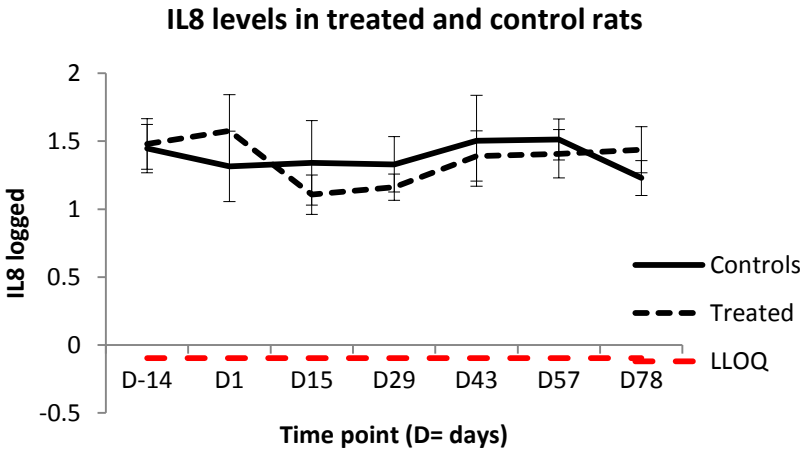

Figure 71. IL8 levels in treated and control rats (n=8 per group). *Rats were dosed once weekly with doxorubicin (1.25 mg/kg, dashed line) or vehicle (solid line) for 8 weeks followed by a 4 week off-dosing period. Error bars represent the standard deviation for the group.*

Appendix 2: Determining the LLOQ for Human Multiplex ELISA

Lower limit of quantification (LLOQ)for multiplex ELISAs

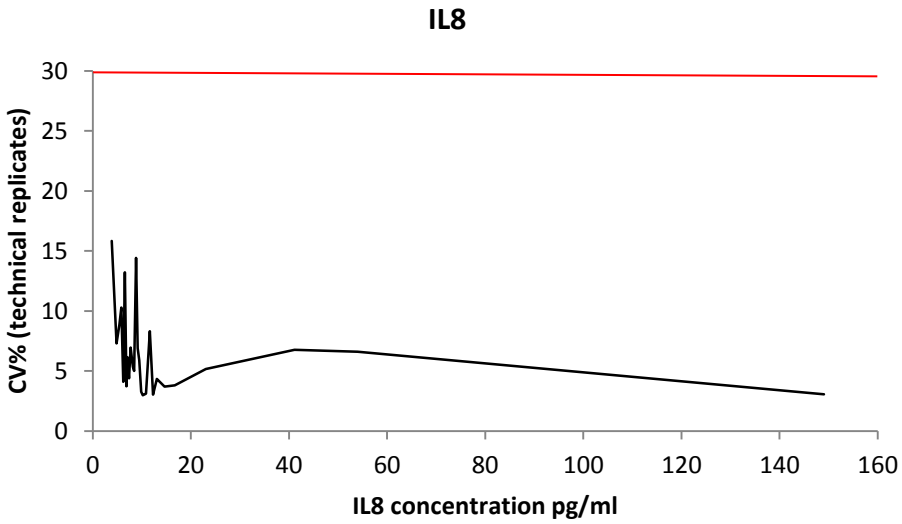

Figure 72. The LLOQ for the IL8 assay was taken as the bottom of the standard curve 0.4pg/ml (x2 for dilution factor) as technical replicate agreement was good above this concentration.

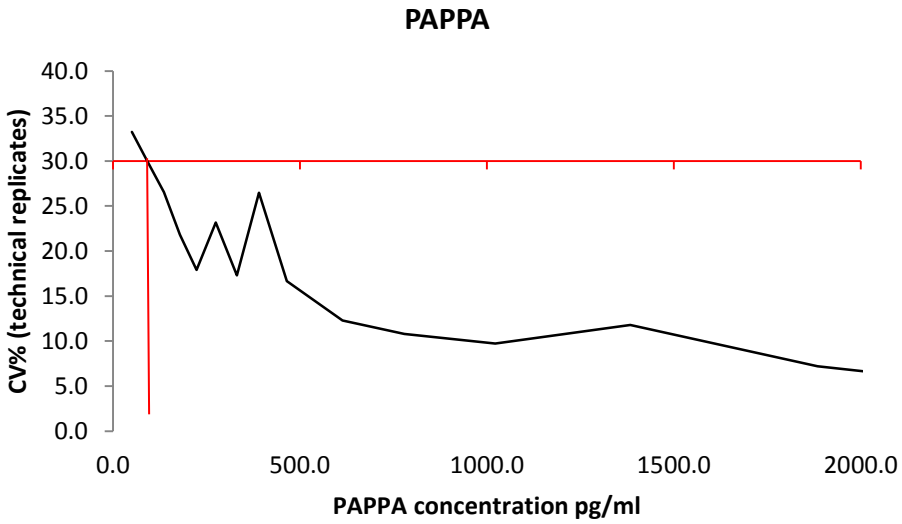

Figure 73. The LLOQ for the PAPPA assay was taken as the bottom of the standard curve 98pg/ml (x2 for dilution factor) as technical replicate agreement was reasonable above this concentration.

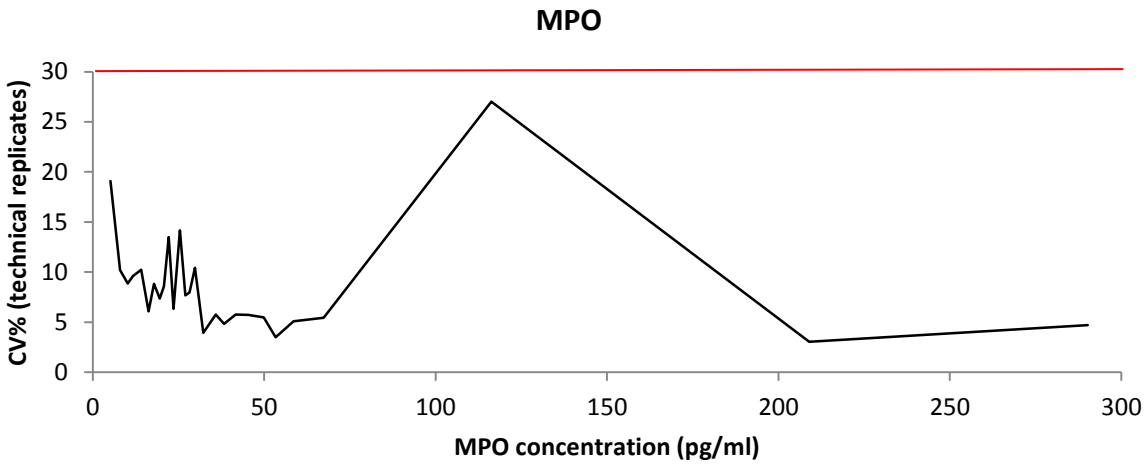

Figure 74. The LLOQ for the MPO assay was taken as the bottom of the standard curve 2pg/ml (x1000 for dilution factor) as technical replicate agreement was reasonable above this concentration.

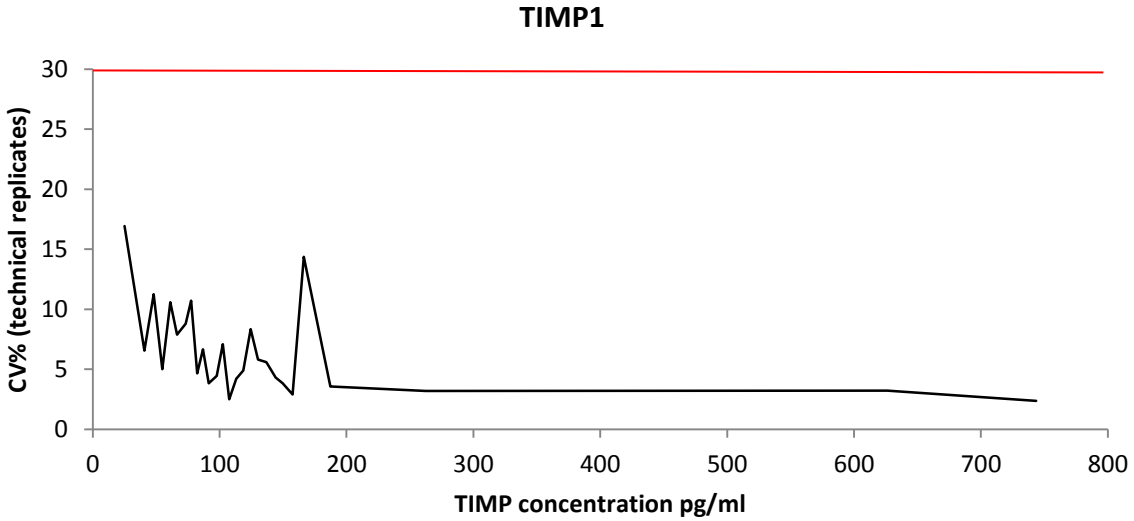

Figure 75. The LLOQ for the TIMP1 assay was taken as the bottom of the standard curve 5pg/ml (x1000 for dilution factor) as technical replicate agreement was good above this concentration.

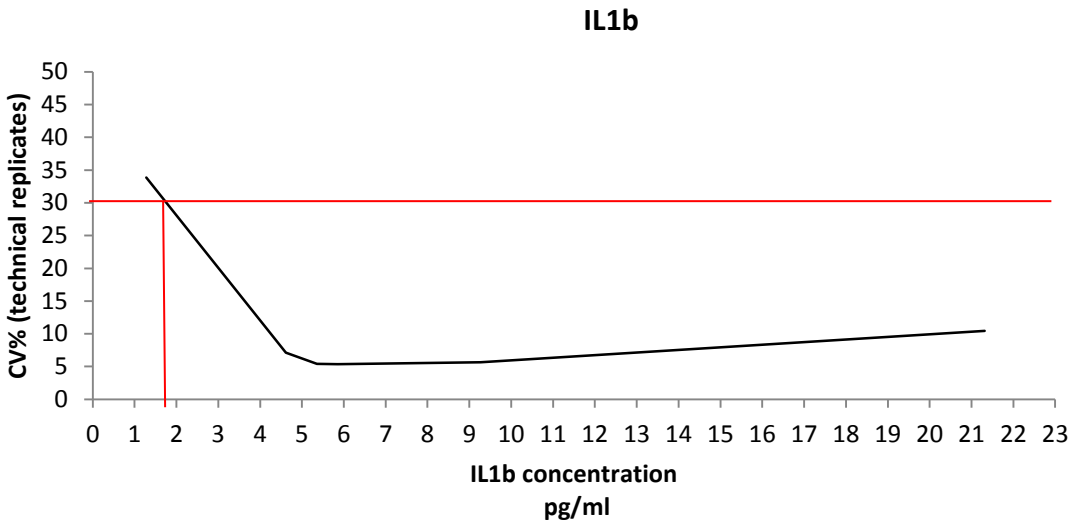

Figure 76. The 30% CV intersects at 1.7pg/ml for the IL1b assay which is above bottom of the standard curve. *Below this point there is a low level of agreement between technical replicates and data is likely to be inaccurate therefore the LLOQ was set at 1.7pg/ml (x2 for dilution factor) therefore LLOQ = 3.4pg/ml.*

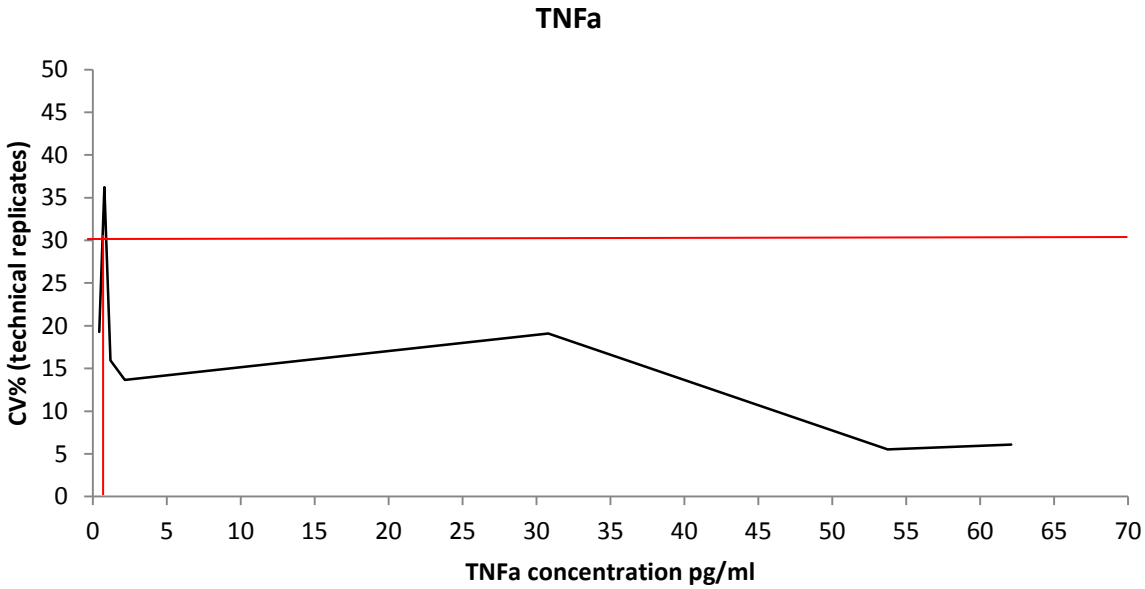

Figure 77. The LLOQ for the TNFa assay was taken as the bottom of the standard curve 2.3pg/ml (x2 for dilution factor) as there was good agreement between technical replicates above this concentration (the 30% CV intersects at 0.9pg/ml).

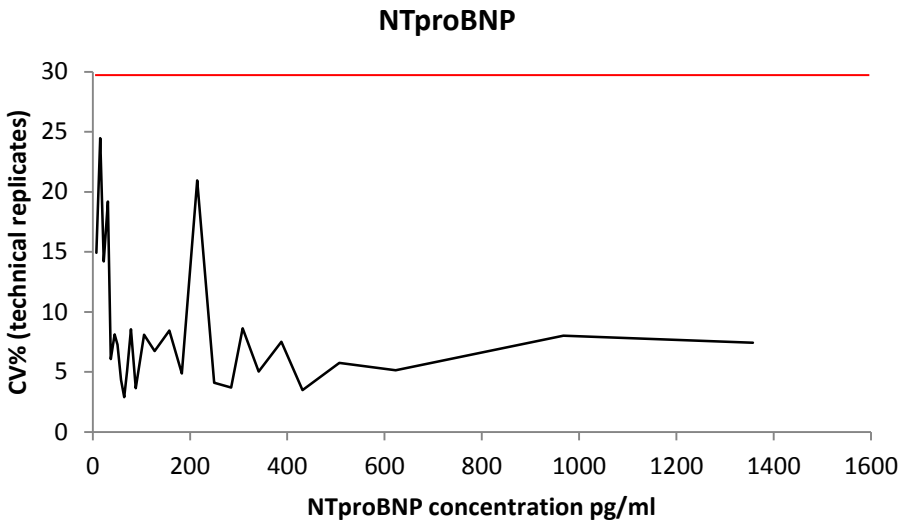

Figure 78. The LLOQ for the NTproBNP assay LLOQ was taken as the bottom of the standard curve 1.4pg/ml (x2 for dilution factor) as there was good agreement between technical replicates above this concentration.

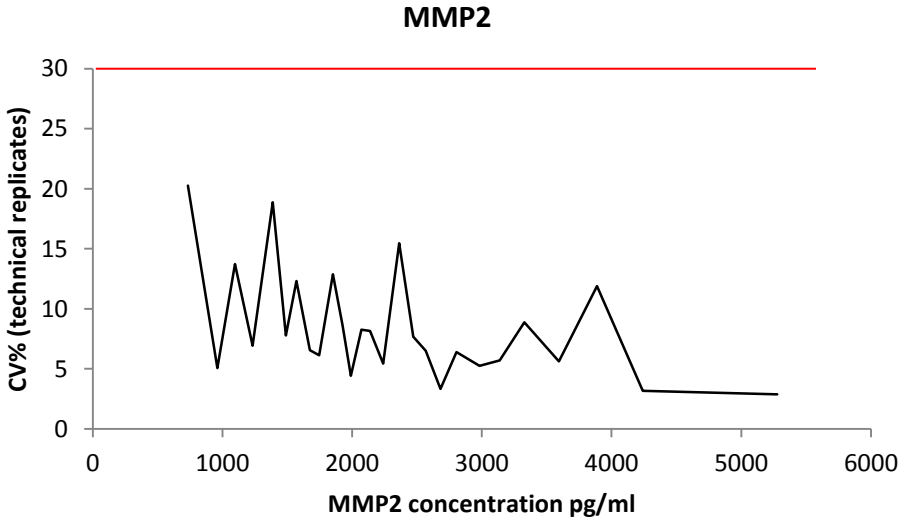

Figure 79. The LLOQ for the MMP2 assay was taken as the bottom of the standard curve 31pg/ml (x100 for dilution factor) as there was good agreement between technical replicates above this concentration.

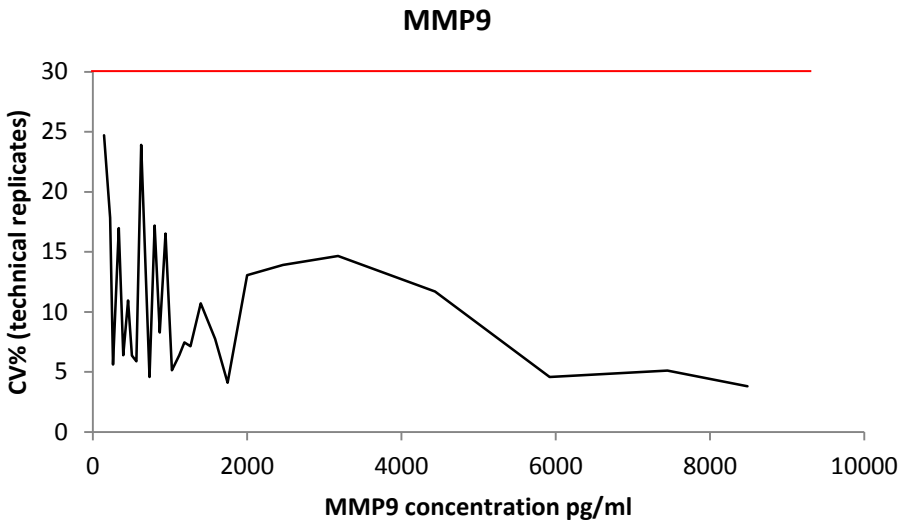

Figure 80. The LLOQ for the MMP9 assay was taken as the bottom of the standard curve 49pg/ml (x 100 for dilution factor) as there was good agreement between technical replicates above this concentration.

Appendix 3: Validation of the Human Multiplex ELISA Platform for Clinical Use

A series of in house validation experiments were carried out on the custom made multiplex ELISA assays to ensure they were 'fit for purpose' (i.e. robust and reproducible) prior to analysis of clinical trial samples. Eight experiments were performed as part of the validation testing and each was performed three times:

1. Standard curve reproducibility
2. Signal interference
3. Antibody cross-reactivity
4. Protein recovery (from human plasma and diluent)
5. Intra and inter-plate variability
6. Freeze/thaw stability
7. Rituximab cross reactivity
8. Observed values in patient samples

All validation experiments were performed using the standard multiplex ELISA technique described in Clinical Study Materials and Methods (section 3.2). Spiking experiments were carried out using the recombinant protein supplied with the above ELISA kits spiked into human plasma from consenting healthy volunteers at the Cancer Research UK, Manchester institute, University of Manchester or foetal calf serum based kit diluent. Blood was also taken from a small number of lymphoma patients who had previously received anthracyclines with and without cardiac morbidity. These patients were consented with the permission of Dr. Alastair Greystoke as part of his ethically approved research protocol looking at biomarkers of epithelial toxicity and cell death with chemotherapy (project number CEP049). Rituximab was purchased from Roche, Germany at 100mg/10ml, product no. B6053B01.

Standard Curve Reproducibility

Quantification of the amount of protein in a sample was determined using a standard concentration curve. The concentration curve was produced by serially diluting a solution containing a known concentration of the protein of interest. Three standard curves were produced for each analyte before testing clinical samples to ensure that each curve had an acceptable line of best fit ($R^2 > 0.985$) with which to interpret sample protein concentrations

and that the curves were reproducible. **Table 21** shows the standard curve and R^2 values for each biomarker and **Figure 81** shows the standard curves themselves.

Biomarker	MMP2 pg/ml	MMP9 pg/ml	MPO pg/ml	TIMP1 pg/ml	NT pro BNP pg/ml	IL1b pg/ml	PAPP A pg/ml	TNFa pg/ml	FABP pg/ml	IL8 pg/ml
Undiluted	512000	800000	28800	80000	22400	3200	1600000	38400	7680000	6400
1 in 16	32000	50000	1800	5000	1400	200	100000	2400	480000	400
1 in 2	16000	25000	900	2500	700	100	50000	1200	240000	200
1 in4	4000	6250	225	625	175	25	12500	300	60000	50
1 in 4	1000	1562.5	56.3	156.3	43.8	6.25	3125	75	15000	12.5
1 in 4	250	390.6	14.1	39.1	10.9	1.56	781.3	18.8	3750	3.1
1 in 4	62.5	97.7	3.5	9.8	2.7	0.4	195.3	4.7	937.5	0.78
1 in 2	31.25	48.8	1.8	4.9	1.4	0.2	97.7	2.3	468.8	0.39
R^2	0.996	0.996	0.996	0.994	0.994	0.994	0.995	0.995	0.998	0.995

Table 21. Standard calibration curves for multiplex ELISAs (n=3)

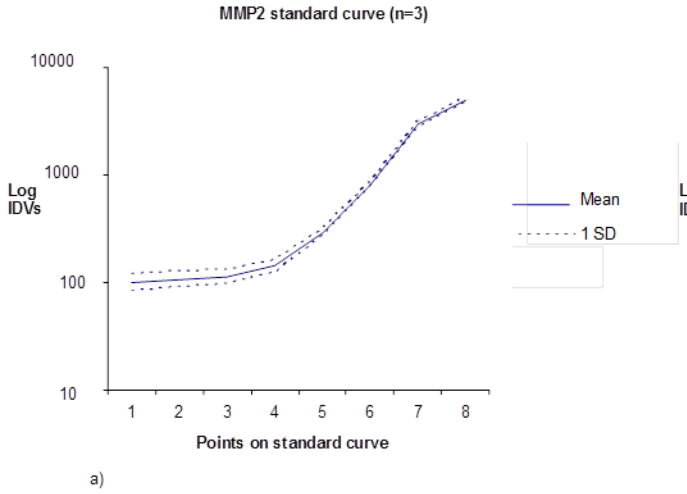
MMP2 standard curve (n=3)
10000
1000
100
10
Log IDVs
1 2 3 4 5 6 7 8
Points on standard curve
Mean
1 SD

a)

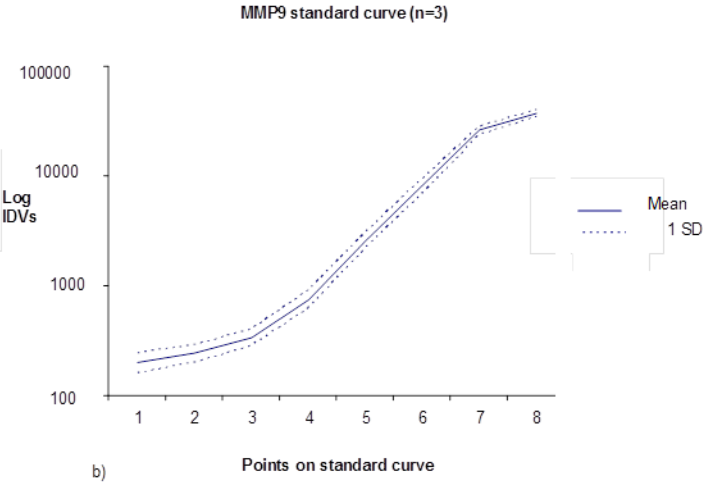
MMP9 standard curve (n=3)
100000
10000
1000
100
Log IDVs
1 2 3 4 5 6 7 8
Points on standard curve
Mean
1 SD

b)

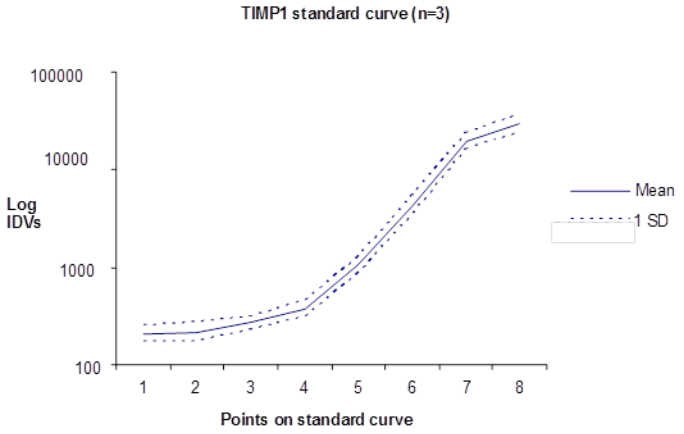
TIMP1 standard curve (n=3)
100000
10000
1000
100
Log IDVs
1 2 3 4 5 6 7 8
Points on standard curve
Mean
1 SD

c)

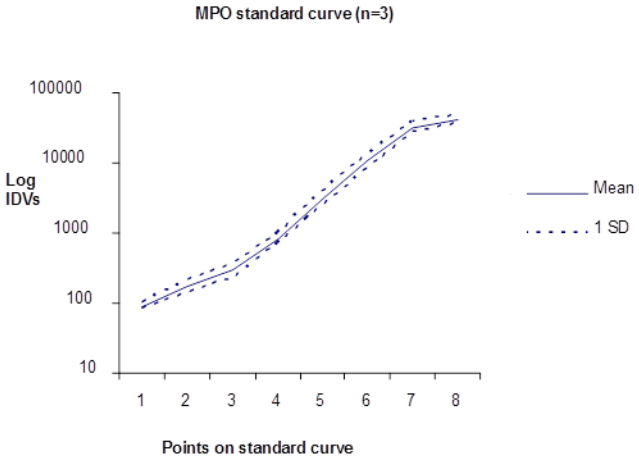
MPO standard curve (n=3)
100000
10000
1000
100
10
Log IDVs
1 2 3 4 5 6 7 8
Points on standard curve
Mean
1 SD

d)

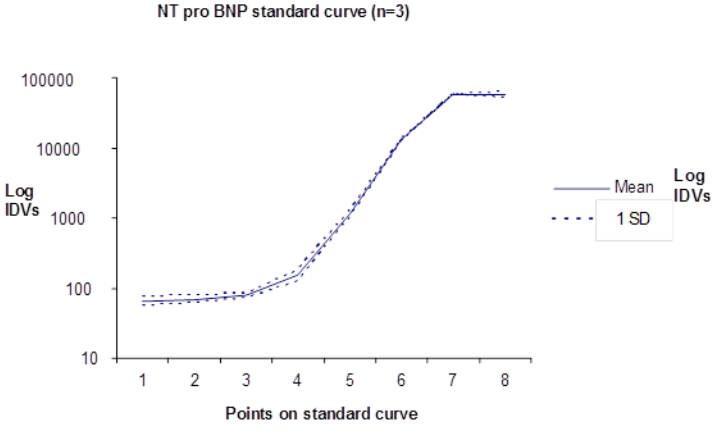
NT pro BNP standard curve (n=3)
100000
10000
1000
100
10
Log IDVs
1 2 3 4 5 6 7 8
Points on standard curve
Mean
1 SD

e)

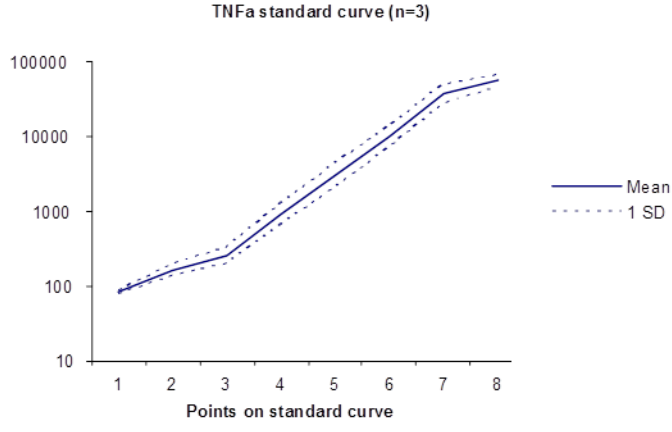
TNFa standard curve (n=3)
100000
10000
1000
100
10
Log IDVs
1 2 3 4 5 6 7 8
Points on standard curve
Mean
1 SD

f)

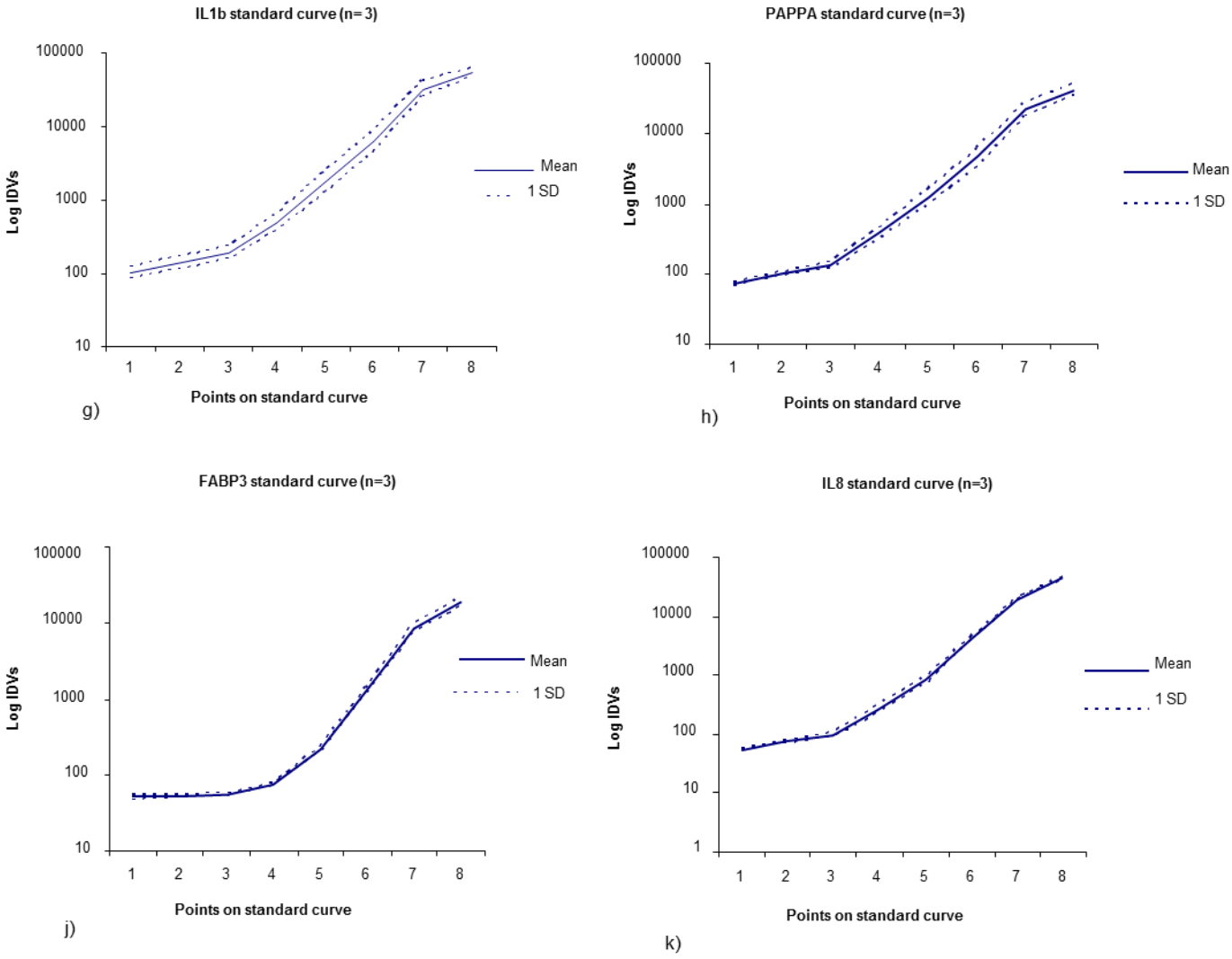

Figure 81. Graphs a) to k) show the standard curves for each assay. *The raw values were logged, the geometric mean and the standard deviation of the logged values were calculated. The values were then plotted graphically to illustrate the standard curves for each analyte showing one standard deviation either side of the mean (dotted line). IDV = integrated density values i.e. signal intensity. Each experiment was carried out 3 times.*

Signal Interference and Antibody Cross-Reactivity

This experiment used a standard curve as a tool to investigate the potential for one assay to affect the others by varying the levels of one analyte whilst keeping the others constant. If the

assays are truly independent, then increasing the concentration of one protein should not affect the other assay results.

Example (**Figure 82**): PAPPA recombinant protein was spiked into kit diluent at a concentration of 12500pg/ml and TNFa recombinant protein was spiked into kit diluent at a concentration of 300pg/ml. The samples were divided into 8 and combined with increasing concentrations of IL1b recombinant protein (by preparing a standard concentration curve). The measurements of TNFa and PAPPA remained constant despite increasing amounts of IL1b in the samples (**Table 22**). The mean TNFa measurement was 331.4pg/ml (SD 22.7pg/ml and CV 5.1% between samples). The mean PAPPA measurement was 13375pg/ml (SD 685.4pg/ml and CV 6.8% between samples). The signal interference results for the remaining multiplex assays are shown in **Table 23 & Table 24.**

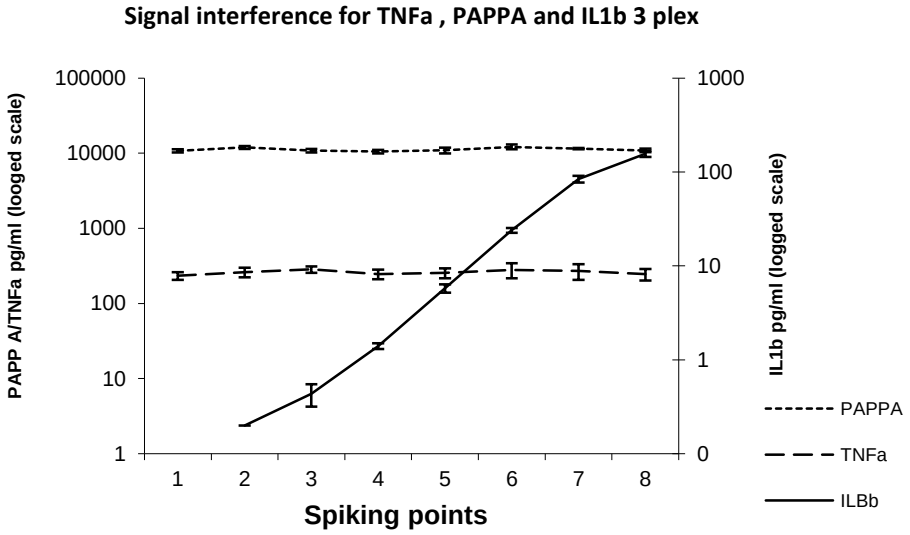

Figure 82. Signal interference for TNFa, PAPPA and IL1b. Stable concentrations of PAPPA and TNFa with increasing IL1b. *The error bars are the standard deviation for 3 experiments.*

Spiking point (n=3)	IL1b pg/ml (stable)	PAPPA pg/ml (stable)	TNFa pg/ml (increasing)	IL1b pg/ml (stable)	PAPPA pg/ml (increasing)	TNFa pg/ml (stable)	IL1b pg/ml (increasing)	PAPPA pg/ml (stable)	TNFa pg/ml (stable)
1	37.7	13490.2	0.0	32.7	16.4	477.2	0.0	13481.6	320.7
2	33.8	14817.3	2.4	37.3	164.6	446.0	0.4	13821.2	361.6
3	38.8	17462.1	5.8	36.9	217.1	651.3	0.5	14061.2	364.2
4	39.2	20270.9	28.7	30.0	766.4	334.4	1.7	12226.6	301.3
5	33.1	14057.2	89.0	31.1	3048.8	405.9	6.9	13041.7	316.7
6	29.1	13541.7	329.3	33.2	12153.3	651.3	27.7	14428.1	351.1
7	31.3	13586.2	1108.3	32.0	41964.7	402.6	98.4	13293.2	326.4
8	28.2	11789.2	1647.8	33.8	71978.8	577.1	170.9	12646.4	309.5
Mean	**33.9**	**14876.9**	**N/A**	**33.4**	**N/A**	**493.2**	**N/A**	**13375.0**	**331.4**
SD	**4.0**	**2533.8**	**N/A**	**2.4**	**N/A**	**112.1**	**N/A**	**685.4**	**22.7**
CV%	**11.9**	**17.0**	**N/A**	**7.3**	**N/A**	**22.7**	**N/A**	**5.1**	**6.8**

Table 22. Signal interference IL1b, PAPPA and TNFa

Spiking point (n=3)	MPO pg/ml (stable)	TIMP pg/ml (increasing)	MPO pg/ml (increasing)	TIMP pg/ml (stable)
1	205.3	0	0	631.8
2	202.0	0	0	582.2
3	216.0	4.3	2.5	542.1
4	196.9	29.0	9.7	554.3
5	221.4	139.9	44.7	621.5
6	215.9	551.4	160.3	586.8
7	206.7	2150.7	533.5	591.2
8	216.5	3798.7	903.4	540.4
Mean	**210**	**N/A**	**N/A**	**581**
SD	**8**	**N/A**	**N/A**	**32.1**
CV%	**4**	**N/A**	**N/A**	**5.5**

Table 23. Signal interference MPO/TIMP1

Spiking Point (n=3)	**IL8 pg/ml (stable)**	**FABP3 pg/ml (increasing)**	**IL8 pg/ml (increasing)**	**FABP3 pg/ml (stable)**
1	44.1	0.0	0.0	58003.6
2	54.2	554.0	0.4	67022.6
3	48.1	1358.7	0.6	63126.3
4	44.8	3768.7	2.5	57456.8
5	44.4	14084.5	9.1	52231.0
6	49.2	57648.5	38.9	57157.8
7	43.2	230207.6	160.0	56209.9
8	45.7	373201.4	298.3	58264.5
Mean	**46.7**	**N/A**	**N/A**	**58684.1**
SD	**3.4**	**N/A**	**N/A**	**4205.7**
CV%	**7.3**	**N/A**	**N/A**	**7.2**

Table 24. Signal interference IL8/FABP3

Antibody Cross Reactivity

The above experiment tests antibody cross reactivity to some extent but this was further tested specifically by measuring levels of recombinant protein alone and in combination with the other proteins to ensure there was no cross reactivity causing non-specific binding and inaccurate results. For each 3 plex and 2 plex the recombinant proteins were spiked into a kit diluent alone and together. The recovery was compared with and without the presence of the other proteins. For the 1 plexes, the recombinant protein was spiked alone and with 3 other proteins and measured to compare recovery with and without the presence of other proteins.

Example (**Figure 83**): Spiked alone and in combination the results for TNFa were 383pg/ml and 397pg/ml respectively (SD 11 CV 3%). Spiked alone and in combination the results for PAPPA were 14772pg/ml and 12664pg/ml respectively (SD 1491 CV 11%). The results for IL1b were 26pg/ml when spiked alone or in combination (SD 0.4 CV% 1.5%)

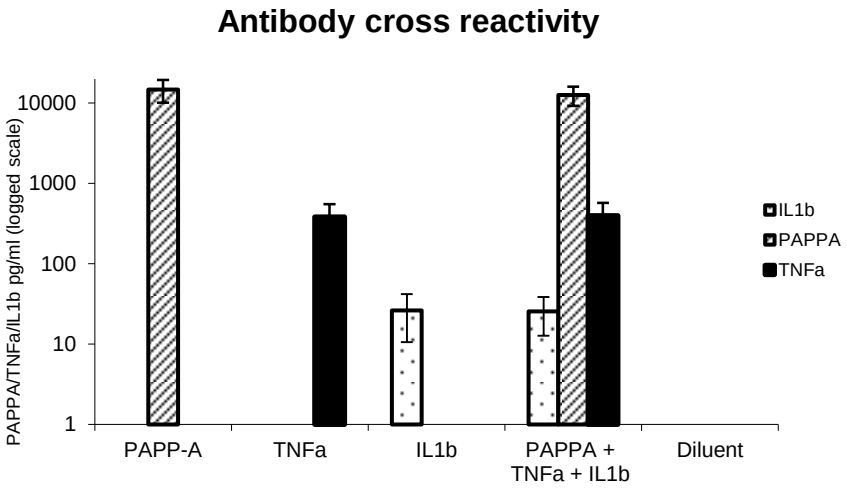

Figure 83. Antibody reactivity of PAPPA, IL1b and TNFa three plex plate. The error bars are the standard deviation for 3 experiments.

Together, the results of these experiments showed that the assays are independent despite being plexed together. The antibody cross reactivity results for the multiplex assays are shown in **Table 25** to
Table 28.

3 plex (n=3)	**TNFa pg/ml**	**IL1b pg/ml**	**PAPPA pg/ml**
Spiked alone	382.6	26.2	14772.4
Spiked together	397.8	25.7	12664.1
Mean	**390.2**	**25.9**	**13718.2**
SD	10.7	0.4	1490.8
CV	2.8	1.5	10.9
Spiked amount	300	25	12500
% recovery	130.1	103.7	109.7

Table 25. Antibody cross reactivity IL1b, PAPPA and TNFa

2 plex (n=3)	**MPO**	**TIMP1**
Spiked alone	193.4	569.3
Spiked together	189.0	547.6
Mean	**191.2**	**558.5**
SD	3.1	15.3
CV	1.6	2.7
Spiked amount	225.0	625.0
% recovery	85.0	89.4

Table 26. Antibody cross reactivity MPO/TIMP1

2 plex (n=3)	**FABP3 pg/ml**	**IL8 pg/ml**
Spiked alone	16752.9	13.9
Spiked together	17427.2	14.6
Mean	**17090.1**	**14.3**
SD	476.8	0.5
CV	2.8	3.5
Spiked amount pg/ml	15000	12.5
% recovery	113.9	114.0

Table 27. Antibody cross reactivity FABP3/IL8

1 plexes (n=3)	**MMP2 pg/ml**	**MMP9 pg/ml**	**NT pro BNP pg/ml**
Spiked alone	2932.7	4331.3	598.1
Spiked together	3031.1	4343.6	666.2
Mean	**2981.9**	**4337.5**	632.2
SD	69.6	8.7	48.1
CV	2.3	0.2	7.6
Spiked amount pg/ml	4000.0	6250.0	600
% recovery	74.5	69.4	114.3

Table 28. Antibody cross reactivity MMP2, MMP9 and NTproBNP single plexes

Protein Recovery

Recovery of recombinant protein spiked into human plasma and kit diluent was measured to ensure that the proteins could be detected and results were and reproducible. Protein recovery from kit diluent was good (>70% for all biomarkers). Recovery from plasma was not as good, ranging from 33% with TNFa to 88% with TIMP1. This could be due to the presence of endogenous proteins in the plasma binding competitively with the recombinant protein and preventing binding to the capture antibody. However, recovery was consistent across each of the 3 experiments showing that results are reasonably reproducible even when there is low recovery allowing us to compare one time point to another in the clinical study and look for changes from baseline in patient samples using patients as their own controls. Results are shown in **Table 29 & Table 30**.

Analyte	Protein recovery	CV%
MPO	79%	18%
TIMP1	83%	18%
MMP2	77%	3%
MMP9	73%	12%
IL1b	92%	15%
PAPPA	87%	4%
TNFa	80%	15%
FABP3	102%	6%
IL8	84%	15%
NTpro BNP	96%	15%

Table 29. Protein recovery from kit diluent. CV% for 3 replicate experiments

Analyte	Protein recovery	CV%
MPO	81%	18%
TIMP1	88%	17%
MMP2	72%	16%
MMP9	52%	22%
IL1b	38%	10%
PAPPA	78%	14%
TNFa	33%	9%
FABP3	51%	12%
IL8	75%	12%
NTpro BNP	47%	5%

Table 30. Protein recovery from human plasma. CV% for 3 replicate experiments

Assay Variability

Intra-plate and inter-plate variability were tested using plasma from healthy volunteers. To test intra-plate variability, plasma was pipetted into replicate wells across one plate. To test inter-plate variability, plasma was pipetted into replicate wells on 3 different plates on 3 separate occasions. Intra-plate and inter-plate variability were reasonable (CV%s <20) for all assays except for MMP9 which had high inter-plate variability, CV=51% (**Table 31 & Table 32**). Due to these findings the clinical samples were analysed in batches with an entire patient sample set on one plate to minimise the effects of inter-plate variation on results.

	MPO	TIMP1	MMP2	MMP9	PAPPA	FABP3	IL8	IL1b	TNFa	NT proBNP
Exp 1	8300	82300	170730	141650	12484	19185	16	4.5	33.8	32.2
Exp 2	9000	86000	185340	136290	14880	22342	22	3.7	28.6	44
Exp 3	9000	99800	189950	153500	10488	25891	24	4.3	33.5	48.4
Mean	8767	89367	182007	143813	12617	22473	21	4.3	32	41.5
SD	404	9223.0	10034	88067	2199	3355	4.2	0.4	2.9	8.4
CV%	4.6	10.3	5.5	6.1	17.4	14.9	20.2	10.1	9.1	20.2

Table 31. Multiplex ELISA intra-plate variability

	MPO	TIMP1	MMP2	MMP9	PAPPA	FABP3	IL8	IL1b	TNFa	NT pro BNP
Plate 1	7700	87000	170730	141650	880	22342	22	4.5	33.8	39.2
Plate 2	8400	69800	169420	56680	1112	22430	19.3	3.8	25.8	32.8
Plate 3	7300	82300	185110	71270	1006	24965	19.8	4.6	27.6	34
Mean	7800	79700	175087	89867	999	23246	20.4	4.3	29.1	35.3
SD	557	8890	8705	45435	116.5	1490	1.4	0.4	4.2	3.4
CV	7.1%	11.2%	5.0%	50.6%	11.7%	6.4%	7.1%	10.1	14.4	9.6%

Table 32. Multiplex ELISA Inter-plate variability

Free Thaw Stability

The freeze-thaw stability of the analytes was investigated by splitting one sample of healthy volunteer human plasma into three aliquots and exposing them to differing freeze-thaw cycles. The three aliquots were removed from -80°C storage and allowed to equilibrate to room temperature for 30 minutes. Two aliquots were then returned to -80°C to re-freeze again. Once frozen they were removed and allowed to equilibrate to room temperature for another 30 minutes before returning one of the aliquots to -80°C to re-freeze for a third time. Finally it was removed again and allowed equilibrate to room temperature for a final 30 minutes. The samples were analysed and the results for samples that had undergone 1, 2 or 3 freeze thaw cycles were compared. The results were highly comparable (CV<15) showing that clinical samples can be refrozen up three times with little effect on accuracy of the result (**Table 33**), however the number of freeze thaw cycles was still minimized where possible. Freeze thaw experiments were unable to be carried out for the FABP3 and IL8 as levels of these proteins in normal human plasma were too low to be detected.

Freeze thaw	MPO	TIMP1	MMP2	MMP9	IL1b	PAPPA	TNFa	NT pro BNP	Trop T
Cycle 1	12500	82800	207930	132395	0.5	6113	15.1	88.7	1979
Cycle 2	10800	92850	210610	139560	0.5	5886	15.5	81.1	1968
Cycle 3	12350	106400	221740	143235	0.4	6053	14.3	81.8	1863
Mean	11883	94017	213427	138397	0.5	6017	15.0	83.9	1937
SD	941	11843	7323	5513	0.1	117	0.6	4.2	64
CV	7.9	12.6	3.4	4.0	14.3	1.9	3.8	5.0	3.3

Table 33. Free thaw effects on sample variability

Stability Over Time

Sample stability over time was tested for analytes that were detectable in normal plasma. Plasma was tested at two time points 6 months apart to assess biomarker instability. No difference was seen between the results when samples were tested 6 months apart with the exception of NTproBNP which measured significantly higher after 6 months storage (**Table 34 & Figure 84**). This knowledge was taken into consideration when interpreting the NTproBNP clinical study results. For biomarkers that were unable to be tested the possibility of analyte instability was factored into result interpretation.

Normal ETDA plasma (stored at -80°)	MPO pg/ml	TIMP1 pg/ml	MMP2 pg/ml	MMP9 pg/ml	PAPPA pg/ml	NTproBNP pg/ml
Month 1	11800	93100	168060	42210	4782	34
Month 6	11400	125500	162110	38530	5580.8	103.2
Mean	11600	109300	165085	40370	5181.4	68.6
STD	282.8	22910.3	4207.3	2602.2	564.8	48.9
CV	2.4	21.0	2.5	6.4	10.9	71.3

Table 34. Stability testing

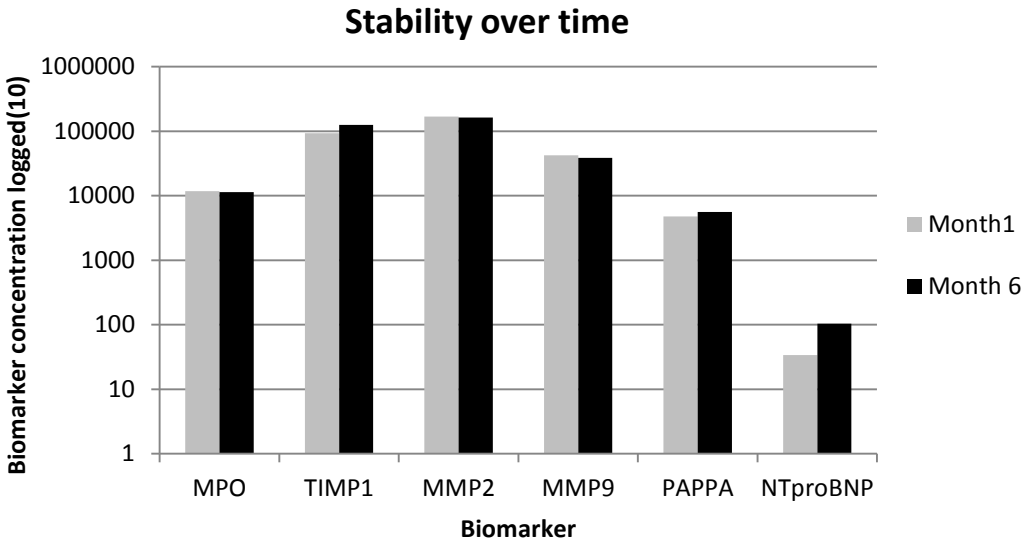

Figure 84. Stability Over Time

Rituximab Cross Reactivity

Patients with aggressive B cell lymphoma also receive monoclonal anti-CD20 antibody therapy rituximab with their anthracycline based chemotherapy (R-CHOP). Rituximab can be detected in the circulation for up to 6 months after therapy due to having a very variable half-life [208]. It is a chimeric (mouse/human) monoclonal antibody against B cell surface marker CD20 therefore has the potential to interfere with the capture antibody on ELISA plates altering results. The specificity of rituximab makes this unlikely but the following experiments were carried out on a sample of the circulating biomarker assays to ensure the results are not grossly affected. Rituximab at a concentration of 300mcg/ml was added to kit diluent alone, human plasma (EDTA), human plasma (EDTA) with recombinant protein spikes and kit diluent with recombinant protein spikes. Results were compared to controls (without rituximab). The dose of 300mcg/ml was chosen as it was approximately the highest concentration of rituximab measured in patient plasma post infusion during the FIZZ study (an international phase II study of rituximab with ^{90}Y-ibritumomab in patients with follicular lymphoma) [209]. There was no significant difference in protein recovery when recombinant proteins were spiked with and without rituximab into diluent or human plasma for the majority of the assays. Rituximab did not appear to bind to the capture antibodies to give falsely high or low results when plexed alone in any of the assays. However, protein recovery of IL8 was slightly lower from human EDTA plasma in the presence of rituximab (20pg/ml

with Rituxmab and 27pg/ml without Rituximab, inter-assay CV of 20%). There was also a discrepancy between the concentration of MPO and TIMP1 measured from human plasma with and without Rituximab (**Figure 85**) but the protein levels were at the lower limit of detection which may account for the inaccuracy as there was no difference between protein recovery from human plasma with and without Rituximab in samples spiked with higher levels of MPO/TIMP1. Raw data for the rituximab testing are shown in **Table 35**.

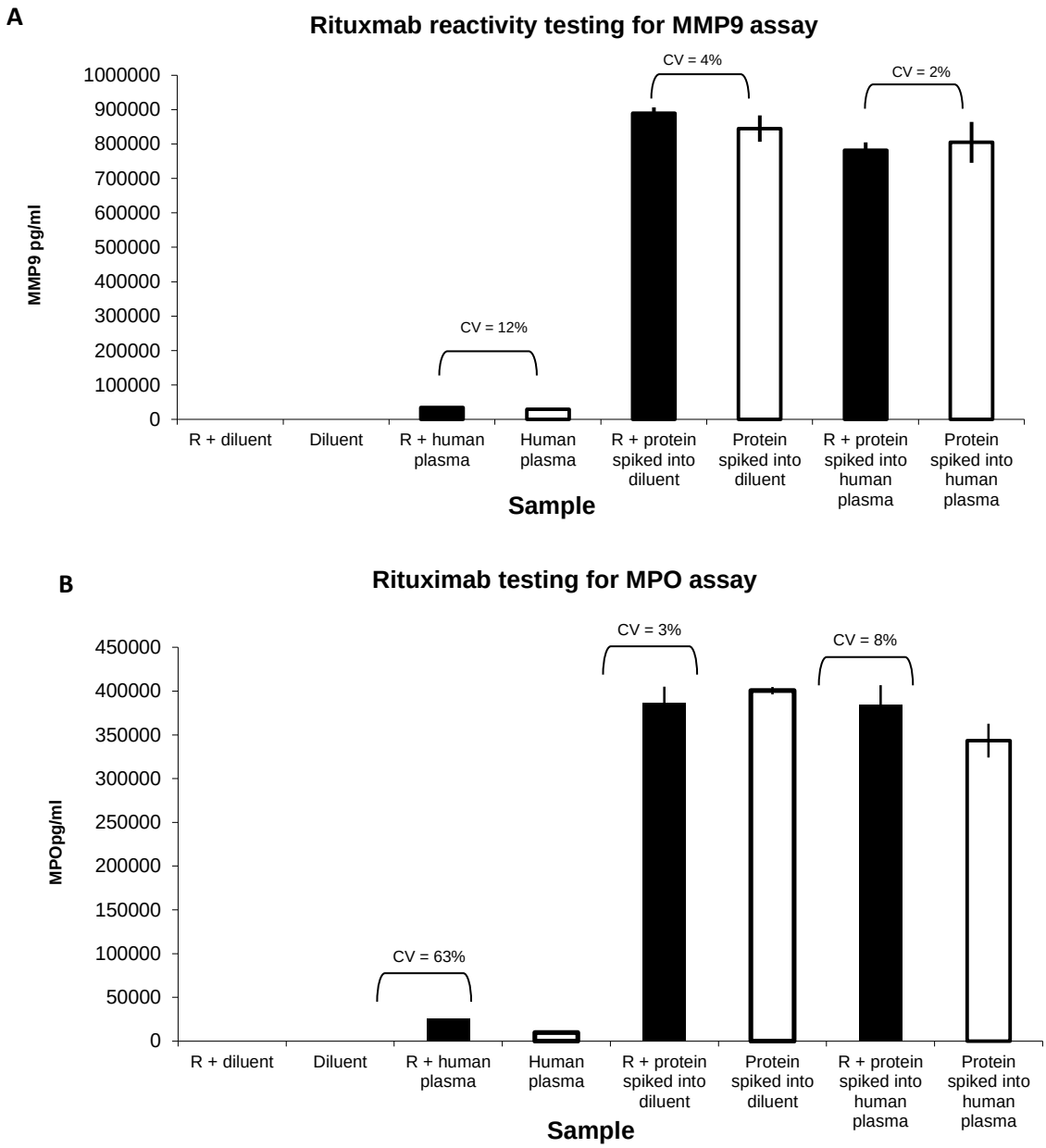

Figure 85. Examples of rituximab cross reactivity testing. The MMP9 assay was unaffected by rituximab (A). The MPO assay may have been affected by rituximab in the presence of low levels of protein (B)

Troponin (n=3)	**Human plasma (healthy volunteer)**	**Protein spiked into diluent**	**Protein spiked into human plasma**
R	965	10190	7564
No R	983	8503	7593
Mean	974	9346	7579
SD	13	1193	20
CV%	1	13	0
IL8 (n=3)	**Human plasma (healthy volunteer)**	**Protein spiked into diluent**	**Protein spiked into human plasma**
R	12	20	20
No R	14	23	27
Mean	13	22	23
SD	2	2	5
CV%	12	10	20
FABP (n=3)	**Human plasma (healthy volunteer)**	**Protein spiked into diluent**	**Protein spiked into human plasma**
R	0	21994	12010
No R	0	23643	11562
Mean	0	22818	11786
SD	0	1166	317
CV%	0	5	3
MPO (n=3)	**Human plasma (healthy volunteer)**	**Protein spiked into diluent**	**Protein spiked into human plasma**
R	25600	386600	384300
No R	9700	400500	343400
Mean	17650	393550	363850
SD	11243	9829	28921
CV%	64	2	8
TIMP1 (n=3)	**Human plasma (healthy volunteer)**	**Protein spiked into diluent**	**Protein spiked into human plasma**
R	214100	1955400	2031900
No R	75400	1934900	1950600
Mean	144750	1945150	1991250
SD	98076	14496	57488
CV%	68	1	3
MMP2 (n=3)	**Human plasma (healthy volunteer)**	**Protein spiked into diluent**	**Protein spiked into human plasma**
R	95020	649700	636070
No R	93920	649640	714760
Mean	94470	649670	675415
SD	778	42	55642
CV%	1	0	8
MMP9	**Human plasma**	**Protein spiked into**	**Protein spiked into human**

(n=3)	**(healthy volunteer)**	**diluent**	**plasma**
R	34380	889520	781750
No R	29120	845230	805160
Mean	31750	867375	793455
SD	3719	31318	16553
CV%	12	4	2

Table 35. Rituximab cross reactivity

Observed Values in Patient Samples

A small pilot study was run by collecting plasma samples from patients who had already received anthracycline based chemotherapy. 7 patients with pre-existing or new cardiac problems and 10 patients with no cardiac morbidity were consented for donation of a single blood sample in order to assess the performance of the assays with clinical samples and get an indication of the likely range of values seen in real life patients.

MPO/TIMP1 Two Plex

The MPO and TIMP1 protein were both detected and were measurable from patient plasma when samples were diluted 1 in 1000 as per manufacturer's guidance (**Figure 86 & Figure 87**). All values lay within the range of the assay, above the lower limit of detection (LLOD depicted by the red line).

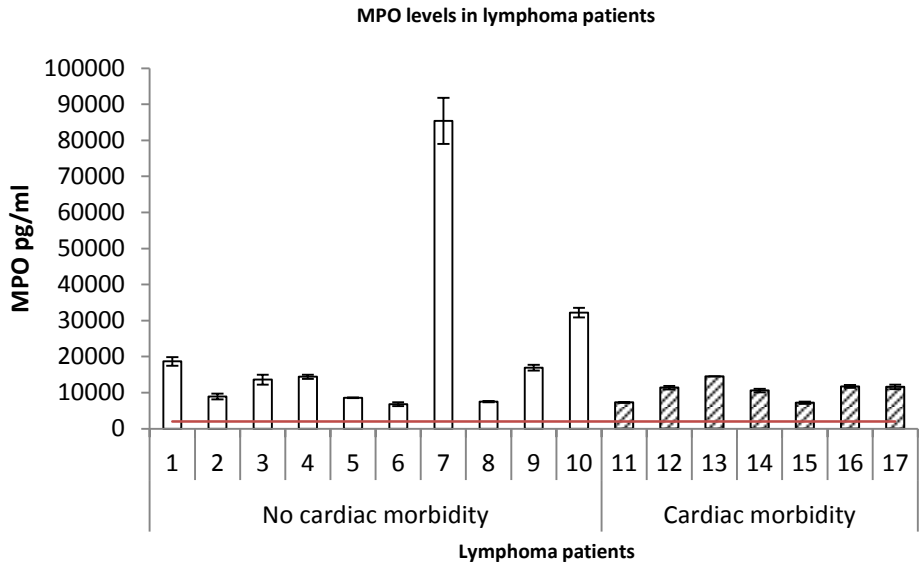

Figure 86. MPO levels in lymphoma patients (pilot data)

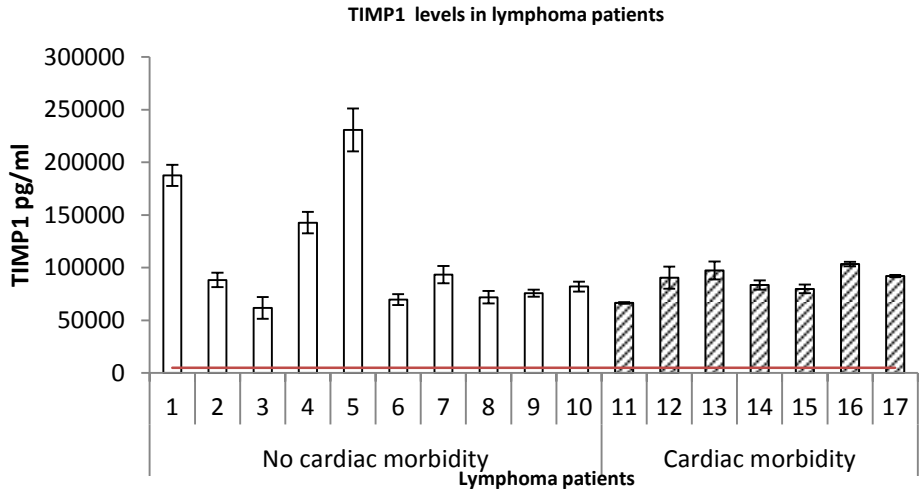

Figure 87. TIMP1 levels in lymphoma patients (pilot data)

FABP3 and IL8 Two Plex

The FABP3 and IL8 proteins were detected and measurable from patient plasma when samples were diluted 1 in 2 as per manufacturer's guidance (**Figure 88 & Figure 89**). All values lay within the range of the IL8 assay however several patient samples had levels of FABP3 which were below the lower limit of detection (LLOD depicted by the red line). FABP3 is a marker of acute cardiac myocyte damage that rises acutely after myocardial infarction and should therefore be undetectable in patients unless they are undergoing acute cardiac damage at the time of sampling.

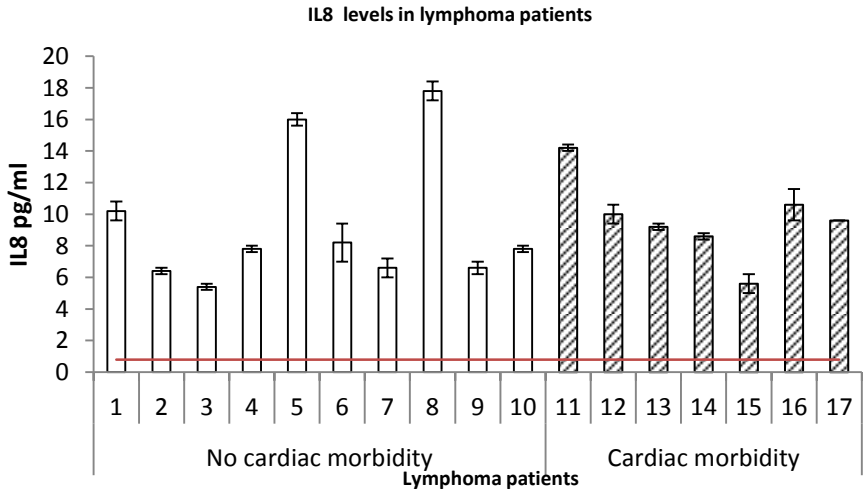

Figure 88. IL8 levels in lymphoma patients (pilot data)

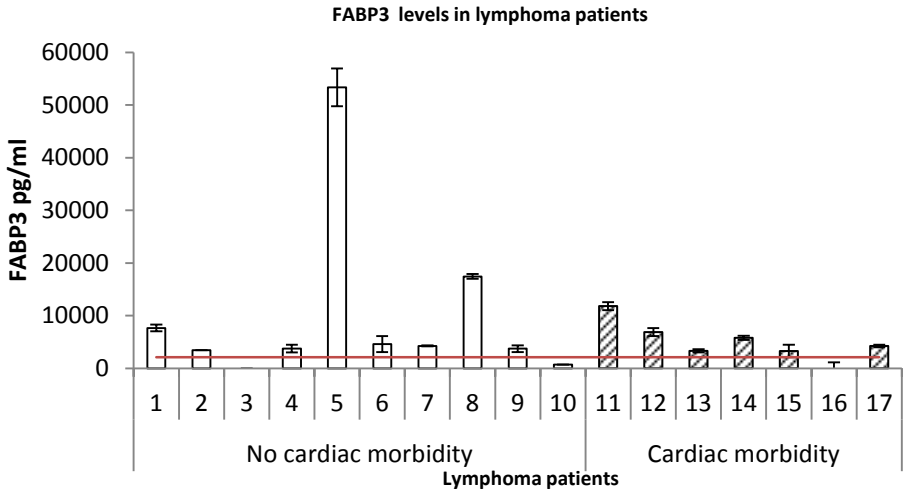

Figure 89. FABP3 levels in lymphoma patients (pilot data)

MMP2, MMP9 and NTproBNP Single Plexes

The MMP2 and MMP9 proteins were detected and measurable from patient plasma when samples were diluted 1 in 100 as per manufacturer's guidance (**Figure 90 & Figure 91**). All values lay within the range of the assay, above the lower limit of detection (LLOD depicted by the red line).

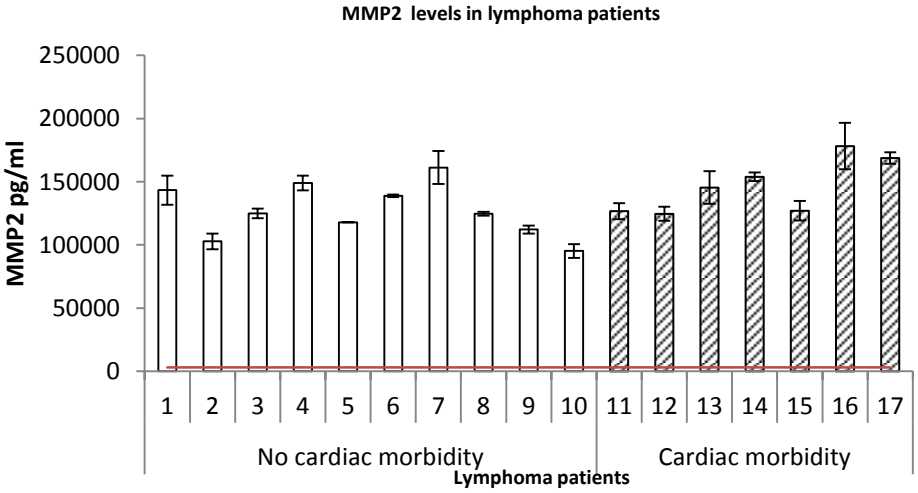

Figure 90. MMP2 levels in lymphoma patients (pilot data)

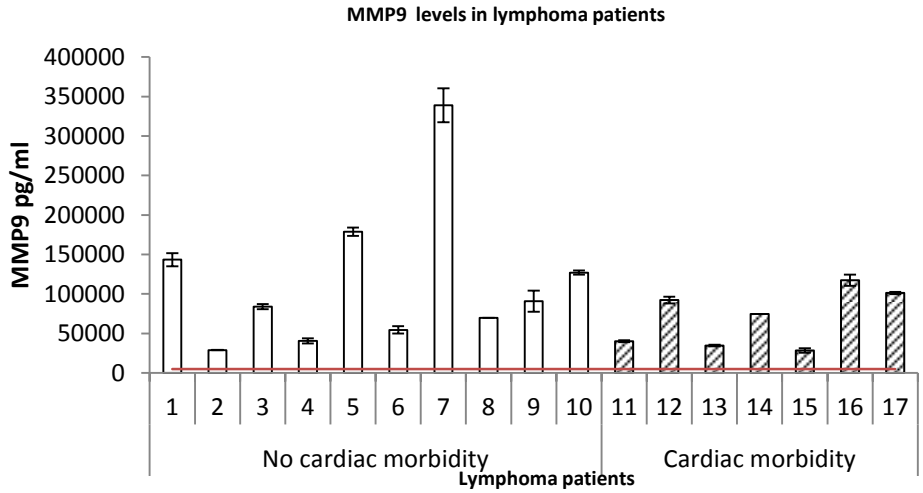

Figure 91. MMP9 levels in lymphoma patients (pilot data)

NTproBNP Single Plex

NTproBNP was detected and measurable from the majority patient plasma samples (diluted 1 in 2) and the samples with elevated levels fell within the range of the assay (**Figure 92**). Only one patient had levels below the limit of detection and this subject had no cardiac morbidly.

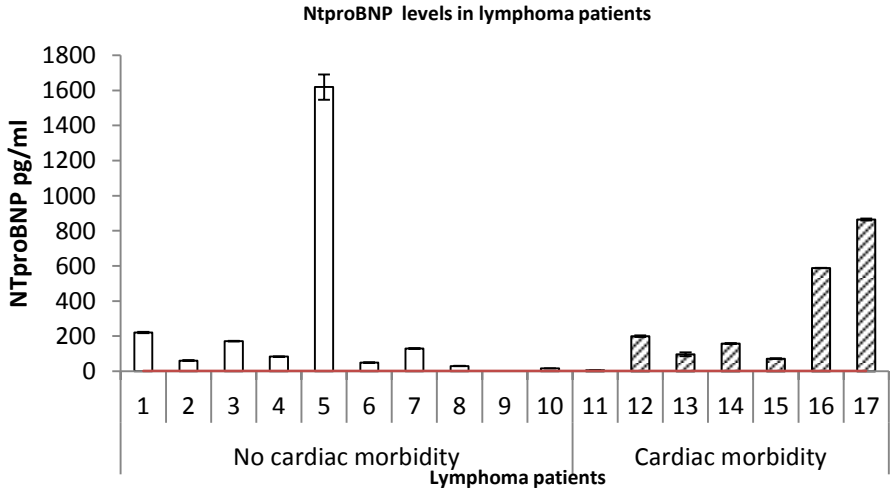

Figure 92. NTproBNP levels in lymphoma patients (pilot data)

PAPPA, IL1b and TNFa Three Plex

PAPPA was measurable in all patient samples (diluted 1 in 2) (**Figure 93**) and levels fell within the range of the assay but IL1b and TNFa were only detectable in 1 patient. The pilot study was a cross sectional study looking at one time point in isolation therefore dynamic

changes during or shortly post therapy were not captured. IL1b and TNFa were therefore still included in the 'Cardiotox' clinical study exploratory biomarker panel to investigate their behaviour over time.

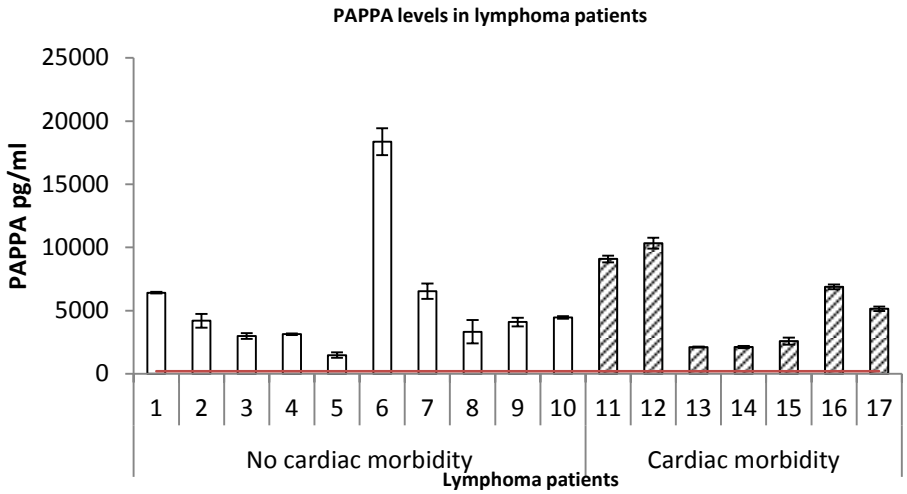

Figure 93. PAPPA levels in lymphoma patients (pilot data)

ELISA Validation Discussion

Eight experimental processes were carried out as part of assay validation; standard concentration curve reproducibility, signal interference, antibody cross reactivity, protein recovery, stability, inter and intra-plate variability, rituximab cross-reactivity and observed values in patient samples. The standard curves for each assay passed the acceptance criteria with R^2 values of >0.985 and results were reproducible over 3 experiements for all assays. Using the standard curve as a tool to look for light scatter, the 'signal interference' experiment was performed by varying one analyte and keeping the other analyte(s) constant. Light scatter is not an issue for single plexes therefore this experiment was only carried out for two and three plexes. The results showed that light scatter does not significantly affect the neighbouring assay in multiplex plates. In the 'antibody cross reactivity' experiment, analytes were spiked at the mid-point of each standard curve both singly and in combination with the other analyte(s). For single plexes the analyte was measure alone and in the presence of three other recombinant proteins and no significant cross-reactivity was seen. Recovery of recombinant protein from diluent and human plasma was performed to determine the sensitivity of the assays. The recovery of protein from diluent was greater than from plasma but recovery was consistent and reproducible from both mediums. Recovery of protein from diluent was >70% for all assays. Recovery from human plasma (EDTA) was generally lower

potentially due to competitive binding. TNFa had the lowest recovery at just 33% however the CV% between experiments was 9% suggesting that recovery is consistently low and therefore comparable from one experiment to another. Recovery of IL1b and NTproBNP were also relatively low from human plasma (38 and 47% respectively) but again the reproducibility was high (CVs of 10 and 5% respectively). Despite the low recovery NTproBNP was detectable in most of the patients in the validation sample set (n=17) however TNFa and IL1b were only detectable in 1 patient. This could be due to poor assay sensitivity but could also be because TNFa and IL1b were truly undetectable in these patients as they did not have active cardiac damage (or active malignancy) at the time of blood draw. However this knowledge was taken into account when interpreting the clinical study biomarker results. It was reassuring that samples with high levels of protein did not exceed the upper limit of the assay ranges and the CV% between technical replicates were under 30% for all the assays except for FABP3 where 2 samples had a CV of over 30%. These samples were near the LLOQ for the assay which may explain the inaccuracy but samples with high CVs in the clinical study were not reported and were re-tested.

The freeze/thaw stability of each analyte was investigated and the low CVs between experiments (<15%) indicated that three rounds of freezing and thawing had little effect on the stability of these analytes. The clinical study samples were therefore limit to three freeze thaw cycles. Analytes appear to remain stable over time when stored at -80˚ with the exception of NTproBNP which appeared to possibly increase with time. This finding was taken into account when looking at the behavior of NTproBNP in the clinical study as, if a general decline was seen in longitudinal analysis, it could be due to analyte instability rather than a true biological effect. The Intra-plate and inter-plate variability for all assays was reasonable with CVs of <20% all experiments. The only exception was inter-plate variability of MMP9 which had a CV of 51%. This may have been due to inconsistencies with plasma dilution as the assay required sample dilution of 1:100. When the experiment was re-run with recombinant protein spikes the results were more reassuring with an inter-plate variability was only 9.3%. This highlights the potential issues surrounding dilution of samples. Samples will therefore be diluted using large volumes in a single step process with adequate mixing to try and minimise inaccuracy. Samples will always be tested in duplicate pairs and samples showing low agreement (high CV >30%) will be re-tested. Where possible, samples from the same patient will be run on the same plate to minimize inter-plate variability and enable accurate comparison of biomarker at different time points.

Rituximab had no effect on the majority of assays. Rituximab did not bind to the assays when plexed alone and did not appear to bind competitively with any of the assays except IL8. Recovery of spiked IL8 from human plasma was slightly lower in the presence of rituximab which could be due to competitive binding with the capture antibody. This could potentially affect the detection of this protein in the clinical samples and negate its' use as a cardiotoxicity biomarker in patients receiving rituximab. A significant difference was seen in the level of MPO and TIMP1 detectable from healthy volunteer human plasma with and without the presence of rituximab. However, the level of MPO and TIMP in human plasma was extremely low and was right at the lower limit of the assay. Recovery of these proteins when spiked into human plasma at higher levels with and without the presence of rituximab was highly comparable which was reassuring and suggests that the lack of reproducibility seen in the un-spiked human plasma samples was due to inaccuracy at the lower end of the assay range rather than competitive binding. If competitive binding was occurring the results suggest that it only occurs when there are very low levels of protein in a sample and should not affect samples with high levels which will be the samples of interest in this study. However, in light of these findings samples from patients receiving rituximab were flagged to ensure that these affects were taken into account when interpreting the clinical study results.

A small proportion of patients exposed to rituximab may also have the potential develop human anti-mouse antibodies (HAMAs) which could also interfere with binding to the capture antibody. This is something that has been discussed as a theoretical problem in the literature regarding accuracy of troponin assays in patients who have received antibody therapies but has not been found to be clinically relevant so far [210]. From previous work performed at the Cancer Research UK Manchester Institute as part of the above FIZZ trial only 3% of patients develop HAMAs and results suggest that the effects of HAMAs are eliminated if samples are diluted [209]. All the multiplex ELISA assays were diluted least 1 in 2 therefore HAMA formation should not be a significant problem.

ELISA Validation Conclusions

Taken together the validation experiments showed that the assays were fit for purpose for the clinical study and that the data generated would be of a high enough quality to be able to draw conclusions about biomarker behavior before, during and after the receipt of anthracyclines. None of the assays were removed from the planned panel in light of the

validation results but the findings were used to aid accurate interpretation of the clinical study data for instance the low sensitivity of TNFa and IL1b and potential instability of NTproBNP over time were taken into account when looking at the clinical biomarker results.

Appendix 4: Optimisation of the Cardiac MRI Protocol

A bespoke imaging protocol was developed specifically for this clinical study therefore several months of optimisation work took place prior to implementation. Five healthy volunteers were scanned under the University of Manchester Imaging Institute ethics to ensure that the scan procedure was tolerable, time efficient and was able to generate high quality robust data. The healthy volunteers were scanned as described in Clinical Study Materials and Methods (section 3.2) without contrast due to the potential risks involved. Volumetric assessment was performed on all five and tissue characterisation was tested on two of the volunteers. Following optimisation, the protocol was deemed tolerable in terms of breath hold duration (<20 seconds) and overall scan duration (~45 minutes for data acquisition).

Validation of Left Ventricular Systolic Functional Assessment

Volumetric analysis was performed by two blinded analysts using the Philips analysis tool to ensure that the measurements obtained were consistent and accurate. Measurements were in line with normal values and inter-operator and intra-patient variability were low (CVs < 5%, **Table 36 &**
Table 37).

Volunteer	Analyst 1 (LVEF%)	Analyst 2 (LVEF%)	Mean (LVE%F)	SD	CV%
1	59	59	59	0.2	0.4
2	72	70	71	2.0	2.8
3	65	64	64	0.7	1.1
4	68	67	67	0.7	1.1
5	77	75	76	1.8	2.3

Table 36. Intra-operative variability of LVEF estimation

Intra-patient variability		Ejection fraction %	CV%
Volunteer 6	Scan 1	57	5
	Scan 2	53	

Table 37. Intra-patient variability of LVEF estimation

Bland Altman Testing

The consistency and agreement between analysts was further tested using the first 100 scans performed in the clinical study to ensure that consistent LVEF% data was being produced for use as main clinical study end point. Bland-Altman testing was carried out and no significant bias was seen (bias 0.08) (sis of the clinical study data.). The median LVEF% for analyst 1 and analyst 2 were 60% and 59% respectively. Results from analyst one were used for interpretation and analysis of the clinical study data.

	Analyst 1 EF%	Analyst 2 EF%
Mean	59	59
SD	7	7
Med	60	59
T test	p=	0.8

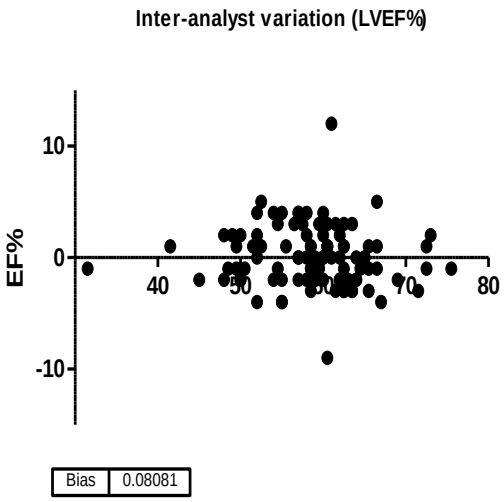

Figure 94. Bland Altman testing of agreement in LVEF% measurements between the two analysts

Optimisation of Tissue Characterisation

The optimisation process proved that it was possible to generate mid-ventricular T1 and T2 maps. Post-acquisition analysis generated robust and reproducible median myocardial T1 or T2 values. The results were slightly higher than previously reported healthy volunteer values (**Table 38**) but results were reproducible and consistent, with low intra-patient variation (CV of <5%) (**Table 39**). The median value of the whole myocardium in diastole was used as this parameter was least effected by erroneous values resulting from imaging or movement artefact.

Volunteer	Med T1 (ms)	Mean T(ms) (984 +/- 28ms)[192]	SD (ms)	Med T2 (ms)	Mean T2 (ms) (52.18 ± 3.4ms)[174]	SD (ms)
1	1085.9	1097.4	110.6	70.8	75.1	36.5
2	1030.6	1058.3	136.1	63.0	65.1	15.9

Table 38. T1 and T2 estimation in healthy volunteers

Intra-patient variability		T1 median (ms)	SD	CV%	T2 median (ms)	SD	CV%
Volunteer 1	Scan 1	1085.9	110.6	1.5	70.8	36.5	1.9
	Scan 2	1118.3	96.1		68.1	76.4	

Table 39. Intra-patient variability of T1 and T2 values

Conclusions

The Cardiac MRI protocol was developed and optimised prior to use in the clinical study. The protocol was tolerable and the data generated was analysable and reproducible. The LVEF values were in line with normal values and there was high agreement between analysts which was paramount as LVEF was be used to report cardiotoxicity in the clinical study. The exploratory elements of T1 and T2 mapping were successful and generated data that was analysable and reproducible for investigation in the clinical study.

Appendix 5: Supplementary Circulating Biomarker Data

Longitudinal Circulating Biomarker Behaviour

Data showing the behaviour of each biomarker over time during and following receipt of anthracyclines therapy is displayed below.

NTproBNP: Significant dynamic changes (outwith baseline variability) were seen in NTproBNP with anthracycline therapy. Levels rose transiently and significantly 48-72 hours post anthracycline dose but returned to baseline prior each cycle (t test 48 hours post dose $p<0.0001$). There was slightly increase again at 12 months but it was not significant (t test $p=0.08$).

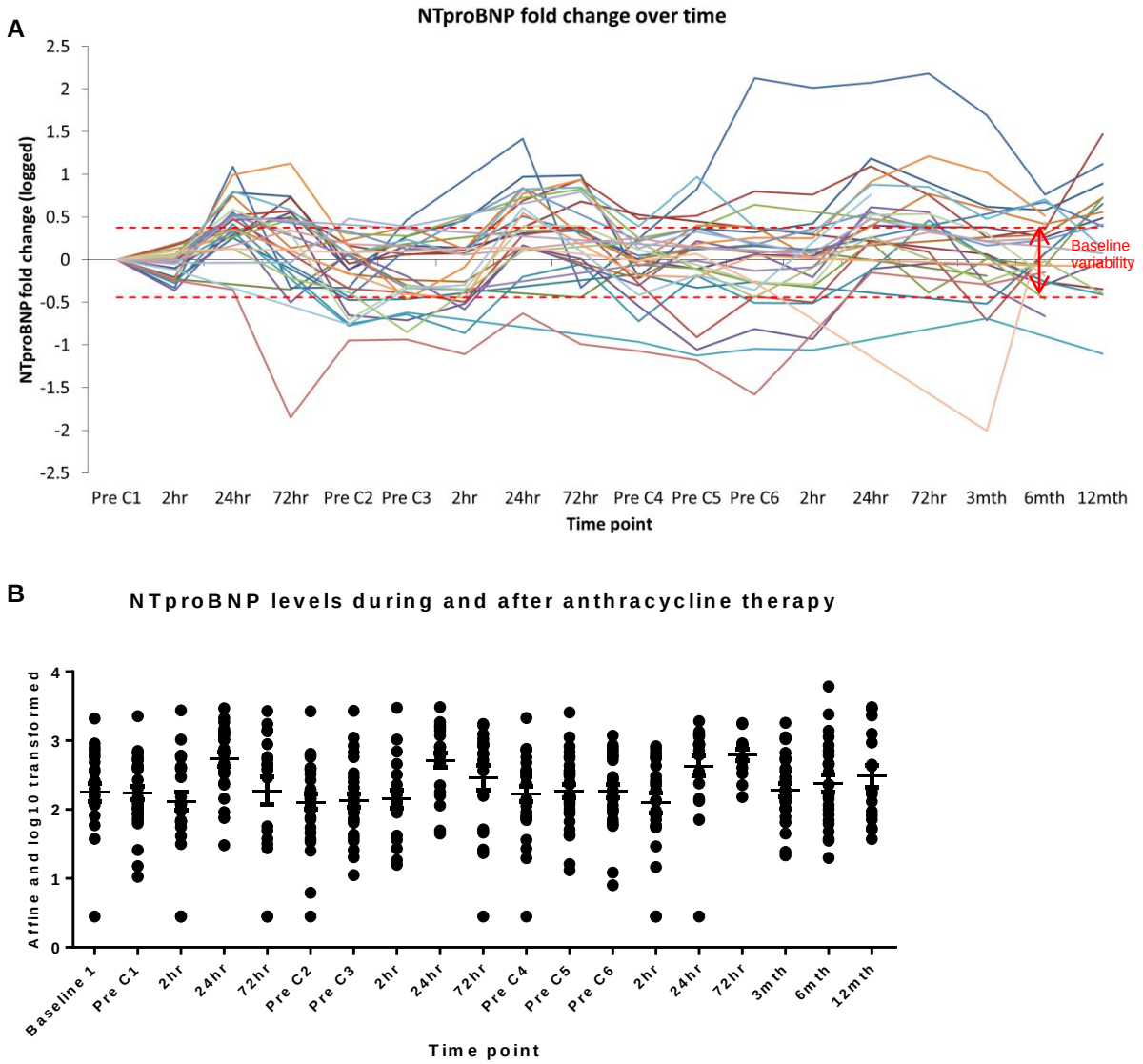

Figure 95. Graph A shows Fold change of circulating NTproBNP (logged) during and after anthracycline therapy. *Each line represents one patient and the dotted red lines show*

the 95% confidence interval for baseline variability. Graph B shows the individual logged values and the population mean and standard deviation at each time point. C= cycle.

PAPPA: PAPPA was detectable at baseline and showed dynamic change over time in a small number of patients but the changes did not correlate with decline in LVEF or the development of cardiac events.

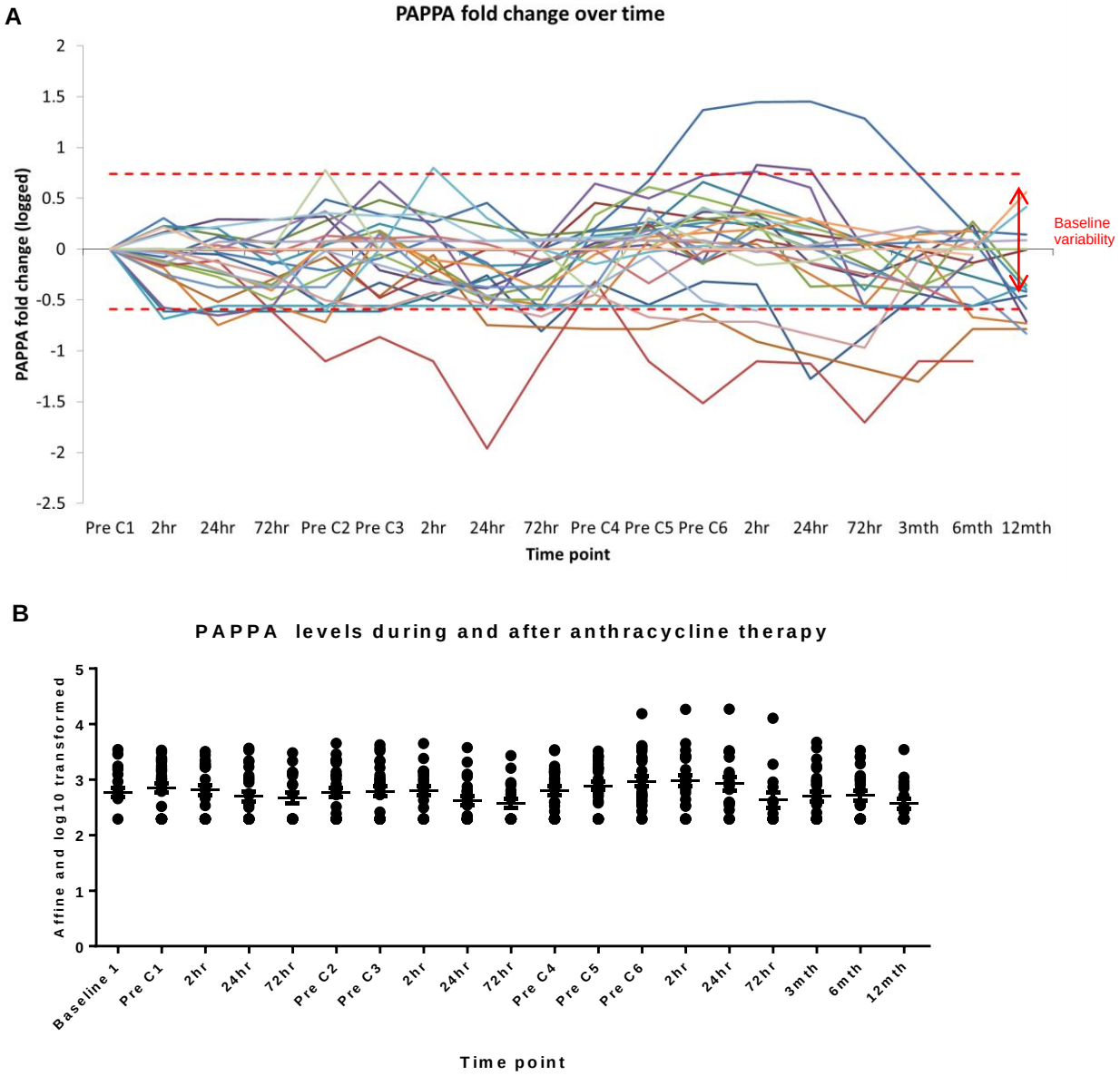

Figure 96. Graph A shows Fold change of circulating PAPPA (logged) during and after anthracycline therapy. *Each line represents one patient and the dotted red lines show the 95% confidence interval for baseline variability. Graph B shows the individual logged values and the population mean and standard deviation at each time point. C= cycle.*

FABP3: FABP3 did not change significantly over time and the one patients with marked increases during cycles 5 and 6 had systemic infection and venous thromboembolism at the time of blood sampling which may have been responsible for changes.

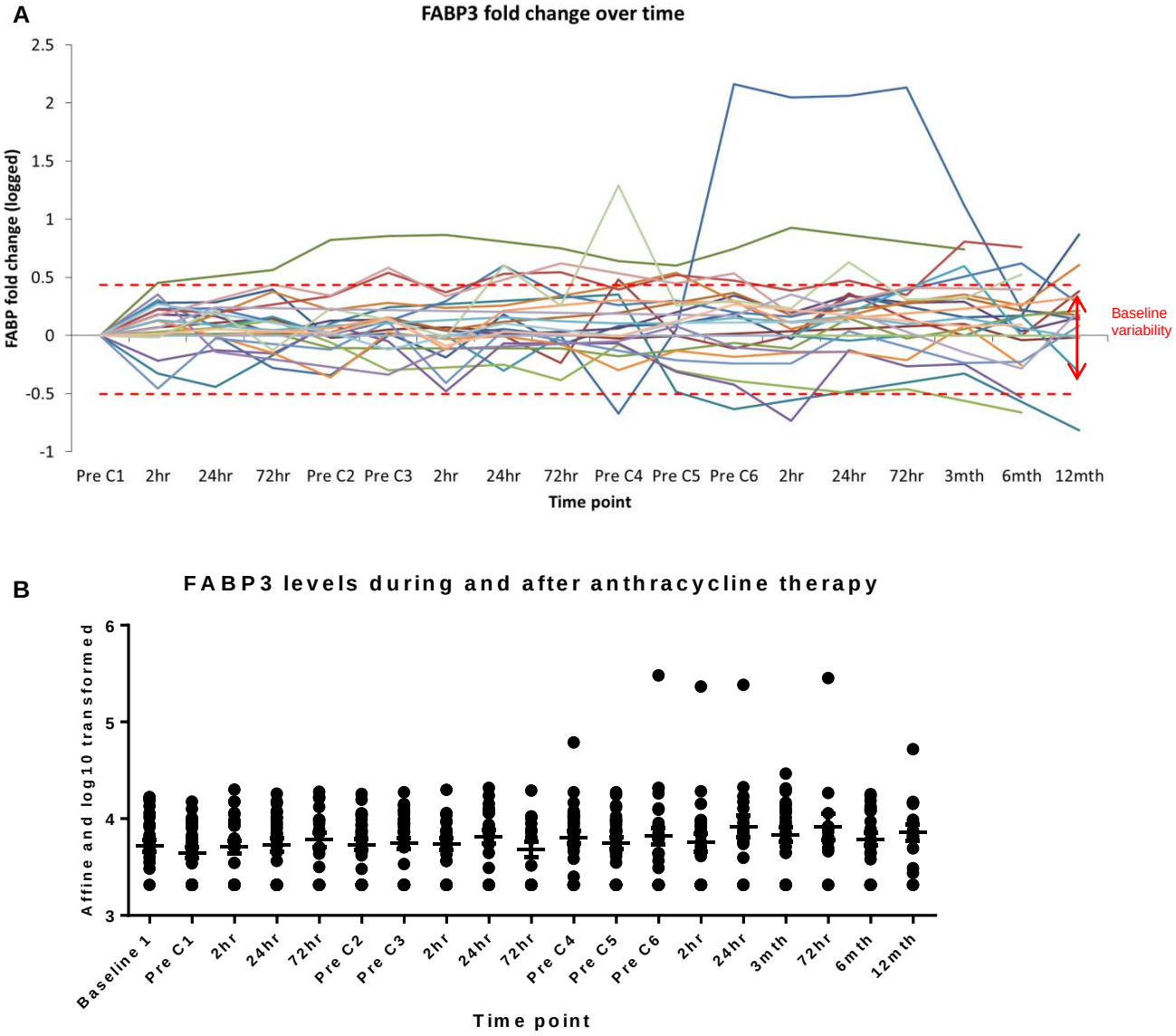

Figure 97. Graph A shows fold change of circulating FABP3 (logged) during and after anthracycline therapy. *Each line represents one patient and the dotted red lines show the 95% confidence interval for baseline variability. Graph B shows the individual logged values and the population mean and standard deviation at each time point. C= cycle.*

MMP9: Behaviour of MMP9 is discussed fully in section 3.6.1.1.3.2 but a significant fall from baseline was seen during treatment that was out with baseline variability.

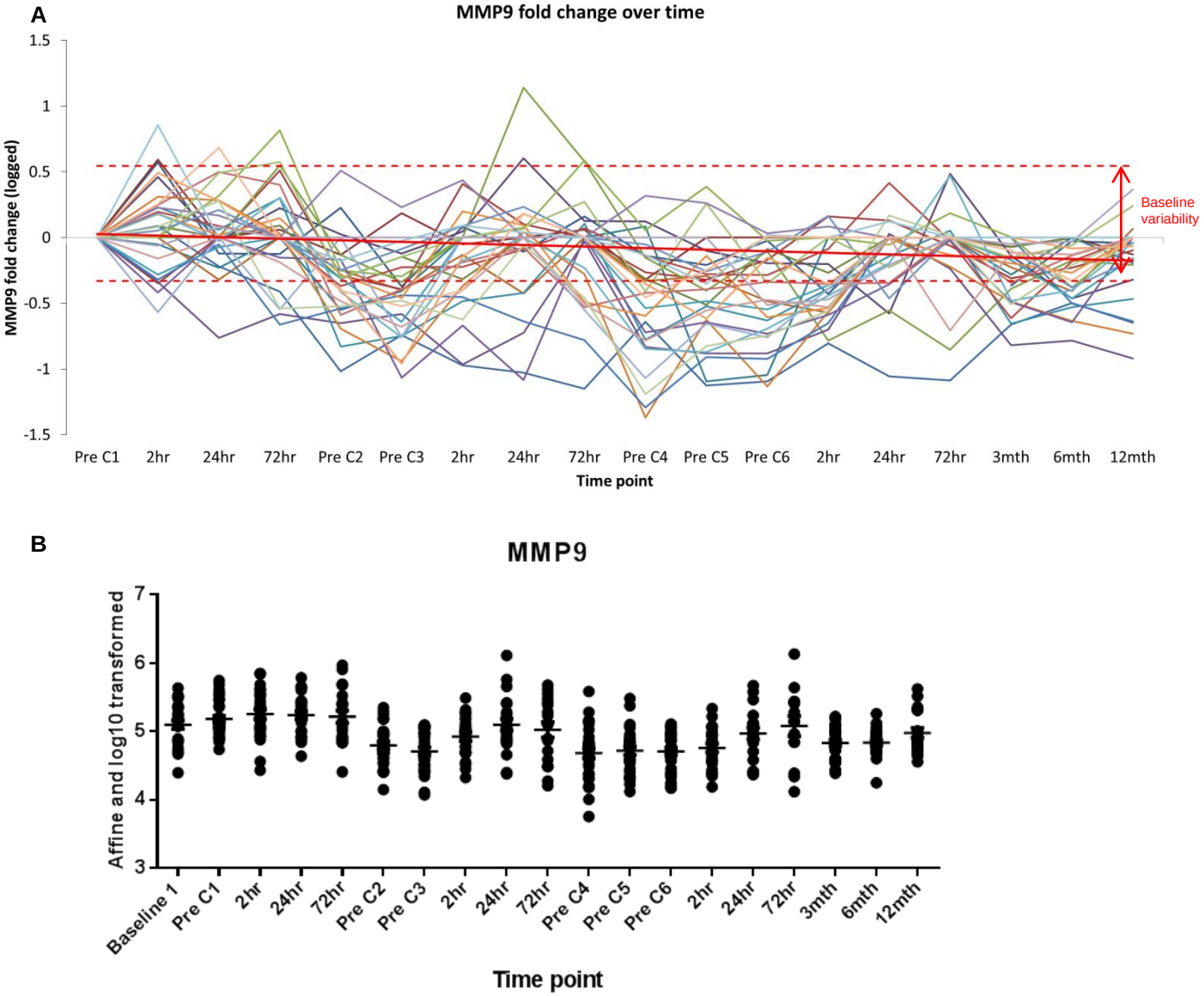

Figure 98. Graph A shows fold change of circulating MMP9 (logged) during and after anthracycline therapy. *Each line represents one patient and the dotted red lines show the 95% confidence interval for baseline variability. Graph B shows the individual logged values and the population mean and standard deviation at each time point. C= cycle.*

TIMP1: Although there were apparent dynamic changes in TIMP1 from baseline the changes were not out with baseline variability therefore no significant change was seen over time.

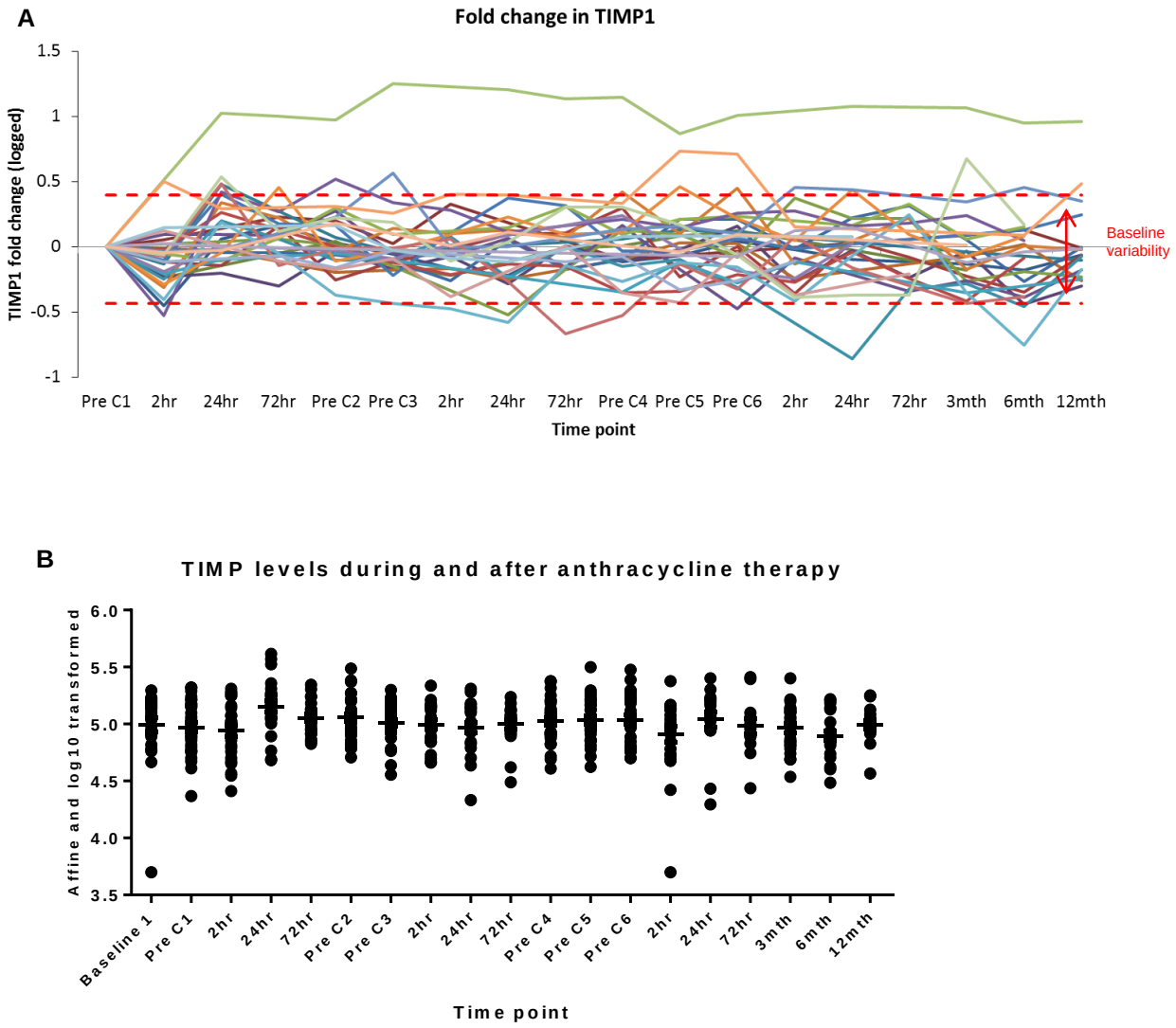

Figure 99. Graph A shows fold change of circulating TIMP1 (logged) during and after anthracycline therapy. *Each line represents one patient and the dotted red lines show the 95% confidence interval for baseline variability. Graph B shows the individual logged values and the population mean and standard deviation at each time point. C= cycle.*

MPO: MPO levels did not change significantly with time.

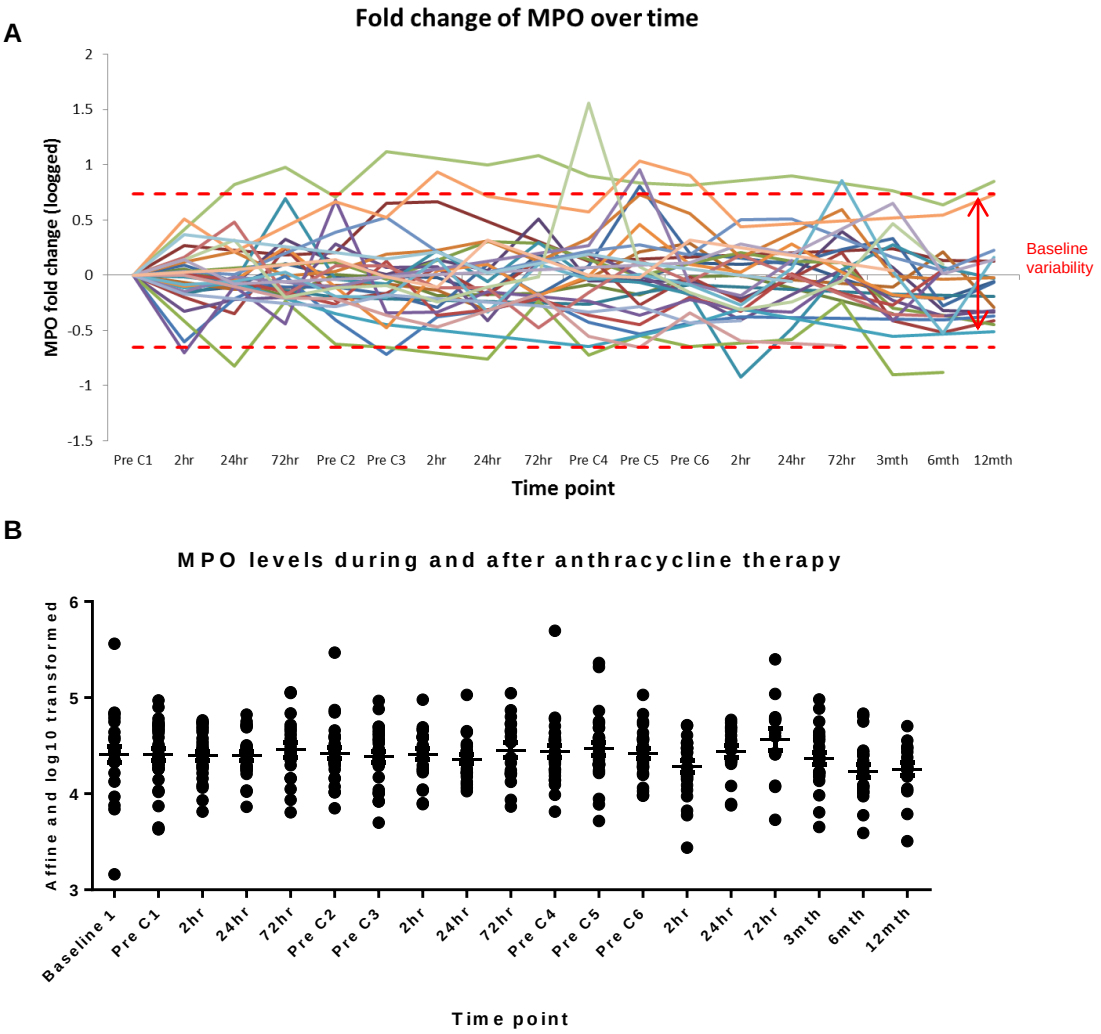

Figure 100. Graph A shows fold change of circulating MPO (logged) during and after anthracycline therapy. *Each line represents one patient and the dotted red lines show the 95% confidence interval for baseline variability. Graph B shows the individual logged values and the population mean and standard deviation at each time point. C= cycle.*

MMP2: MMP2 was detectable at baseline but did not change significantly over time. The changes seen all remained within the limits of baseline variability.

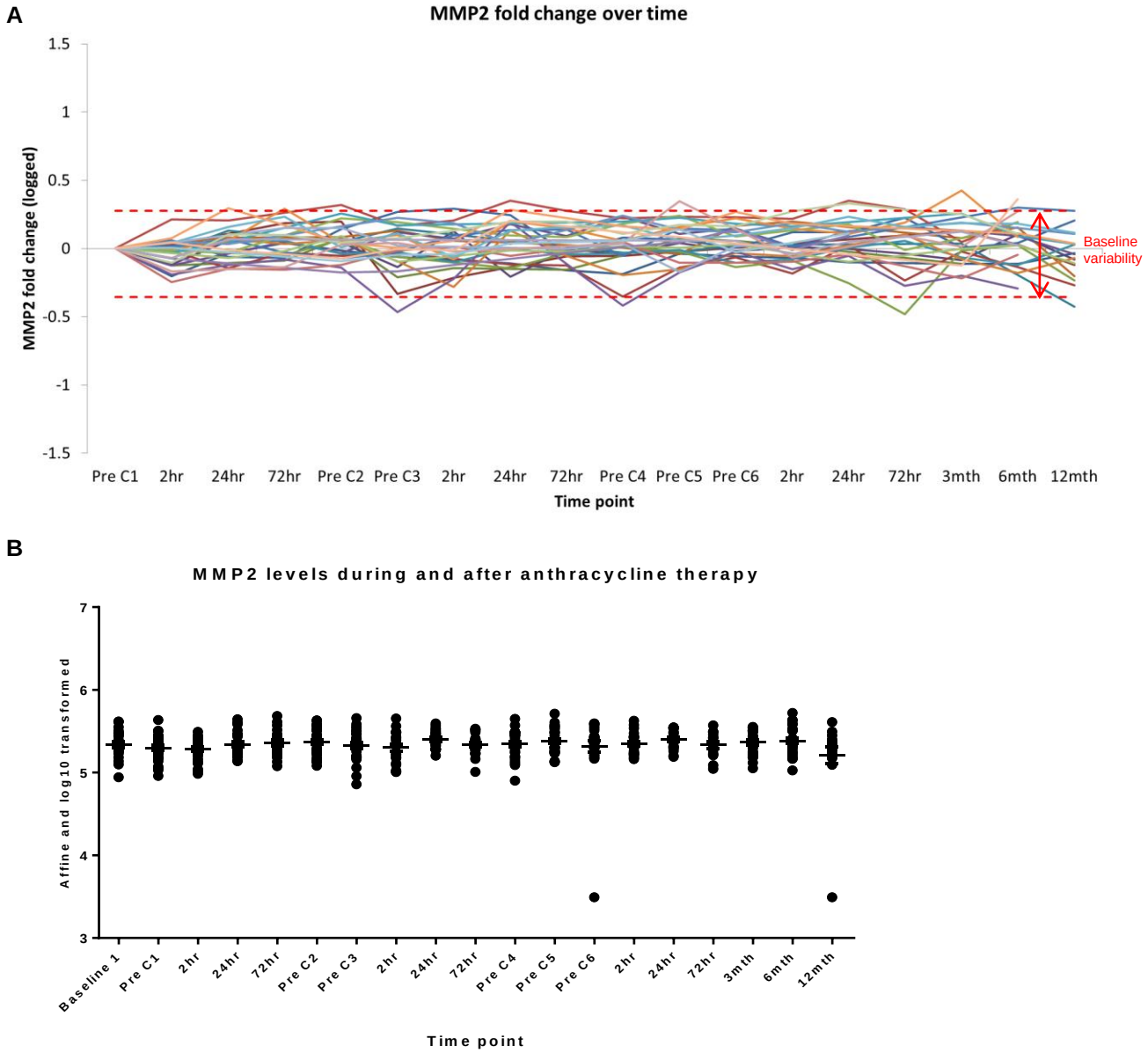

Figure 101. Graph A shows fold change of circulating MMP2 (logged) during and after anthracycline therapy. *Each line represents one patient and the dotted red lines show the 95% confidence interval for baseline variability. Graph B shows the individual logged values and the population mean and standard deviation at each time point. C= cycle.*

IL8: IL8 levels rose transiently 24 hours after the first dose of chemotherapy which may have been due to an initial anti-tumour effects or tumour flare rather than cardiac toxicity. Very little change form baseline was seen during the rest of the study. High levels were seen in one patient during an episode of sepsis complicated by thromboembolism.

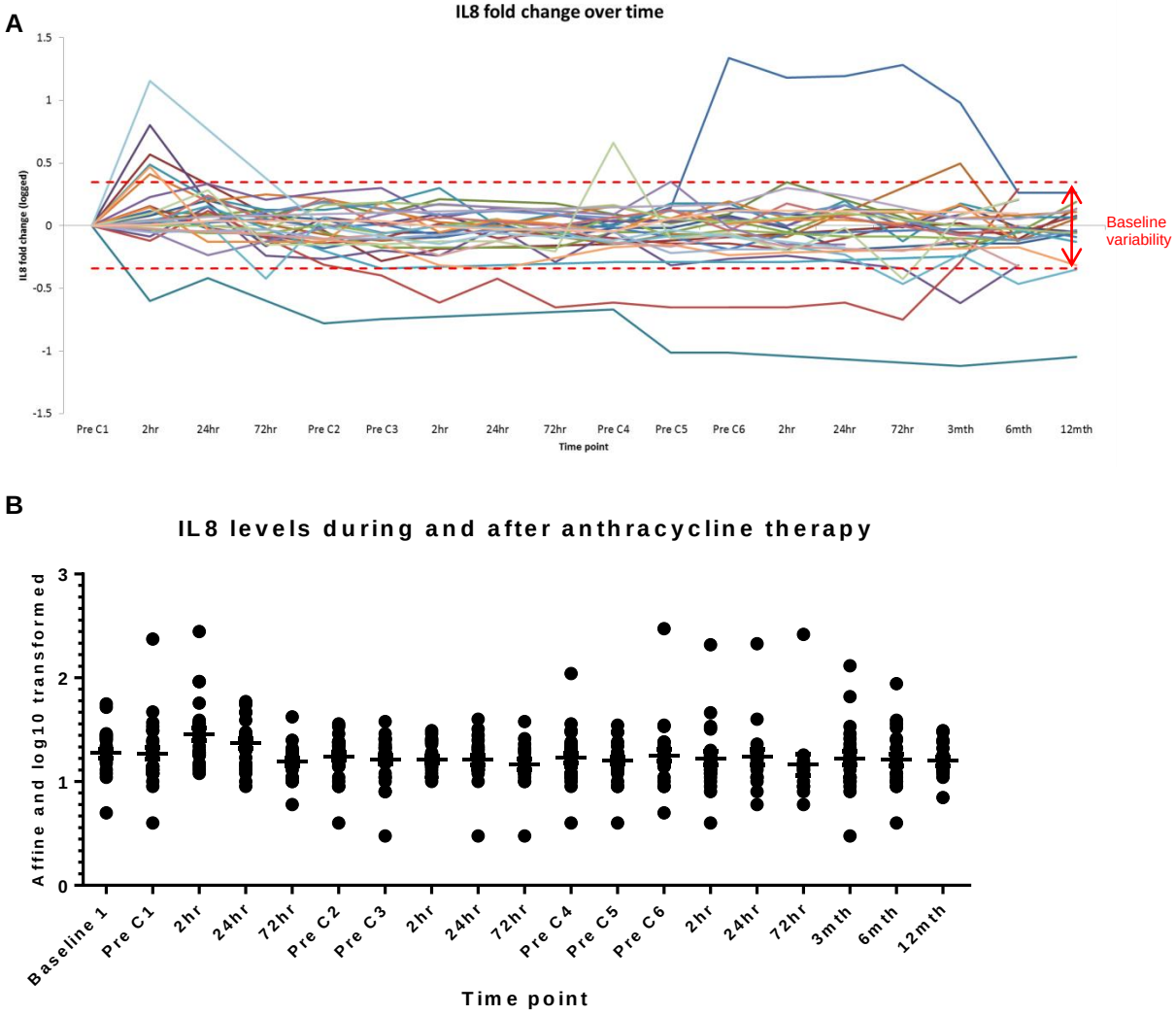

Figure 102. Graph A shows fold change of circulating IL8 (logged) during and after anthracycline therapy. *Each line represents one patient and the dotted red lines show the 95% confidence interval for baseline variability. Graph B shows the individual logged values and the population mean and standard deviation at each time point. C= cycle.*

IL1b and TNFa: IL1b and TNFa were rejected as potential biomarkers as they were undetectable at baseline and showed no significant dynamic change over time. High levels were seen in one patient (008) during cycle 6 in the presence of systemic infection and a venous thromboembolism but very few patients had significant elevations (patient 008 = dark blue line).

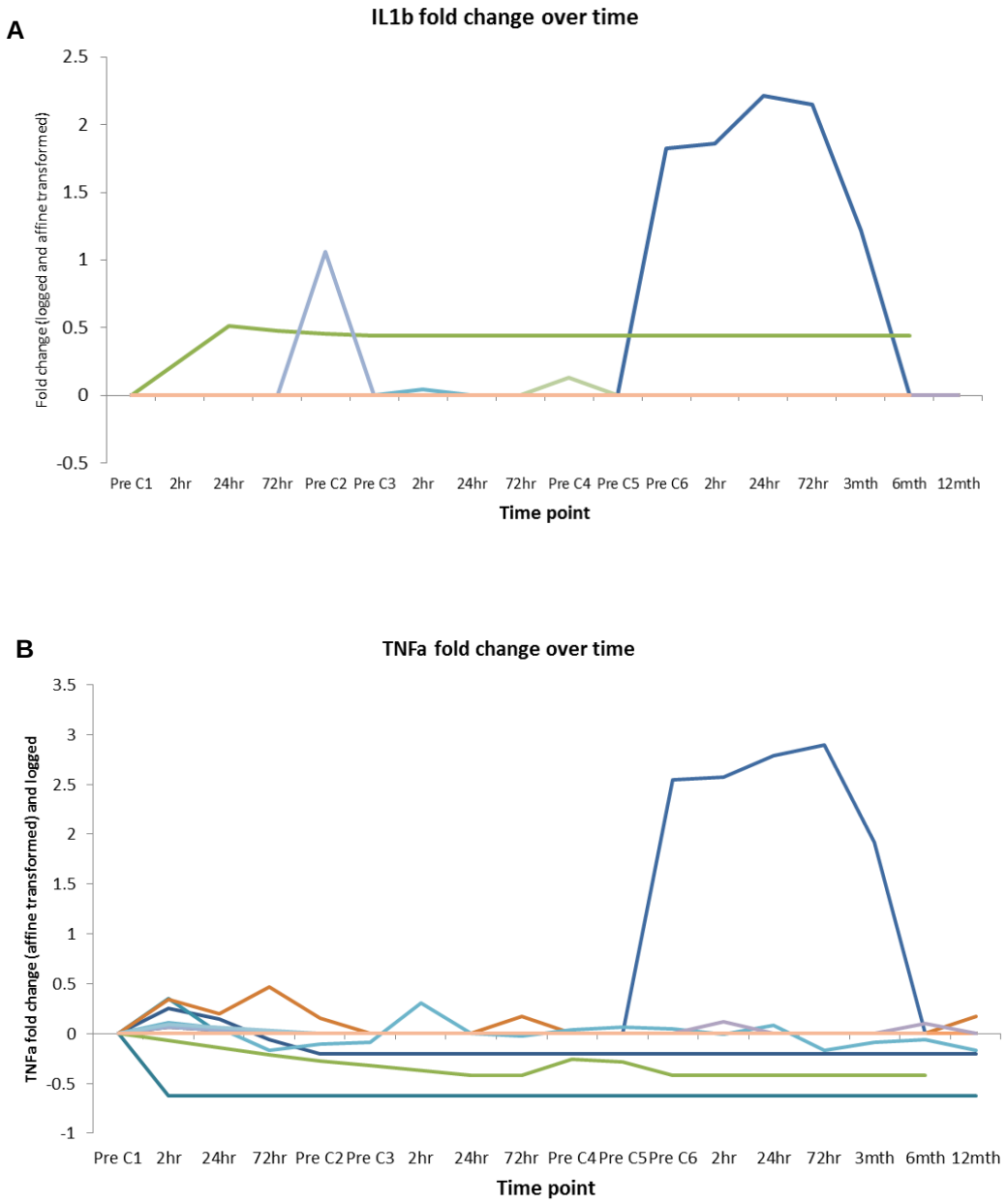

Figure 103. Graph A shows fold change in IL1b (logged) and graph B showed change in TNFa (logged) during and after anthracycline therapy in all patients. *Each line represents one patient. C= cycle.*

Example of a Scatterplot Matrix

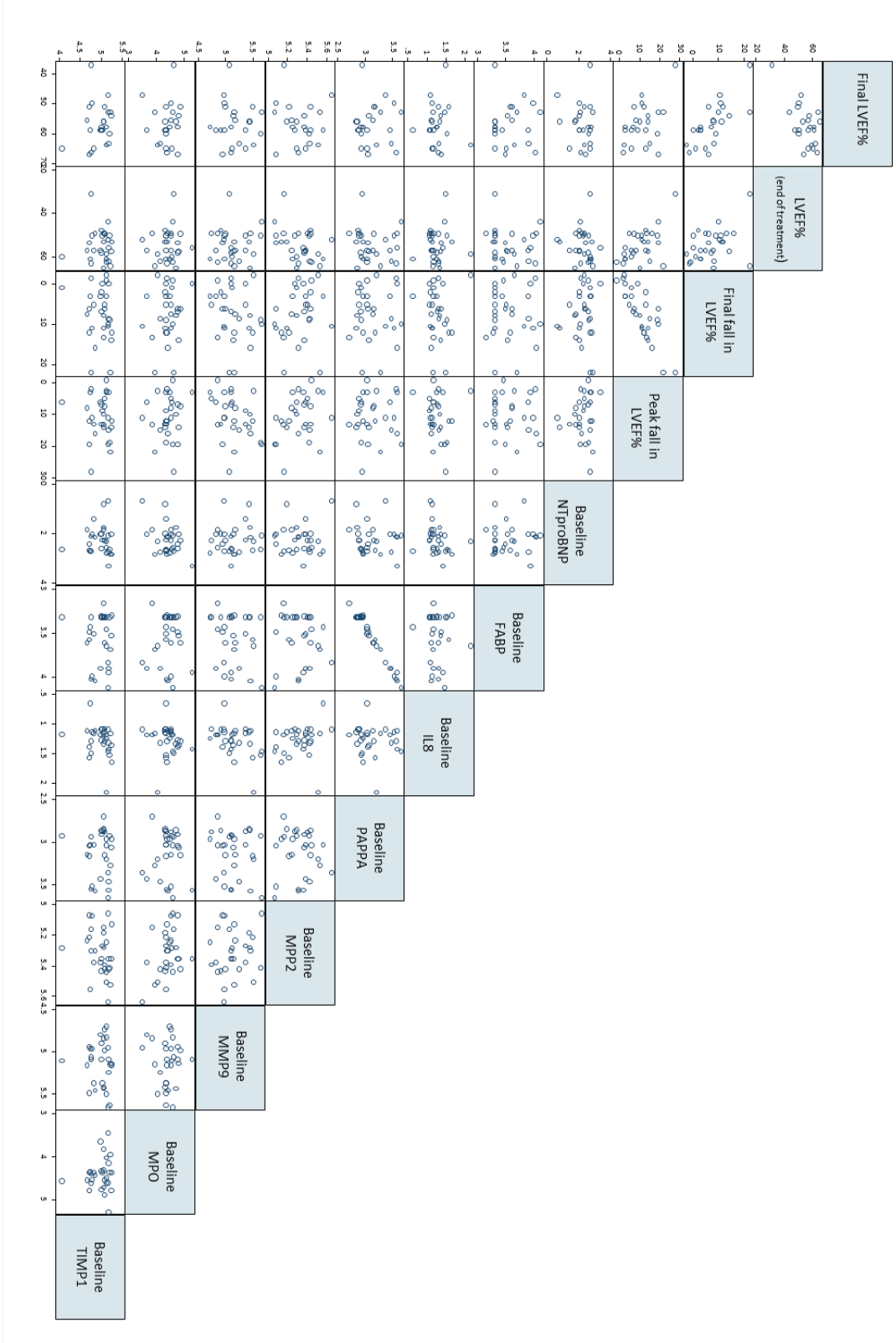

Figure 104. Example of a scatterplot matrix used to explore correlations between baseline biomarkers and LVEF

MMP2 and MMP9 ROC Analysis

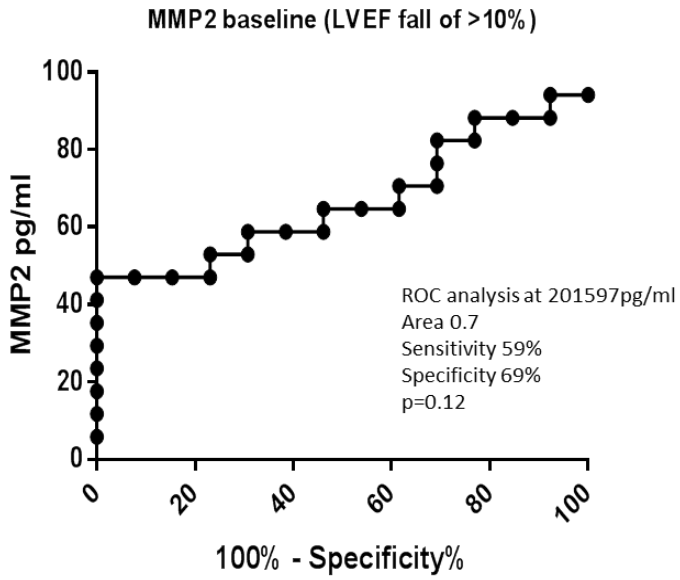

Figure 105. ROC analysis to determine the optimal sensitivity and specificity of MMP2 as a baseline prognostic bio marker

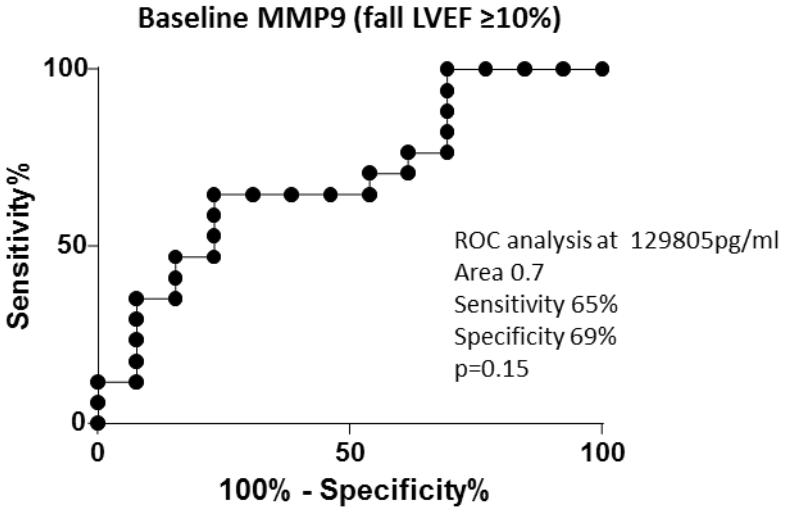

Figure 106. ROC analysis to determine the optimal sensitivity and specificity of MMP9 as a baseline prognostic bio marker

References

1. Trachtenberg, B.H., et al., Anthracycline-Associated Cardiotoxicity in Survivors of Childhood Cancer. Pediatr Cardiol, 2011.
2. Mertens, A.C., et al., Late mortality experience in five-year survivors of childhood and adolescent cancer: the Childhood Cancer Survivor Study. J Clin Oncol, 2001. 19(13): p. 3163-72.
3. Oeffinger, K.C., et al., Chronic health conditions in adult survivors of childhood cancer. N Engl J Med, 2006. 355(15): p. 1572-82.
4. Mertens, A.C., et al., Cause-specific late mortality among 5-year survivors of childhood cancer: the Childhood Cancer Survivor Study. J Natl Cancer Inst, 2008. 100(19): p. 1368-79.
5. Mulrooney, D.A., et al., Cardiac outcomes in a cohort of adult survivors of childhood and adolescent cancer: retrospective analysis of the Childhood Cancer Survivor Study cohort. BMJ, 2009. 339: p. b4606.
6. Carver, J.R., et al., American Society of Clinical Oncology clinical evidence review on the ongoing care of adult cancer survivors: cardiac and pulmonary late effects. J Clin Oncol, 2007. 25(25): p. 3991-4008.
7. Lenihan, D.J. Internation Cardio-oncology Society. in Internation Cardio-oncology Society Annual Meeting. 2011. Milan, Italy.
8. Dolci, A., et al., Biochemical markers for prediction of chemotherapy-induced cardiotoxicity: systematic review of the literature and recommendations for use. Am J Clin Pathol, 2008. 130(5): p. 688-95.
9. Bovelli, D., G. Plataniotis, and F. Roila, Cardiotoxicity of chemotherapeutic agents and radiotherapy-related heart disease: ESMO ClinicalPractice Guidelines. Annals of Oncology, 2010. 21.
10. Macmillan and BHF, Heart Health and Cancer Treatment, A Practical Guide to Living with and after Cancer. 2014.
11. Vander, A., J. Sherman, and D. Luciano, Human Physiology - The heart, in Human Physiology - The Mechanisms of Body Function. 1998, McGraw-Hill Companies, Inc. : Boston, Massachusetts. p. 387-407.
12. Walker, C.A. and F.G. Spinale, The structure and function of the cardiac myocyte: a review of fundamental concepts. J Thorac Cardiovasc Surg, 1999. 118(2): p. 375-82.
13. Unverferth, D.V., et al., Doxorubicin cardiotoxicity. Cancer Treat Rev, 1982. 9(2): p. 149-64.
14. Gianni, L., et al., Anthracycline cardiotoxicity: from bench to bedside. J Clin Oncol, 2008. 26(22): p. 3777-84.
15. Nysom, K., Late cardiotoxicity following anthracycline therapy for childhood cancer. Progress in pediatric cardiology, 1998. 8: p. 121-138.
16. Kremer, L.C., et al., Frequency and risk factors of subclinical cardiotoxicity after anthracycline therapy in children: a systematic review. Ann Oncol, 2002. 13(6): p. 819-29.
17. Vandecruys, E., et al., Late cardiotoxicity after low dose of anthracycline therapy for acute lymphoblastic leukemia in childhood. J Cancer Surviv, 2011.
18. Hequet, O., et al., Subclinical late cardiomyopathy after doxorubicin therapy for lymphoma in adults. J Clin Oncol, 2004. 22(10): p. 1864-71.
19. Swerdlow, A.J., et al., Myocardial infarction mortality risk after treatment for Hodgkin disease: a collaborative British cohort study. J Natl Cancer Inst, 2007. 99(3): p. 206-14.

20. Trudeau, M., et al., Selection of adjuvant chemotherapy for treatment of node-positive breast cancer. Lancet Oncol, 2005. 6(11): p. 886-98.
21. Maehara, Y., et al., 4'-O-tetrahydropyranyladriamycin has greater antineoplastic activity than adriamycin in various human tumours in vitro. Anticancer Res, 1989. 9(2): p. 387-9.
22. Ganzina, F., 4'-epi-doxorubicin, a new analogue of doxorubicin: a preliminary overview of preclinical and clinical data. Cancer Treat Rev, 1983. 10(1): p. 1-22.
23. Cardinale, D., et al., Trastuzumab-induced cardiotoxicity: clinical and prognostic implications of troponin I evaluation. J Clin Oncol, 2010. 28(25): p. 3910-6.
24. Gharib, M.I. and A.K. Burnett, Chemotherapy-induced cardiotoxicity: current practice and prospects of prophylaxis. Eur J Heart Fail, 2002. 4(3): p. 235-42.
25. Von Hoff, D.D., et al., Risk factors for doxorubicin-induced congestive heart failure. Ann Intern Med, 1979. 91(5): p. 710-7.
26. Swain, S.M., F.S. Whaley, and M.S. Ewer, Congestive heart failure in patients treated with doxorubicin: a retrospective analysis of three trials. Cancer, 2003. 97(11): p. 2869-79.
27. Peng, X., et al., The cardiotoxicology of anthracycline chemotherapeutics: translating molecular mechanism into preventative medicine. Mol Interv, 2005. 5(3): p. 163-71.
28. Eschenhagen, T., et al., Cardiovascular side effects of cancer therapies: a position statement from the Heart Failure Association of the European Society of Cardiology. Eur J Heart Fail, 2011. 13(1): p. 1-10.
29. ElGhandour, A.H., et al., Human heart-type fatty acid-binding protein as an early diagnostic marker of doxorubicin cardiac toxicity. 2009. Vol. 1. 2009.
30. Sawyer, D.B., et al., Mechanisms of anthracycline cardiac injury: can we identify strategies for cardioprotection? Prog Cardiovasc Dis, 2010. 53(2): p. 105-13.
31. Gewirtz, D.A., A critical evaluation of the mechanisms of action proposed for the antitumor effects of the anthracycline antibiotics adriamycin and daunorubicin. Biochem Pharmacol, 1999. 57(7): p. 727-41.
32. Joplin, C.E., Sleep; Marina, Raya; Merce, Marti; Angel, Raya; Juan, Carlos, Izipsua, Belmonte, Zebrafish heart regeneration occurs by cardiomyocyte dedifferentiation and proliferation. Nature, 2010. 464(7288): p. 606-609.
33. Jones, R.L., C. Swanton, and M.S. Ewer, Anthracycline cardiotoxicity. Expert Opin Drug Saf, 2006. 5(6): p. 791-809.
34. Anderson, E.J., L.A. Katunga, and M.S. Willis, Mitochondria as a source and target of lipid peroxidation products in healthy and diseased heart. Clin Exp Pharmacol Physiol, 2012. 39(2): p. 179-93.
35. Chandran, K., et al., Doxorubicin inactivates myocardial cytochrome c oxidase in rats: cardioprotection by Mito-Q. Biophys J, 2009. 96(4): p. 1388-98.
36. Damy, T., et al., Glutathione deficiency in cardiac patients is related to the functional status and structural cardiac abnormalities. PLoS One, 2009. 4(3): p. e4871.
37. Sawyer, D.B., et al., Daunorubicin-induced apoptosis in rat cardiac myocytes is inhibited by dexrazoxane. Circ Res, 1999. 84(3): p. 257-65.
38. Doroshow, J.H., Anthracycline antibiotic-stimulated superoxide, hydrogen peroxide, and hydroxyl radical production by NADH dehydrogenase. Cancer Res, 1983. 43(10): p. 4543-51.
39. Mihm, M.J. and J.A. Bauer, Peroxynitrite-induced inhibition and nitration of cardiac myofibrillar creatine kinase. Biochimie, 2002. 84(10): p. 1013-9.
40. Chen, B., et al., Molecular and cellular mechanisms of anthracycline cardiotoxicity. Cardiovasc Toxicol, 2007. 7(2): p. 114-21.

41. Xu, X., H.L. Persson, and D.R. Richardson, Molecular pharmacology of the interaction of anthracyclines with iron. Mol Pharmacol, 2005. 68(2): p. 261-71.
42. Simunek, T., et al., Anthracycline-induced cardiotoxicity: overview of studies examining the roles of oxidative stress and free cellular iron. Pharmacol Rep, 2009. 61(1): p. 154-71.
43. Degli Esposti, M., Mitochondria in apoptosis: past, present and future. Biochem Soc Trans, 2004. 32(Pt3): p. 493-5.
44. Montaigne, D., et al., Stabilization of mitochondrial membrane potential prevents doxorubicin-induced cardiotoxicity in isolated rat heart. Toxicol Appl Pharmacol, 2010. 244(3): p. 300-7.
45. Sardao, V.A., S.L. Pereira, and P.J. Oliveira, Drug-induced mitochondrial dysfunction in cardiac and skeletal muscle injury. Expert Opin Drug Saf, 2008. 7(2): p. 129-46.
46. Mukhopadhyay, P., et al., Role of superoxide, nitric oxide, and peroxynitrite in doxorubicin-induced cell death in vivo and in vitro. Am J Physiol Heart Circ Physiol, 2009. 296(5): p. H1466-83.
47. Unverferth, D.V., et al., The effect of first-dose doxorubicin on the cyclic nucleotide levels of the human myocardium. Toxicol Appl Pharmacol, 1981. 60(1): p. 151-4.
48. Cardinale, D., et al., Left ventricular dysfunction predicted by early troponin I release after high-dose chemotherapy. J Am Coll Cardiol, 2000. 36(2): p. 517-22.
49. Cardinale, D. and M.T. Sandri, Role of biomarkers in chemotherapy-induced cardiotoxicity. Prog Cardiovasc Dis, 2010. 53(2): p. 121-9.
50. Wang, S., et al., Activation of nuclear factor-kappaB during doxorubicin-induced apoptosis in endothelial cells and myocytes is pro-apoptotic: the role of hydrogen peroxide. Biochem J, 2002. 367(Pt 3): p. 729-40.
51. Nachtigal, P., et al., Daunorubicin does not induce immunohistochemically detectable endothelial dysfunction in rabbit aorta and femoral artery. Histol Histopathol, 2011. 26(5): p. 551-62.
52. Ito, H., et al., Doxorubicin selectively inhibits muscle gene expression in cardiac muscle cells in vivo and in vitro. Proc Natl Acad Sci U S A, 1990. 87(11): p. 4275-9.
53. Bian, Y., et al., Neuregulin-1 attenuated doxorubicin-induced decrease in cardiac troponins. Am J Physiol Heart Circ Physiol, 2009. 297(6): p. H1974-83.
54. Zhang, Y., et al., Doxorubicin Induces Sarcoplasmic Reticulum Calcium Regulation Dysfunction via the Decrease of SERCA2 and Phospholamban Expressions in Rats. Cell Biochem Biophys, 2014. 70(3): p. 1791-8.
55. Felker, G.M., et al., Underlying causes and long-term survival in patients with initially unexplained cardiomyopathy. N Engl J Med, 2000. 342(15): p. 1077-84.
56. Cardinale, D., et al., Anthracycline-induced cardiomyopathy: clinical relevance and response to pharmacologic therapy. J Am Coll Cardiol, 2010. 55(3): p. 213-20.
57. Wells, Q.S. and D.J. Lenihan, Reversibility of left ventricular dysfunction resulting from chemotherapy: can this be expected? Prog Cardiovasc Dis, 2010. 53(2): p. 140-8.
58. Albini, A., et al., Cardiotoxicity of anticancer drugs: the need for cardio-oncology and cardio-oncological prevention. J Natl Cancer Inst, 2010. 102(1): p. 14-25.
59. Jones, L.W., et al., Early breast cancer therapy and cardiovascular injury. J Am Coll Cardiol, 2007. 50(15): p. 1435-41.
60. Singal, P.K. and N. Iliskovic, Doxorubicin-induced cardiomyopathy. N Engl J Med, 1998. 339(13): p. 900-5.
61. Unverferth, B.J., et al., Early changes in human myocardial nuclei after doxorubicin. Cancer, 1983. 52(2): p. 215-21.

62. Bristow, M.R., et al., Dose-effect and structure-function relationships in doxorubicin cardiomyopathy. Am Heart J, 1981. 102(4): p. 709-18.
63. Rahman, A.M., S.W. Yusuf, and M.S. Ewer, Anthracycline-induced cardiotoxicity and the cardiac-sparing effect of liposomal formulation. Int J Nanomedicine, 2007. 2(4): p. 567-83.
64. De Gruttola, V.G., et al., Considerations in the evaluation of surrogate endpoints in clinical trials. summary of a National Institutes of Health workshop. Control Clin Trials, 2001. 22(5): p. 485-502.
65. Cummings, J., et al., Biomarker method validation in anticancer drug development. Br J Pharmacol, 2008. 153(4): p. 646-56.
66. Hodgson, D.R., et al., Biomarkers in oncology drug development. Mol Oncol, 2009. 3(1): p. 24-32.
67. Greystoke, A., et al., Assessment of circulating biomarkers for potential pharmacodynamic utility in patients with lymphoma. Br J Cancer, 2011. 104(4): p. 719-25.
68. Mair, J., et al., Cardiac troponin I in the diagnosis of myocardial injury and infarction. Clin Chim Acta, 1996. 245(1): p. 19-38.
69. Gomes, A.V., J.D. Potter, and D. Szczesna-Cordary, The role of troponins in muscle contraction. IUBMB Life, 2002. 54(6): p. 323-33.
70. Lipshultz, S.E., et al., Predictive value of cardiac troponin T in pediatric patients at risk for myocardial injury. Circulation, 1997. 96(8): p. 2641-8.
71. Cardinale, D., et al., Prognostic value of troponin I in cardiac risk stratification of cancer patients undergoing high-dose chemotherapy. Circulation, 2004. 109(22): p. 2749-54.
72. Auner, H.W., et al., Prolonged monitoring of troponin T for the detection of anthracycline cardiotoxicity in adults with hematological malignancies. Ann Hematol, 2003. 82(4): p. 218-22.
73. Morris, P.G., et al., Troponin I and C-Reactive Protein are Commonly Detected in Patients with Breast Cancer Treated with Dose-Dense Chemotherapy Incorporating Trastuzumab and Lapatinib. Clin Cancer Res, 2011.
74. Katsurada, K., et al., High-sensitivity troponin T as a marker to predict cardiotoxicity in breast cancer patients with adjuvant trastuzumab therapy. Springerplus, 2014. 3: p. 620.
75. Salvatici, M., et al., TnI-Ultra assay measurements in cancer patients: comparison with the conventional assay and clinical implication. Scand J Clin Lab Invest, 2014. 74(5): p. 385-91.
76. Cardinale, D., et al., Myocardial injury revealed by plasma troponin I in breast cancer treated with high-dose chemotherapy. Ann Oncol, 2002. 13(5): p. 710-5.
77. Kilickap, S., et al., cTnT can be a useful marker for early detection of anthracycline cardiotoxicity. Ann Oncol, 2005. 16(5): p. 798-804.
78. Lipshultz, S.E., et al., Abstract 20432: Diagnostic Value of Cardiac Troponin T, N-Terminal Pro-Brain Natriuretic Peptide, and High-Sensitivity C-Reactive Protein During Doxorubicin Therapy in Children with Acute Lymphoblastic Leukemia. Circulation. 122(21_MeetingAbstracts): p. A20432-.
79. Sandri, M.T., et al., Minor increases in plasma troponin I predict decreased left ventricular ejection fraction after high-dose chemotherapy. Clin Chem, 2003. 49(2): p. 248-52.
80. Sawaya, H., et al., Early detection and prediction of cardiotoxicity in chemotherapy-treated patients. Am J Cardiol, 2011. 107(9): p. 1375-80.

81. O'Brien, P.J., Cardiac troponin is the most effective translational safety biomarker for myocardial injury in cardiotoxicity. Toxicology, 2008. 245(3): p. 206-18.
82. Adamcova, M., et al., In vitro and in vivo examination of cardiac troponins as biochemical markers of drug-induced cardiotoxicity. Toxicology, 2007. 237(1-3): p. 218-28.
83. Simunek, T., et al., Cardiac troponin T as an indicator of reduced left ventricular contractility in experimental anthracycline-induced cardiomyopathy. Cancer Chemother Pharmacol, 2003. 52(5): p. 431-4.
84. Koh, E., T. Nakamura, and H. Takahashi, Troponin-T and brain natriuretic peptide as predictors for adriamycin-induced cardiomyopathy in rats. Circ J, 2004. 68(2): p. 163-7.
85. Gardner, R.S., et al., N-terminal pro-brain natriuretic peptide. A new gold standard in predicting mortality in patients with advanced heart failure. Eur Heart J, 2003. 24(19): p. 1735-43.
86. McCullough, P.A., T. Omland, and A.S. Maisel, B-type natriuretic peptides: a diagnostic breakthrough for clinicians. Rev Cardiovasc Med, 2003. 4(2): p. 72-80.
87. Felker, G.M., et al., Biomarker-guided therapy in chronic heart failure: a meta-analysis of randomized controlled trials. Am Heart J, 2009. 158(3): p. 422-30.
88. Paulus, W.J., et al., How to diagnose diastolic heart failure: a consensus statement on the diagnosis of heart failure with normal left ventricular ejection fraction by the Heart Failure and Echocardiography Associations of the European Society of Cardiology. Eur Heart J, 2007. 28(20): p. 2539-50.
89. Mair, J., Biochemistry of B-type natriuretic peptide--where are we now? Clin Chem Lab Med, 2008. 46(11): p. 1507-14.
90. Aggarwal, S., et al., B-type natriuretic peptide as a marker for cardiac dysfunction in anthracycline-treated children. Pediatr Blood Cancer, 2007. 49(6): p. 812-6.
91. Daugaard, G., et al., Natriuretic peptides in the monitoring of anthracycline induced reduction in left ventricular ejection fraction. Eur J Heart Fail, 2005. 7(1): p. 87-93.
92. Nousiainen, T., et al., Natriuretic peptides as markers of cardiotoxicity during doxorubicin treatment for non-Hodgkin's lymphoma. Eur J Haematol, 1999. 62(2): p. 135-41.
93. Mavinkurve-Groothuis, A.M., et al., Abnormal NT-pro-BNP levels in asymptomatic long-term survivors of childhood cancer treated with anthracyclines. Pediatr Blood Cancer, 2009. 52(5): p. 631-6.
94. Romano, S., et al., Serial measurements of NT-proBNP are predictive of not-high-dose anthracycline cardiotoxicity in breast cancer patients. Br J Cancer, 2011. 105(11): p. 1663-8.
95. Pichon, M.F., et al., Drug-induced cardiotoxicity studied by longitudinal B-type natriuretic peptide assays and radionuclide ventriculography. In Vivo, 2005. 19(3): p. 567-76.
96. McCann, C.J., et al., Investigation of a multimarker approach to the initial assessment of patients with acute chest pain. Adv Ther, 2009. 26(5): p. 531-4.
97. Chen, L., X. Guo, and F. Yang, Role of heart-type fatty acid binding protein in early detection of acute myocardial infarction in comparison with cTnI, CK-MB and myoglobin. J Huazhong Univ Sci Technolog Med Sci, 2004. 24(5): p. 449-51, 459.
98. Horacek, J.M., et al., The use of cardiac biomarkers in detection of cardiotoxicity associated with conventional and high-dose chemotherapy for acute leukemia. Exp Oncol, 2010. 32(2): p. 97-9.

99. Ingelsson, E., et al., Inflammation, as measured by the erythrocyte sedimentation rate, is an independent predictor for the development of heart failure. J Am Coll Cardiol, 2005. 45(11): p. 1802-6.
100. Mann, D.L., Inflammatory mediators and the failing heart: past, present, and the foreseeable future. Circ Res, 2002. 91(11): p. 988-98.
101. Vasan, R.S., et al., Inflammatory markers and risk of heart failure in elderly subjects without prior myocardial infarction: the Framingham Heart Study. Circulation, 2003. 107(11): p. 1486-91.
102. Rauchhaus, M., et al., Plasma cytokine parameters and mortality in patients with chronic heart failure. Circulation, 2000. 102(25): p. 3060-7.
103. Tsutamoto, T., et al., Interleukin-6 spillover in the peripheral circulation increases with the severity of heart failure, and the high plasma level of interleukin-6 is an important prognostic predictor in patients with congestive heart failure. J Am Coll Cardiol, 1998. 31(2): p. 391-8.
104. Ortolani, P., et al., Predictive value of high sensitivity C-reactive protein in patients with ST-elevation myocardial infarction treated with percutaneous coronary intervention. Eur Heart J, 2008. 29(10): p. 1241-9.
105. Ridker, P.M. and D.A. Morrow, C-reactive protein, inflammation, and coronary risk. Cardiol Clin, 2003. 21(3): p. 315-25.
106. Heslop, C.L., J.J. Frohlich, and J.S. Hill, Myeloperoxidase and C-reactive protein have combined utility for long-term prediction of cardiovascular mortality after coronary angiography. J Am Coll Cardiol, 2010. 55(11): p. 1102-9.
107. Brennan, M.L., et al., Prognostic value of myeloperoxidase in patients with chest pain. N Engl J Med, 2003. 349(17): p. 1595-604.
108. Velasquez, I.M., et al., Association of interleukin 8 with myocardial infarction: results from the Stockholm Heart Epidemiology Program. Int J Cardiol, 2014. 172(1): p. 173-8.
109. Bujak, M. and N.G. Frangogiannis, The role of IL-1 in the pathogenesis of heart disease. Arch Immunol Ther Exp (Warsz), 2009. 57(3): p. 165-76.
110. Zhu, J., et al., Recombinant human interleukin-1 receptor antagonist protects mice against acute doxorubicin-induced cardiotoxicity. Eur J Pharmacol, 2010. 643(2-3): p. 247-53.
111. Tsavaris, N., et al., Immune changes in patients with advanced breast cancer undergoing chemotherapy with taxanes. Br J Cancer, 2002. 87(1): p. 21-7.
112. Shaker, O. and D.A. Sourour, How to protect doxorubicin-induced cardiomyopathy in male albino rats? J Cardiovasc Pharmacol, 2010. 55(3): p. 262-8.
113. Spinale, F.G., Novel approaches to retard ventricular remodeling in heart failure. Eur J Heart Fail, 1999. 1(1): p. 17-23.
114. Schulz, R., Intracellular targets of matrix metalloproteinase-2 in cardiac disease: rationale and therapeutic approaches. Annu Rev Pharmacol Toxicol, 2007. 47: p. 211-42.
115. Barton, P.J., et al., Increased expression of extracellular matrix regulators TIMP1 and MMP1 in deteriorating heart failure. J Heart Lung Transplant, 2003. 22(7): p. 738-44.
116. Goetzenich, A., et al., Alteration of matrix metalloproteinases in selective left ventricular adriamycin-induced cardiomyopathy in the pig. J Heart Lung Transplant, 2009. 28(10): p. 1087-93.
117. Ahmed, S.H., et al., Matrix metalloproteinases/tissue inhibitors of metalloproteinases: relationship between changes in proteolytic determinants of matrix composition and structural, functional, and clinical manifestations of hypertensive heart disease. Circulation, 2006. 113(17): p. 2089-96.

118. Kai, H., et al., Peripheral blood levels of matrix metalloproteases-2 and -9 are elevated in patients with acute coronary syndromes. J Am Coll Cardiol, 1998. 32(2): p. 368-72.
119. Yamazaki, T., et al., Circulating matrix metalloproteinase-2 is elevated in patients with congestive heart failure. Eur J Heart Fail, 2004. 6(1): p. 41-5.
120. Shirakabe, A., et al., Clinical significance of matrix metalloproteinase (MMP)-2 in patients with acute heart failure. Int Heart J, 2010. 51(6): p. 404-10.
121. Bonaca, M.P., et al., Prospective evaluation of pregnancy-associated plasma protein-a and outcomes in patients with acute coronary syndromes. J Am Coll Cardiol, 2012. 60(4): p. 332-8.
122. Zhang, Z., et al., Elevated pregnancy-associated plasma protein A predicts myocardial dysfunction and death in severe sepsis. Ann Clin Biochem, 2014. 51(Pt 1): p. 22-9.
123. Constantine, G., et al., Role of MRI in clinical cardiology. Lancet, 2004. 363(9427): p. 2162-71.
124. Shan, K., et al., Role of cardiac magnetic resonance imaging in the assessment of myocardial viability. Circulation, 2004. 109(11): p. 1328-34.
125. Korkusuz, H., et al., Accuracy of cardiovascular magnetic resonance in myocarditis: comparison of MR and histological findings in an animal model. J Cardiovasc Magn Reson, 2010. 12: p. 49.
126. Marijianowski, M.M., et al., Dilated cardiomyopathy is associated with an increase in the type I/type III collagen ratio: a quantitative assessment. J Am Coll Cardiol, 1995. 25(6): p. 1263-72.
127. Perel, R.D., R.E. Slaughter, and W.E. Strugnell, Subendocardial late gadolinium enhancement in two patients with anthracycline cardiotoxicity following treatment for Ewing's sarcoma. J Cardiovasc Magn Reson, 2006. 8(6): p. 789-91.
128. Catalano, O., et al., Contrast-enhanced cardiac magnetic resonance in a patient with chemotoxic cardiomyopathy. J Cardiovasc Med (Hagerstown), 2007. 8(3): p. 214-5.
129. Wassmuth, R., et al., Subclinical cardiotoxic effects of anthracyclines as assessed by magnetic resonance imaging-a pilot study. Am Heart J, 2001. 141(6): p. 1007-13.
130. Oberholzer, K., et al., [Anthracycline-induced cardiotoxicity: cardiac MRI after treatment for childhood cancer]. Rofo, 2004. 176(9): p. 1245-50.
131. Lunning, M.A., et al., Cardiac magnetic resonance imaging for assessment of cardiac structure and function following doxorubicin-based chemotherapy for newly diagnosed non-hodgkin lymphoma. Annals of oncology, 2011. 22(supl 4).
132. Nagueh, S.F., et al., Recommendations for the evaluation of left ventricular diastolic function by echocardiography. Eur J Echocardiogr, 2009. 10(2): p. 165-93.
133. Stoodley, P.W., et al., Two-dimensional myocardial strain imaging detects changes in left ventricular systolic function immediately after anthracycline chemotherapy. Eur J Echocardiogr, 2011. 12(12): p. 945-52.
134. Kang, Y., et al., Early detection of anthracycline-induced cardiotoxicity using two-dimensional speckle tracking echocardiography. Cardiol J, 2013. 20(6): p. 592-9.
135. Mornos, C., et al., The value of left ventricular global longitudinal strain assessed by three-dimensional strain imaging in the early detection of anthracyclinemediated cardiotoxicity. Hellenic J Cardiol, 2014. 55(3): p. 235-44.
136. Mewton, N., et al., Assessment of myocardial fibrosis with cardiovascular magnetic resonance. J Am Coll Cardiol, 2011. 57(8): p. 891-903.
137. Miller, C.A., et al., Comprehensive validation of cardiovascular magnetic resonance techniques for the assessment of myocardial extracellular volume. Circ Cardiovasc Imaging, 2013. 6(3): p. 373-83.

138. Neilan, T.G., et al., Myocardial extracellular volume by cardiac magnetic resonance imaging in patients treated with anthracycline-based chemotherapy. Am J Cardiol, 2013. 111(5): p. 717-22.
139. Tham, E.B., et al., Diffuse myocardial fibrosis by T1-mapping in children with subclinical anthracycline cardiotoxicity: relationship to exercise capacity, cumulative dose and remodeling. J Cardiovasc Magn Reson, 2013. 15: p. 48.
140. Takaseya, T., et al., Mechanical unloading improves intracellular Ca2+ regulation in rats with doxorubicin-induced cardiomyopathy. J Am Coll Cardiol, 2004. 44(11): p. 2239-46.
141. Yilmaz, S., et al., Protective effect of lycopene on adriamycin-induced cardiotoxicity and nephrotoxicity. Toxicology, 2006. 218(2-3): p. 164-71.
142. Date, T., et al., Myocardial expression of baculoviral p35 alleviates doxorubicin-induced cardiomyopathy in rats. Hum Gene Ther, 2003. 14(10): p. 947-57.
143. Weiss, R.B., The anthracyclines: will we ever find a better doxorubicin? Semin Oncol, 1992. 19(6): p. 670-86.
144. Cochet, A., et al., Baseline diastolic dysfunction as a predictive factor of trastuzumab-mediated cardiotoxicity after adjuvant anthracycline therapy in breast cancer. Breast Cancer Res Treat, 2011. 130(3): p. 845-54.
145. Christian, J.B., et al., Cardiac imaging approaches to evaluate drug-induced myocardial dysfunction. Am Heart J, 2012. 164(6): p. 846-55.
146. Elliott, P., Pathogenesis of cardiotoxicity induced by anthracyclines. Semin Oncol, 2006. 33(3 Suppl 8): p. S2-7.
147. Levey, G.S., et al., Selective inhibition of rat and human cardiac guanylate cyclase by doxorubicin (adriamycin): possible link to anthracycline cardiotoxicity. Trans Assoc Am Physicians, 1979. 92: p. 303-8.
148. Czarnecki, C.M., Animal models of drug-induced cardiomyopathy. Comp Biochem Physiol C, 1984. 79(1): p. 9-14.
149. Arola, O.J., et al., Acute doxorubicin cardiotoxicity involves cardiomyocyte apoptosis. Cancer Res, 2000. 60(7): p. 1789-92.
150. Heiberg, E., et al., Design and validation of Segment--freely available software for cardiovascular image analysis. BMC Med Imaging, 2010. 10: p. 1.
151. Puchtler, H., F.S. Waldrop, and L.S. Valentine, Polarization microscopic studies of connective tissue stained with picro-sirius red FBA. Beitr Pathol, 1973. 150(2): p. 174-87.
152. Junqueira, L.C., G. Bignolas, and R.R. Brentani, Picrosirius staining plus polarization microscopy, a specific method for collagen detection in tissue sections. Histochem J, 1979. 11(4): p. 447-55.
153. McMurray, J.J., et al., ESC guidelines for the diagnosis and treatment of acute and chronic heart failure 2012: The Task Force for the Diagnosis and Treatment of Acute and Chronic Heart Failure 2012 of the European Society of Cardiology. Developed in collaboration with the Heart Failure Association (HFA) of the ESC. Eur J Heart Fail, 2012. 14(8): p. 803-69.
154. Saraste, A., S. Nekolla, and M. Schwaiger, Contrast-enhanced magnetic resonance imaging in the assessment of myocardial infarction and viability. J Nucl Cardiol, 2008. 15(1): p. 105-17.
155. Tjeerdsma, G., et al., Early detection of anthracycline induced cardiotoxicity in asymptomatic patients with normal left ventricular systolic function: autonomic versus echocardiographic variables. Heart, 1999. 81(4): p. 419-23.

156. Marchandise, B., et al., Early detection of doxorubicin cardiotoxicity: interest of Doppler echocardiographic analysis of left ventricular filling dynamics. Am Heart J, 1989. 118(1): p. 92-8.
157. Lee, B.H., et al., Alterations in left ventricular diastolic function with doxorubicin therapy. J Am Coll Cardiol, 1987. 9(1): p. 184-8.
158. Schwarz, E.R., et al., A small animal model of non-ischemic cardiomyopathy and its evaluation by transthoracic echocardiography. Cardiovasc Res, 1998. 39(1): p. 216-23.
159. Dodos, F., et al., Usefulness of myocardial performance index and biochemical markers for early detection of anthracycline-induced cardiotoxicity in adults. Clin Res Cardiol, 2008. 97(5): p. 318-26.
160. Lefrak, E.A., et al., A clinicopathologic analysis of adriamycin cardiotoxicity. Cancer, 1973. 32(2): p. 302-14.
161. Herman, E.H., et al., Use of cardiac troponin T levels as an indicator of doxorubicin-induced cardiotoxicity. Cancer Res, 1998. 58(2): p. 195-7.
162. Lauer, B., et al., Cardiac troponin T in patients with clinically suspected myocarditis. J Am Coll Cardiol, 1997. 30(5): p. 1354-9.
163. Jaffe, A.S., L. Babuin, and F.S. Apple, Biomarkers in acute cardiac disease: the present and the future. J Am Coll Cardiol, 2006. 48(1): p. 1-11.
164. Jaffe, A.S., Cardiovascular biomarkers: the state of the art in 2006. Clin Chim Acta, 2007. 381(1): p. 9-13.
165. Adamcova, M., et al., Troponin as a marker of myocardiac damage in drug-induced cardiotoxicity. Expert Opin Drug Saf, 2005. 4(3): p. 457-72.
166. Jaffe, A.S. and A.H. Wu, Troponin release--reversible or irreversible injury? Should we care? Clin Chem, 2012. 58(1): p. 148-50.
167. Migrino, R.Q., et al., Early detection of doxorubicin cardiomyopathy using two-dimensional strain echocardiography. Ultrasound Med Biol, 2008. 34(2): p. 208-14.
168. Lightfoot, J.C., et al., Novel approach to early detection of doxorubicin cardiotoxicity by gadolinium-enhanced cardiovascular magnetic resonance imaging in an experimental model. Circ Cardiovasc Imaging, 2010. 3(5): p. 550-8.
169. Pfreundschuh, M., et al., CHOP-like chemotherapy with or without rituximab in young patients with good-prognosis diffuse large-B-cell lymphoma: 6-year results of an open-label randomised study of the MabThera International Trial (MInT) Group. Lancet Oncol, 2011. 12(11): p. 1013-22.
170. Cardinale, D., et al., Prevention of high-dose chemotherapy-induced cardiotoxicity in high-risk patients by angiotensin-converting enzyme inhibition. Circulation, 2006. 114(23): p. 2474-81.
171. Sawaya, H., J.C. Plana, and M. Scherrer-Crosbie, Newest echocardiographic techniques for the detection of cardiotoxicity and heart failure during chemotherapy. Heart Fail Clin, 2011. 7(3): p. 313-21.
172. Colombo, A., et al., Managing cardiotoxicity of chemotherapy. Curr Treat Options Cardiovasc Med, 2013. 15(4): p. 410-24.
173. Jiamsripong, P., et al., Three methods for evaluation of left atrial volume. Eur J Echocardiogr, 2008. 9(3): p. 351-5.
174. Giri, S., et al., T2 quantification for improved detection of myocardial edema. J Cardiovasc Magn Reson, 2009. 11: p. 56.
175. Messroghli, D.R., et al., Optimization and validation of a fully-integrated pulse sequence for modified look-locker inversion-recovery (MOLLI) T1 mapping of the heart. J Magn Reson Imaging, 2007. 26(4): p. 1081-6.

176. Wong, T.C., et al., Association between extracellular matrix expansion quantified by cardiovascular magnetic resonance and short-term mortality. Circulation, 2012. 126(10): p. 1206-16.
177. Yu, C.M., J.J. Bax, and J. Gorcsan, 3rd, Critical appraisal of methods to assess mechanical dyssynchrony. Curr Opin Cardiol, 2009. 24(1): p. 18-28.
178. Gorcsan, J., 3rd, et al., Echocardiography for cardiac resynchronization therapy: recommendations for performance and reporting--a report from the American Society of Echocardiography Dyssynchrony Writing Group endorsed by the Heart Rhythm Society. J Am Soc Echocardiogr, 2008. 21(3): p. 191-213.
179. Gresele, P., et al., Platelets release matrix metalloproteinase-2 in the coronary circulation of patients with acute coronary syndromes: possible role in sustained platelet activation. European Heart Journal, 2011(32): p. 316–325.
180. Voller, A., et al., The detection of viruses by enzyme-linked immunosorbent assay (ELISA). J Gen Virol, 1976. 33(1): p. 165-7.
181. Goode, V., et al., An audit of the consent and management of cardiotoxicity in lymphoma patients. 2014.
182. Consensus, Guidelines for the treatment of Lymphoma. 2011, Greater Manchester and Cheshire Cancer Network.
183. McGale, P., et al., Incidence of heart disease in 35,000 women treated with radiotherapy for breast cancer in Denmark and Sweden. Radiother Oncol, 2011. 100(2): p. 167-75.
184. Lunning, M.A., et al., Cardiac Magnetic Resonance Imaging for the Assessment of the Myocardium After Doxorubicin-based Chemotherapy. Am J Clin Oncol, 2013.
185. Drafts, B.C., et al., Low to moderate dose anthracycline-based chemotherapy is associated with early noninvasive imaging evidence of subclinical cardiovascular disease. JACC Cardiovasc Imaging, 2013. 6(8): p. 877-85.
186. Jordan, J.H., et al., Longitudinal assessment of concurrent changes in left ventricular ejection fraction and left ventricular myocardial tissue characteristics after administration of cardiotoxic chemotherapies using t1-weighted and t2-weighted cardiovascular magnetic resonance. Circ Cardiovasc Imaging, 2014. 7(6): p. 872-9.
187. Praga, C., et al., Adriamycin cardiotoxicity: a survey of 1273 patients. Cancer Treat Rep, 1979. 63(5): p. 827-34.
188. Hilmer, S.N., et al., The hepatic pharmacokinetics of doxorubicin and liposomal doxorubicin. Drug Metab Dispos, 2004. 32(8): p. 794-9.
189. Minow, R.A., et al., Adriamycin cardiomyopathy--risk factors. Cancer, 1977. 39(4): p. 1397-402.
190. Grenier, M.A. and S.E. Lipshultz, Epidemiology of anthracycline cardiotoxicity in children and adults. Semin Oncol, 1998. 25(4 Suppl 10): p. 72-85.
191. Cottin, Y., et al., Impairment of diastolic function during short-term anthracycline chemotherapy. Br Heart J, 1995. 73(1): p. 61-4.
192. Reiter, U., et al., Normal diastolic and systolic myocardial T1 values at 1.5-T MR imaging: correlations and blood normalization. Radiology, 2014. 271(2): p. 365-72.
193. Smith, L.A., et al., Cardiotoxicity of anthracycline agents for the treatment of cancer: systematic review and meta-analysis of randomised controlled trials. BMC Cancer, 2010. 10: p. 337.
194. Jerosch-Herold, M., et al., Cardiac magnetic resonance imaging of myocardial contrast uptake and blood flow in patients affected with idiopathic or familial dilated cardiomyopathy. Am J Physiol Heart Circ Physiol, 2008. 295(3): p. H1234-H1242.
195. Wu, S., et al., Adriamycin-induced cardiomyocyte and endothelial cell apoptosis: in vitro and in vivo studies. J Mol Cell Cardiol, 2002. 34(12): p. 1595-607.

196. Hare, J.L., et al., Use of myocardial deformation imaging to detect preclinical myocardial dysfunction before conventional measures in patients undergoing breast cancer treatment with trastuzumab. Am Heart J, 2009. 158(2): p. 294-301.
197. Ky, B., et al., Early increases in multiple biomarkers predict subsequent cardiotoxicity in patients with breast cancer treated with doxorubicin, taxanes, and trastuzumab. J Am Coll Cardiol, 2014. 63(8): p. 809-16.
198. Sawaya, H., et al., Assessment of echocardiography and biomarkers for the extended prediction of cardiotoxicity in patients treated with anthracyclines, taxanes, and trastuzumab. Circ Cardiovasc Imaging, 2012. 5(5): p. 596-603.
199. Ye, Z.X., et al., Baseline serum matrix metalloproteinase-9 level predicts long-term prognosis after coronary revascularizations in stable coronary artery disease. Clin Biochem, 2008. 41(4-5): p. 292-8.
200. DeCoux, A., et al., Myocardial matrix metalloproteinase-2: inside out and upside down. J Mol Cell Cardiol, 2014.
201. Ivanova, M., et al., Chronic cardiotoxicity of doxorubicin involves activation of myocardial and circulating matrix metalloproteinases in rats. Acta Pharmacol Sin, 2012. 33(4): p. 459-69.
202. Fang, L., et al., Activation of peripheral blood mononuclear cells and extracellular matrix and inflammatory gene profile in acute myocardial infarction. Clin Sci (Lond), 2010. 119(4): p. 175-83.
203. Kiczak, L., et al., Matrix metalloproteinase 9/neutrophil gelatinase associated lipocalin/tissue inhibitor of metalloproteinasess type 1 complexes are localized within cardiomyocytes and serve as a reservoir of active metalloproteinase in porcine female myocardium. J Physiol Pharmacol, 2014. 65(3): p. 365-75.
204. Ishimura, S., et al., Circulating levels of fatty acid-binding protein family and metabolic phenotype in the general population. PLoS One, 2013. 8(11): p. e81318.
205. Horacek, J.M., et al., Use of multiple biomarkers for evaluation of anthracycline-induced cardiotoxicity in patients with acute myeloid leukemia. Exp Oncol, 2008. 30(2): p. 157-9.
206. Horacek, J.M., et al., Biochemical markers and assessment of cardiotoxicity during preparative regimen and hematopoietic cell transplantation in acute leukemia. Exp Oncol, 2007. 29(3): p. 243-7.
207. Messroghli, D.R., et al., Assessment of diffuse myocardial fibrosis in rats using small-animal Look-Locker inversion recovery T1 mapping. Circ Cardiovasc Imaging, 2011. 4(6): p. 636-40.
208. Berinstein, N.L., et al., Association of serum Rituximab (IDEC-C2B8) concentration and anti-tumor response in the treatment of recurrent low-grade or follicular non-Hodgkin's lymphoma. Ann Oncol, 1998. 9(9): p. 995-1001.
209. Illidge, T.M., et al., Fractionated (9)(0)Y-ibritumomab tiuxetan radioimmunotherapy as an initial therapy of follicular lymphoma: an international phase II study in patients requiring treatment according to GELF/BNLI criteria. J Clin Oncol, 2014. 32(3): p. 212-8.
210. Melanson, S.E., M.J. Tanasijevic, and P. Jarolim, Cardiac troponin assays: a view from the clinical chemistry laboratory. Circulation, 2007. 116(18): p. e501-4.